AD NUMBER
AD477758
LIMITATION CHANGES
TO: **Approved for public release; distribution is unlimited.**
FROM: **Distribution authorized to U.S. Gov't. agencies and their contractors; Critical Technology; NOV 1965. Other requests shall be referred to Air Force Flight Dynamics, Wright-Patterson AFB, OH 45433. This document contains export-controlled technical data.**
AUTHORITY
AFFDL ltr, 25 Oct 1972

AFFDL-TR-65-155

X-20 HIGH TEMPERATURE SIDE WINDOW TEST EVALUATION

JOHN C. McGINNIS

THE BOEING COMPANY

TECHNICAL REPORT No. AFFDL-TR-65-155

NOVEMBER 1965

AIR FORCE FLIGHT DYNAMICS LABORATORY
RESEARCH AND TECHNOLOGY DIVISION
AIR FORCE SYSTEMS COMMAND
WRIGHT-PATTERSON AIR FORCE BASE, OHIO

NOTICES

When Government drawings, specifications, or other data are used for any purpose other than in connection with a definitely related Government procurement operation, the United States Government thereby incurs no responsibility nor any obligation whatsoever; and the fact that the Government may have formulated, furnished, or in any way supplied the said drawings, specifications, or other data, is not to be regarded by implication or otherwise as in any manner licensing the holder or any other person or corporation, or conveying any rights or permission to manufacture, use, or sell any patented invention that may in any way be related thereto.

Copies of this report should not be returned to the Research and Technology Division unless return is required by security considerations, contractual obligations, or notice on a specific document.

200 - January 1966 - 24-488-773

X-20 HIGH TEMPERATURE SIDE WINDOW TEST EVALUATION

JOHN C. McGINNIS

THE BOEING COMPANY

FOREWORD

This program is an extension of the X-20 (Dyna-Soar) structural development in the area of high temperature windows. The program was sponsored by the Air Force Flight Dynamics Laboratory (AFFDL), Research and Technology Division, Air Force Systems Command, United States Air Force. Initially listed under Project Number 620A, Task Number 620A, Item Number 2-9, this work was accomplished under Contract AF 33(615)-2013; Project Number 1368; Task Number 136802, "Window Systems Concepts".

The hot side window assembly of an X-20 (Dyna-Soar) was fabricated by The Boeing Company, Aerospace Division, Seattle, Washington under EWA 00114. Vibration, air, and thermal load tests were accomplished by the Structures Test Branch (FDTT) at AFFDL, Wright-Patterson AFB, Ohio.

The first test of the series was conducted on 20 January 1965 with termination occurring on 2 April 1965 during Test No. 3 when the window failed during heating. The tabulated data on all tests performed are stored at the Structures Test Branch (FDTT), AFFDL and at The Boeing Company, Aerospace Division.

Acknowledgment is given to Lt. J. Pharmer (FDTS), Program Coordinator, and Mr. Murry England (FDTT), Test Project Engineer, of the Air Force Flight Dynamics Laboratory for supplying photographs, drawings, descriptions and test data.

The manuscript was released by the author in August 1965 under Boeing Document No. D2-81310-1 for publication as an RTD Technical Report.

Publication of this report does not constitute Air Force approval of the report's findings or conclusions. It is published only for the exchange and stimulation of ideas.

Frederick C. Krug

FREDERICK C. KRUG
Colonel USAF
Chief, Structures Division

ABSTRACT

This document presents the results of testing an X-20A (Dyna-Soar) high temperature side window assembly under vibration, air, and thermal loading.

The purpose of this program was to experimentally verify the X-20A side window assembly and provide experience for improved window design. The objective of this program was to verify the structural integrity of an X-20A high temperature window design in the X-20A flight environment and provide test data to evaluate the design analysis and development procedures utilized.

The X-20 side window provides pilot vision throughout all phases of flight, and is exposed to all flight environments. The side window is triangular in shape (28 inches by 24 inches by 16 inches) with rounded corners. The window assembly includes three separate glass panes of fused silica, seals fabricated from Hastelloy-X wire mesh with foil covering, Superalloy Rene' 41 mounting springs, fairing, and frame.

The window was subjected to a low-level boost vibration environment, limit boost pressure of -7 pounds/inch^2 (gage) and a simulated re-entry heating time-temperature history.

The window failed during the re-entry temperature cycle. The primary cause of failure was the high temperature gradient through the depth of the window frame of approximately 850°F which exceeded by a factor of 2 the ultimate design value. The extreme thermal gradient caused thermal curvature of the window frame which induced glass curvature in excess of allowable.

Measured temperatures and deflections are presented and compared with analytical values. A thermal analysis is presented and compared with test values. Deficiencies of the X-20 window design as determined from the test program are pointed out and suggested methods of improvement are given.

TABLE OF CONTENTS

LIST OF ILLUSTRATIONS

LIST OF ILLUSTRATIONS (Continued)

LIST OF ILLUSTRATIONS (Continued)

LIST OF ILLUSTRATIONS (Concluded)

LIST OF TABLES

NOMENCLATURE

A	= Aluminum plate thermocouple
C	= Control Thermocouple
CPS	= Cycles/second
DA	= Deflection indicator - section A-A
DB	= Deflection indicator - section B-B
DC	= Deflection indicator - section C-C
DD	= Deflection indicator - section D-D
DE	= Deflection indicator - section E-E
F	= Fairing thermocouple
g	= Acceleration - 32.2 ft/sec^2
I	= Moment of inertia - in^4
I.R.	= Infrared
J	= Polar moment of inertia - in^4
M_x,M_y	= Bending moment - in.lbs./inch
psi	= Pressure lbs/in^2
P	= Load lbs or lbs/in
P_S	= Surface pressure - lbs/ft^2
P_V	= Vent pressure - lbs/ft^2
P_∞	= Free stream pressure - lbs/ft^2
PSD	= Power spectral density - g^2/CPS
Q_x,Q_y	= Shear lbs/in
Q	= Amplification factor - g's output/g's input
rms	= Root mean square

NOMENCLATURE (Continued)

R_x, R_y	= Rotation - radians
T	= Thermocouple or temperature-°F
TM	= Thermistor
TCPL	= Thermocouple
V	= Shear - pounds
Z	= Vertical deflection - inches
σ_{xx}, σ_{yy}	= Stress - lbs/in^2
τ_{xy}	= Shear stress - lbs/in^2

1 INTRODUCTION

1.1 GENERAL DESCRIPTION

The requirement for pilot vision necessitated the installation of five windows within the cooled pilots compartment and the surrounding primary hot structure of the X-20A (Dyna-Soar) vehicle. The three forward facing windows require thermal protection during re-entry, which is provided by an ejectable windshield cover. This cover is ejected following re-entry at velocities between Mach 6 and Mach 4. This allows the pilot to make a visual approach and landing. The left and right side windows are provided for pilot vision throughout all phases of flight, and are exposed to all flight environments, boost through landing.

This program deals with the test of one of the hot side windows only. The hot side windows must prevent the hot gas plasma associated with aerodynamic heating from entering the fuselage cavity. The hot windows are triple pane, 100 percent fused-silica, polished plates having an infrared coating on all surfaces except on the outer surface. The window panes are of a triangular shape approximately 24 inches by 28 inches by 16 inches with rounded corners. Each of the window installations consists of three panes of glass mounted in a continuous superalloy (Rene' 41) frame, as shown on page 3 . Each frame is mounted on a three-point suspension pivot principle so as to allow the glass to carry only normal loads either to the edge or the face of the pane. The attachments shown on page 20 show the hot frames are fully restrained at only one pivot point. This restraint point will accept all inertia loads as well as dampen vibrations of the installation. The "hot" glass, itself, is mounted in the frame in such a manner as to prevent the glass from coming free when the frame expands under high-temperature conditions. This is accomplished by use of flat Rene' 41 side springs and Rene' 41 leaf spring in series with the seals. The seal material for this "hot" environment consists of five pads of Hastelloy-X wire mesh wrapped in Hastelloy-X foil nominally clamped up at 35 pounds per lineal inch of periphery. Under the "hot" environment the material retains a clamped up pressure of approximately 8 pounds per lineal inch of periphery.

The "hot" structural window assembly is directly adjacent to the "cold" windows of the pilots compartment. The pilots compartment is suspended within the glider primary structure in such a manner as not to accept basic structural loads. The cold window is a laminated two-pane low-expansion, alumino-silicate polished plate having an infrared reflective coating on the outboard surface. These panes are mounted in a silicone rubber seal that is clamped in place to provide for a near-zero leakage rate of the pressurized pilots compartment. The "cold" windows are not a part of this test program.

The "hot" side window test specimen was instrumented with accelerometers for determining response of the structural system during vibration testing; thermistors for measurement of the fused silica glass pane temperatures; thermocouples for measurement of the window frame, cab frame, and support structure temperatures; and deflection gages for measurement of window and

1.1 GENERAL DESCRIPTION (Continued)

cab frame translations and/or rotations. The window test setup is instrumented to measure net pressure on the window and leakage rates through the seals during the boost air load test No. 2. All instrumentation data is recorded, reduced, and is documented herein.

An outline of the test plan as prepared in Reference 4 is shown on page 3. The planned test series were not completed due to the failure of the glass during Test Condition 3; Re-entry Thermal Cycle. Although the full planned program of tests was not completed, limited tests were run for each of the three design environments—pressure, vibration and temperature.

This report presents the results of the tests completed and a comparison with analytical data. A thermal and stress analysis of the window assembly is included. The cause of the window failure is discussed and methods of improvement are suggested.

Developmental testing and stress analysis for the X-20 "hot" side window in support of X-20A drawing release has been documented in Reference 5.

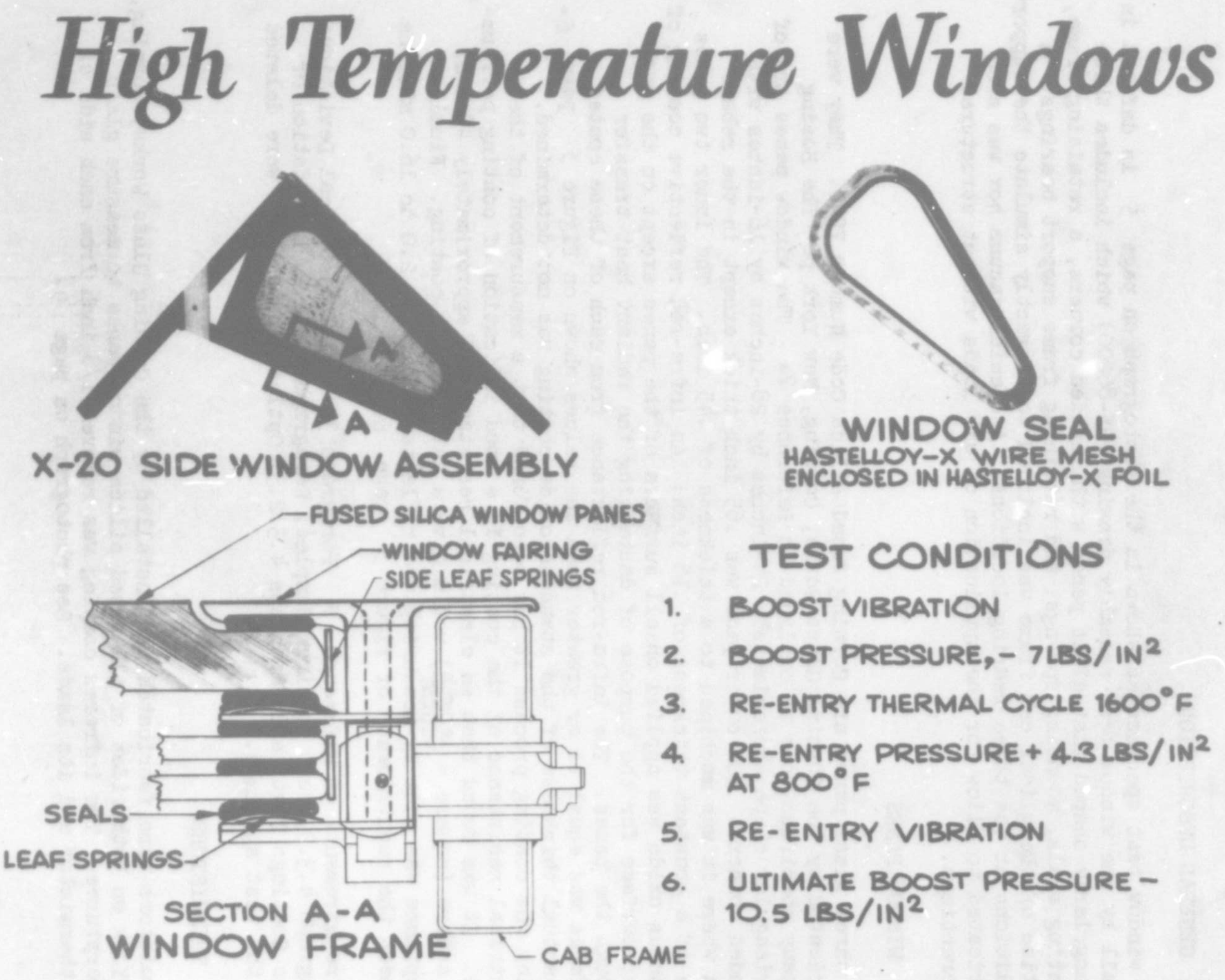

FIGURE 1 X-20 High Temperature Window Test Plan

2 TEST SPECIMEN

2.1 GENERAL DESCRIPTION

The window test specimen as shown in the photograph on page 5 is defined in detail by the window test assembly drawing (25-86200) which includes three triangularly shaped flat glass panes with rounded corners, a retaining frame, mounting seals, mounting springs, and retaining frame support bearings. A portion of the glider cab frame was included to correctly simulate the support conditions at the three bearing locations. A special vacuum box was also fabricated to allow for the application of air loads without structural interactions.

2.2 WINDOW PANES

The three glass panes are Corning fused silica Code Number 7940. They were fabricated by the Corning Glass Works, Corning, New York per The Boeing Company specifications as outlined in Reference 7. The window panes are of a triangular shape approximately 24-inches by 28-inches by 16-inches with rounded corners. The outer pane was .65 inch thick except in the rebate area where it was machined to a thickness of .45 inch. The inner two panes were of a constant thickness of .18 inch. An infra-red reflective coating of stannous oxide was applied on all surfaces of the panes except on the most outer surface for the purpose of decreasing the radiant heat transfer through the panes. The infra-red reflectance from each of these coated surfaces was equal to or greater than the values shown on Figure 3 page 6. The actual thickness of the stannous oxide coating was not determined. During the coating process it has been found that a measurement of the electrical resistance of the coating is a good indication of coating performance. It was found that an electrical resistance of approximately 40 ohms per square (square = $\frac{\text{length}}{\text{width}}$) would give a satisfactory coating. Final acceptance was made by measuring the reflectance between 2.0 to 16.0 microns to meet the requirements of Figure 3 page 6.

The requirements of Reference 7 Paragraph 3.1.2.1.1.6, Optical Deviation; Paragraph 4.3.2, Test Specimen Samples; Paragraph 4.3.2.2, Degradation of Glass Coatings Test; and Paragraph 4.3.2.3, Optical Inspection, were deleted for the test specimen.

2.3 THERMISTORS

Thermistors were fabricated and installed by the Corning Glass Works, Corning, New York on both sides of all fused silica window panes to measure glass temperatures. The infrared coating was removed 1/8 inch from each side of the thermistor and its leads. See photograph on page 9.

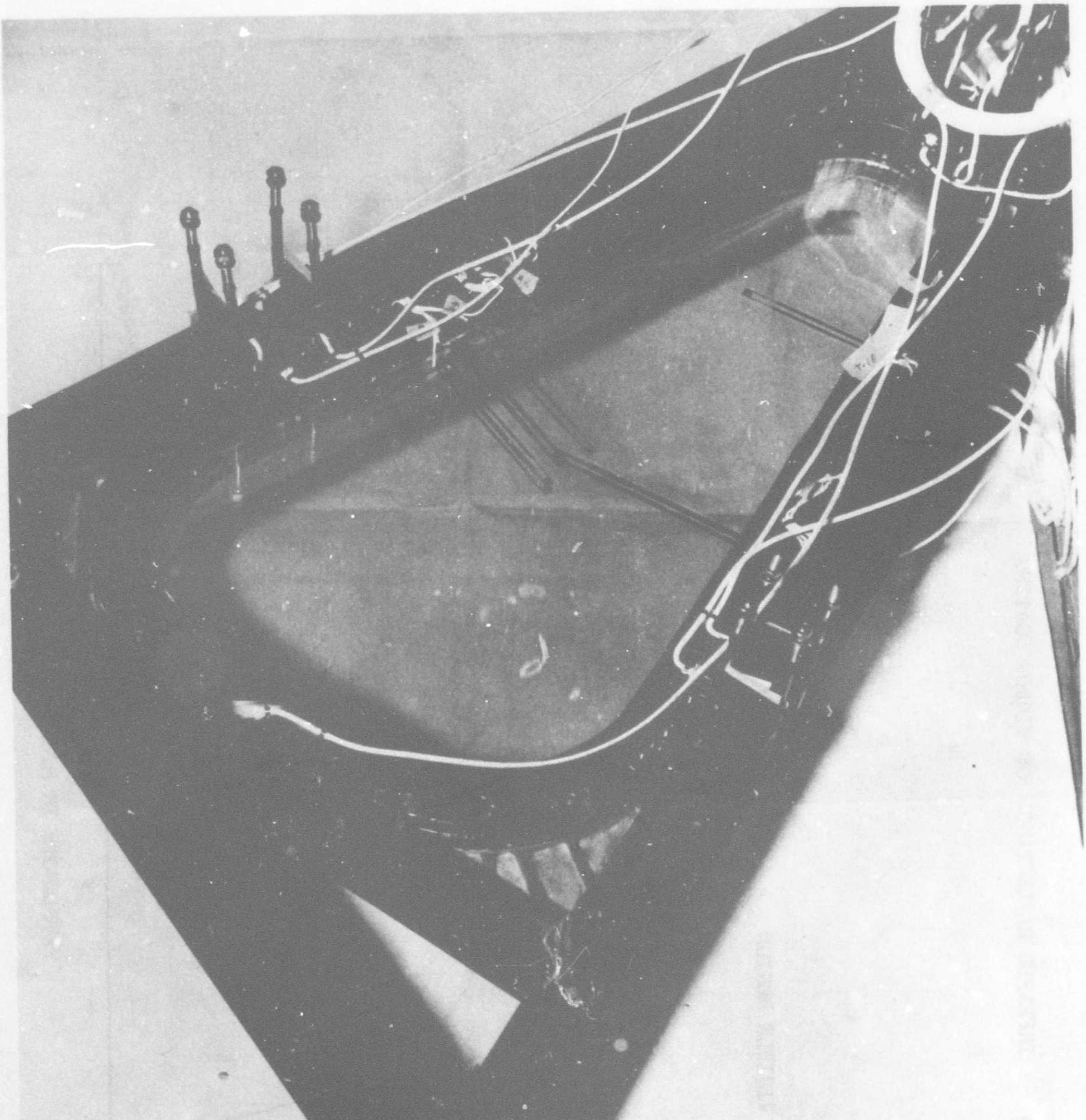

FIGURE 2 X-20 SIDE WINDOW ASSEMBLY

FIGURE 3 INFRARED REFLECTANCE OF WINDOW COATING

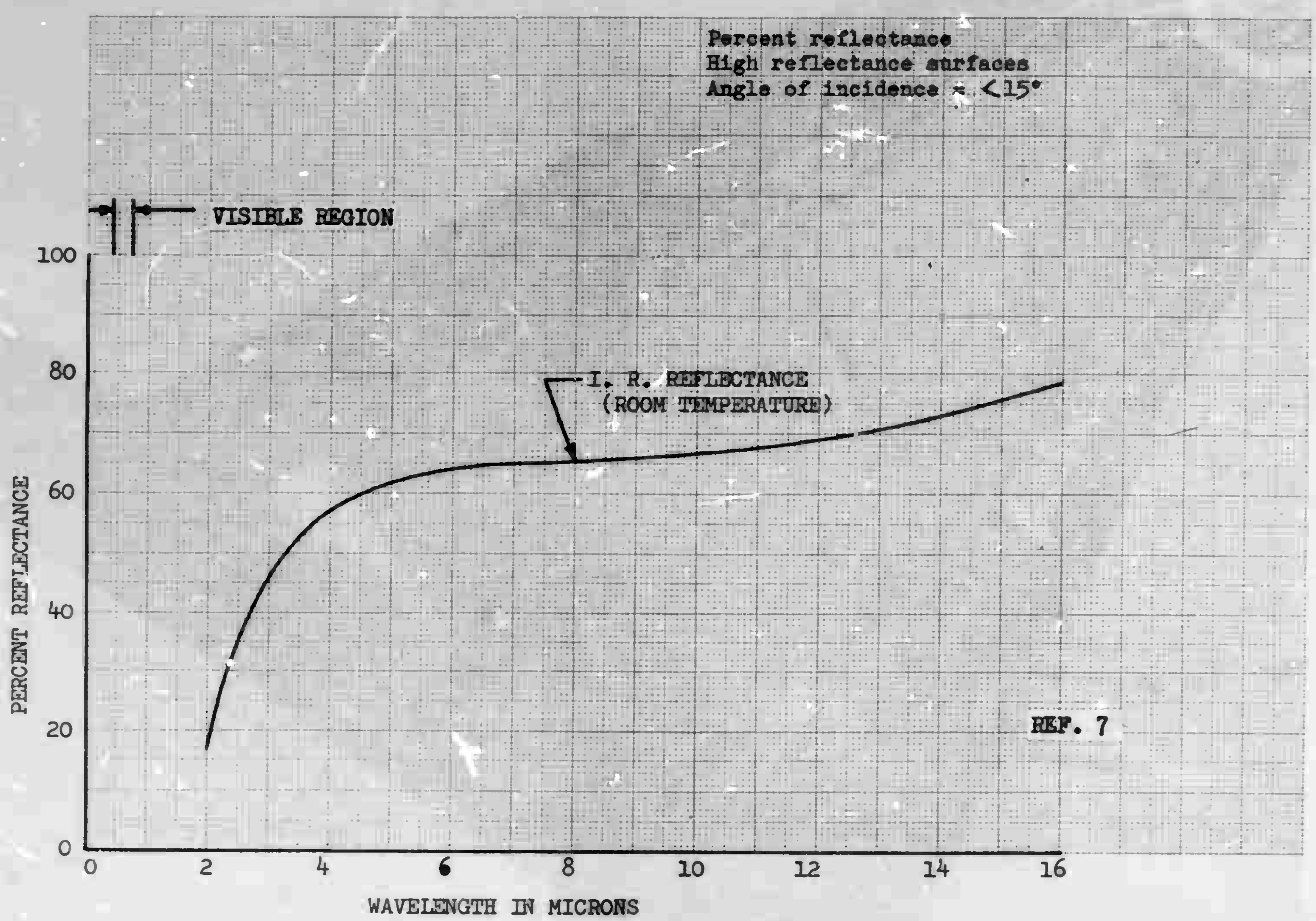

2.3 THERMISTORS (Continued)

Thermistors (a contraction of thermally sensitive resistors) are electrical circuit elements formed of solid semiconducting materials which are characterized by a high negative coefficient of resistivity. Their use for temperature measurement is based on the direct or indirect determination of the resistance of a thermistor immersed in the environment whose temperature is to be measured. Thermistors are quite stable where they are properly aged before use (less than .1% drift in resistance per month—according to most data). Thermistors exhibit great temperature sensitivity (up to 10 times the sensitivity of the usual base-metal thermocouples) while thermistor response can be in the order of milliseconds. Accuracies of 0.1°F are not unusual. However, the current through the thermistor must be limited to a value which does not increase its temperature by resistant (I^2R) heating.

A program was initiated under Air Force Contract AF 33(657)8922 to improve upon existing surface temperature measurements of transparent materials applicable to aircraft glazing. The initial investigation was to develop a thermistor bolometer using high resistance tin oxide films doped with materials that give a high negative temperature coefficient. These films were successful for a high T.C. but became unstable for a temperature range above 500°F which is of primary concern on research aircraft. At this point effort was shifted to a noble metal bolometer.

The Boeing Company Experimental Laboratories had conducted tests on thin film type heat sensors for use in the hot-shot and shock tunnels. Such films as tungsten, and tantalum applied to quartz have been tested. A sample of a silicon-platinum sensor using gold thin film leads installed on fused silica was received from the Corning Glass Works. It was evaluated by the Experimental Laboratories and found to measure temperatures with accuracy.

The bolometer made for special application by Corning Glass Works is a platinum pattern, silk screened on the glass surface and fired in a temperature in excess of 1200°F. The thin film gold leads as well as the silicon-platinum sensor are applied in the form of a paste by a silk screen method. The platinum sensor is fired on first, followed by the gold leads. During the firing processes the platinum sensor and the gold leads are cohesion bonded to the fused silica. The actual firing temperature depends to a large extent on the end use and the glass substrate.

Since the material used is a relatively thin film the actual resistance of the bolometer depends on the number of squares being used. (A square = $\frac{\text{length}}{\text{width}}$.) Platinum generally will have a resistivity of 10 ohms/square.

Calibration has shown the bolometer to be completely stable to 1400°F on Vycor or fused silica. The resistance/temperature curve is a straight line between 0°F and 1400°F. The temperature coefficient in parts/million is 1200 ($\frac{\Delta R}{R_x \Delta T}$ x 10^6). Gold film used for leads to the sensors have been very successful.

2.3 THERMISTORS (Continued)

A sensor of this type had been used on the X-15 and reached temperatures of 1700°F+.

One point to remember is that high heat flux on external sensors is shorted out by ionized gases at high temperatures—effectively a parallel conductor.

These sensors have been compared against platinum disc type sensors and with various radiation blocking devices. The thermistors are intimately in contact with the glass and do not promote any stress risers to weaken the surface of the glass. They stay on as long as the glass retains its integrity. The thermistors are not adversely affected by optical glass cleaning methods but can be damaged by abrasion.

A total of eight (8) thermistors are used to measure the glass temperature. Six thermistors are located on the inside and outside surfaces of each glass pane. The remaining two are located on the exterior surface of the external glass pane, and the internal surface of the internal glass pane. Figure 17 on page 27 shows the location of all thermistors.

The gold thermistor leads are .002 inch thick and are parallel to each other. They lead to the edge of the glass in the same direction for each pane. The leads are terminated at the edge of the glass by forming 1/4 inch by 1/4 inch square gold contact patches.

An external electrical connection is made using a .010 diameter gold wire as a lead through the window frame. The end of the .010 diameter gold wire is flattened to a thickness of .001 to .002. The flattened end is thermo-compression bonded (spotwelded) to the thermistor lead at the edge of the glass using a layer of .001 gold foil superimposed. This bonded connection then has a one square inch refrasil tape pad, .010 inch thick, impregnated and tapered out with "Ecco-ceram" compound to act as an electrical insulator. See photograph on page 11. The gold wire is insulated with refrasil tubing except for the leads of the outer pane which must be sealed. At this location 1 mm quartz tubing is used for sealing purposes. Expansion loops are provided. The photograph on page 11 shows the thermistor lead wires. This installation was expected to withstand the vibration and heat environment without failure due to the malleable characteristics of the gold wire with adequate expansion loops provided.

The photograph on page 9 shows one thermistor lead wire after the spotwelded connection was made while the other lead has "Ecco-ceram" compound applied over the connection. The photograph on page 10 shows a close-up view after the same operations have been completed. Figures 6&7 pages 11&12 shows how the thermistor lead wires were routed through the window frame and seals. Only four lead connections occurred at the same location, however.

FIGURE 4 Thermistor Application

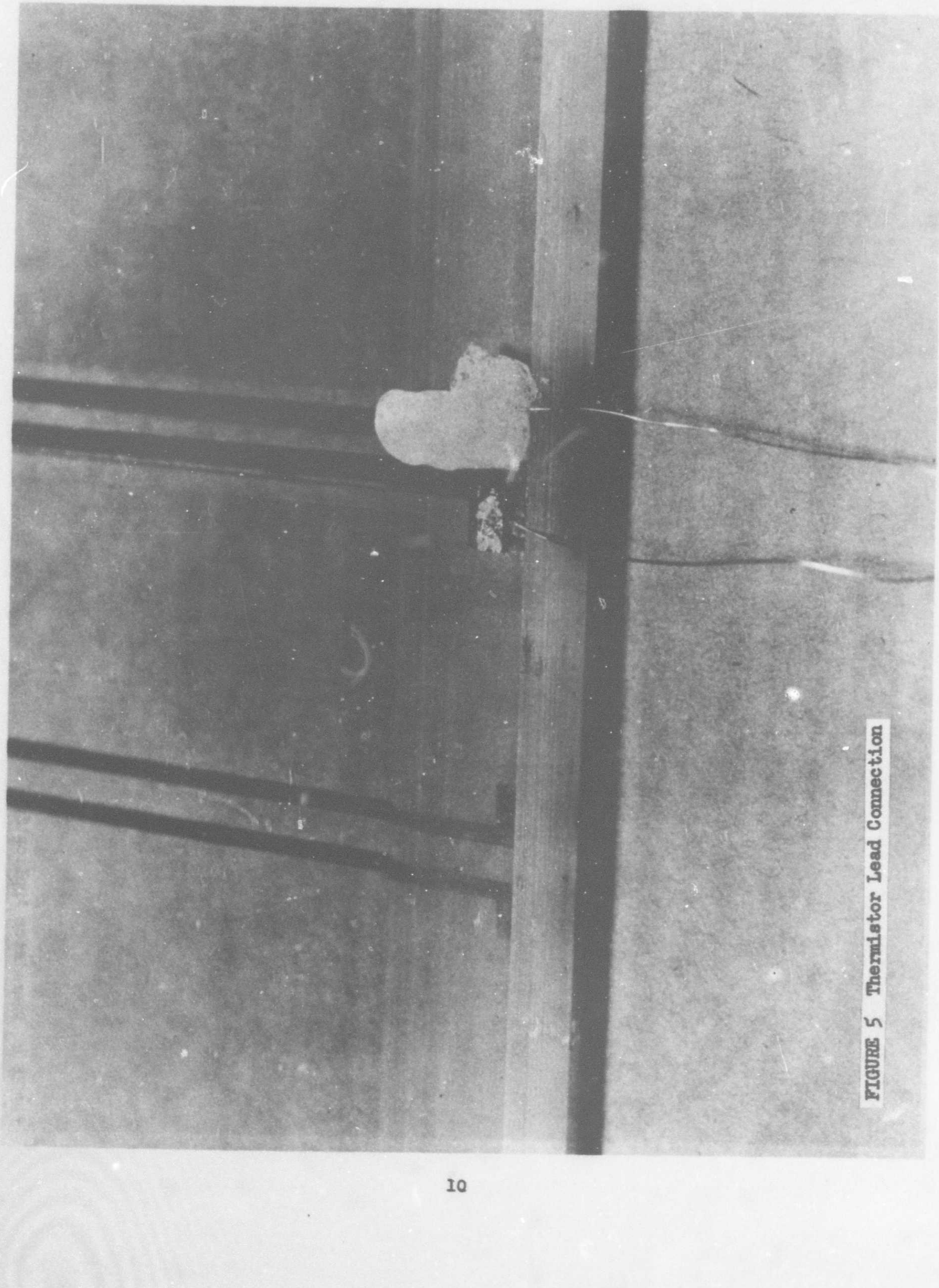

FIGURE 5 Thermistor Lead Connection

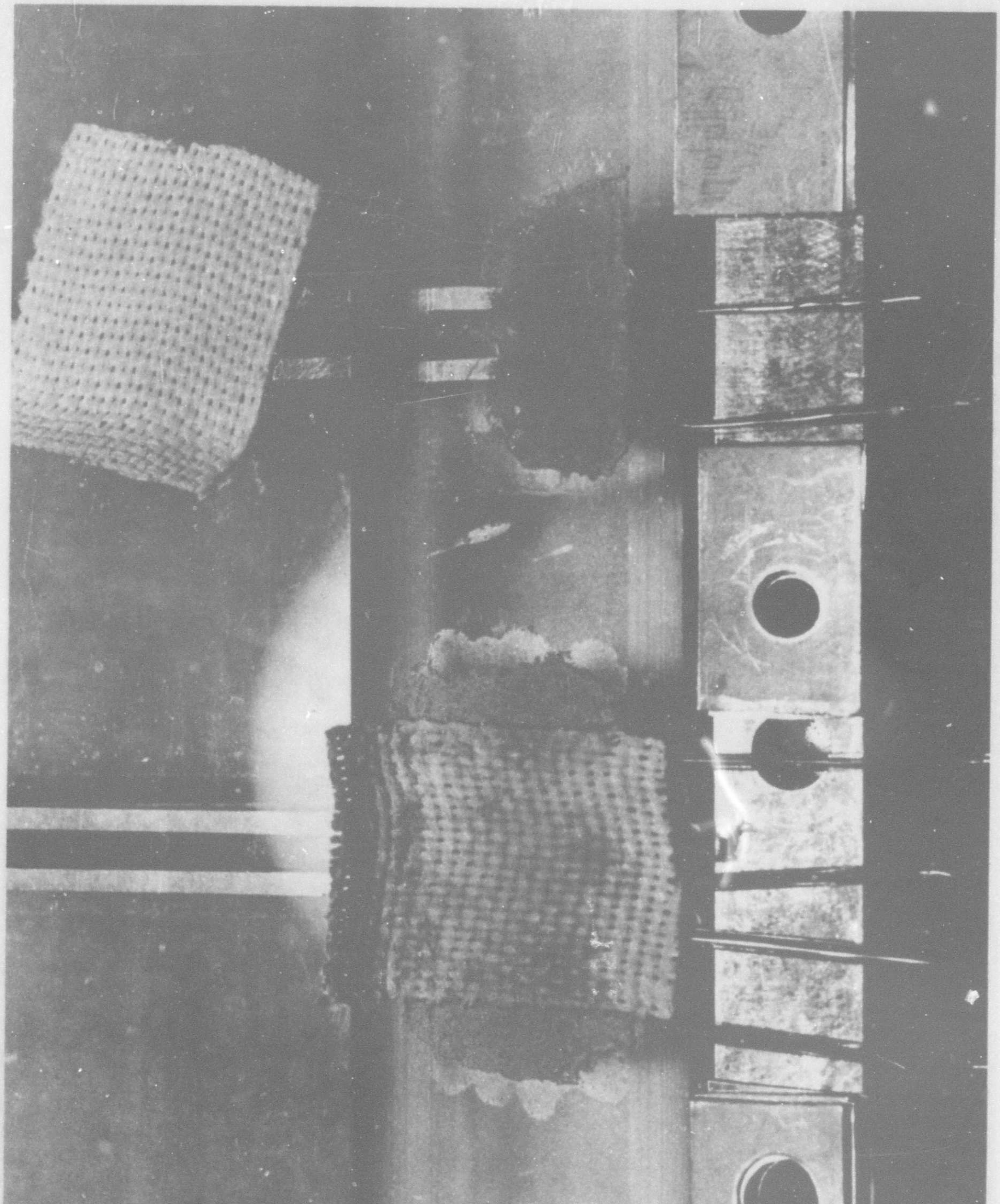

FIGURE 6 THERMISTOR LEAD INSULATION AND ROUTING

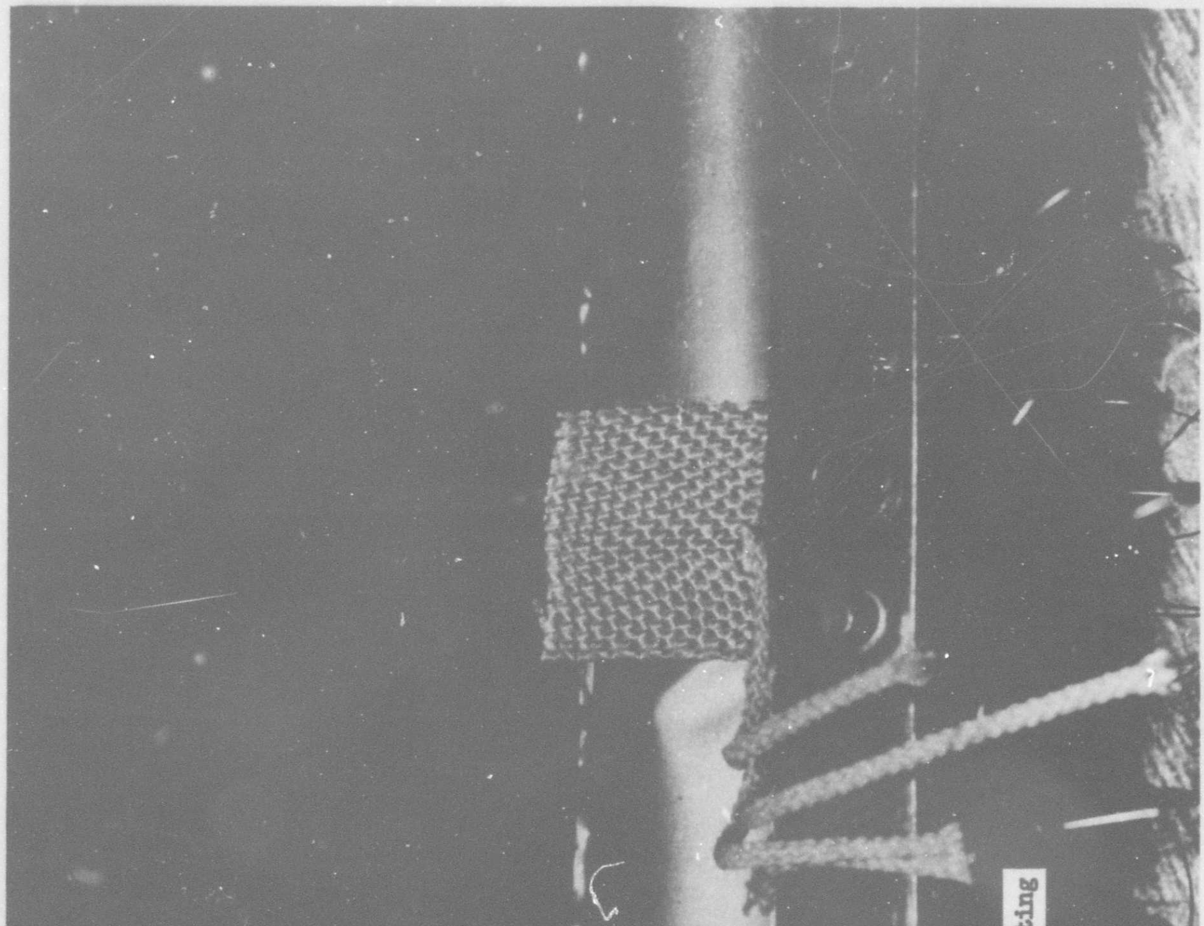

FIGURE 7 Thermistor Lead Insulation And Routing

2.4 WINDOW FRAME

The glass panes are supported by a Rene' 41 multi-layered retaining frame. The edges of the panes are clamped between protruding layers of the retaining frame, see page 15. The upper portion of the frame is a continuous rectangular ring section .50-inch wide by .625-inch fabricated from Rene' 41. The lower frame portion is a rectangular section .50-inch wide by .724-inch. The lower portion of the frame is removed at the intersection of the three bearing blocks. The bearing blocks splice this portion of the frame that is removed. The two frame halves are counterbored and riveted together with 3/16 inch diameter Rene' rivets as shown on page 14. This riveting process provides shear continuity between the frame members and also ties in the inner two seals, leaf spring and center backup strip. The outer fairing and inner backup strip are continuous members and are considered as effective frame material.

2.5 WINDOW SEALS

The seals are made of a Hastelloy-X wire matrix manufactured by Johns-Manville and enclosed in a wrapping of Hastelloy-X foil which is .002 inch thick. All seals are made from the same size oval-shaped Hastelloy-X wire mesh. The outer seal is made with a continuous covering to act as a seal plane to restrict the flow of hot gas plasma into the fuselage cavity. All seals are wrapped in a jacket that is .80 inch wide except the seal that is between the two .18 inch thick inner glass panes. This seal has a jacket width that is .60 inch wide to give a greater window spacing between these glasses to assure adequate clearance during out of phase vibrations. The seals are approximately .21 inch to .25 inch thick in the uncompressed position. The seals offer a cushion for the glass panes as they are clamped between the layers of the window frame. Tests were run on the window seal configuration to obtain their spring rate and the stress relaxation at high temperature. This information is presented in the Appendix on page 181. A photograph showing the complete seals is shown on page 17. Figures 11 and 12 show positioning of the metallic window seals during assembly.

2.6 WINDOW SPRINGS

Rene' 41 leaf springs are installed in series with the seals. These springs eliminate the slack in the seal system which results from installation tolerances and relative motion and relaxation in the assembly when subjected to heat and load. These springs provide clamping forces after exposure to the maximum temperature environment and allow the window to withstand re-entry and approach vibrations. Two sets of the leaf springs are used. They are fabricated from 5 layers of .008 Rene' 41 material. The maximum spring travel is .04 inch. The leaf springs flatten to an overall thickness of .05 inch under a loading of 35 pounds per running inch. The leaf springs exhibit a spring constant of 875 pounds/in per inch of length at room temperature. The seals are nominally clamped up at 35 pounds per lineal inch at room temperature. Under the "hot" environment the springs retain a clamped up pressure of approximately 8 pounds per lineal inch of periphery in the window assembly.

FIGURE 8 WINDOW AND FRAME ASSEMBLY - Nomenclature

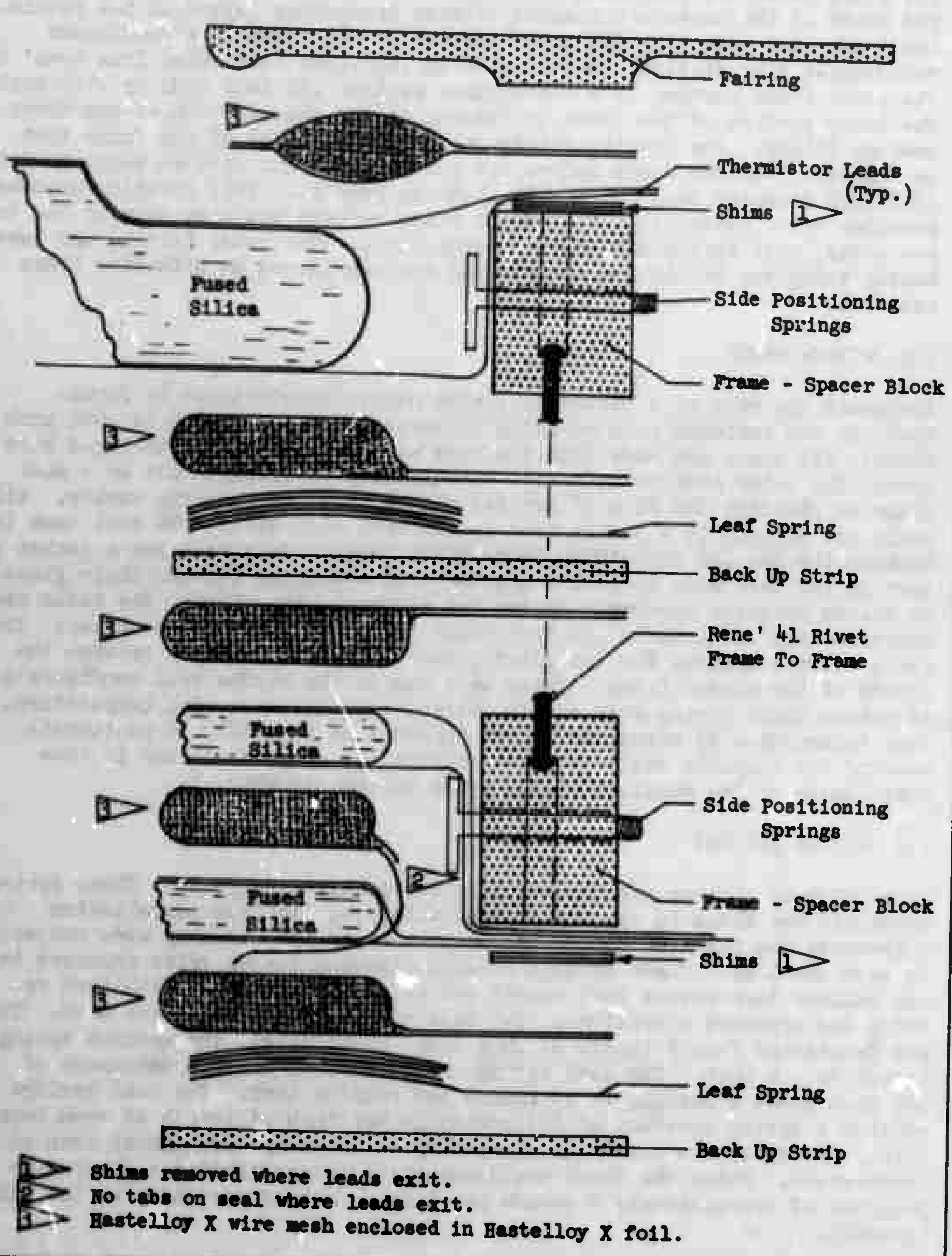

FIGURE 9 WINDOW AND FRAME ASSEMBLY - Dimensions

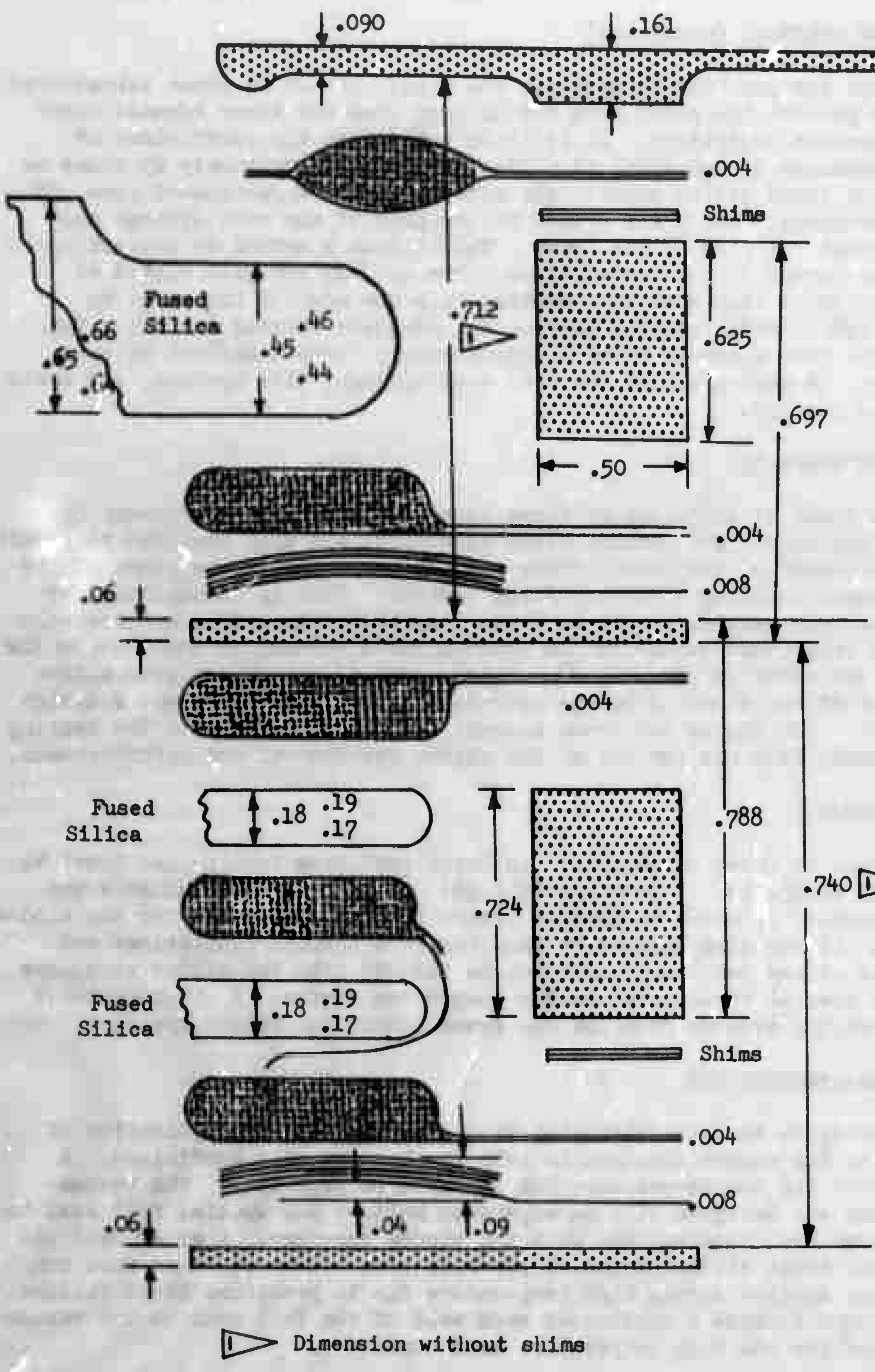

2.6 WINDOW SPRINGS (Continued)

Side springs are provided to position the glass, absorb in plane vibrational loads, and prevent the glass from coming free when the frame expands under high temperature conditions. It is to be noted that the coefficient of thermal expansion of the Rene' 41 window frame is approximately 25 times as great as the fused silica glass. The side springs are fabricated from .05 Rene' 41 material. Studs are welded to the peak of the side springs and extend through the side of the frame. This allows a method of retracting the springs during window installation. The springs are gold plated at their peaks where they come into contact with the edge of the glass to provide a low friction sliding surface and adequate bearing surface. The side springs have a spring rate of approximately 720 pounds/inch at room temperature. A photograph of the leaf seal springs, side springs, and seals is shown on page 17.

2.7 WINDOW SUPPORTS

The window frame is supported at three locations around its periphery by spherical bearings. The bearing block assemblies are also designed to permit relative movement of the window frame and the cab frame in the plane of the window without inducing redundant force systems. This is accomplished by allowing certain bearing shafts to slide longitudinally and/or transversely in the cab frame. Photographs of the bearing block assemblies attached to the cab frame are shown on pages 20-22. This method of attachment also allows for removal of the window from the outside of the glider which was a design requirement. The window and frame assembly can be unbolted from the bearing block assembly from the outside of the glider for removal and refurbishment.

2.8 CAB FRAME

The cab frame as shown on page 20 is fabricated from rectangular Rene' 41 tubing (2.5 inches by 1.0 inch by .09 inch). The cab frame simulates the glider structure in order to provide proper support conditions for the window structure. It was also desired to show that the thermal elongations and distortions of the cab frame would not be induced into the window structure due to the special three-point window suspension system. A .05 inch thick Rene' 41 fairing extends from the cab frame around the window specimen.

2.9 VACUUM-PRESSURE BOX

A vacuum-pressure box was fabricated from Rene' 41 for the application of air loads to the window specimen in both the hot and cold conditions. A photograph of the vacuum-pressure box is shown on page 23. The vacuum-pressure box was designed with an expansion bellows and special foil seal to prevent structural interactions with the window specimen. A mylar seal was used for the boost airload negative pressure test. No conditions were run with airload applied during high temperature due to premature glass failure. It was planned to make a continuous seam weld of the foil seal to the vacuum-pressure box for the high temperature load condition.

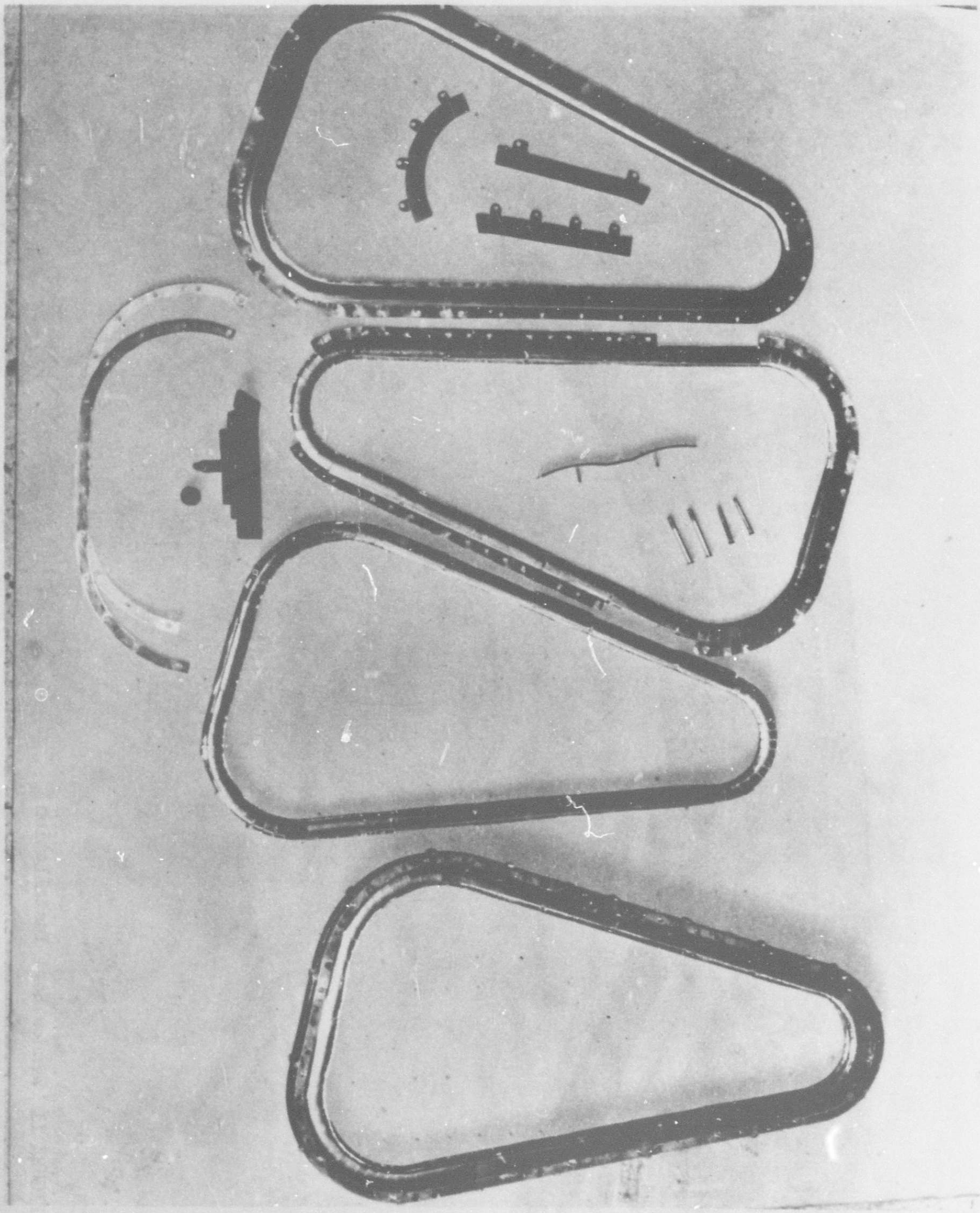

FIGURE 10 WINDOW SEALS AND SPRINGS

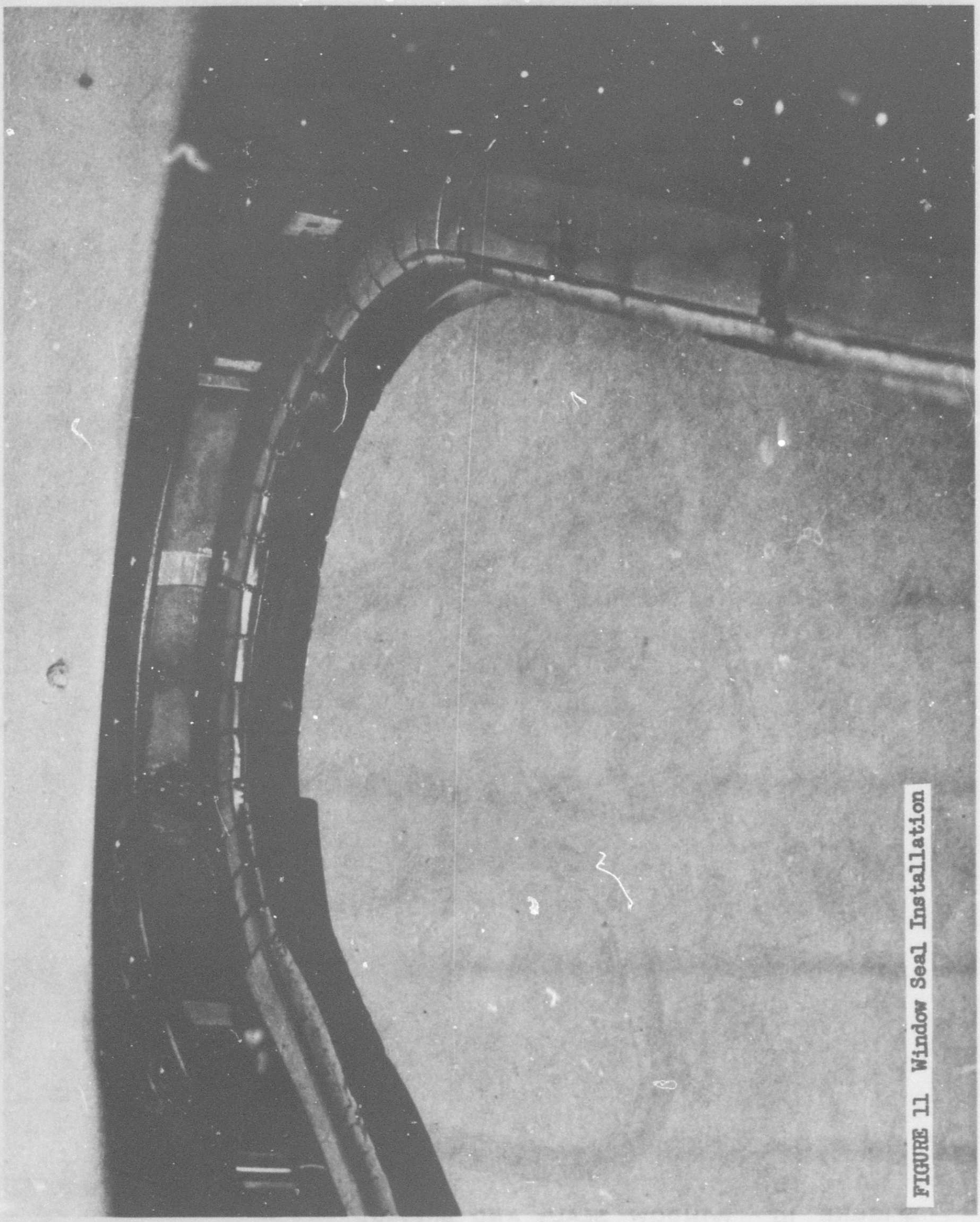

FIGURE 11 Window Seal Installation

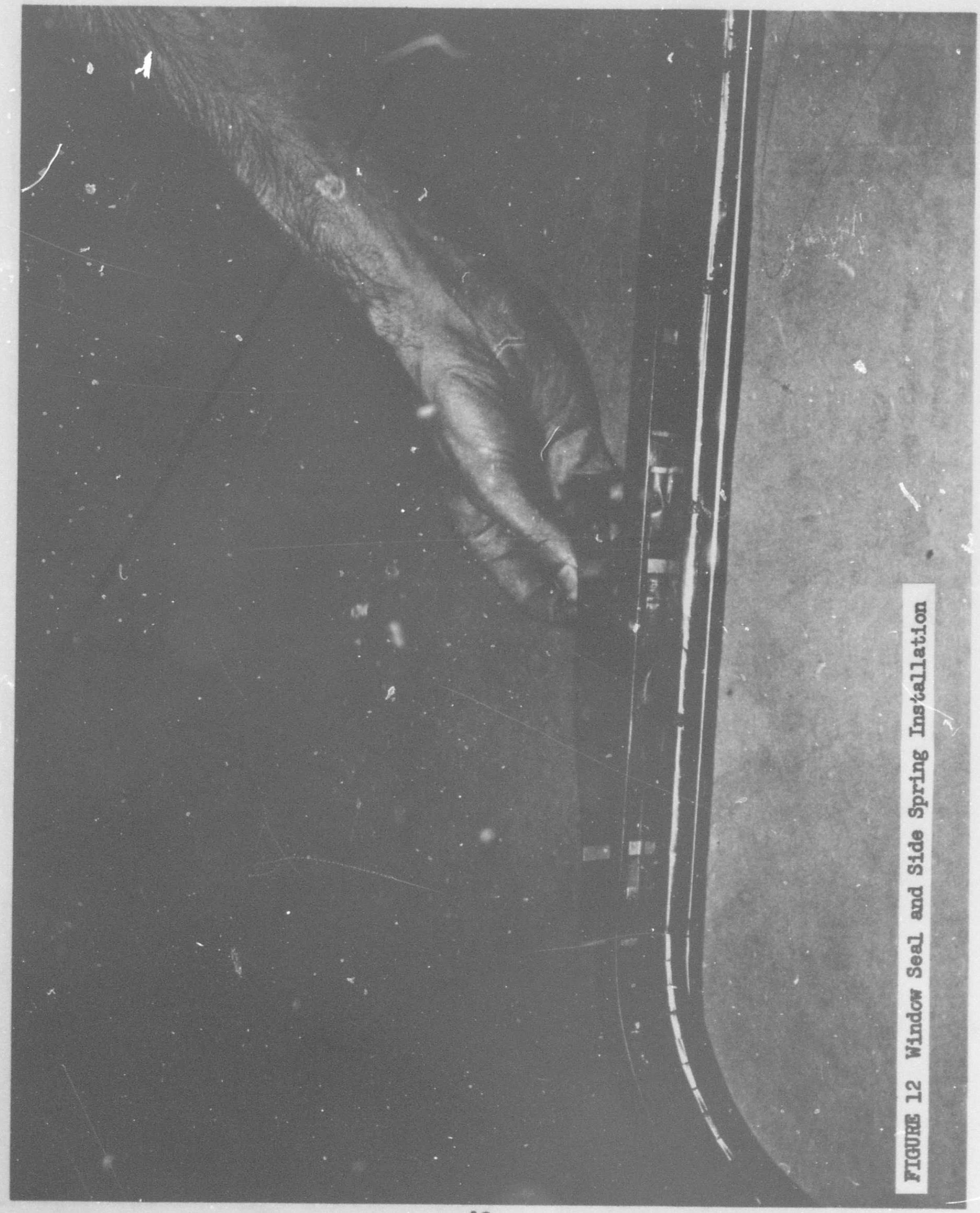

FIGURE 12 Window Seal and Side Spring Installation

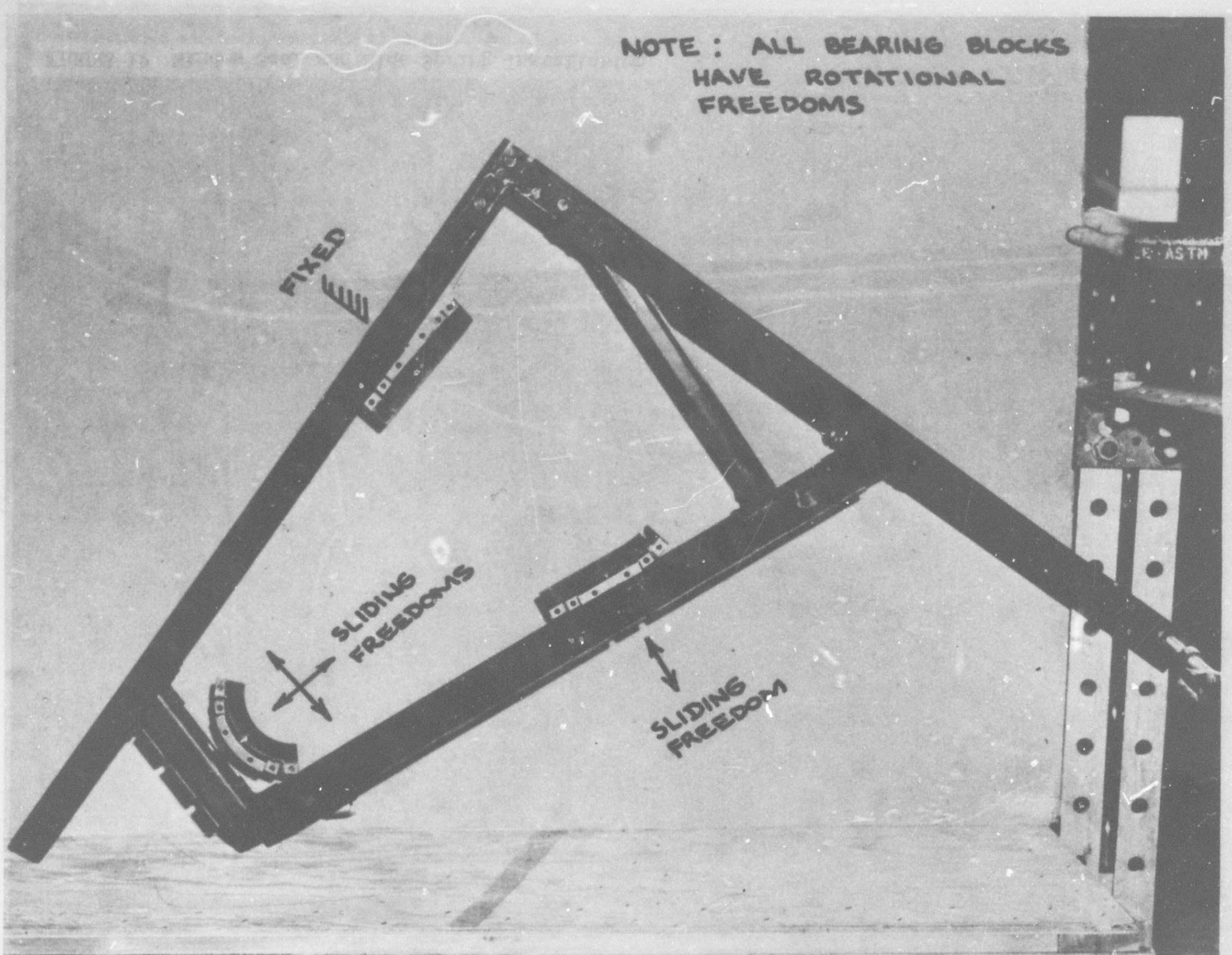

FIGURE 13 Cab Frame and Window Support

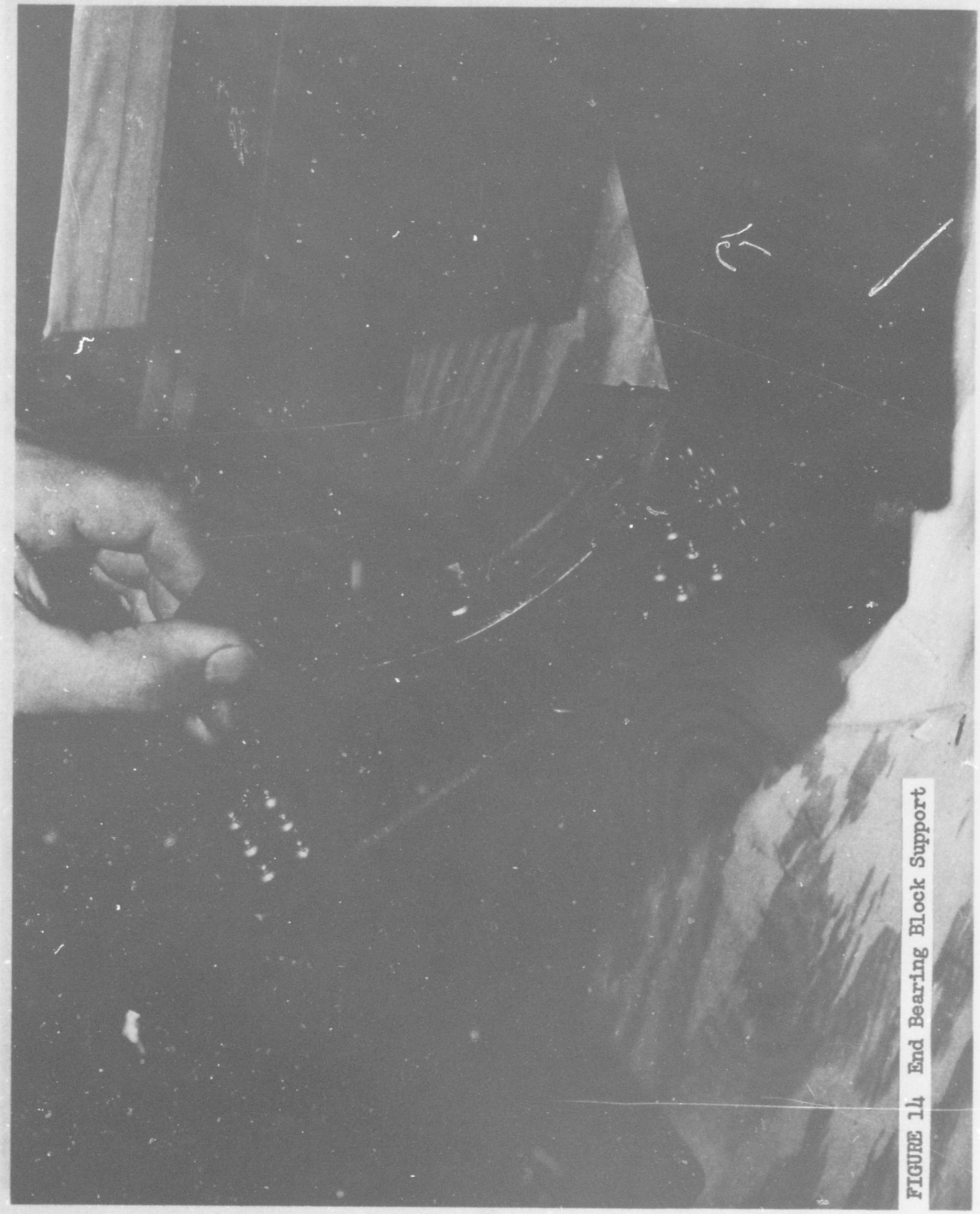

FIGURE 14 End Bearing Block Support

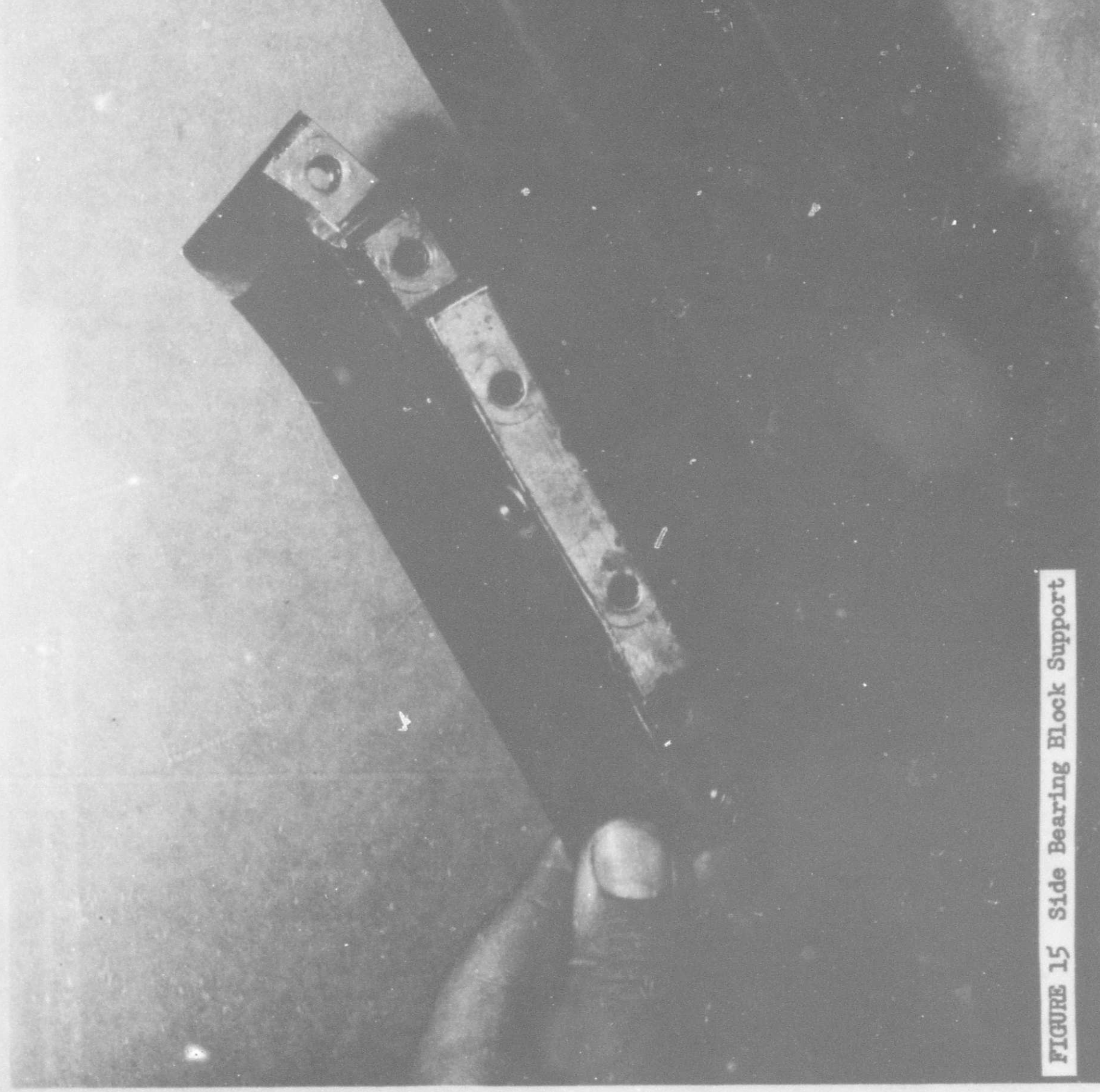

FIGURE 15 Side Bearing Block Support

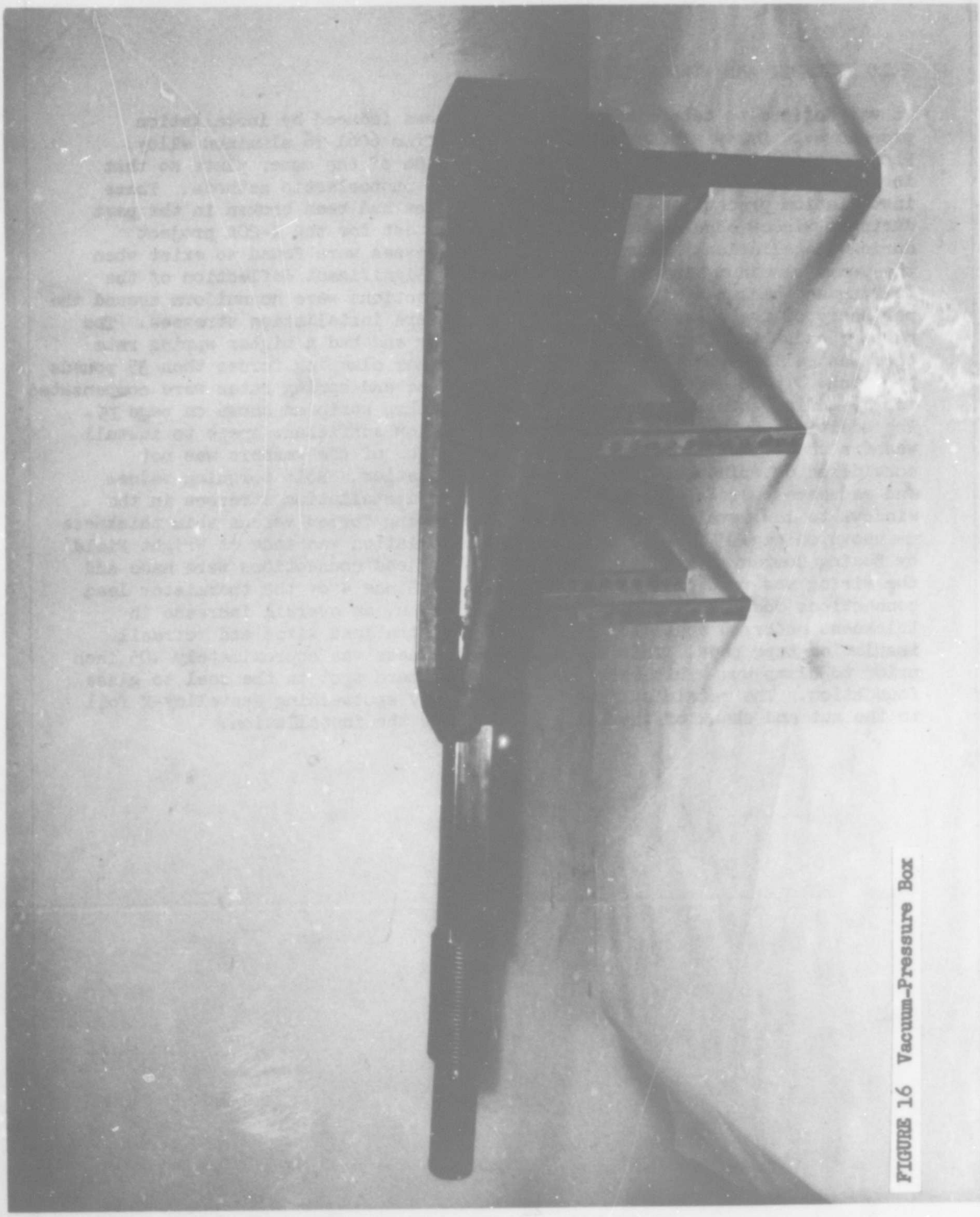

FIGURE 16 Vacuum-Pressure Box

2.10 ASSEMBLY AND WINDOW INSTALLATION

It was desired to determine the glass stresses induced by installation procedures. Dummy windows were fabricated from 6061-T6 aluminum alloy. Photoelastic plastic was bonded to the outside of the outer plate so that installation stresses could be determined by photoelastic methods. These installation precautions were taken as a glass had been broken in the past during a window edge attachment development test for the X-20A project during installation. Large installation stresses were found to exist when the dummy aluminum windows were installed. Significant deflection of the fairing and backup strip occurred. The deflections were nonuniform around the periphery of the glass which lead to the severe installation stresses. The primary cause was that the seals were thicker and had a higher spring rate than was called for by the design giving higher clamping forces than 35 pounds per inch. These differences in seal thickness and spring rates were compensated for by adding shims under the fairing and backup strip as shown on page 15. The addition of the shims however did not allow sufficient space to install washers under the retaining nuts. The deletion of the washers was not considered deterimental to the window installation. Bolt torquing values and sequences were established to reduce the installation stresses in the windows to low levels. Calculations of clamping forces versus shim thickness are shown on page 191. The final glass installation was made at Wright Field by Boeing Company personnel. The thermistor lead connections were made and the wiring was routed as shown on page 14. Since 4 of the thermistor lead connections occurred at the same frame location, an overall increase in thickness occurred equal to the thickness of the lead wires and refrasil insulation tape pads. This increase in thickness was approximately .05 inch prior to clamp up. This resulted in a small hard spot in the seal to glass foundation. The retaining nuts were locked by spotwelding Hastelloy-X foil to the nut and shank of the bolts to complete the installation.

3 INSTRUMENTATION

Instrumentation of the test specimen and supporting test fixtures includes accelerometers, thermistors, thermocouples, deflection gages, pressure gage, and flowmeters. A detailed description of instrumentation and its location follows:

3.1 ACCELEROMETERS

Accelerometers were of the crystal piezoelectric type. Control accelerometers were installed rigidly to the specimen. Glass accelerometers were installed with double-backed tape. Locations of the accelerometers are shown on pages 42 and 44.

3.2 THERMISTORS

Thermistors are of the thin film type as described on page 4 . A total of eight thermistors are used to measure the glass temperature. Six thermistors are located on the inside and outside surfaces of each glass pane. The remaining two are located on the exterior surface of the external glass pane, and the internal surface of the internal glass pane. Figure 17 on page 27 shows the locations of all thermistors.

3.3 THERMOCOUPLES

A total of 19 Refrasil-insulated, 22 gage, Type K (chromel-alumel) thermocouples are spotwelded to the Rene' 41 window frame assembly and cab frame as follows: 7 on the window frame outer fairing, 6 on the window frame at the bearings, 2 on the window frame at the inner flanged backup ring, and 4 on the cab frame. See figure 17 page 27 for locations.

These thermocouples are used to establish temperatures and gradients of the window frame and cab frame.

Where possible, the thermal junction was formed by spotwelding the individual thermocouple wires to the specimen parallel to each other and approximately 1/10 inch apart, thereby including a small section of the Rene' 41 specimen in the thermocouple circuit. The ends of the Refrasil insulation wire covers were treated with Synar (trade name for a silica acid solution manufactured by the Pennsylvania Salt Company) to inhibit raveling.

3.4 DEFLECTION GAGES

A total of 24 deflection measurements were made as shown in Figures 17 through 19 pages 27 through 37 for heat and load test conditions. A system employing low thermal expansion quartz rods in conjunction with strain gage-cantilever beam deflection transducer devices was used for all deflection measurements. The deflection transducer devices were manufactured by Structures Branch FDTT at the Flight Dynamics Laboratory.

3.5 PRESSURE GAGE AND FLOWMETER

Pressure and flow measurements for the pressure box test fixture were made using the following equipment: Meriam Laminar Flow Meter Element - Model 50MH10; Meriam Inclined Manometer - Model 40HE 34; Meriam Mercury Pressure Manometer - Model 33BA and Air Temperature Sensor manufactured by the Structures Branch (FDTT).

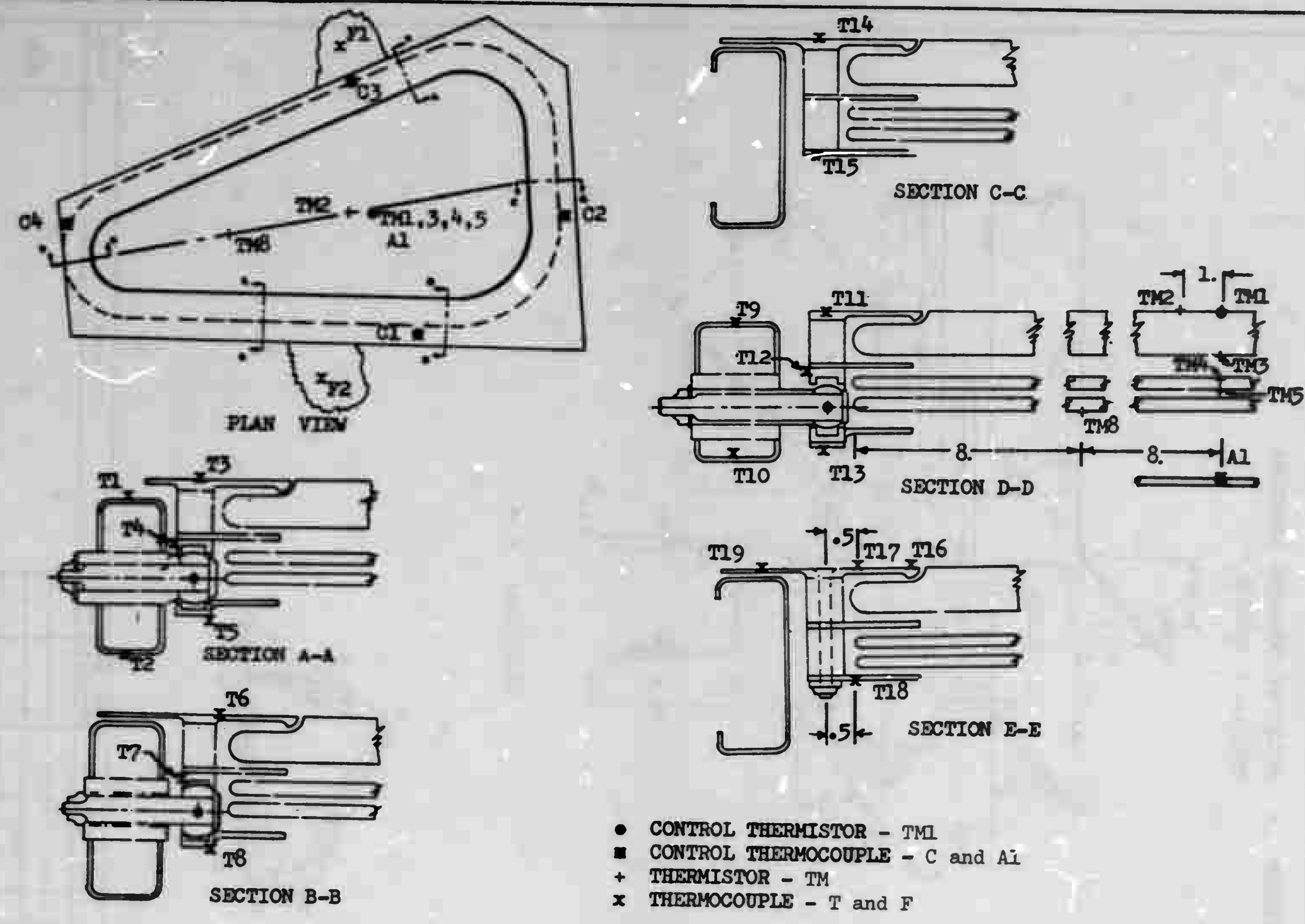

FIGURE 17 THERMISTOR AND THERMOCOUPLE LOCATIONS

FIGURE 18 DEFLECTION INDICATOR LOCATIONS
TEST NO. 2 SECTION A-A

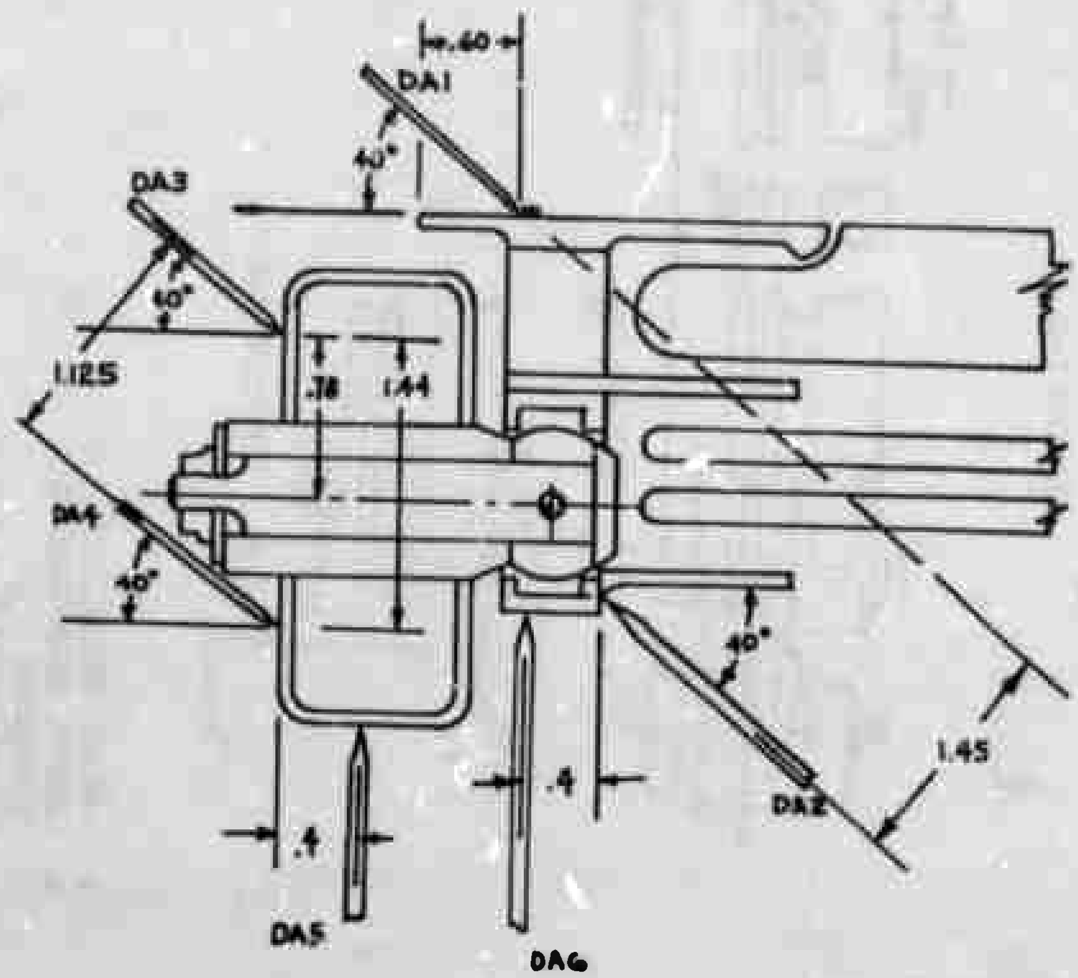

SECTION A-A

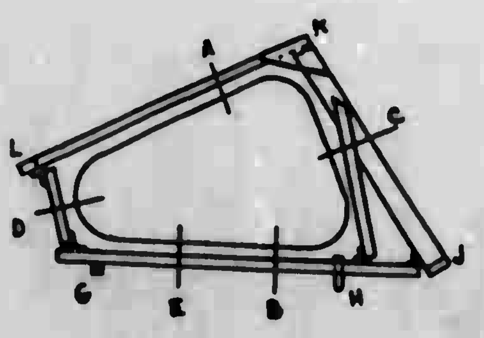

	INITIALS	DATE	REV BY INITIALS	DATE	TITLE	MODEL
CALC						X-20
CHECK						
APPD.						
APPD.						

FIGURE 18 DEFLECTION INDICATOR LOCATIONS TEST NO. 2 SECTION B-B

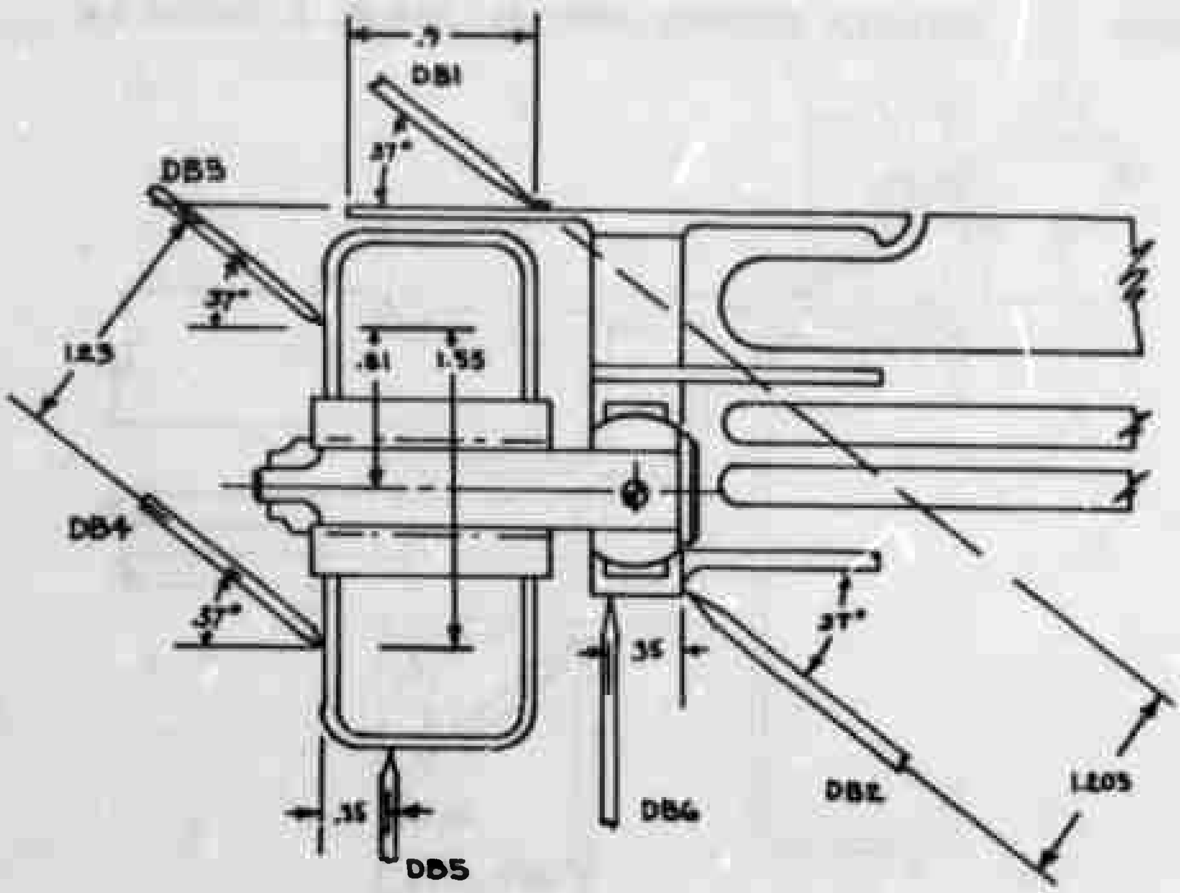

SECTION B-B

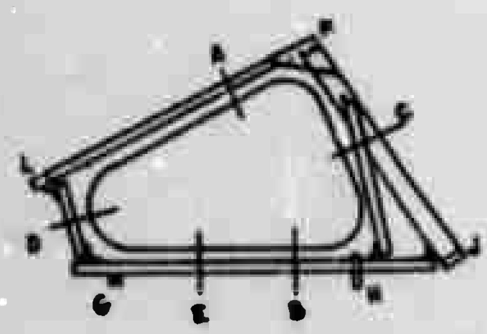

	INITIALS	DATE	REV BY INITIALS	DATE	TITLE	MODEL
CALC						X-20
CHECK						
APPD.						
APPD.						

FIGURE 18 DEFLECTION INDICATOR LOCATIONS TEST NO. 2 SECTION C-C

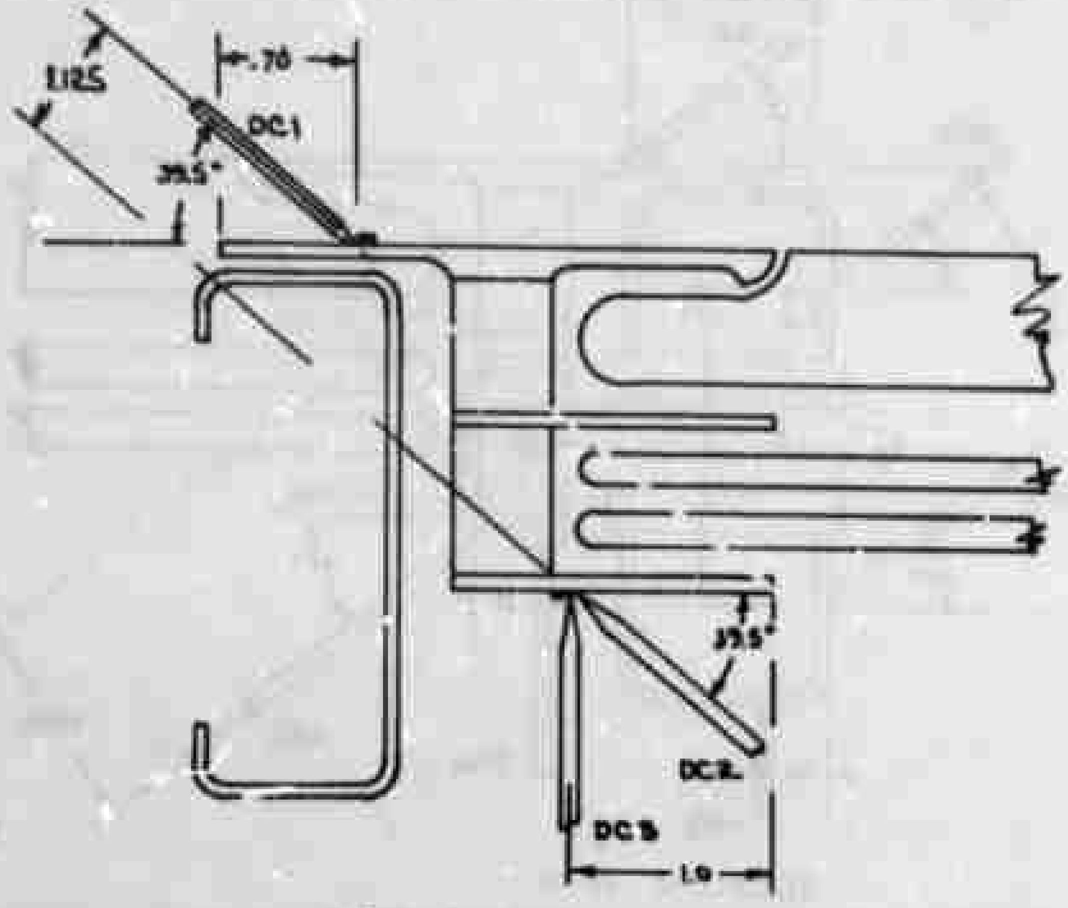

SECTION C-C

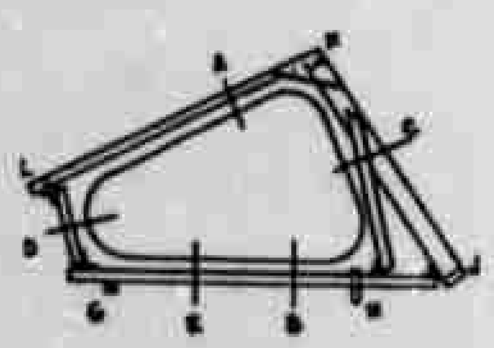

	INITIALS	DATE	REV BY INITIALS	DATE	TITLE	MODEL
CALC						
CHECK						X-20
APPD.						
APPD.						

FIGURE 18 DEFLECTION INDICATOR LOCATIONS TEST NO. 2 SECTION D-D

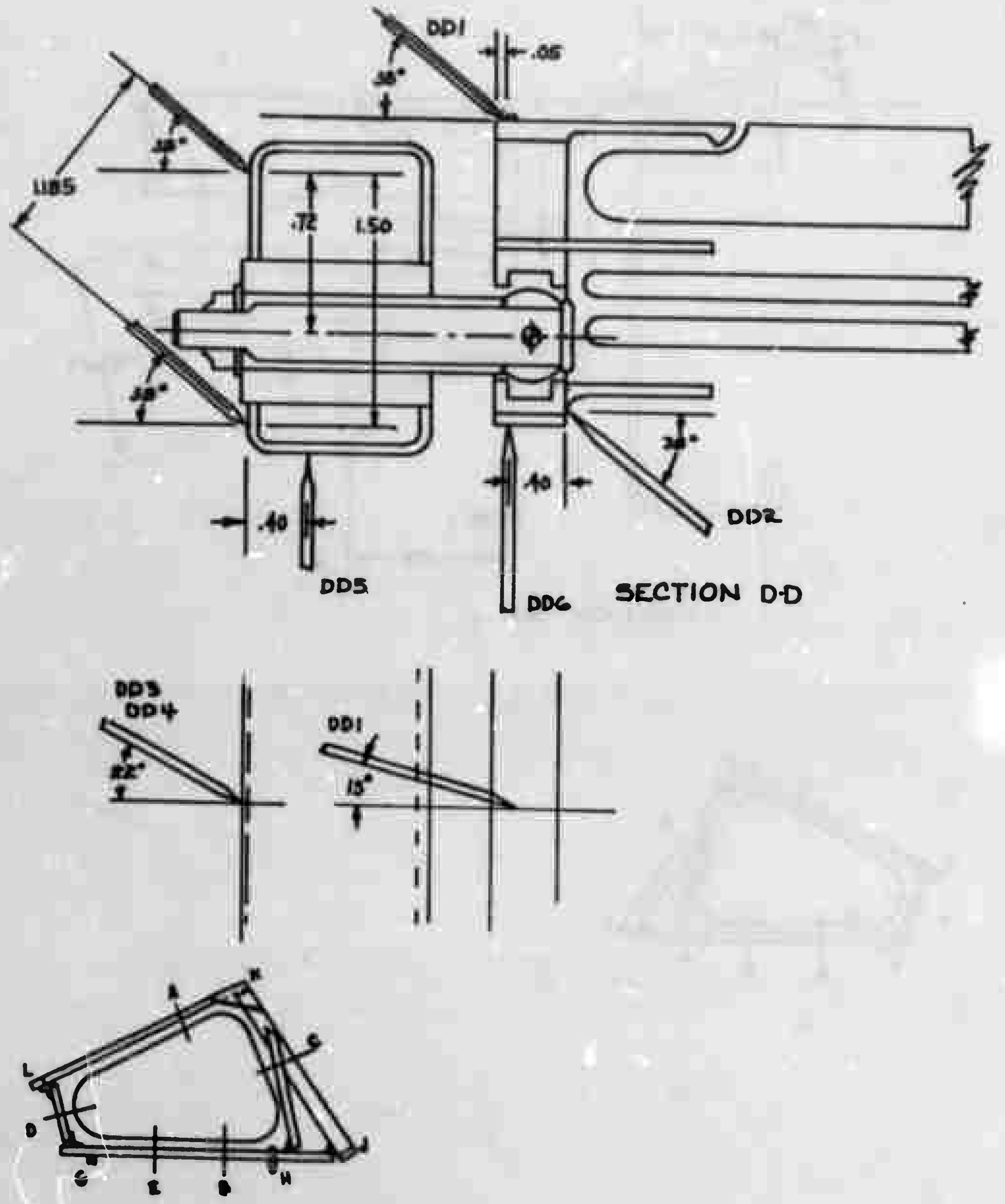

	INITIALS	DATE	REV BY INITIALS	DATE	TITLE	MODEL
CALC						X-20
CHECK						
APPD.						
APPD.						

FIGURE 18 DEFLECTION INDICATOR LOCATIONS TEST NO. 2 SECTION E-E

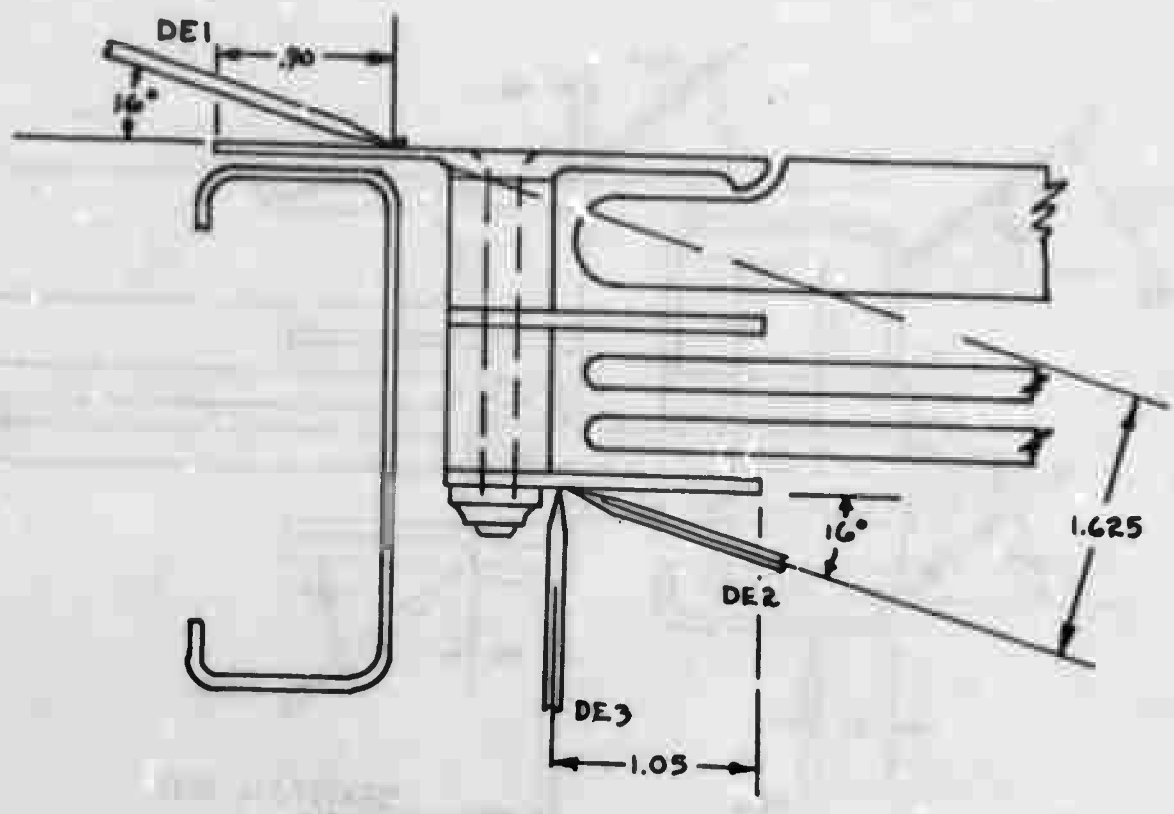

SECTION E-E

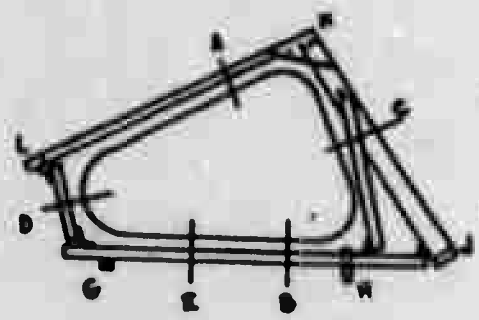

	INITIALS	DATE	REV BY INITIALS	DATE	TITLE	MODEL
CALC						
CHECK						X-20
APPD.						
APPD.						

FIGURE 19 DEFLECTION INDICATOR LOCATIONS TEST NO. 3 SECTION A-A

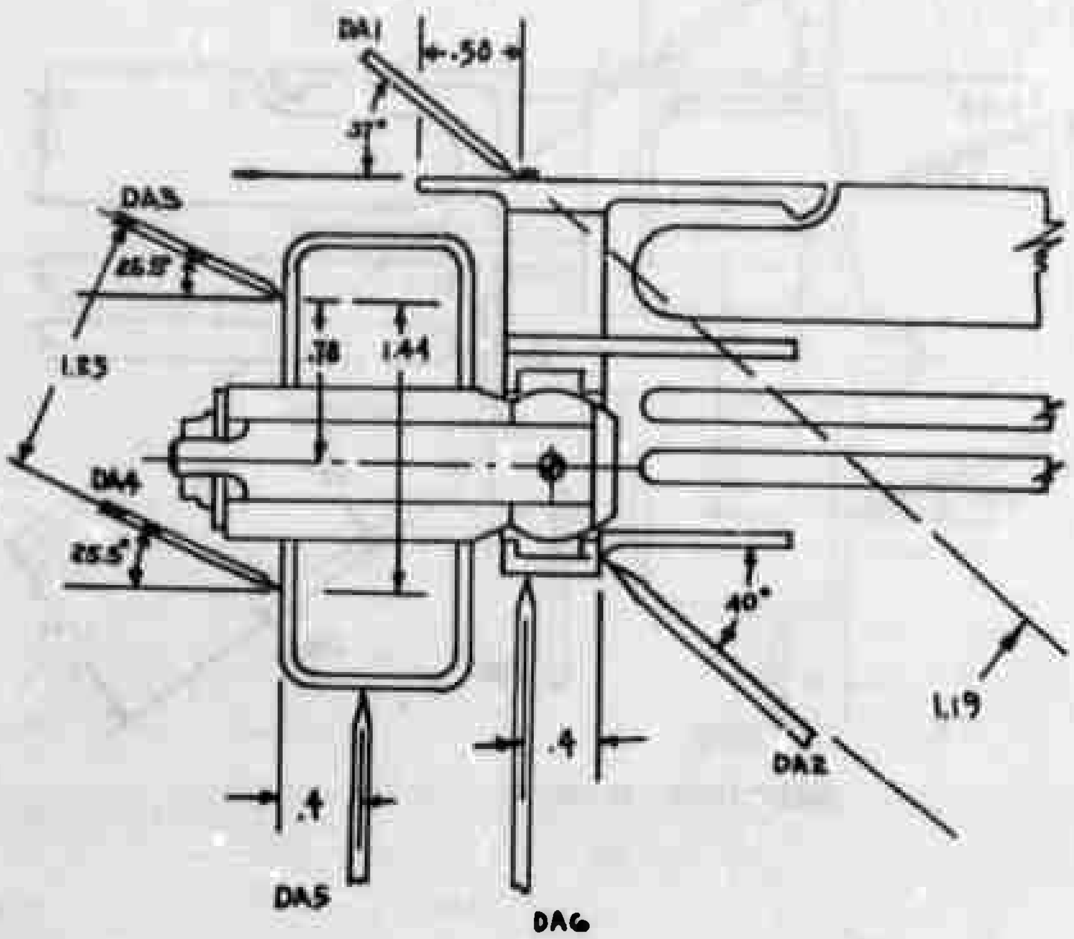

SECTION A-A

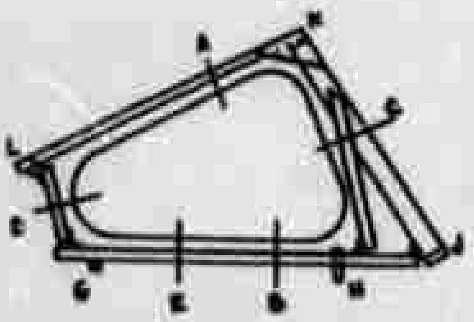

	INITIALS	DATE	REV BY INITIALS	DATE	TITLE	MODEL
CALC						
CHECK						
APPD.						X-20
APPD.						

FIGURE 19 DEFLECTION INDICATOR LOCATIONS TEST NO. 3 SECTION B-B

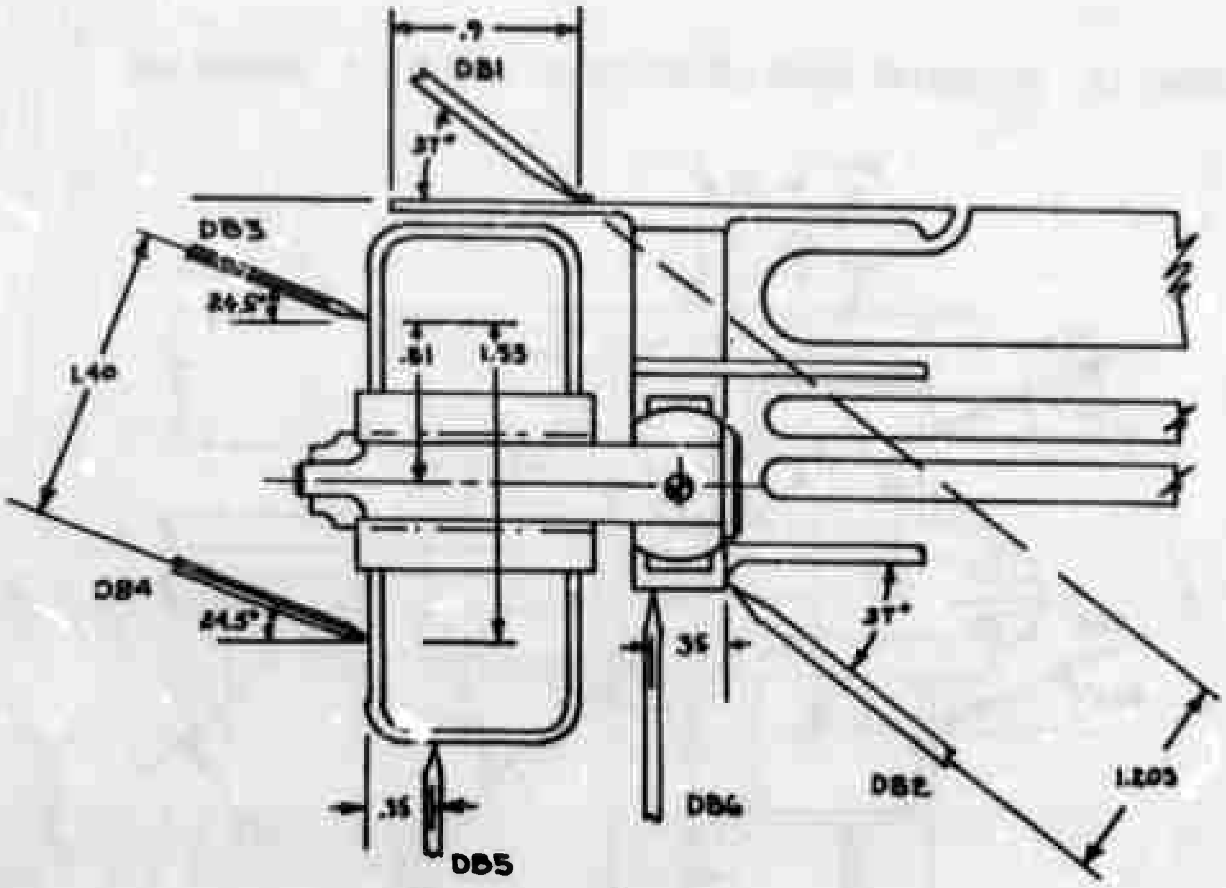

SECTION B-B

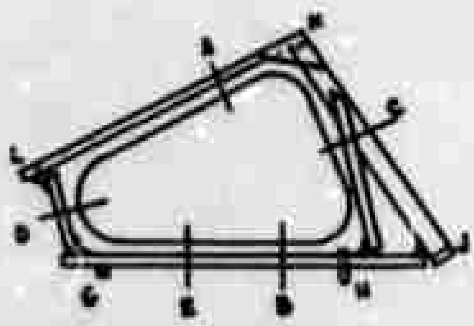

	INITIALS	DATE	REV BY INITIALS	DATE	TITLE	MODEL
CALC						X-20
CHECK						
APPD.						
APPD.						

FIGURE 19 DEFLECTION INDICATOR LOCATIONS TEST NO. 3 SECTION C-C

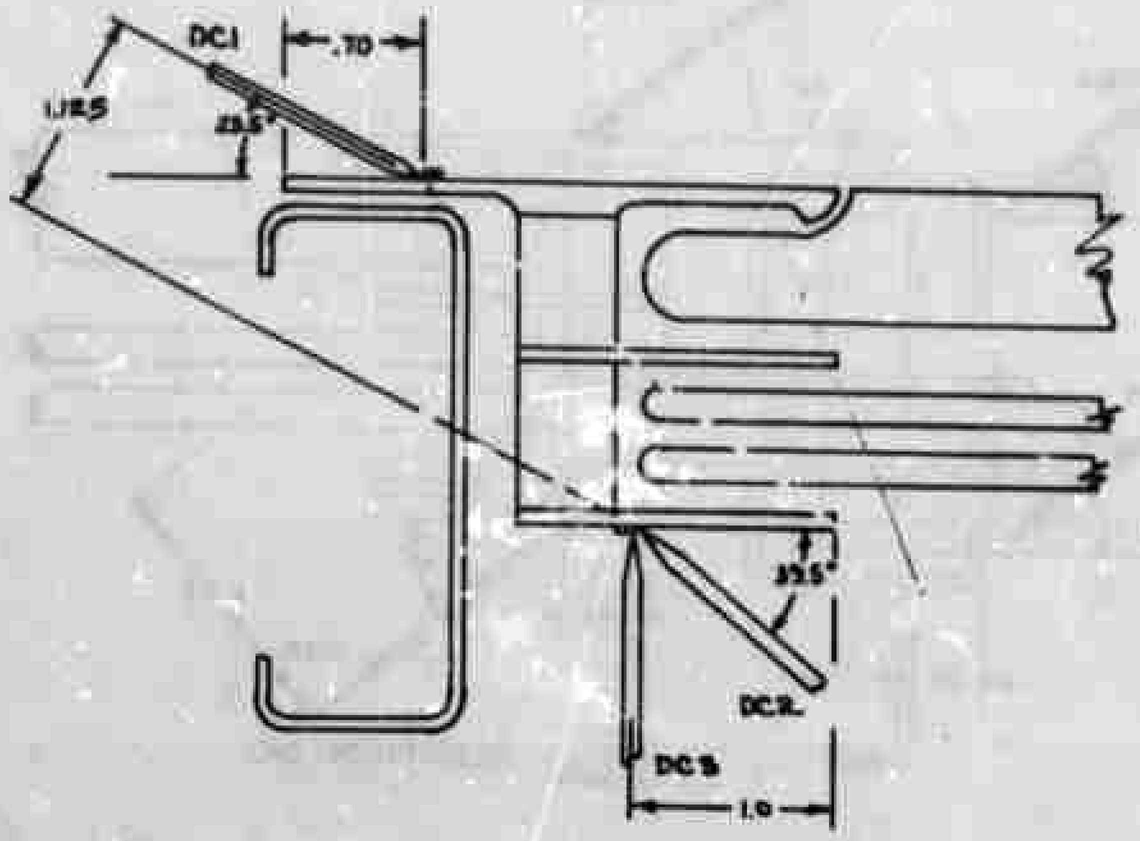

SECTION C-C

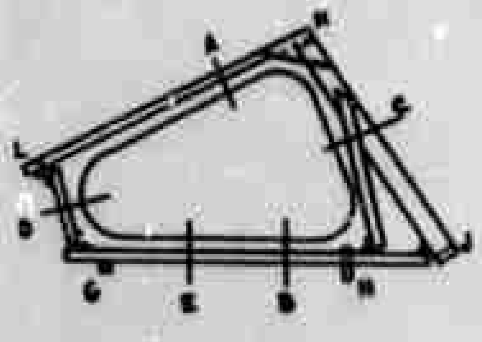

	INITIALS	DATE	REV BY INITIALS	DATE	TITLE	MODEL
CALC						
CHECK						
APPD.						X-20
APPD.						

FIGURE 19 DEFLECTION INDICATOR LOCATIONS TEST NO. 3 SECTION D-D

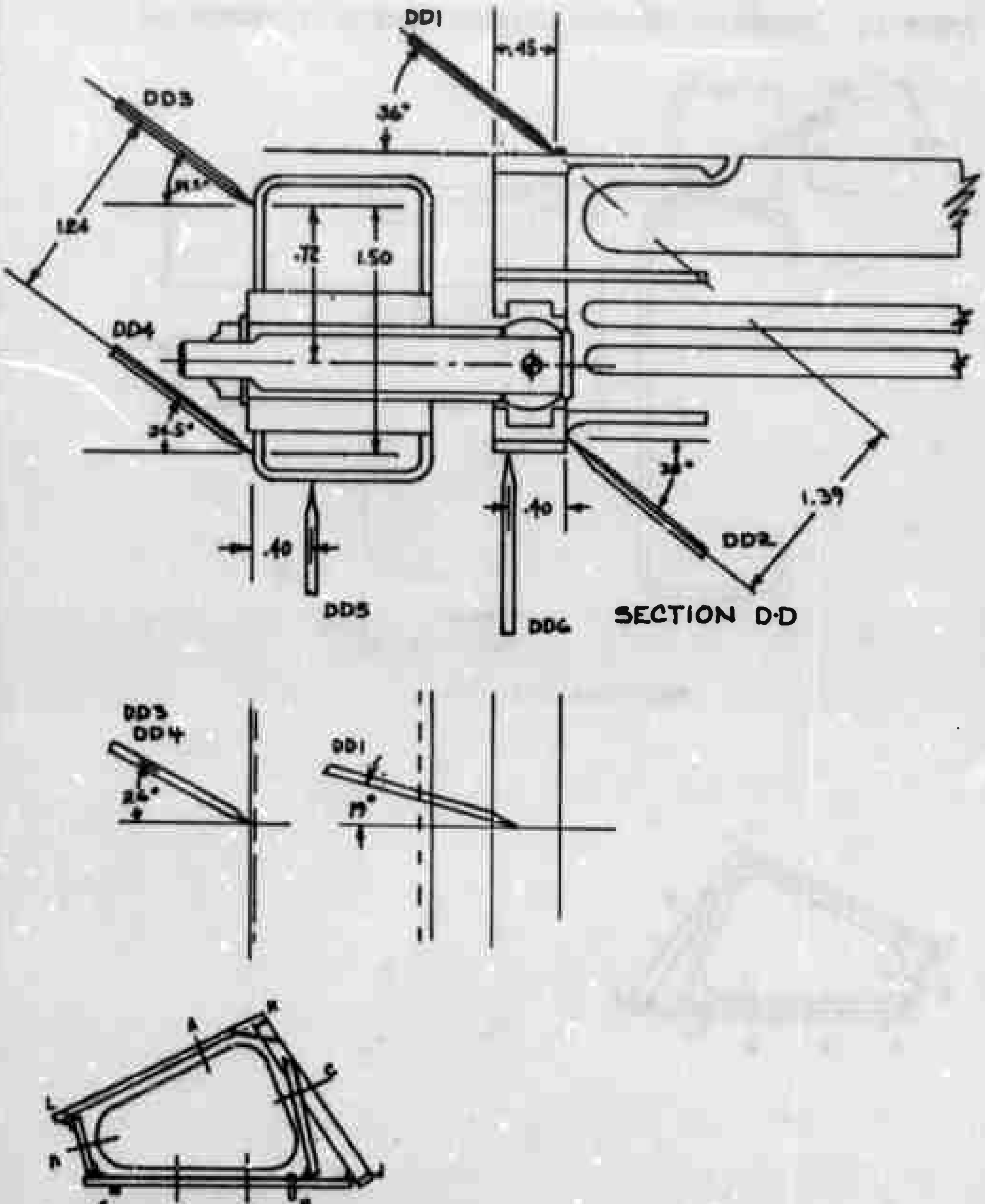

	INITIALS	DATE	REV BY INITIALS	DATE	TITLE	MODEL
CALC						X-20
CHECK						
APPD.						
APPD.						

FIGURE 19 DEFLECTION INDICATOR LOCATIONS TEST NO. 3 SECTION E-E

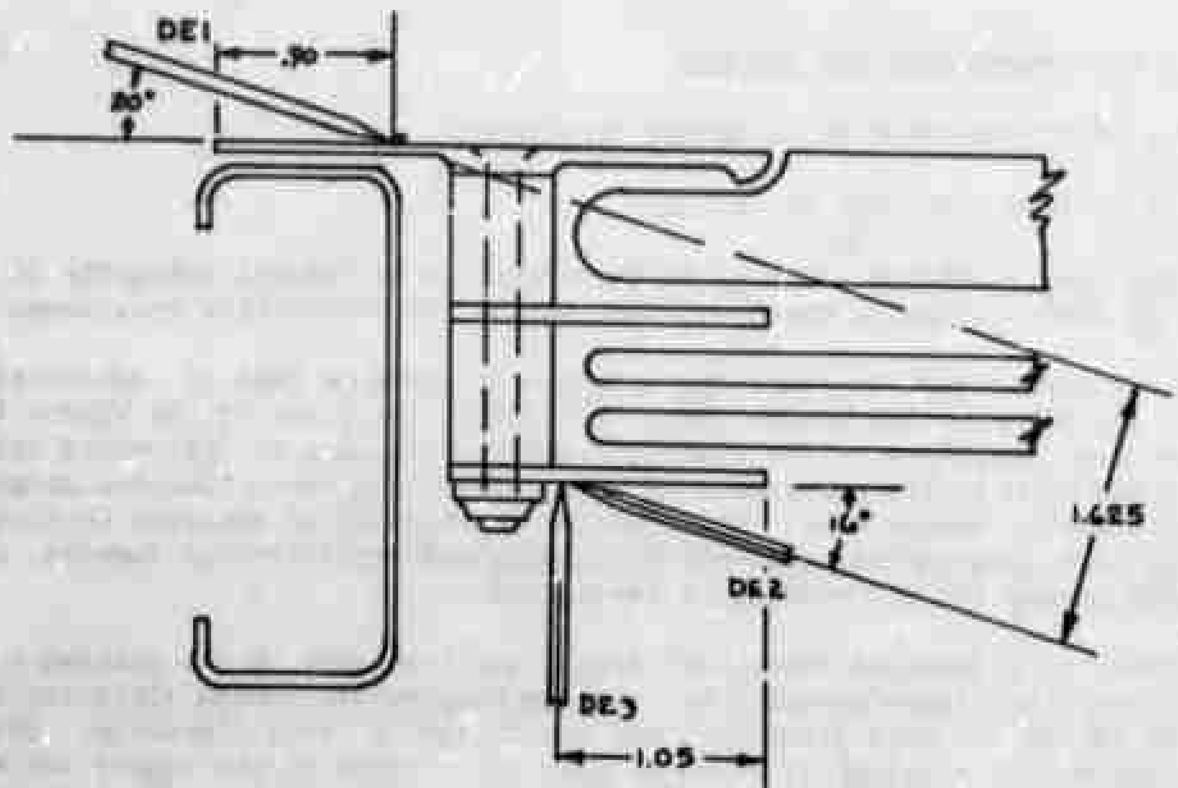

SECTION E-E

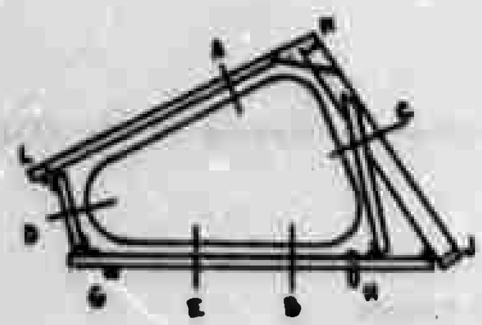

	INITIALS	DATE	REV BY INITIALS	DATE	TITLE	MODEL
CALC						X-20
CHECK						
APPD.						
APPD.						

4 TEST PROCEDURES AND RESULTS

4.1 TEST CONDITION NO. 1 (BOOST VIBRATION)

4.1.1 TEST CONDITION NO. 1 PLAN

This test condition was planned to verify the structural integrity of the X-20 window assembly when subjected to the boost vibration environment.

Sinusoidal vibration scans were planned as shown on page 39 conducted normal to the plane of the window (Axis "A") and in the plane of the window (Axis "B"). Resonant responses of the window assembly could thus be determined between 50 and 2000 cycles per second by using travelling accelerometers attached with double-backed tape. These measurements could be analyzed to show resonant frequencies, resonant bandwidths and amplification factors, and mode shapes for all measurable resonances.

After the sinusoidal vibration testing was completed it was planned to subject the window assembly to two room temperature random vibration tests, one in the "A"-axis direction, and one in the "B"-axis direction. The planned test envelope is shown on page 40. Input to the shaker while supporting the specimen could be limited at specific frequencies as necessary so that resonant responses of the window assembly would not exceed the upper tolerance of the test envelope. The test duration of 10 minutes for each axis was planned. A record of the acceleration power spectrum and overall acceleration applied in each axis at each monitor point could then be prepared.

4.1.2 VIBRATION EQUIPMENT

The largest shaker system available for the vibration testing at the Flight Dynamics Laboratory consisted of:

Ling Electronics

A-300B Shaker, Maximum Load = 300 Pounds

PP20/35 Power Amplifier

R1003C Sine Console

R1001-2 Random Console

ASD-20 26 Channel Analyzer

ESD-20 Equilizer (Band Width varies from 17 cps at 100 cps to 100 at 700 cps and on)

Since the weight of the window test specimen assembly was approximately 100 pounds, the test fixture weight was limited so as not to exceed the maximum load capability of the shaker. The test fixture consisted of a two inch thick aluminum plate.

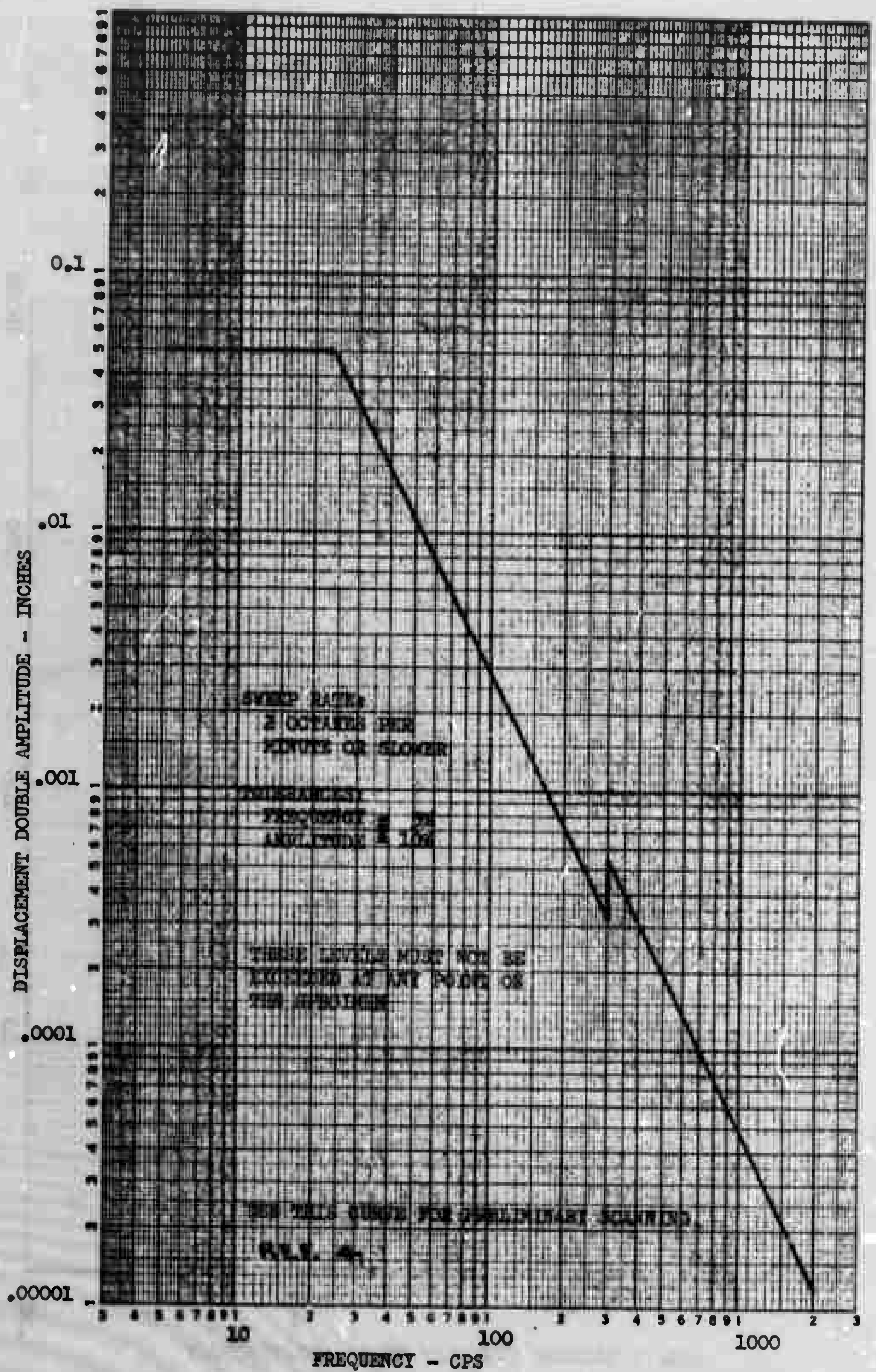

FIGURE 20 PRELIMINARY SINUSOIDAL VIBRATION TEST PLAN - TEST NO. 1

FIGURE 21 X-20 BOOST VIBRATION TEST ENVELOPE - TEST PLAN CONDITION NO. 1

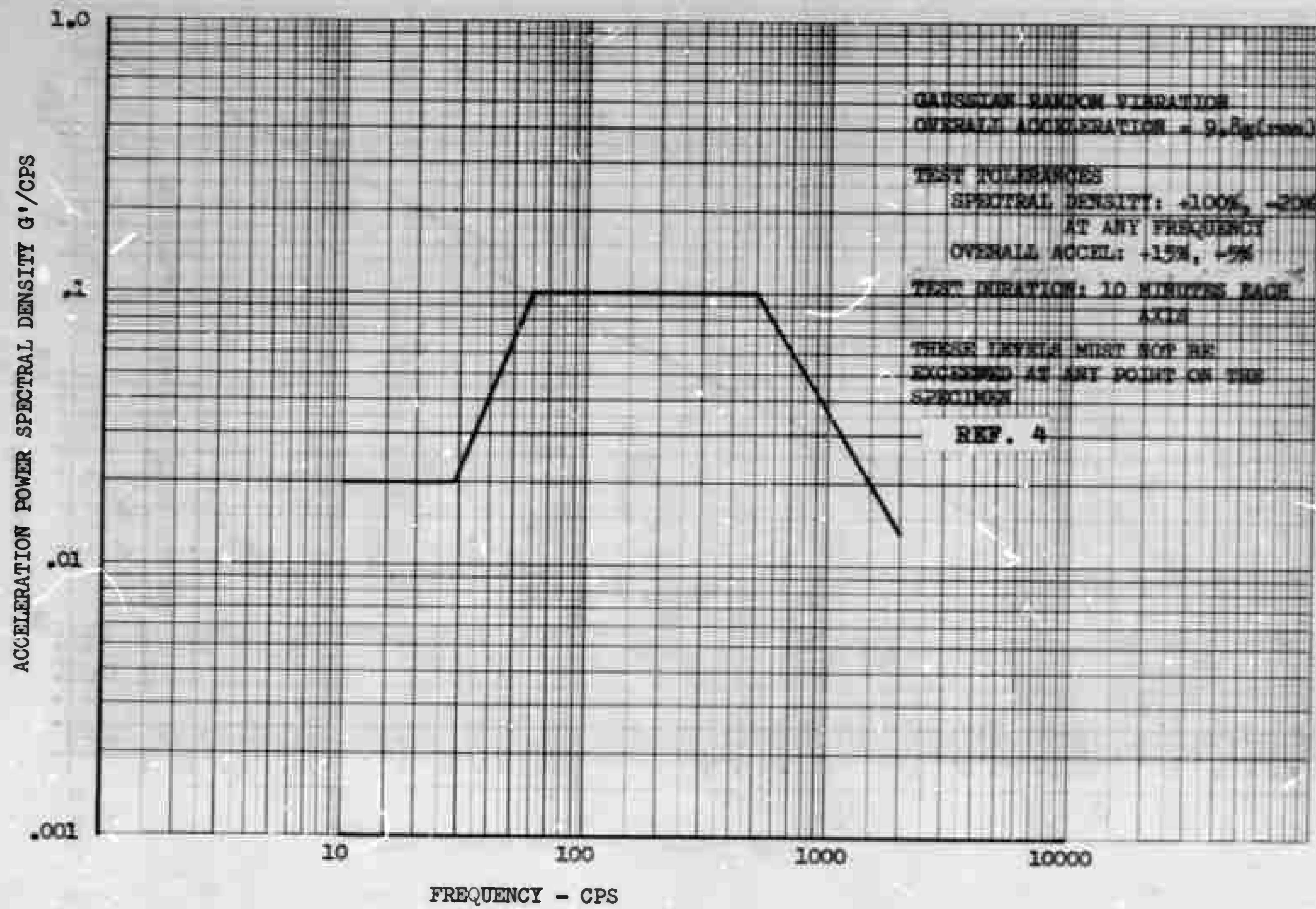

4.1.3 TEST PROCEDURES

The following paragraphs are a record of the vibration tests as conducted.

The window frame was rigidly attached to the test fixture and a Ling Model A300 vibration exciter. Vibration was first applied vertically, perpendicular to the plane of the glass.

For preliminary information, initial scanning was accomplished for the vertical direction by performing a sinusoidal frequency sweep from 5 cps to 2000 cps. The sweep rate was less than 2 octaves/minute. The input double amplitude was 0.025 inch from 5 cps to 23 cps and 0.2 g from 23 cps to 2000 cps.

Rather severe resonances were found to exist in the A-frame members which overhung the edge of the fixture. Consequently, the two projecting members were removed at the fixture edge by means of a high speed cutting wheel.

The fixture without the window test specimen was installed on the shaker and a complete dynamic survey was conducted on the fixture alone. An amplification factor (Q) of 56 was noted at one point on the fixture (2 g input gave 112 g's on plate). This data indicated that the fixture did not have sufficient stiffness to accurately control the vibration levels.

The fixture and specimen were then instrumented to determine the resonant modes of the upper glass pane and the frame unit in which it was installed.

The window was again mounted on the fixture and a complete dynamic survey of the fixture and specimen was accomplished. The Q of the fixture had dropped from 56 to 15 at the most severe point. The outer .65 inch thick window had a Q of approximately 30. Wide band random vibration was then applied to the specimen, perpendicular to the plane of the glass. The random vibration input was applied at extremely low level, 0.001 PSD maximum, in lieu of 0.1 PSD as recommended by Boeing Document D2-81293, Window Test Plan, Reference 4. The test plan level is shown on page 40. The response of the upper glass was monitored and the input vibration level was reduced so that the response of the glass would not exceed twice the input PSD value. A recording and analysis of this data was made so that it could be compared with data planned to be taken after the heat test.

The specimen and test fixture were next mounted on an oil film table, oriented so that vibration was applied horizontally, along the "B" axis, as shown on page 44. Initial scanning was accomplished for this direction by means of a sinusoidal frequency sweep from 5 cps to 2000 cps, with an applied double amplitude of 0.025 inch from 5 to 23 cps, and 0.2 g from 23 cps to 2000 cps. Resonant responses of the upper glass pane and frame were recorded.

FIGURE 22 RESONANT RESPONSES - VERTICAL DIRECTION

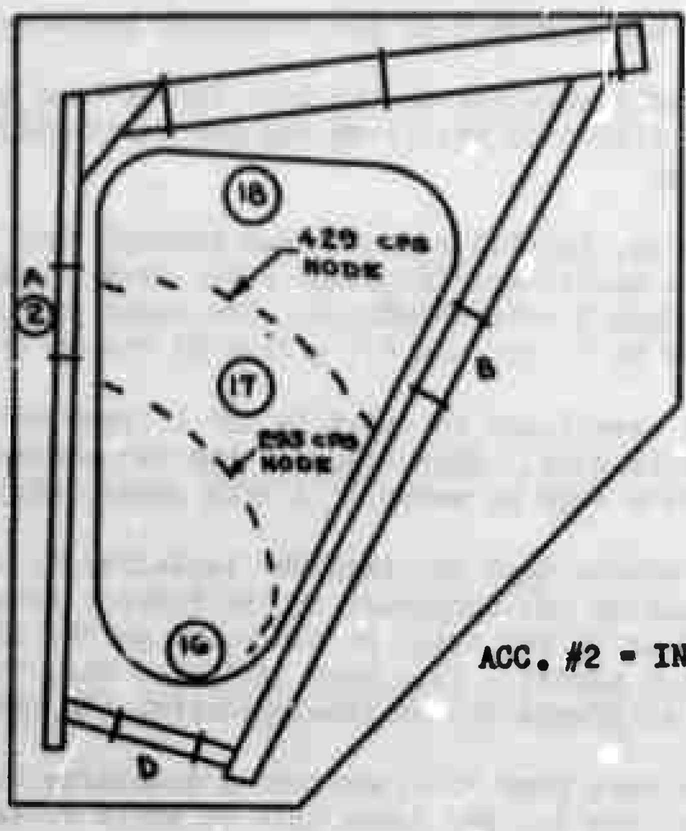

ACC. #2 = INPUT CONTROL

ACC. #	FREQUENCY (cps) 135	293	429	619
2	0.2 g	0.2 g	0.2 g	0.2 g
16	0.66	2.5	1.6	2.0
17	0.75	1.5	3.0	0.7
18	1.2	0.9	0.5	1.5

Note: For 135 cps, amplification began at about 120 cps, and extended to approximately 150 cps.

For 293 cps, amplification began at about 285 cps and extended to approximately 315 cps.

For 429 cps, amplification began at about 415 cps and extended to approximately 452 cps.

For 619 cps, amplification began at about 609 cps and extended to approximately 629 cps.

4.1.3 TEST PROCEDURES (Continued)

Wide band random vibration was then applied for this "B" axis direction, also at the extremely low level of 0.001 PSD maximum, in lieu of 0.1 PSD. A recording and analysis of this data was also made for comparison with data planned to be taken after the heat test.

A review of the vibration test data was made. The following factors were areas which were found to exist that could result in overtesting the X-20 side window specimen during the required random vibration testing:

a. Due to equipment force limitations and physical size limitations, the vibration fixture design had very limited parameters and therefore several resonances (two severe) exist in the fixture which may cause serious over-testing at these frequencies.

b. The test plan (Reference 4) requires that all responses are to be limited to the overall upper tolerance level (100% above spectrum) of the random vibration spectrum. Due to limitations of analyzing equipment, this requirement will be difficult to meet. There are also areas of the specimen (the two lower glass panes) that cannot be instrumented so control at these points will not be accomplished.

c. The equalizing equipment is manually operated for adjustment purposes so it must be adjusted while exciting the specimen and therefore, may result in short periods of overtesting. A dummy mass in this case would not help unless it were a dynamic simulation of the specimen. There is approximately a factor of 5 difference in the fixture amplification factor between the fixture alone and the fixture with the window mounted. (Q = 56 unloaded, Q = 15 with specimen mounted.)

Since the above uncontrollable areas were present a possibility of window failure due to overtesting existed. It was decided to postpone the full-scale boost vibration testing until after the heat and load test had been accomplished.

4.1.4 TEST RESULTS

Significant resonant frequency data recorded during the initial sinusoidal frequency surveys are as follows:

4.1.4.1 RESONANT FREQUENCIES - VIBRATION APPLIED PERPENDICULAR TO GLASS - AXIS "A"

a. No resonances were detected below 120 cps.

b. 120 cps to 150 cps, chatter occurred which was manifested in movement of the sliding joint at point D, Reference 4 & page 42. Maximum chatter was observed at 135 cps. This chattering motion resulted in amplification factors as high as 6, when measured on the upper pane of glass and on the frame immediately adjacent to the glass. (See Figure 22 page42).

FIGURE 23
ACCELEROMETER LOCATIONS AND RESULTS - HORIZONTAL VIBRATION

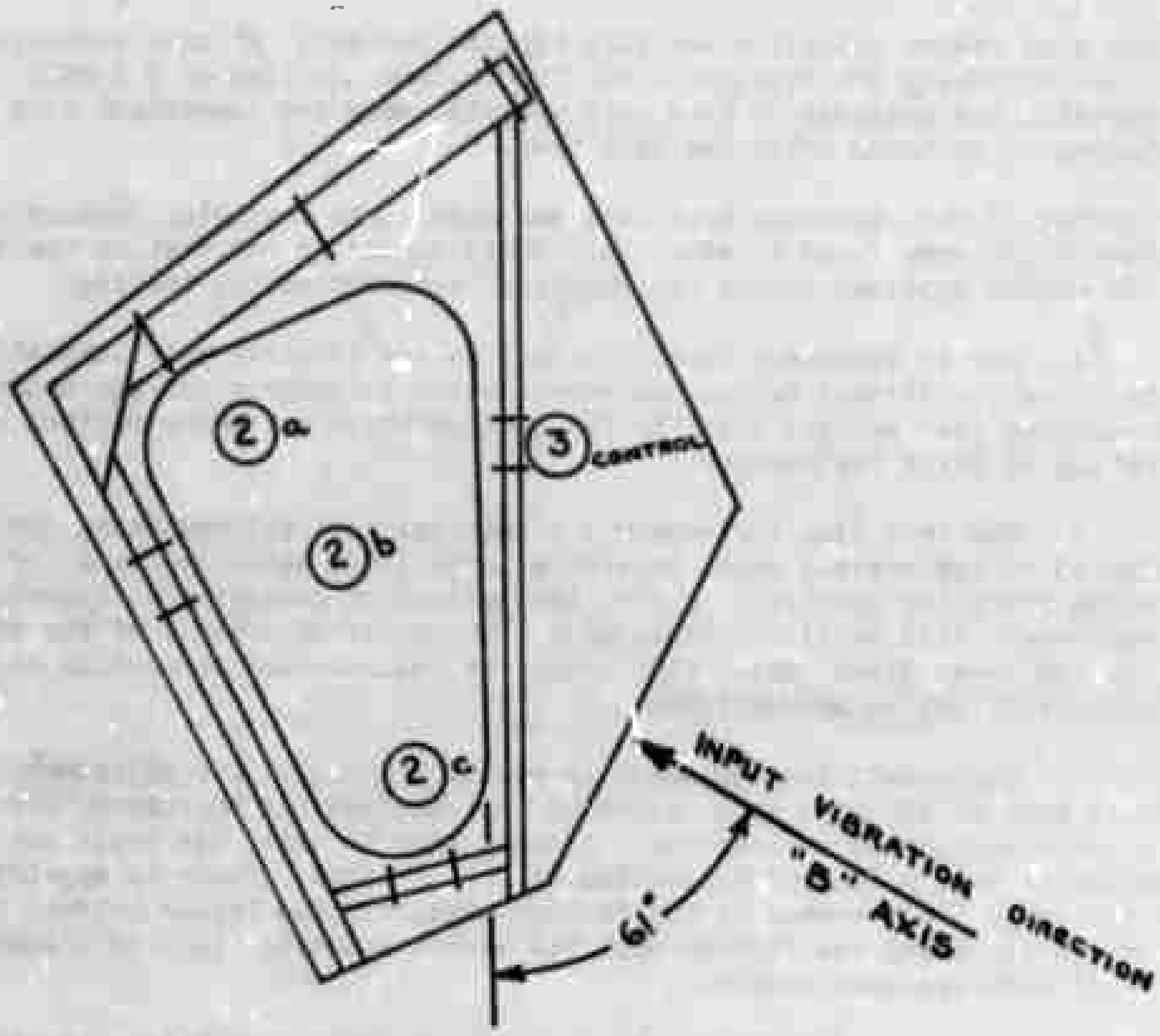

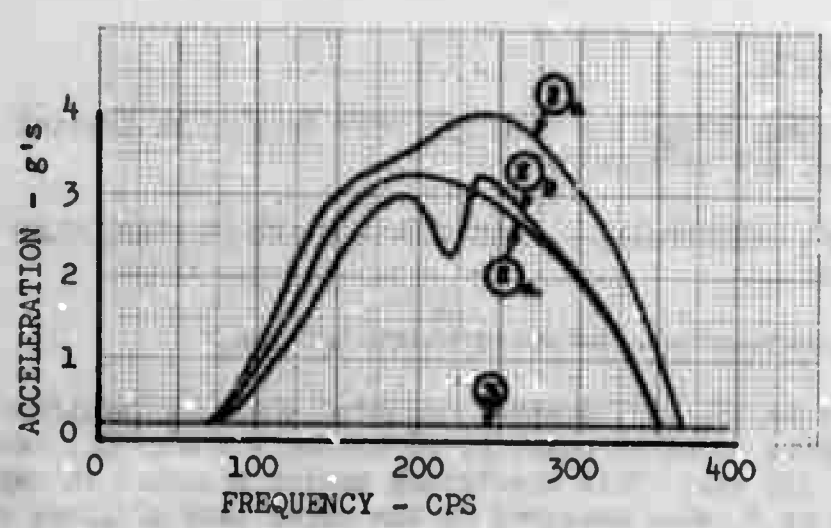

4.1.4.1 RESONANT FREQUENCIES - AXIS "A" (Continued)

c. The only resonances of the upper glass pane for which a mode shape could be drawn were observed at 293 cps and 429 cps. The frequency of 293 cps was attributed to a fixture resonance. The frequency of 429 cps is the only authentic glass pane resonance found. (See Figure 22 page 42). It has an amplification factor of 15 at the center of the glass.

4.1.4.2 RESONANT FREQUENCIES - VIBRATION APPLIED HORIZONTALLY IN A PARALLEL PLANE WITH GLASS - AXIS "B"

a. A very gradual buildup in amplification for accelerometer locations on the glass began at around 70 cps. For location 2a, Figure 23 page 44 the gradual rise reached a maximum amplification of 3.25 at 190 cps, 3.0 at 240 cps, continuing at 2.5 up to 275 cps, dropping to input level at 350 cps.

b. For location 2b, Figure 23 page 44 initial amplification began at around 70 cps, with a gradual rise to a maximum of 3.0 at 190 cps, 2.25 at 220 cps, 3.25 at 240 cps, continuing at approximately 2.5 to 280 cps, dropping to input level at 350 cps.

c. For location 2c, Figure 23 page 44initial amplification began at around 70 cps, with gradual rise to a maximum of 2.75 at 140 cps, 3.5 at 190 cps, 4.0 at 240 cps, 3.75 at 270 cps, dropping to input level at 365 cps.

4.2 TEST CONDITION 2

4.2.1 TEST CONDITION 2 PROCEDURE

The window specimen was pressure loaded with air at room temperature to a negative 7 psi (outward acting). This pressure simulates the X-20 boost limit pressure and is the limit load design condition for the window.

The window was mounted securely to the test stand. The pressure-vacuum box was mounted on the window. Mylar was initially proposed to seal the pressure box to the window frame for this test condition. The mylar was installed but did not provide a satisfactory seal. It was removed and zinc chromate putty was used to make a satisfactory seal. A photograph of the test set-up is shown on page 52.

Pressure was applied to the specimen as shown on page49. The pressure leakage rate, and window and cab frame deflections were recorded for all test times.

A schematic of the apparatus for measuring the air leakage is shown on page47. Prior to the test, the vacuum line was capped off at the test specimen. The valve was closed and the pump shut off to assure that no leakage existed.

The procedure followed during the test was to close Bleed Valve B until the pressure manometers read the correct pressure in the pressure box and then read the Meriam Flow Meter. This indicated the amount of air flowing back to the vacuum pump and thus the amount leaking into the pressure box through the window seals. The flow meter was calibrated to read up to 1.6 SCFM with water in the manometer. When it became apparent the leakage was going to exceed 1.6 cfm, mercury was substituted for the water in the inclined manometer to extend the range.

Following the test, a valve was installed at the test specimen end of the vacuum line and a series of flow versus pressure readings were made with the valve opened to different amounts in order to verify the linearity of the flow meter up to the flow value measured during the test.

4.2.2 TEST CONDITION 2 RESULTS

4.2.2.1 WINDOW SEAL LEAKAGE RATE

The target leakage rate as defined in Reference 2 is 1.17×10^{-4} ft^2 per foot of seal with a corresponding leakage rate of .55 x 10-5 pounds/second per foot, for choked flow at standard conditions. These target requirements were set-up to control the design from the standpoint of aerodynamic heating. The above sealing capability was desired at the time of high heating during re-entry in order to seal the hot gas plasma from heating the internal fuselage cavity. Fortunately the maximum pressure during the critical heating

FIGURE 24 VACUUM SYSTEM SCHEMATIC TEST CONDITION 2

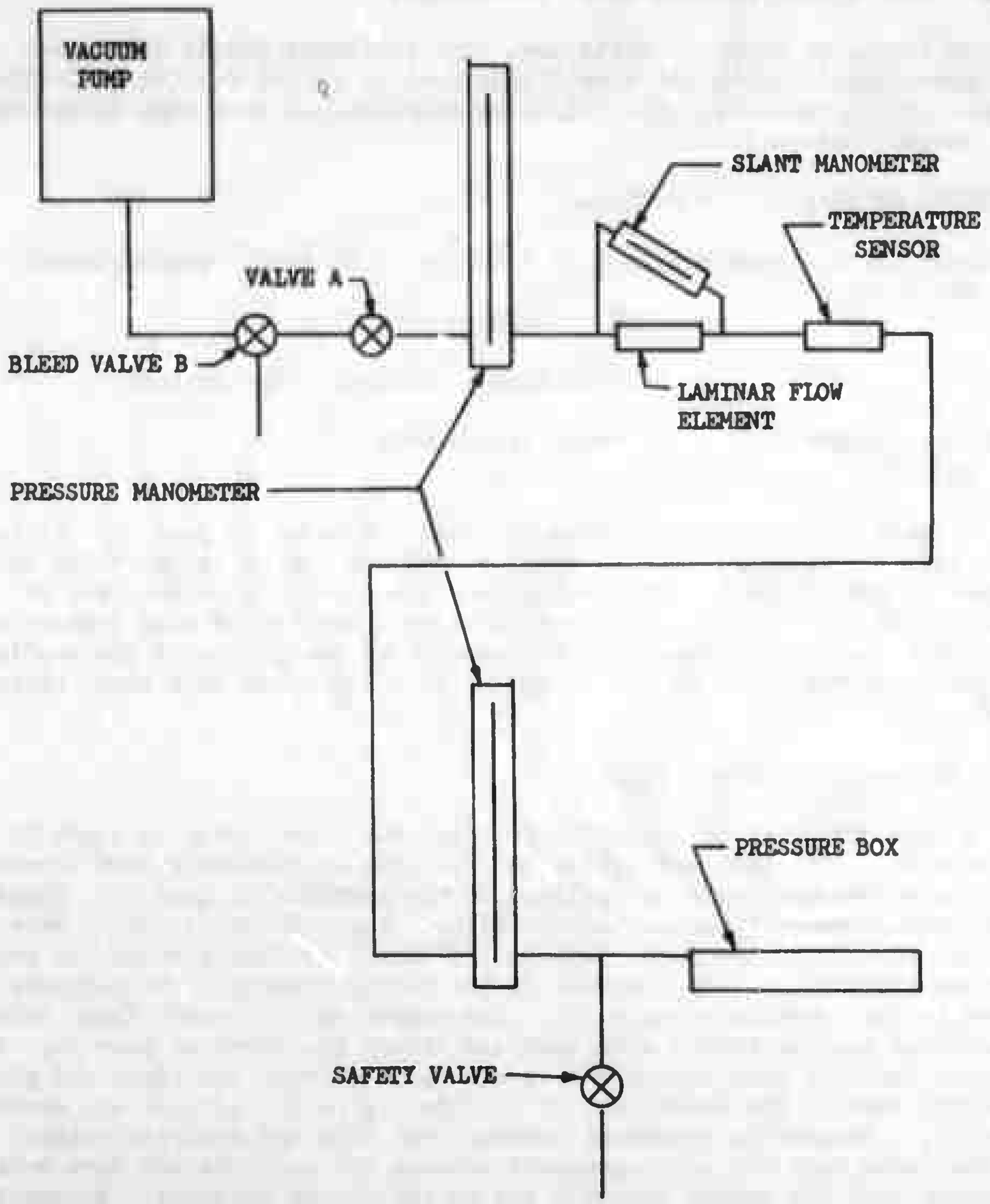

	INITIALS	DATE	REV BY INITIALS	DATE	TITLE	MODEL
CALC					VACUUM SYSTEM SCHEMATIC TEST CONDITION 2	X-20
CHECK						
APPD.						
APPD.						

4.2.2.1 WINDOW SEAL LEAKAGE RATE (Continued)

period during re-entry is quite low. The pressures should not exceed .50 pound/inch^2 during the significant heating period for the X-20 side window during re-entry. The following calculations were made to determine the target leakage rate:

LENGTH OF SEAL = 5.58 Feet

TARGET LEAKAGE RATE AT .5 PSI = 5.58 (.55 x 10^{-5}) = 3.06 x 10^{-5} pounds/second

= .001836 pounds/minute

= .001836/.0766 = .024 cubic feet/minute

TARGET LEAKAGE RATE AT 7 PSI = .34 cubic feet/minute

The leakage rates recorded during the test are shown on page 49. It is seen that the recorded leakage rates exceed the design target value by a factor of 10. Since the thermistor lead wires ran across the seal as outlined on page 24, it is believed this resulted in the high leakage rate. Therefore the leakage rates are not considered conclusive of the sealing qualities of the seals as the flight article would not have these thermistor leads.

4.2.3 DEFLECTIONS AND ROTATIONS

Deflection and rotation locations for Test No. 2 are shown on pages 50 through 51. The test deflection and rotation measurements were corrected for rigid body movements as outlined in the Appendix on page 195. These data were then compared with calculated values. The calculated values were determined from an analysis based on the direct stiffness method as programmed for the digital IBM 7094 computer by The Boeing Company. The analysis is shown in the Appendix on page 195. The comparison of window frame rotations (torsional angular twist) with analysis values are shown on page 50. It is seen that the test values lie in most part between the fixed and pinned analysis cases. The comparison of vertical frame deflections are shown on page 51. Reasonable agreement between test data and analysis exists. It is concluded that the good agreement between the analysis and test data is evidence that the window assembly has no structural weakness. Extrapolation of this data to ultimate load indicates that the window assembly could withstand the ultimate load without failure.

The window frame to glass gaps were recorded before and after the test as shown on page 121.

FIGURE 25 TEST HISTORY - TEST CONDITION 2 (BOOST PRESSURE)

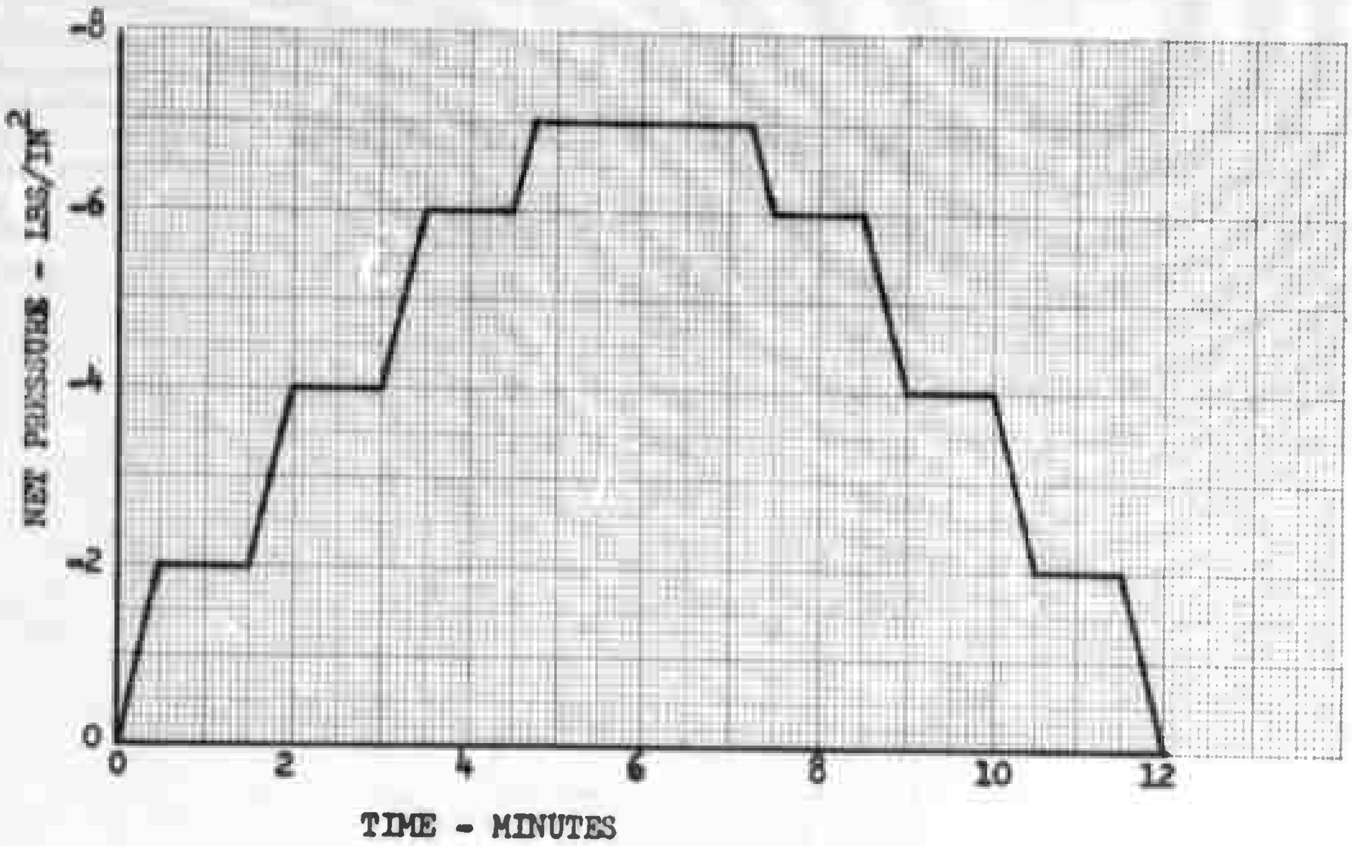

FIGURE 26 WINDOW SEAL LEAKAGE RATE
TEST CONDITION 2 (BOOST PRESSURE)

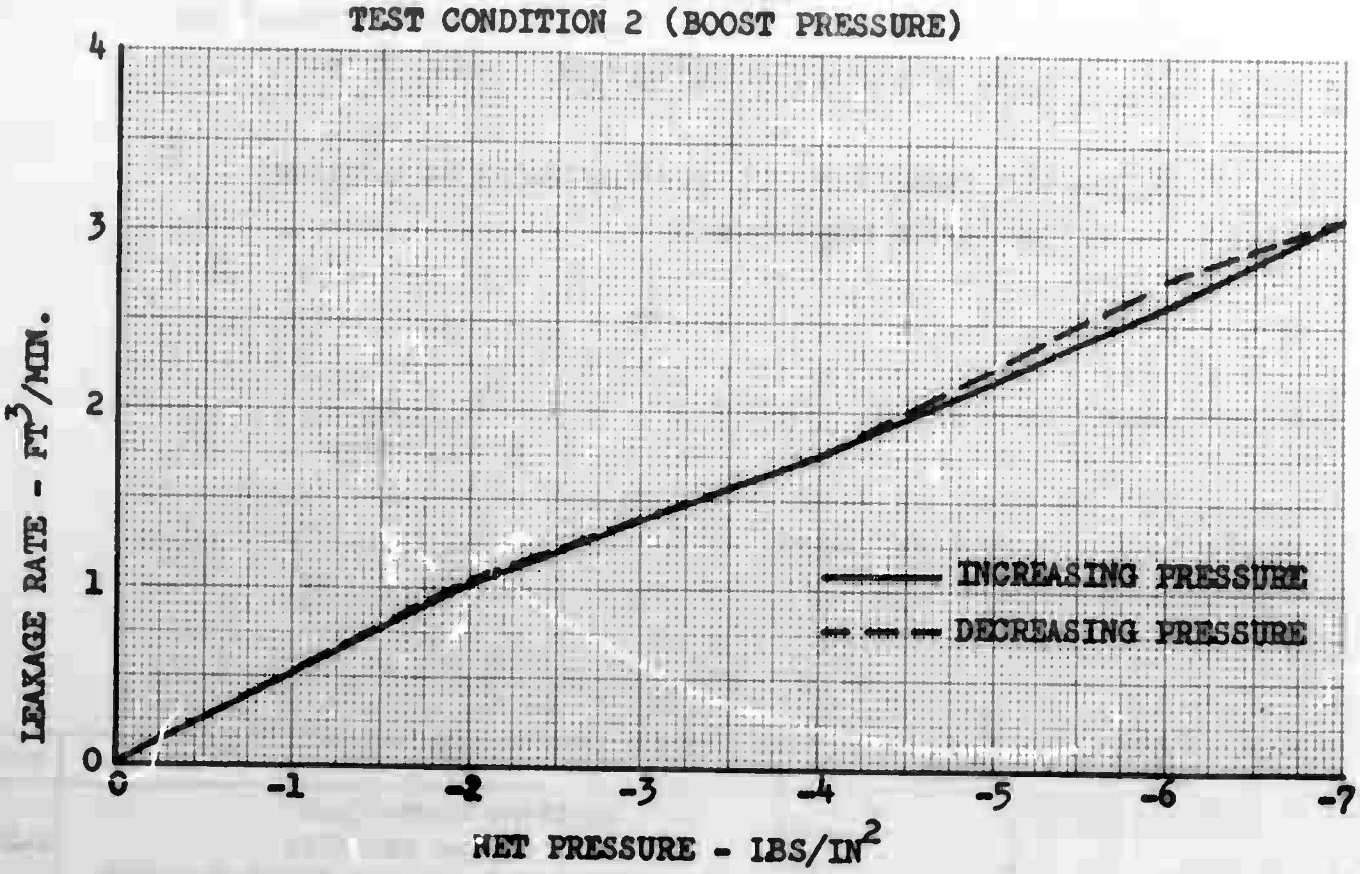

TABLE 1 ROTATION COMPARISON AT -7 LBS/IN^2 PRESSURE

POINT	WINDOW FRAME ROTATION - RADIANS		
	ANALYTIC DATA [1]		TEST DATA
	FIXED	PINNED	
A	-.002352	-.009152	-.003743
B	-.002430	-.008462	-.005619
C	+.001072	+.005617	-.000714
D	-.001553	-.001055	[2]
E	-.000821	-.006124	-.004128

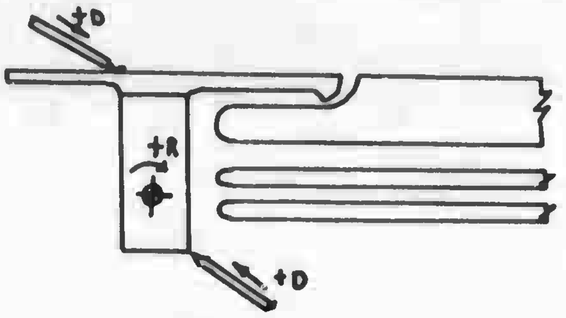

SIGN CONVENTION (TYPICAL SECTION)

[1] ANALYSIS ASSUMES BOTH A FIXED AND PINNED BOUNDARY FOR GLASS TO FRAME-SEAL CONNECTION. REF. P. 130

[2] DATA INVALIDATED BY NON-PARALLELISM OF ROTATION DEFLECTION MEASUREMENTS.

	INITIALS	DATE	REV BY INITIALS	DATE	TITLE	MODEL
CALC	Abrend	6/23/65			ROTATION COMPARISON TEST versus ANALYSIS TEST CONDITION 2 - LIMIT BOOST PRESSURE	X-20
CHECK						
APPD.						
APPD.						

FIGURE 27 VERTICAL DEFLECTION COMPARISON - TEST NO. 2

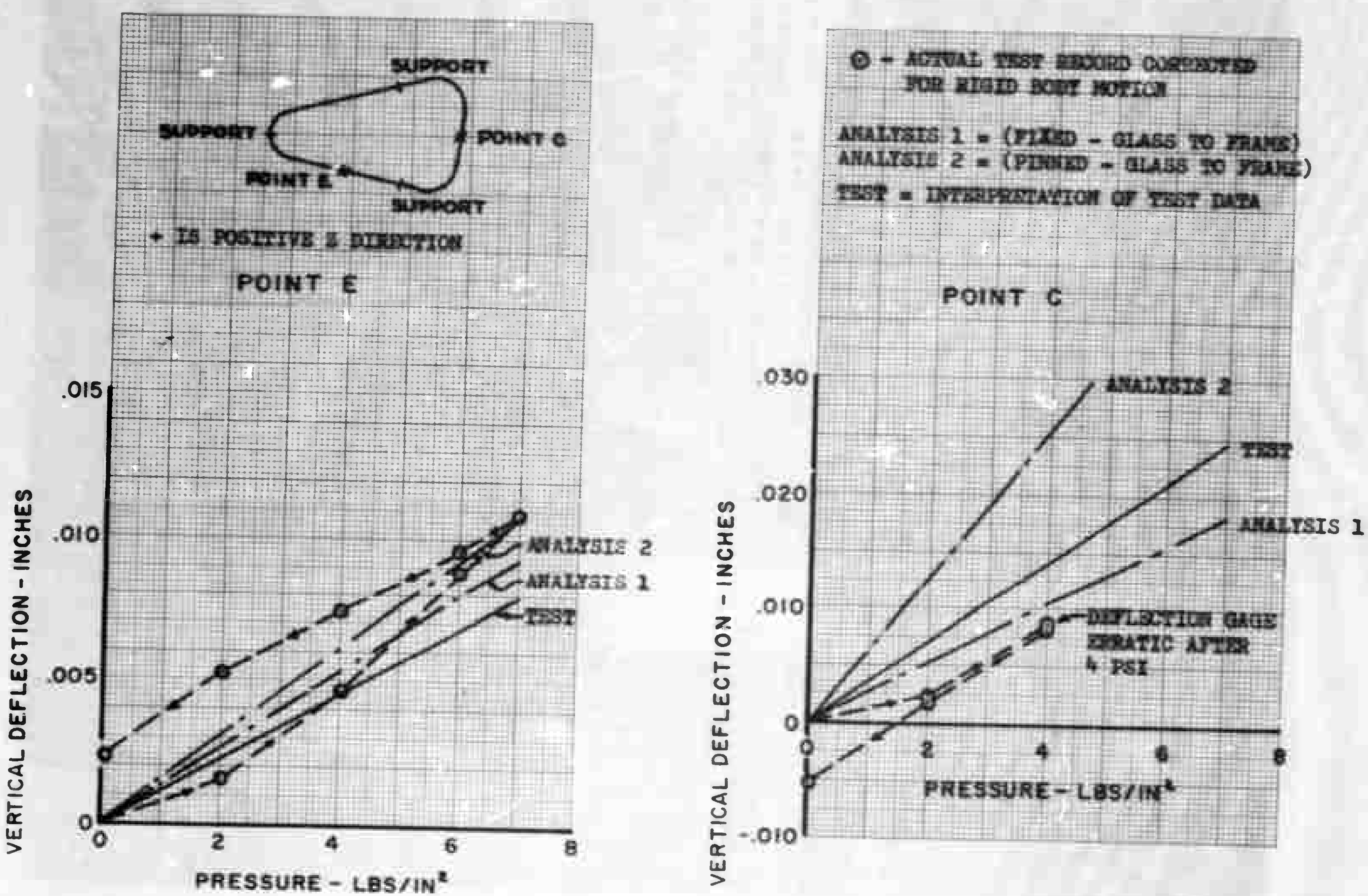

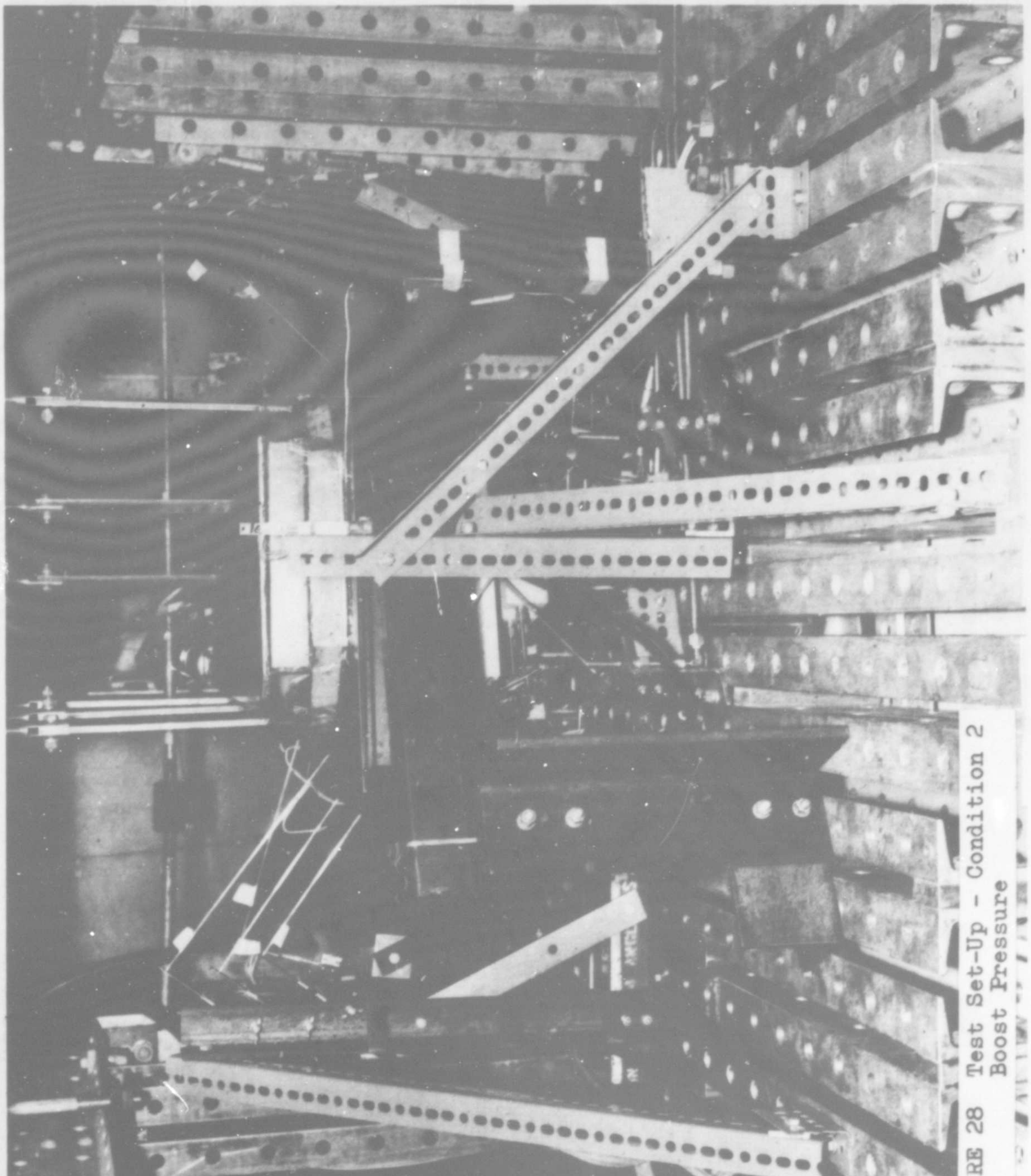

FIGURE 28 Test Set-Up - Condition 2
Boost Pressure

4.3 TEST CONDITION 3 (RE-ENTRY THERMAL CYCLE)

4.3.1 TEST CONDITION 3 PROCEDURE

The window specimen was to be heated as shown in Figure 29 page 54. The time-temperature requirements represent a thermal cycle which simulates the X-20 maximum lateral range re-entry. Figure 30 page 57 is a photograph of the test set-up. The test specimen support conditions are shown on page 58.

Efficiency tests conducted prior to the actual test indicated the silicon carbide powder installed per the test plan (Reference 4) over the surface of the outer glass to aid heating caused the glass to heat much too rapidly. The silicon carbide powder was removed with a vacuum cleaner, which left a small residue, for the actual test.

Figure 32 page 59 shows the upper surface lamp layout and also the location of the four control thermocouples (C_1, C_2, C_3, C_4) and the two fairing thermocouples (F_1 and F_2). The deflection and rotation measurement locations for Test No. 3 are shown on pages 33 through 37.

The electrical power applied to the lamps in each control area was determined by the Structures Test Branch (FDTT) Heat Rate Computer which matches the actual temperature of the control thermocouple or thermistor with the desired temperature as programmed on a magnetic drum and adjusts heat lamp voltages accordingly.

4.3.2 TEST CONDITION 3 RESULTS

Two efficiency tests were conducted on the test specimen to check out heating set-up. These consisted of applying a constant voltage to all heat lamps and recording temperatures from all the thermocouples and thermistors and all deflections. This data is on file at the Structures Branch FDTT of the Air Force Flight Dynamics Laboratory.

Included in the data under Serial No. 206 are the temperatures and deflections recorded during a run which lasted 80 seconds and was then aborted when the ignitrons malfunctioned. The plotted data for this rapid rate heating is on file as noted above. Following this run the specimen was inspected and no damage was observed.

The final test was terminated after 380 seconds when it was observed that the top glass had broken. From the data it appears the break occurred after 352 seconds. A photograph of the failed glass is shown on page 61. An accurate drawing of the failed glass is shown on page 63. The test set-up after the glass failure is shown on page 62. Only the top glass failed and no apparent damage was sustained by the rest of the test specimen.

FIGURE 29 X-20 HOT SIDE WINDOW - TEMPERATURE HISTORY TEST PLAN 3

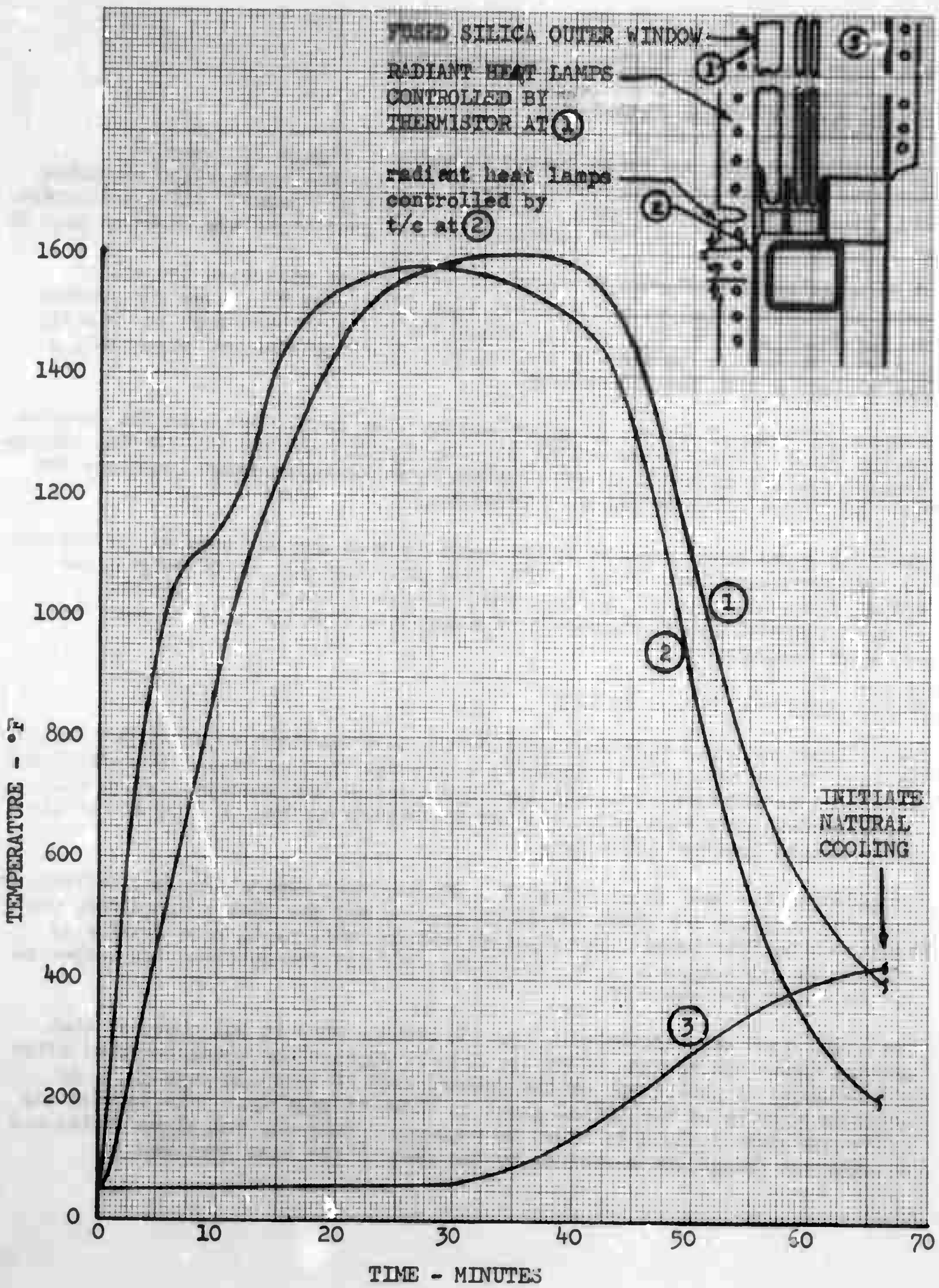

4.3.2 TEST CONDITION 3 RESULTS (Continued)

The heat lamps in the control zone directly over the glass and controlled by Thermistor No. 1 did not come on. This was because sufficient heat was arriving from the area of Control Zone 2 for Heat Control Zone 1 to follow the planned temperature profile. The lower surface lamps heating the aluminum dummy window did not come on since heating was not programmed until later in the cycle.

Results of the final Test Condition 3 are presented in plotted form under Serial No. 207 on pages 65 through 120 Figure 37 page 121 shows the window gap measurements.

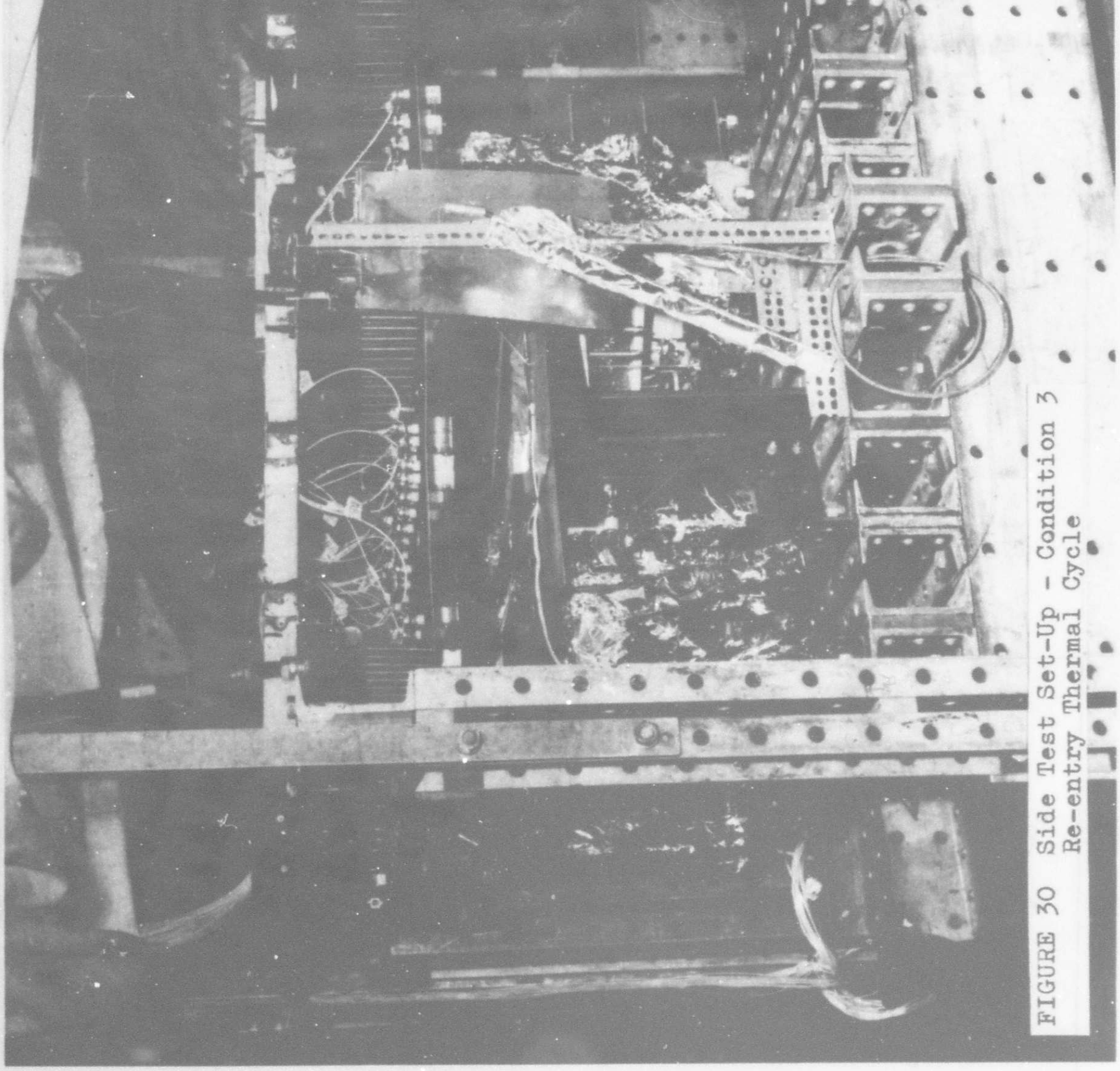

FIGURE 30 Side Test Set-Up - Condition 3
Re-entry Thermal Cycle

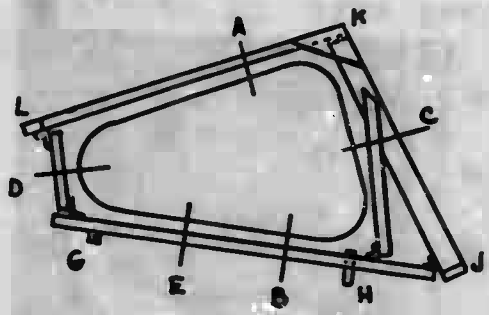

POINT "G" RESTRAINS IN ALL DIRECTIONS.
POINT "H" RESTRAINS DOWNWARD & TRANSVERSELY.
POINTS "J, K, L" RESTRAINS DOWNWARD ONLY.

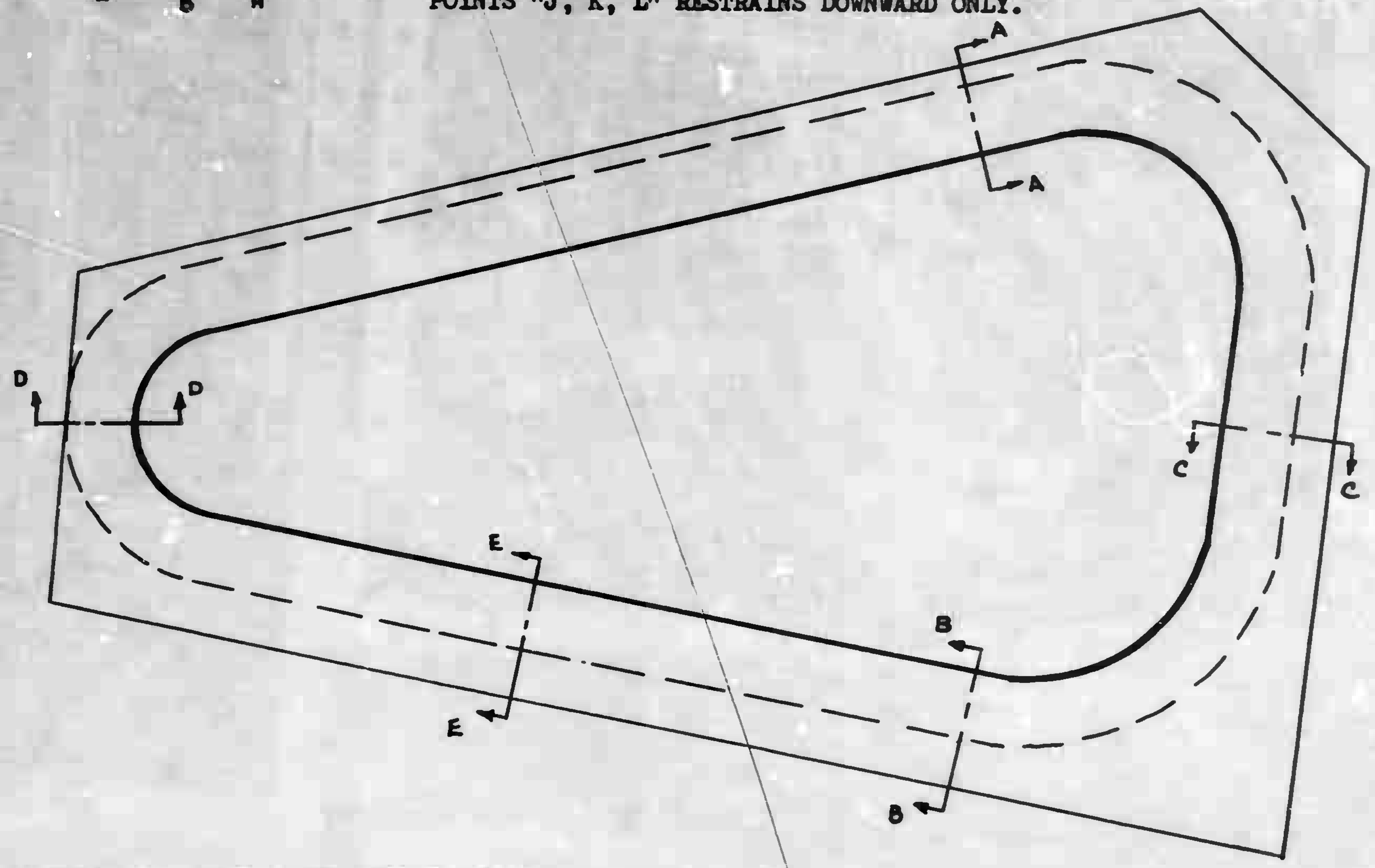

FIGURE 31 WINDOW SUPPORT FOR TEST CONDITION 3

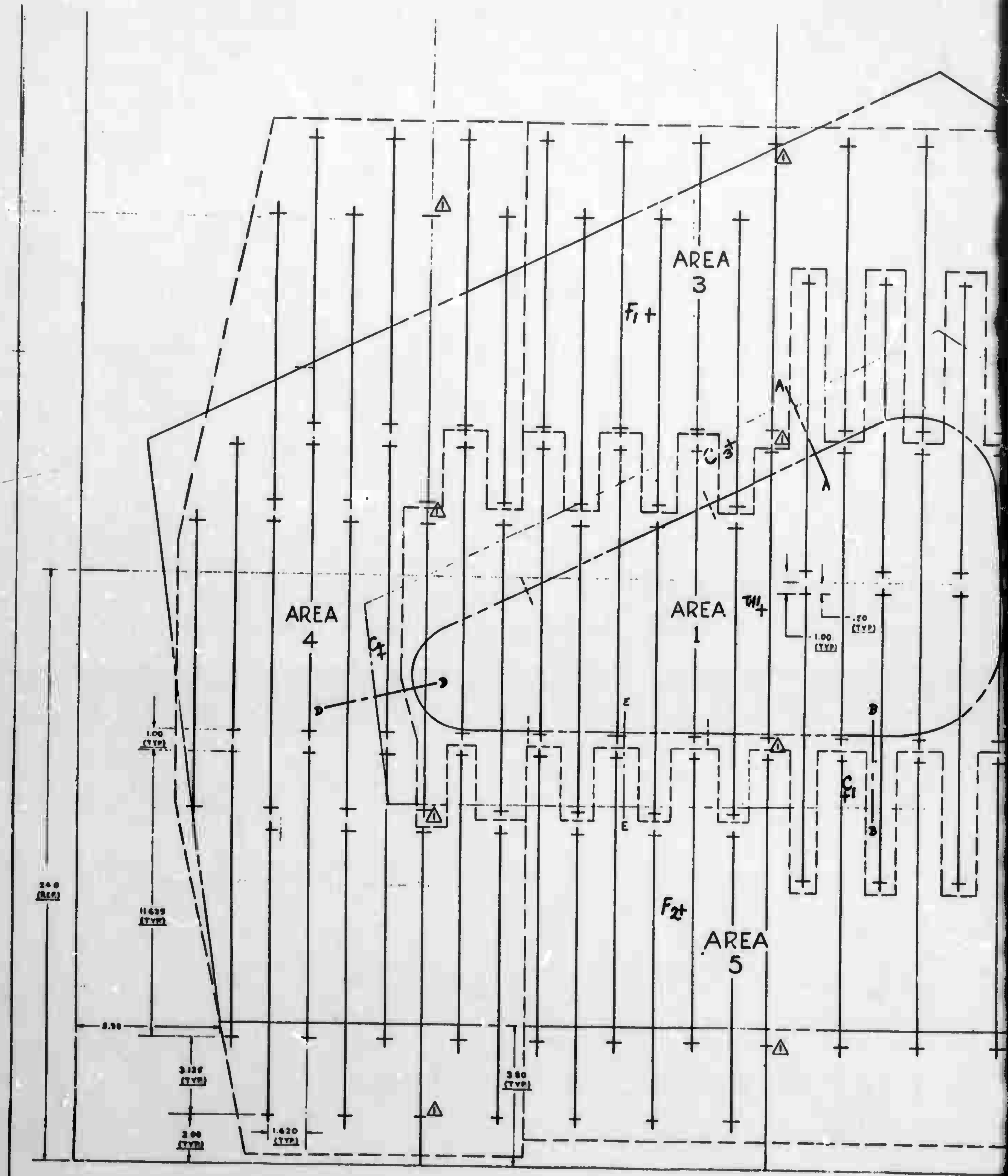

NOTES:

4. RESEARCH INC WATER COOLED REFLECTORS (8 EA)
3. INSTALL G.E. 1500 WATT T3 LAMPS.
2. ALL TOLERANCES ±.03
△1 THESE HOLES TO BE DRILLED AT JUNCTION OF REFLECTORS.

TEST 3

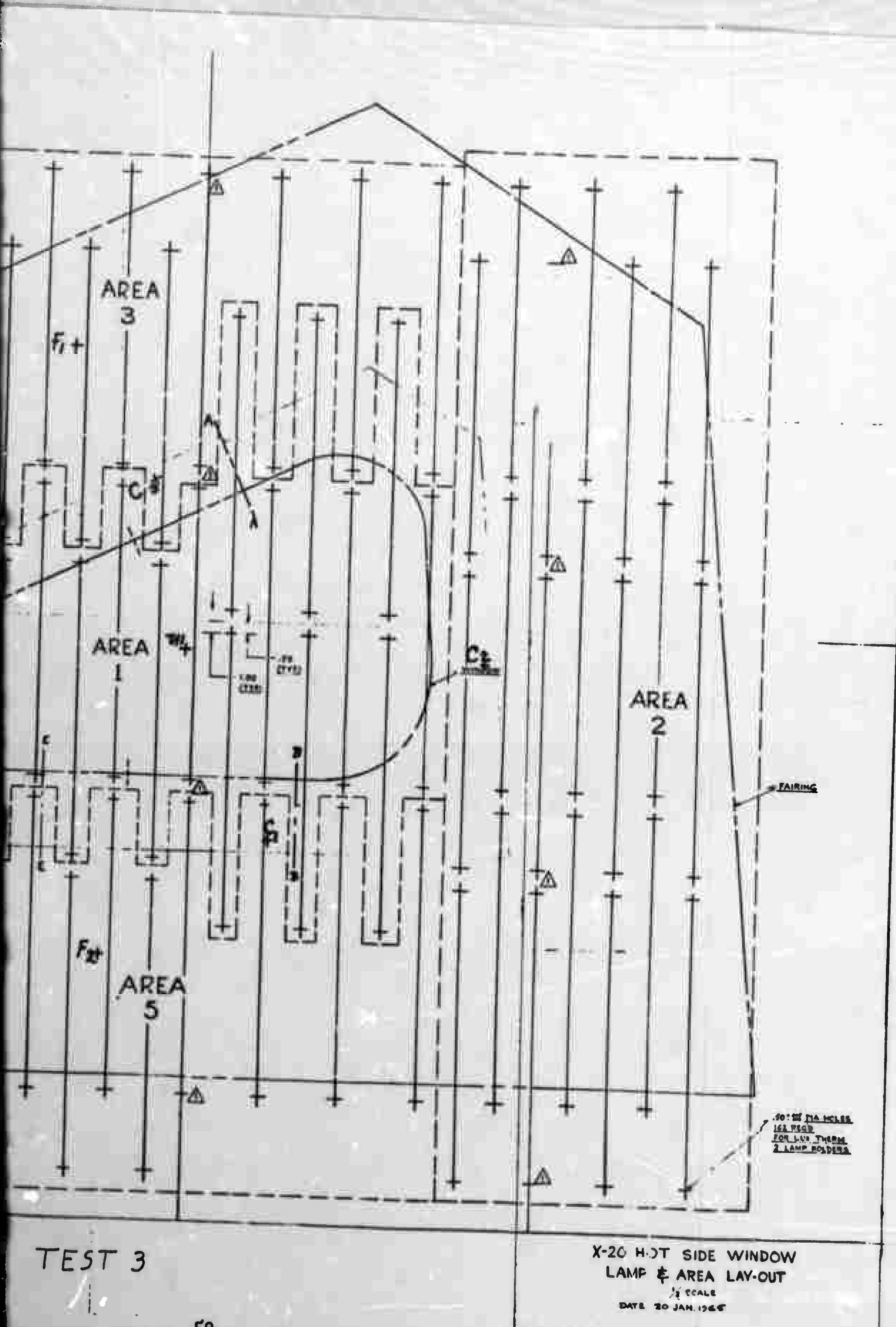
AREA 3
AREA 1
AREA 2
AREA 5
FAIRING
TEST 3
X-20 HOT SIDE WINDOW
LAMP & AREA LAY-OUT
½ SCALE
DATE 20 JAN. 1965

FIGURE 32

2

FIGURE 33 Photograph of Window Fracture

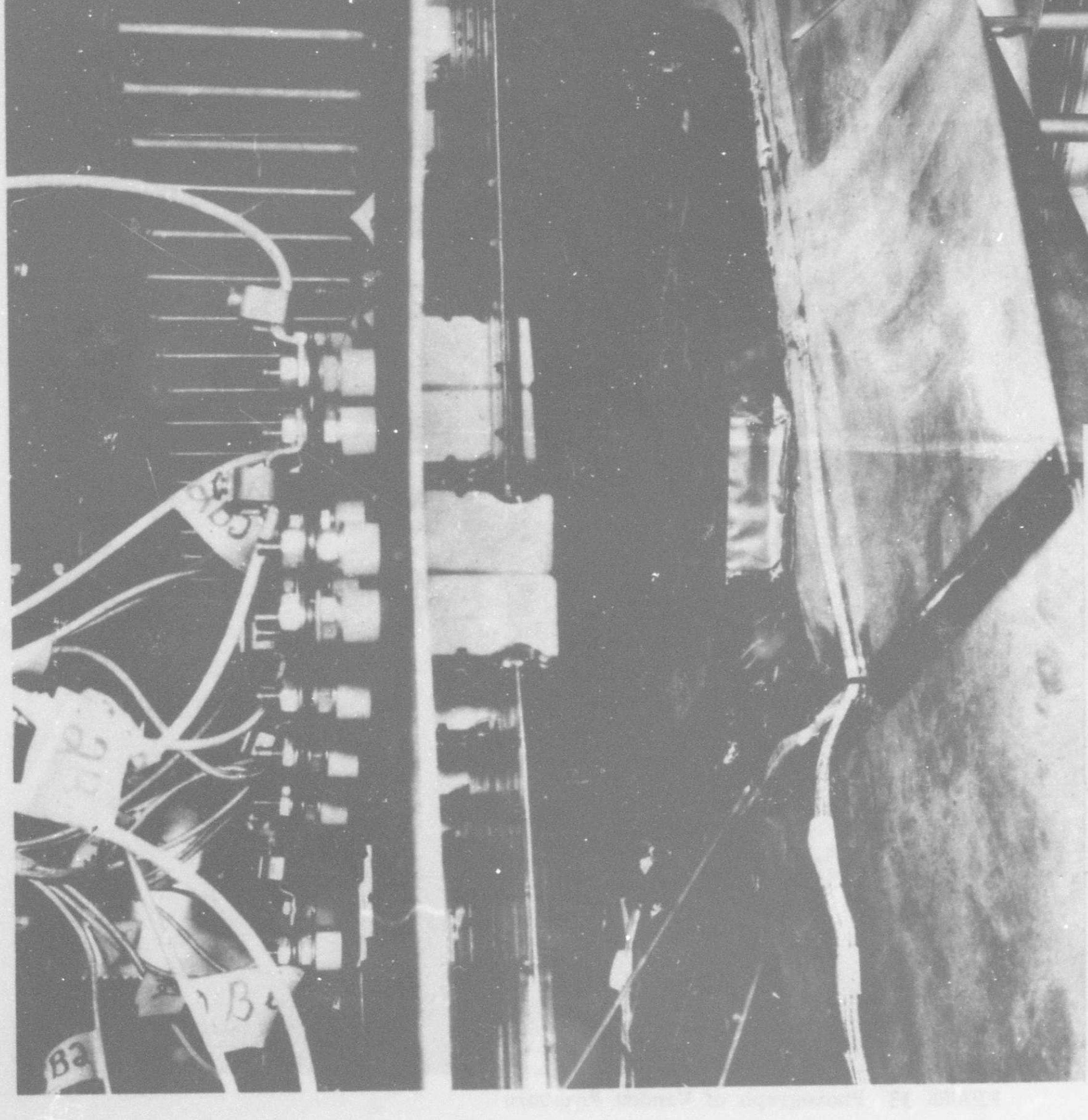

FIGURE 34 Test Set-Up After Failure - Condition 3

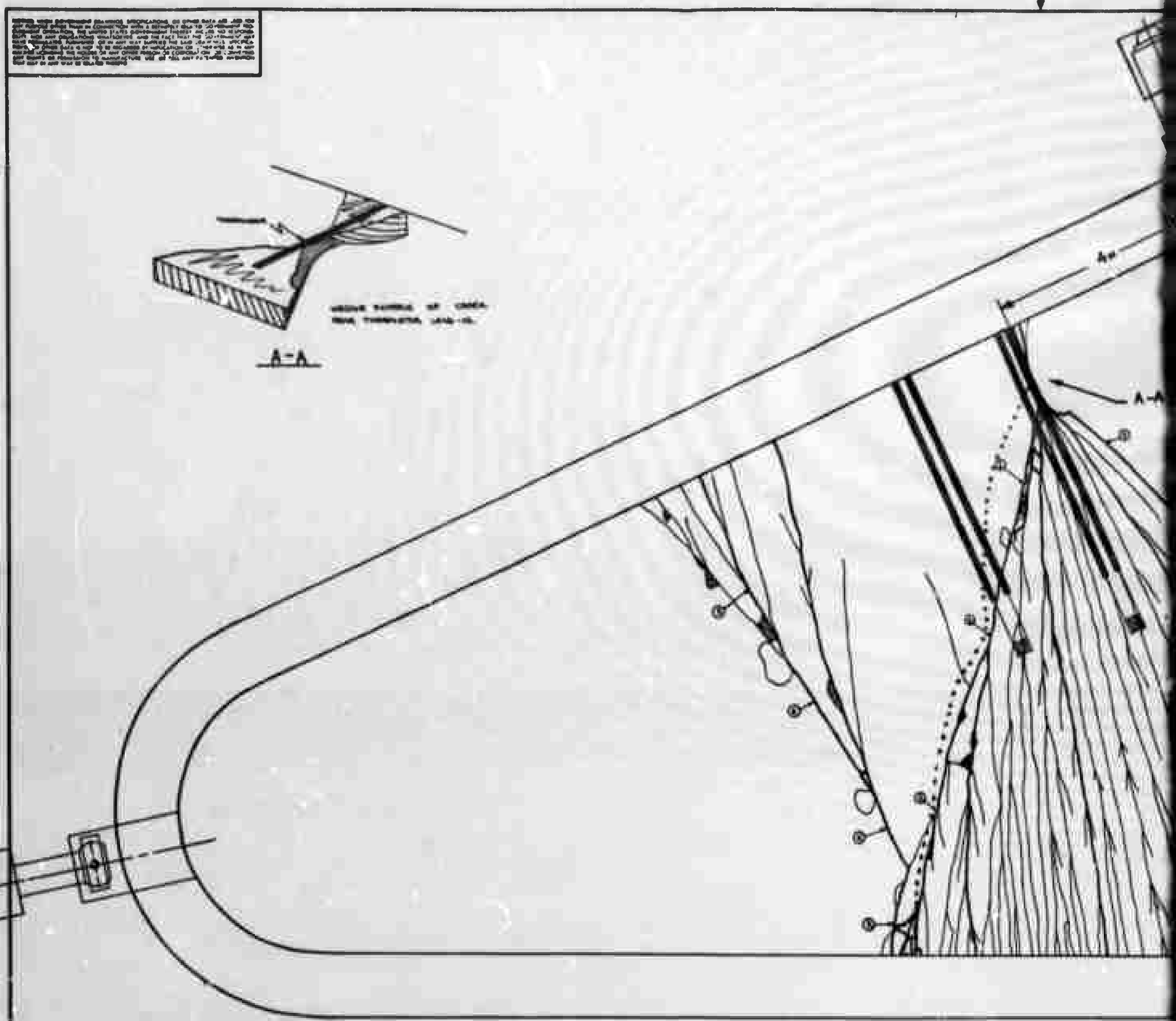

① CRACK THRU SURFACE – MAJOR SLOPE OF CRACK RUNS FROM SOLID CRACK ... GLASS TO OTHER SURFACE OF GLAZING DESIGNATED BY .... LINE. THIS ... – JUST TO INDICATE SLOPING CRACK THRU GLASS AT THIS POINT.

② MOST PROMINENT CRACK THRU SURFACE. A "MAJOR" CRACK IN THE FULL ... NOTE: THIS CRACK IS MIDWAY BETWEEN BEARING POINTS (AT POINT WHERE ... WOULD BE EXPECTED TO OCCUR). CRACK IS PERPENDICULAR FOR MOST ... SLOPING. SEE PHOTOS ...

③ CRACK THRU SURFACE & THOSE FROM ③ TO ① ARE DEFINITELY PERPEN... PHOTO ... ESPECIALLY & ALSO ...

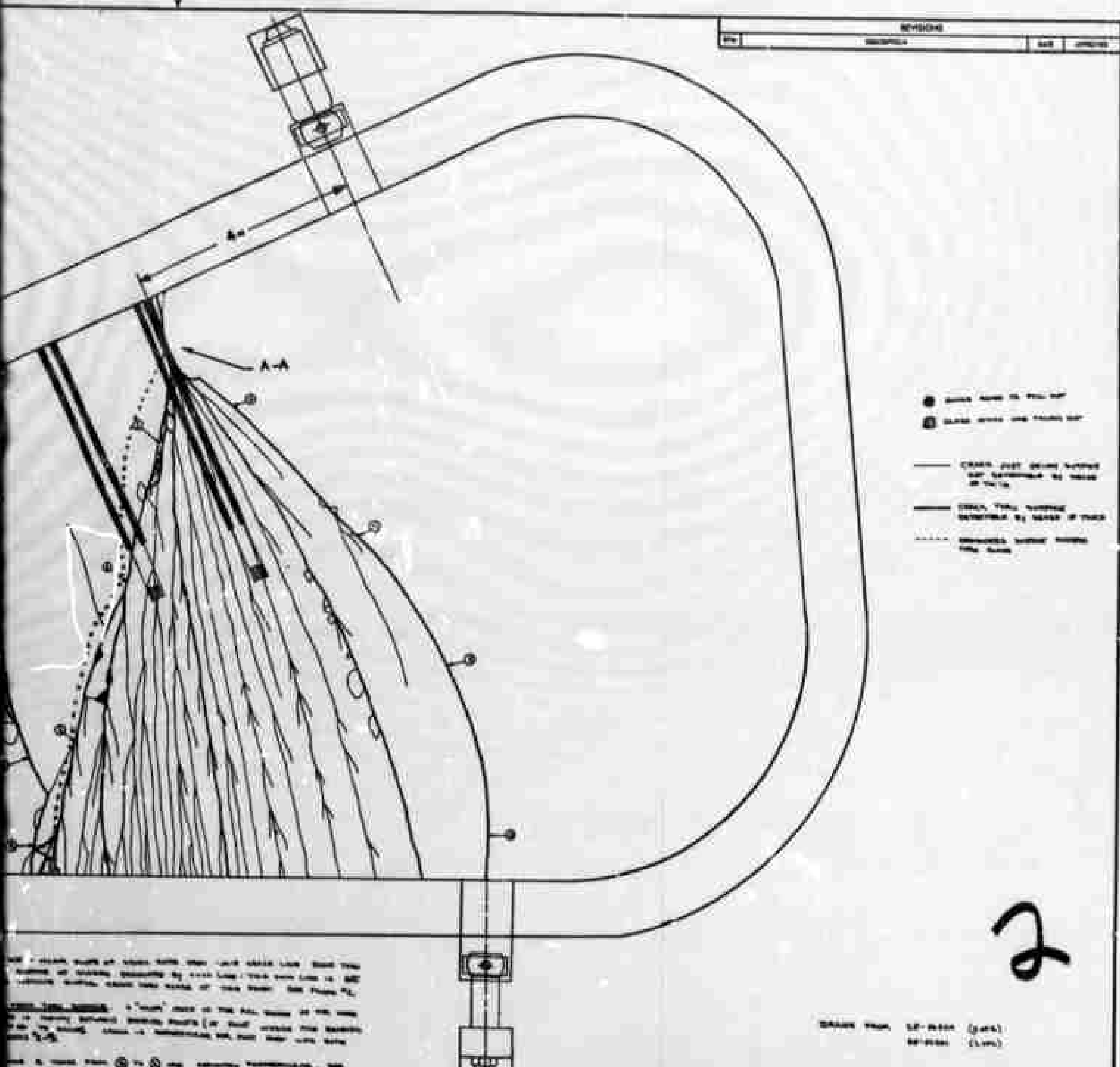

Lt Pharmer

U.S. AIR FORCE

FIGURE 35
Crack pattern: surface
.66 in. fused-silica.
2 Apr 1965 WPAFB, Ohio

DESIGN ACTIVITY AUTHENTICATION

AF33(615) 2013

D

SCALE 1/1

ENGINEERING DRAWING LAYOUT D

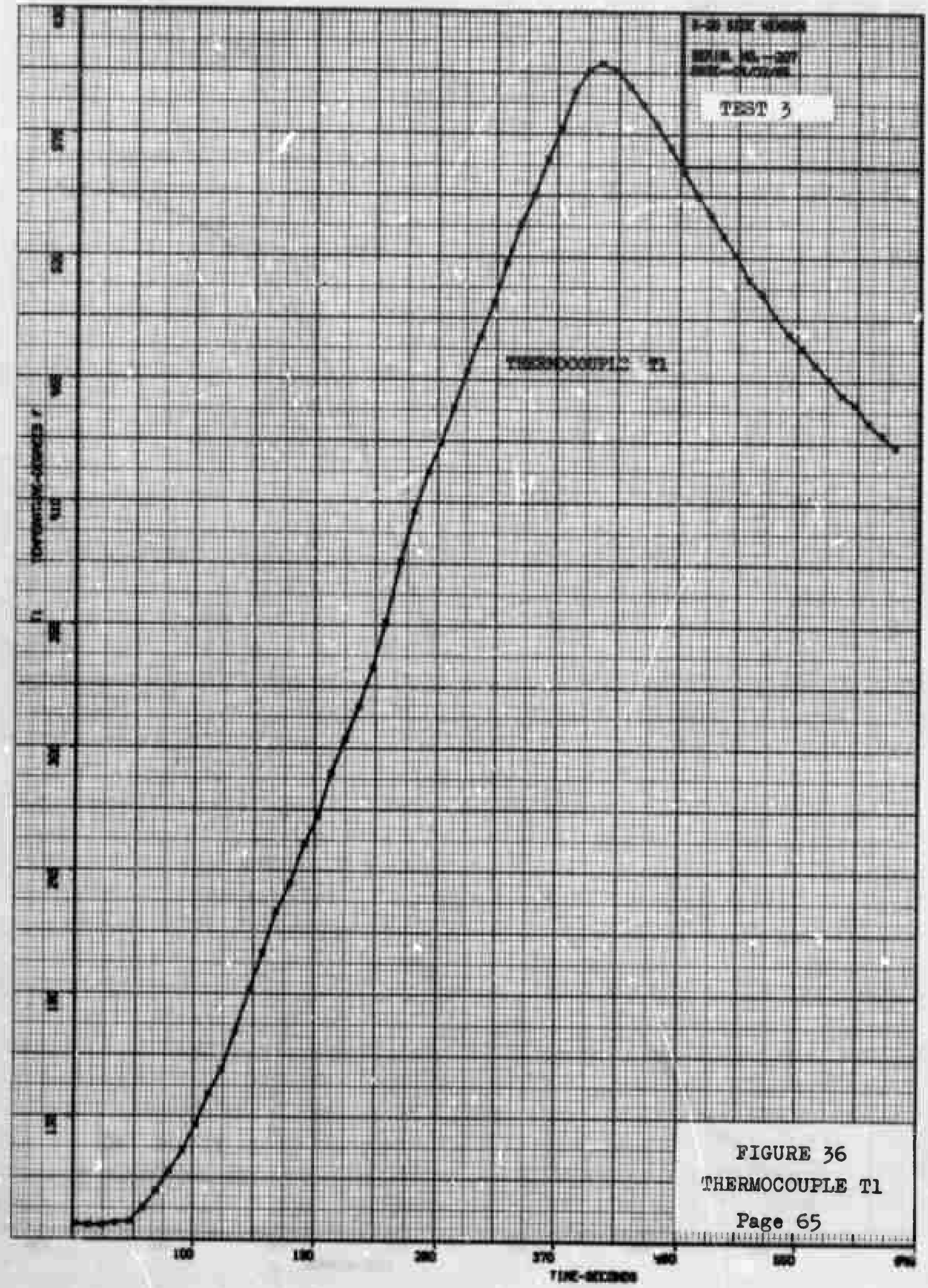

FIGURE 36
THERMOCOUPLE T1

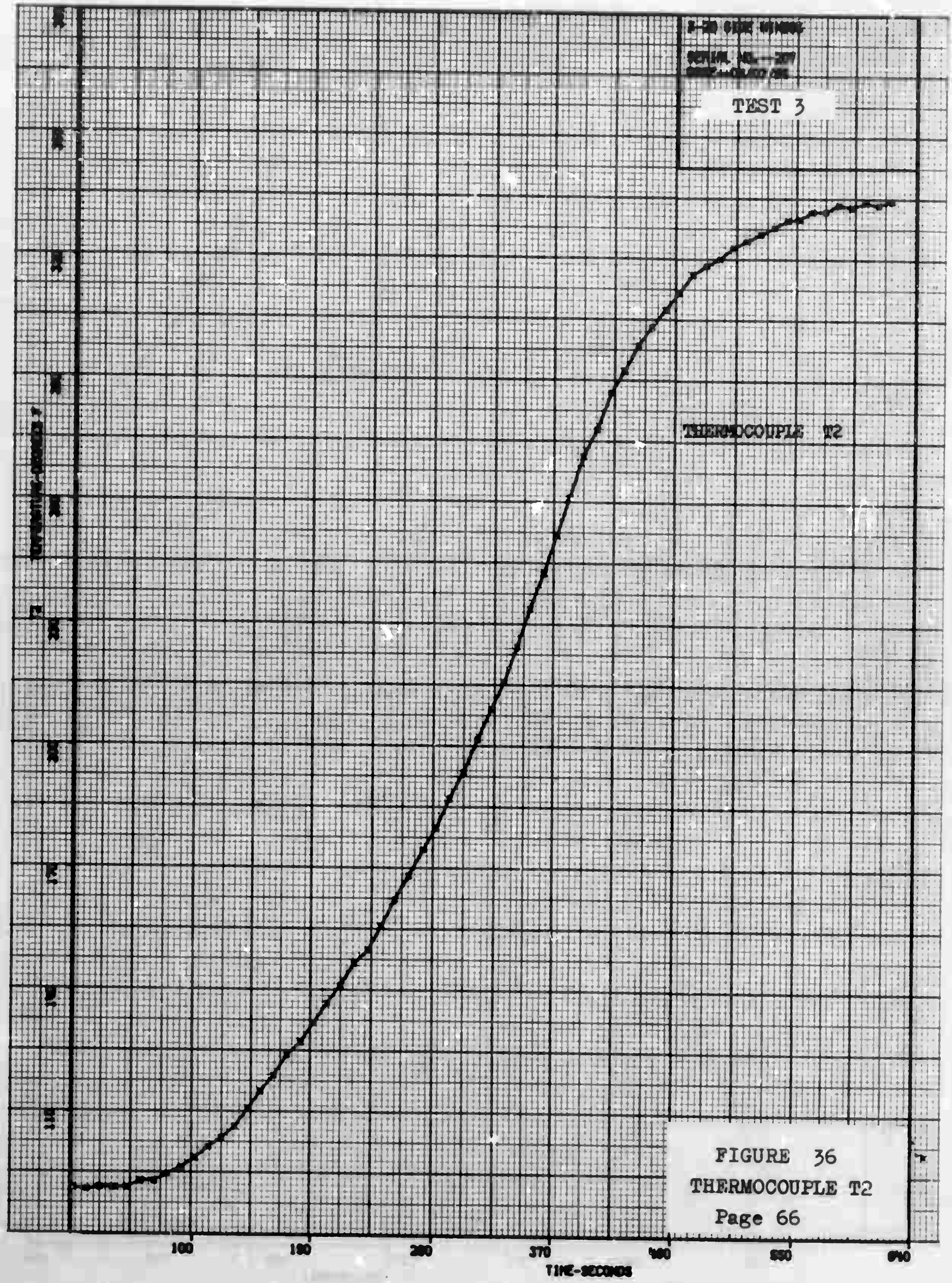

FIGURE 36
THERMOCOUPLE T2

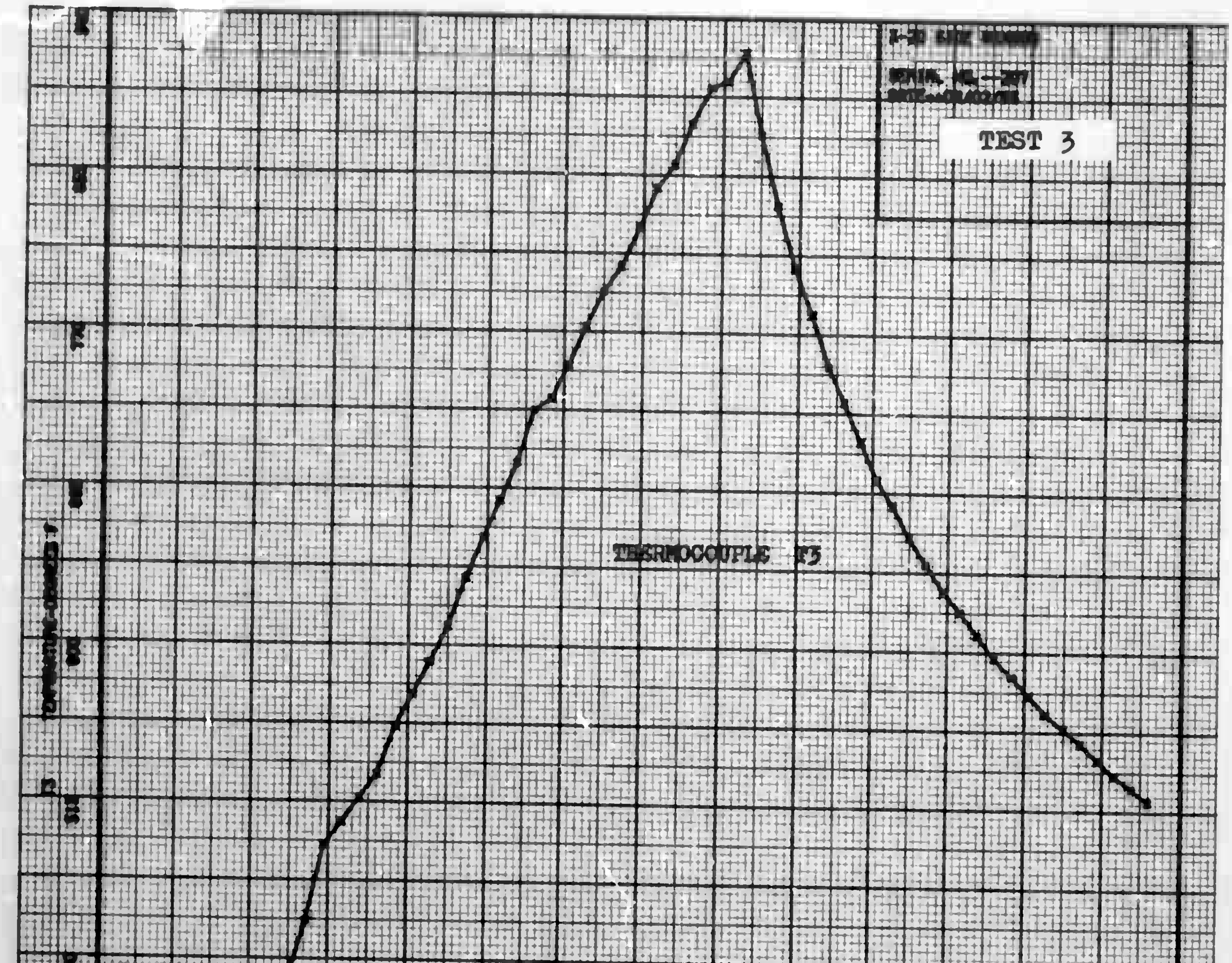

FIGURE 36
THERMOCOUPLE T3

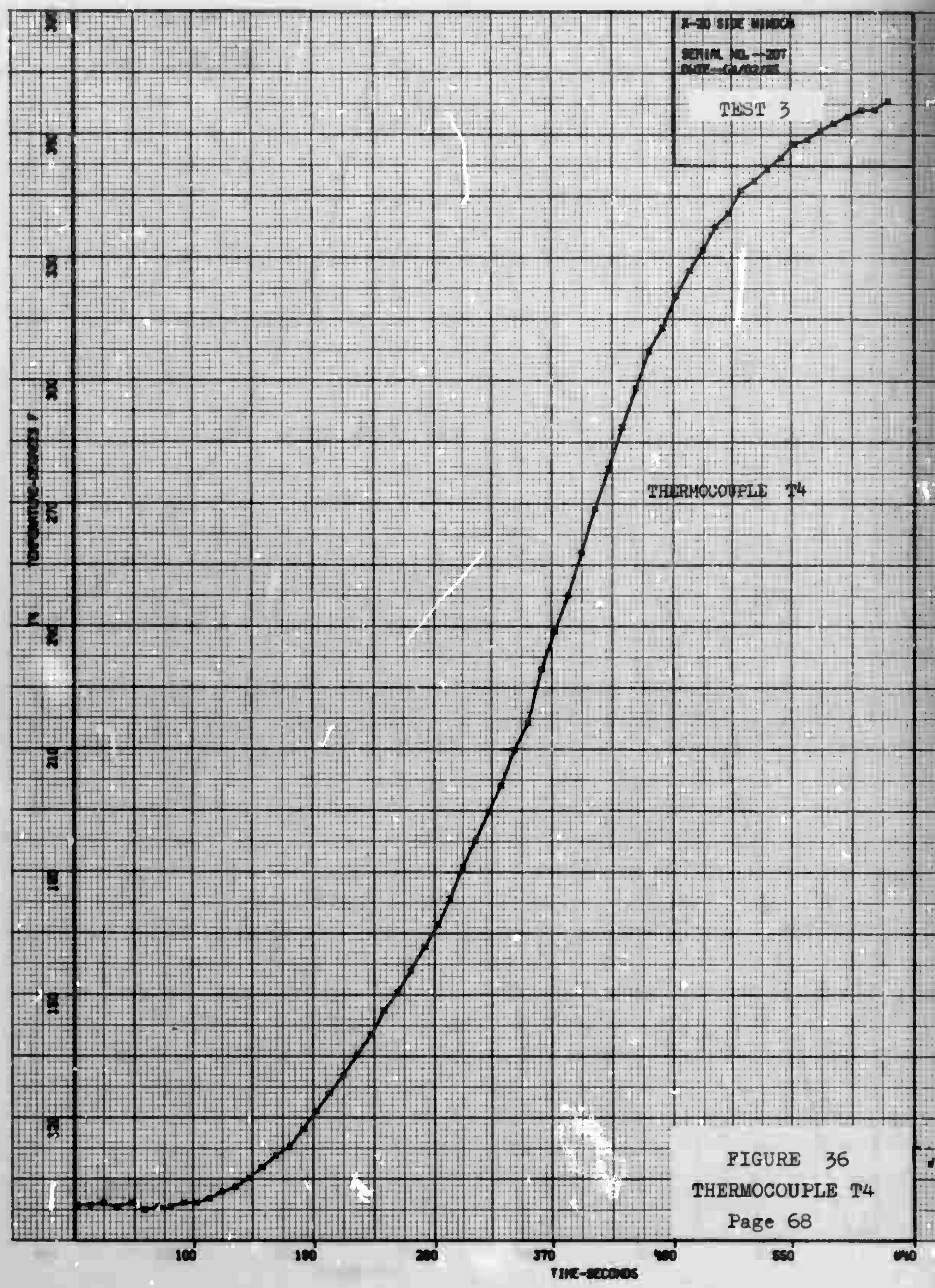

FIGURE 36
THERMOCOUPLE T4
Page 68

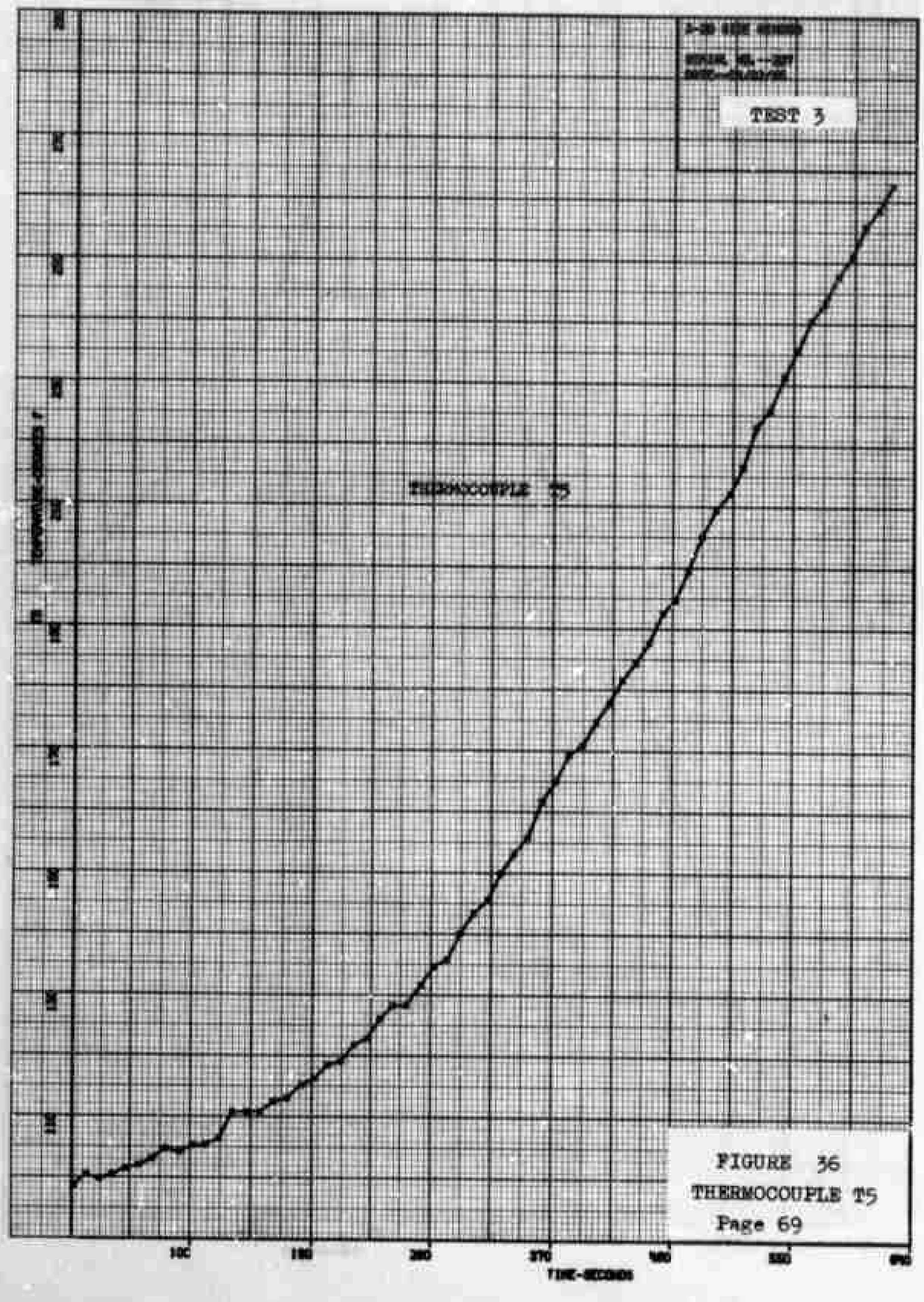

FIGURE 36
THERMOCOUPLE T5
Page 69

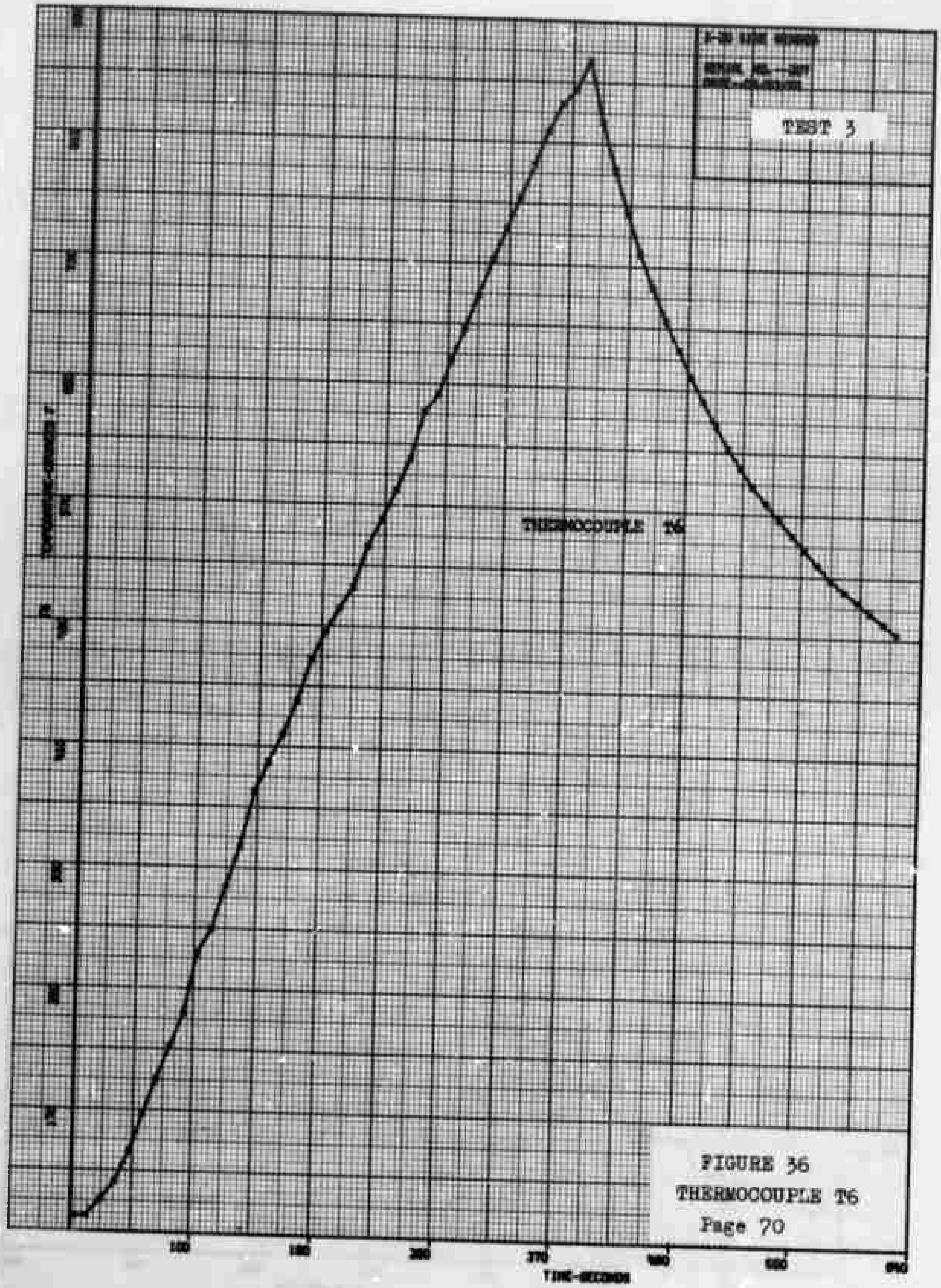

FIGURE 36
THERMOCOUPLE T6
Page 70

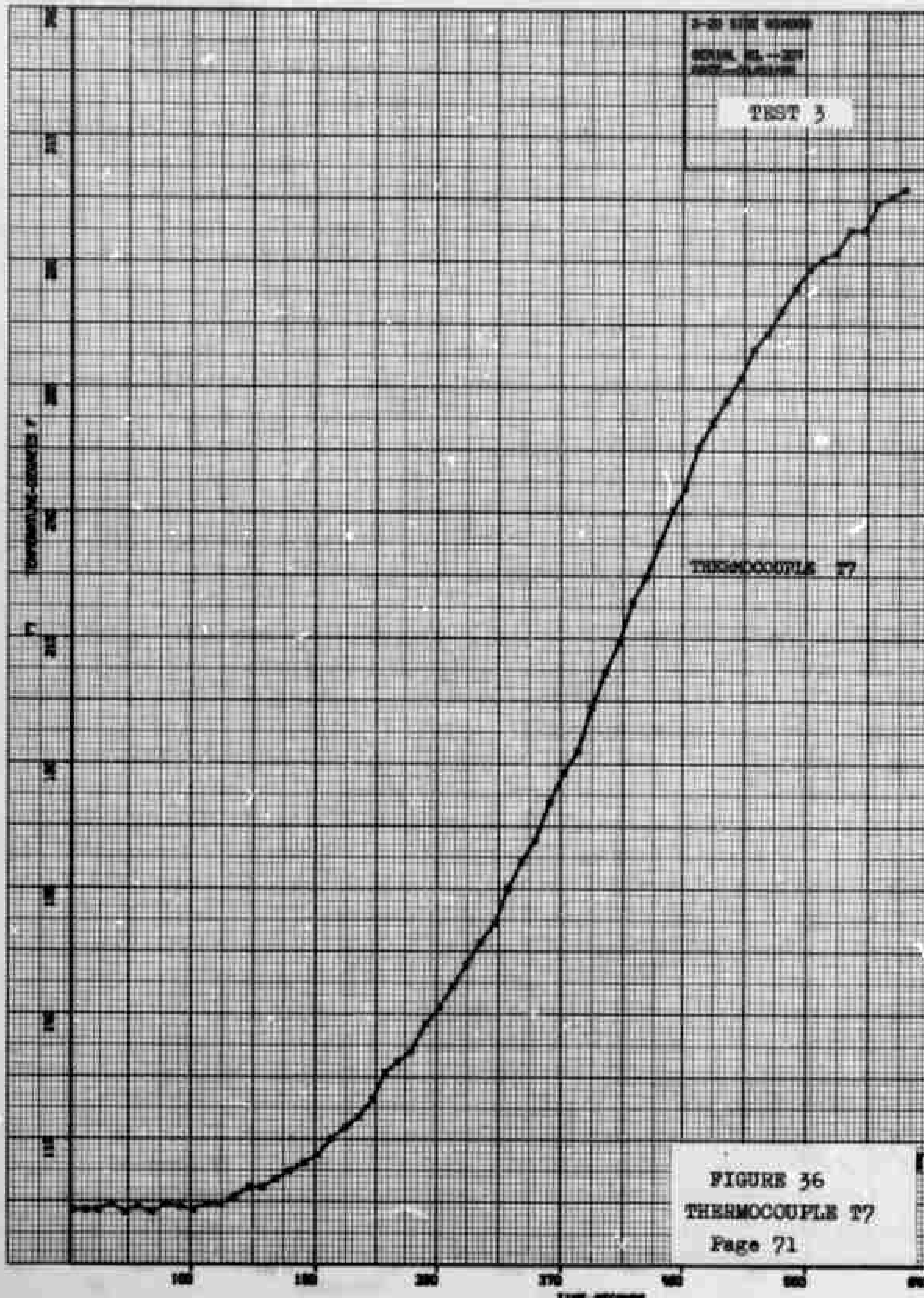

FIGURE 36
THERMOCOUPLE T7
Page 71

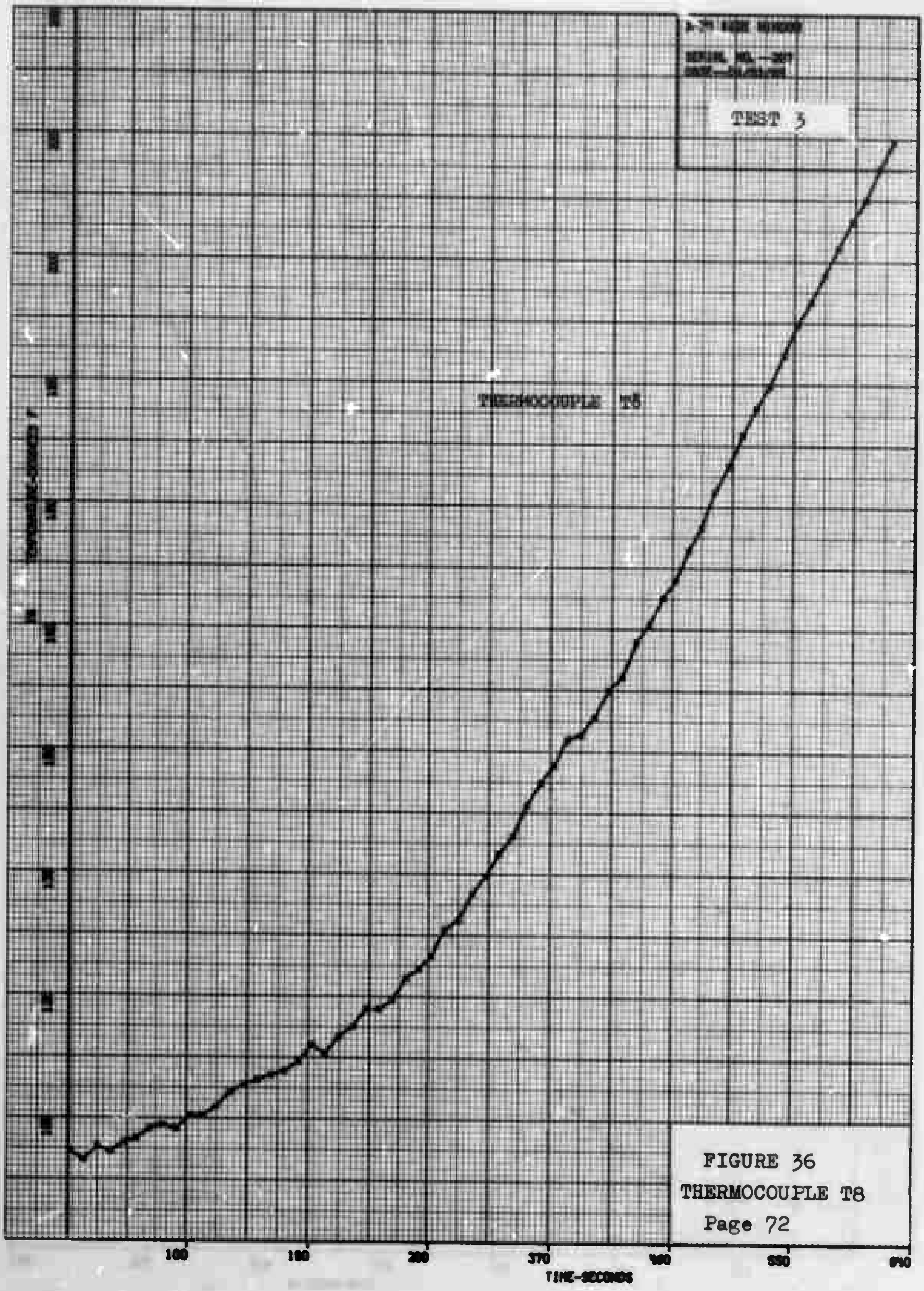

FIGURE 36
THERMOCOUPLE T8
Page 72

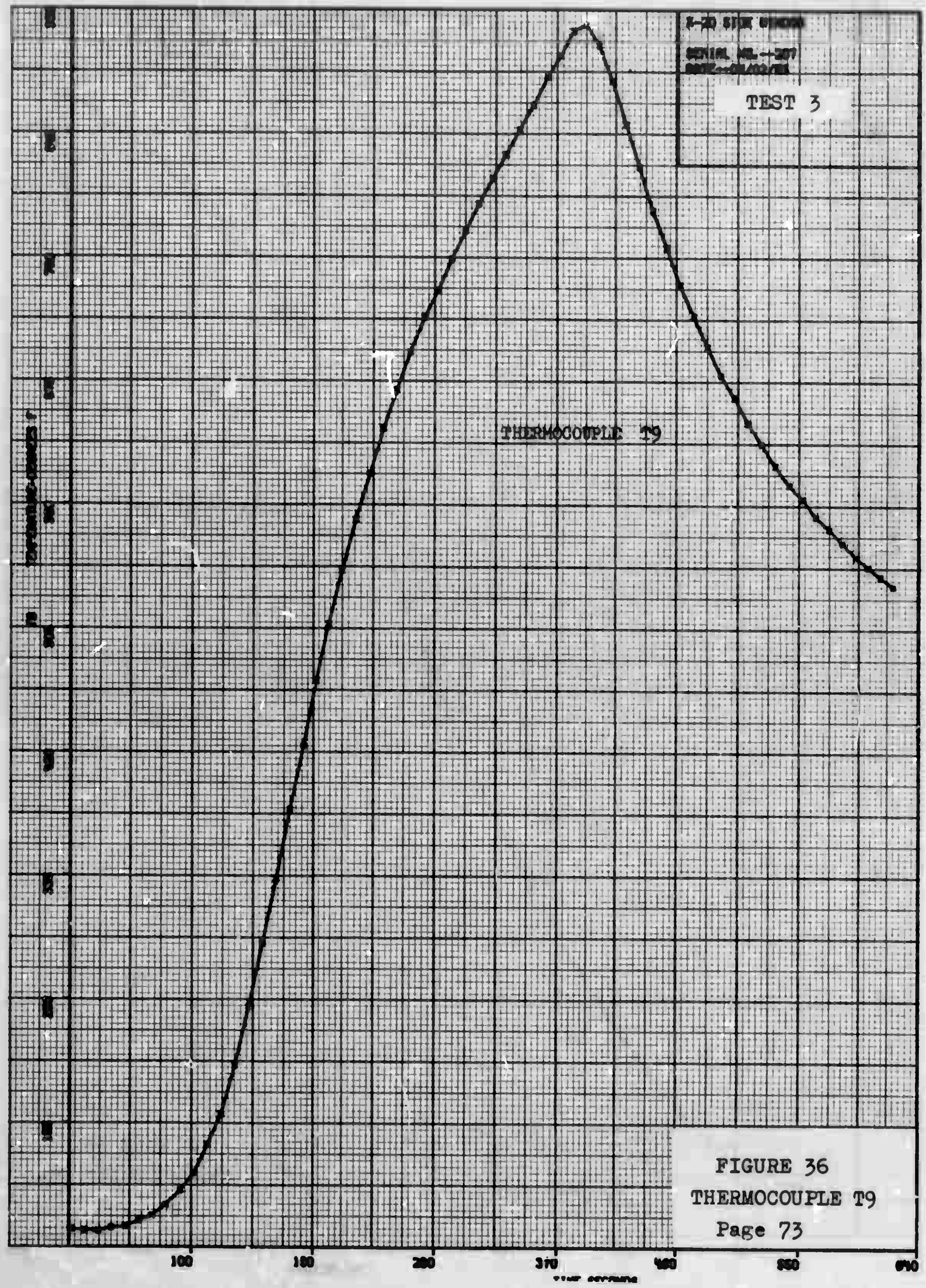

FIGURE 36
THERMOCOUPLE T9

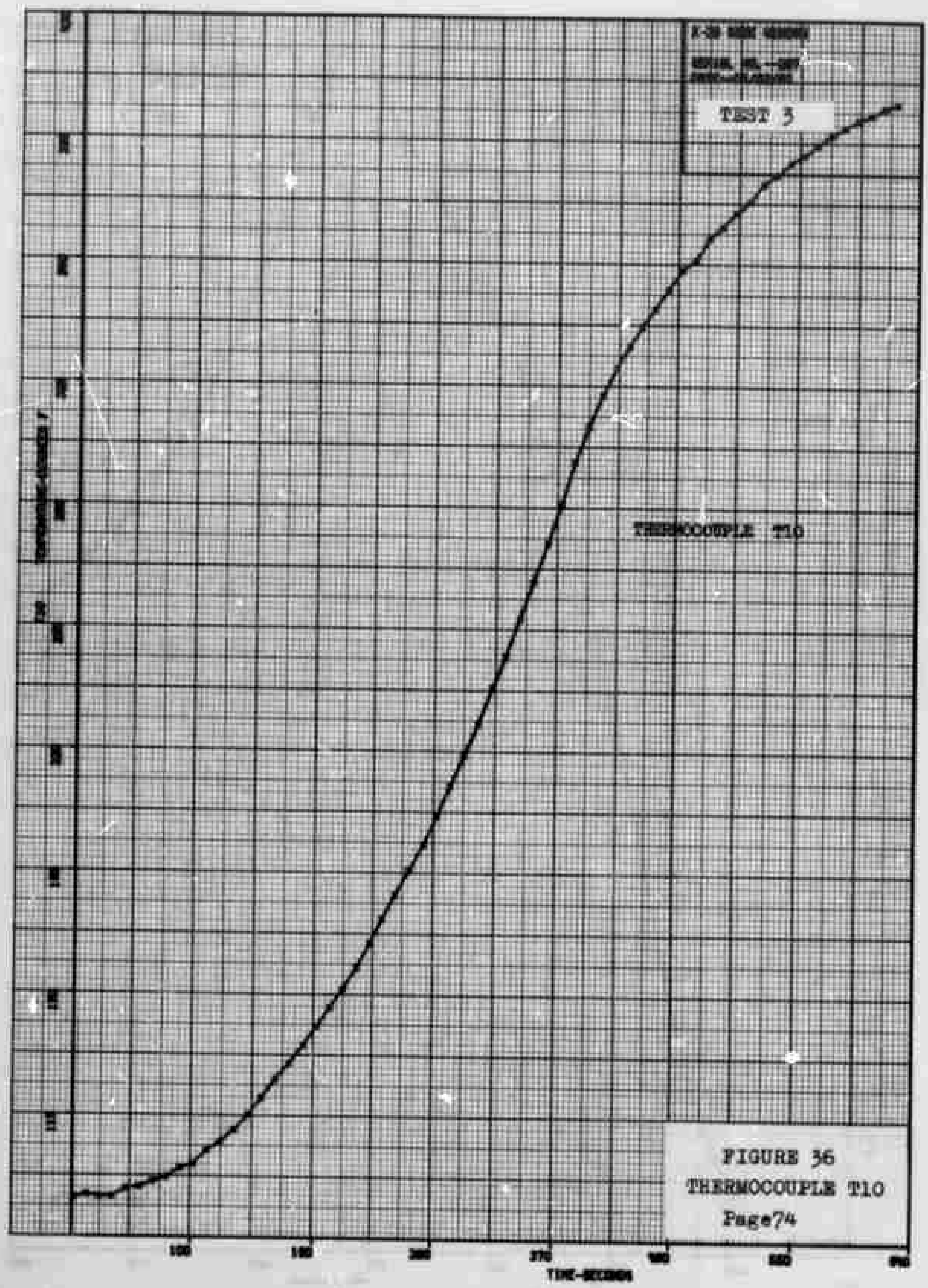

FIGURE 36
THERMOCOUPLE T10
Page74

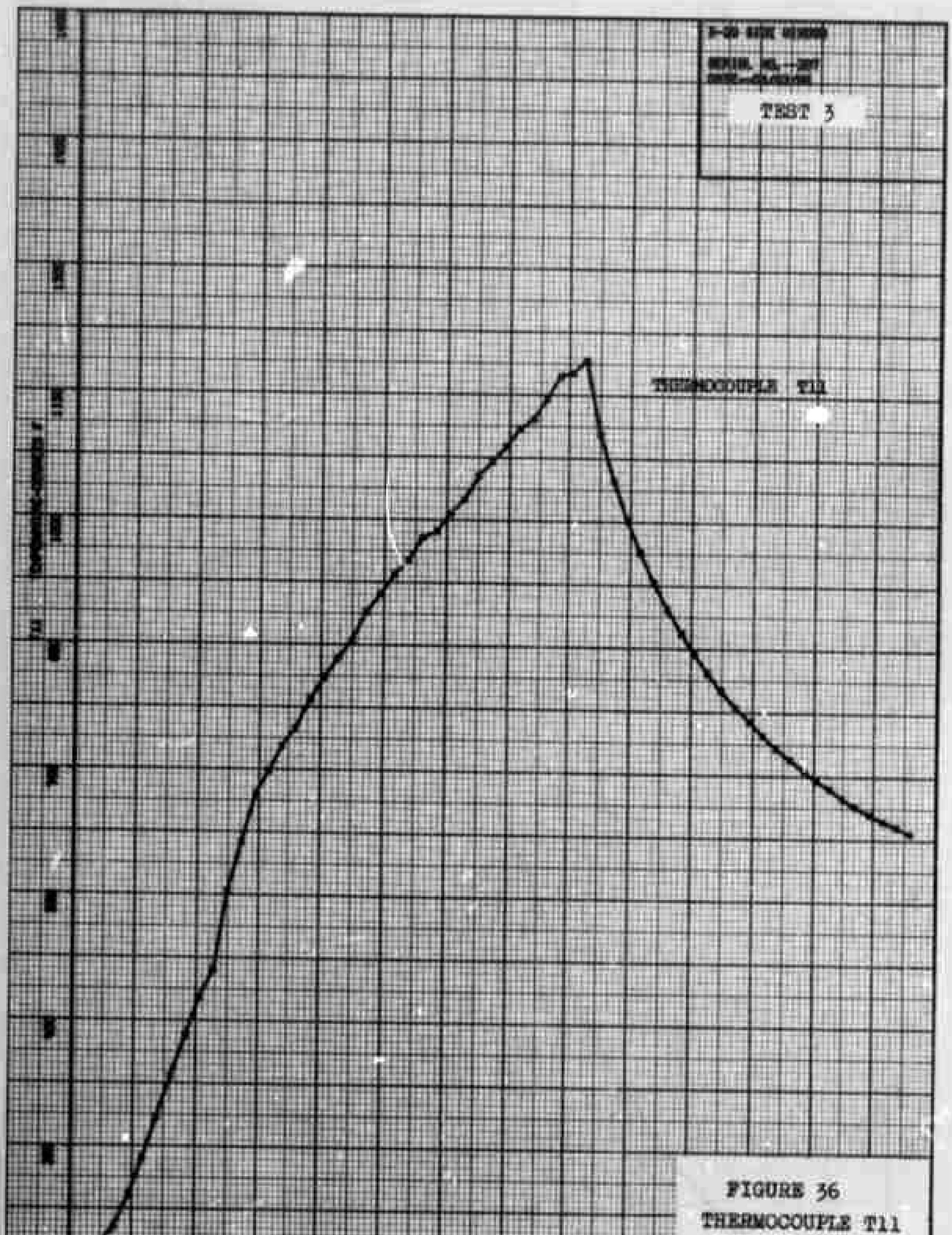

FIGURE 36
THERMOCOUPLE T11

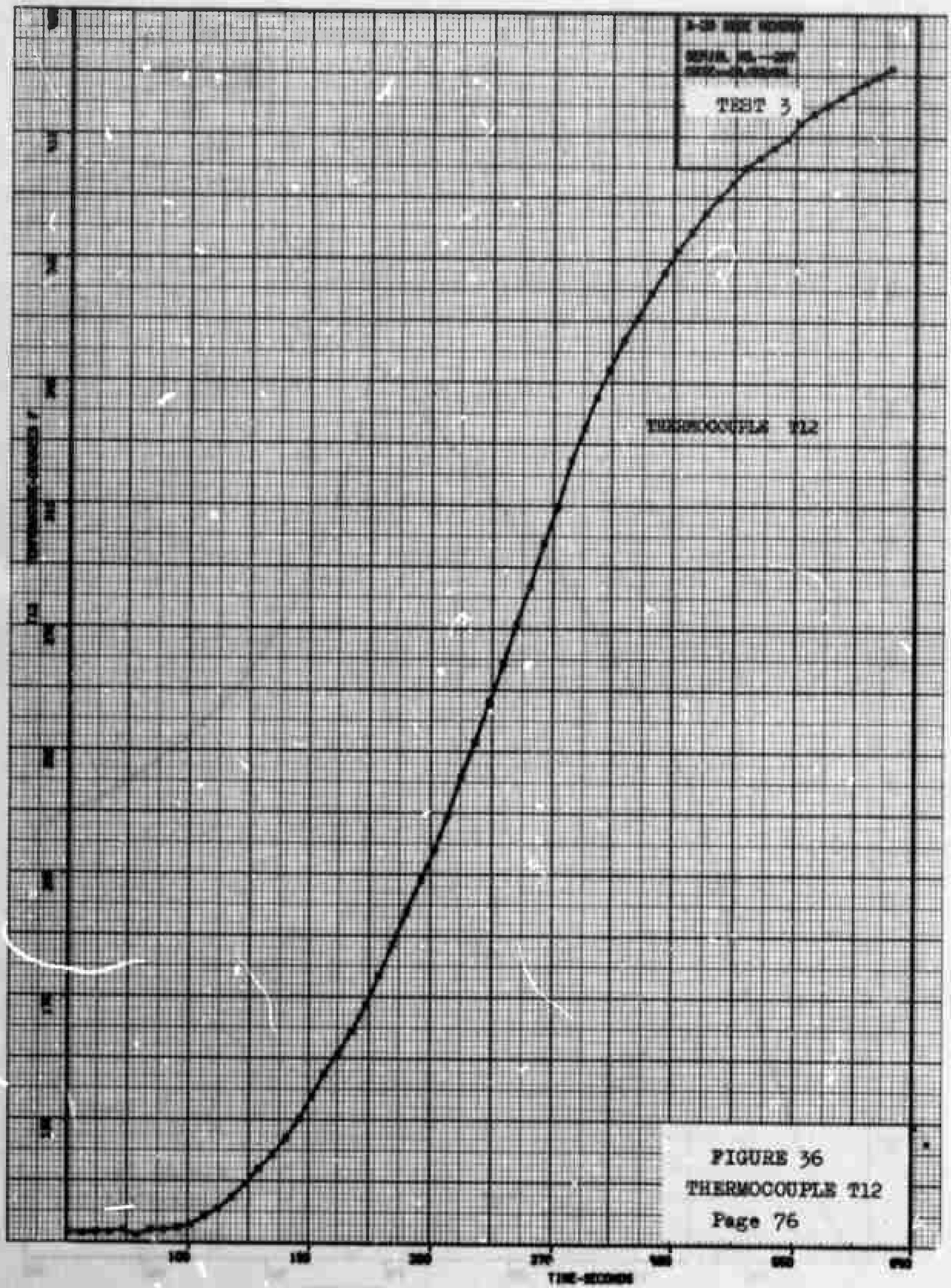

FIGURE 36
THERMOCOUPLE T12
Page 76

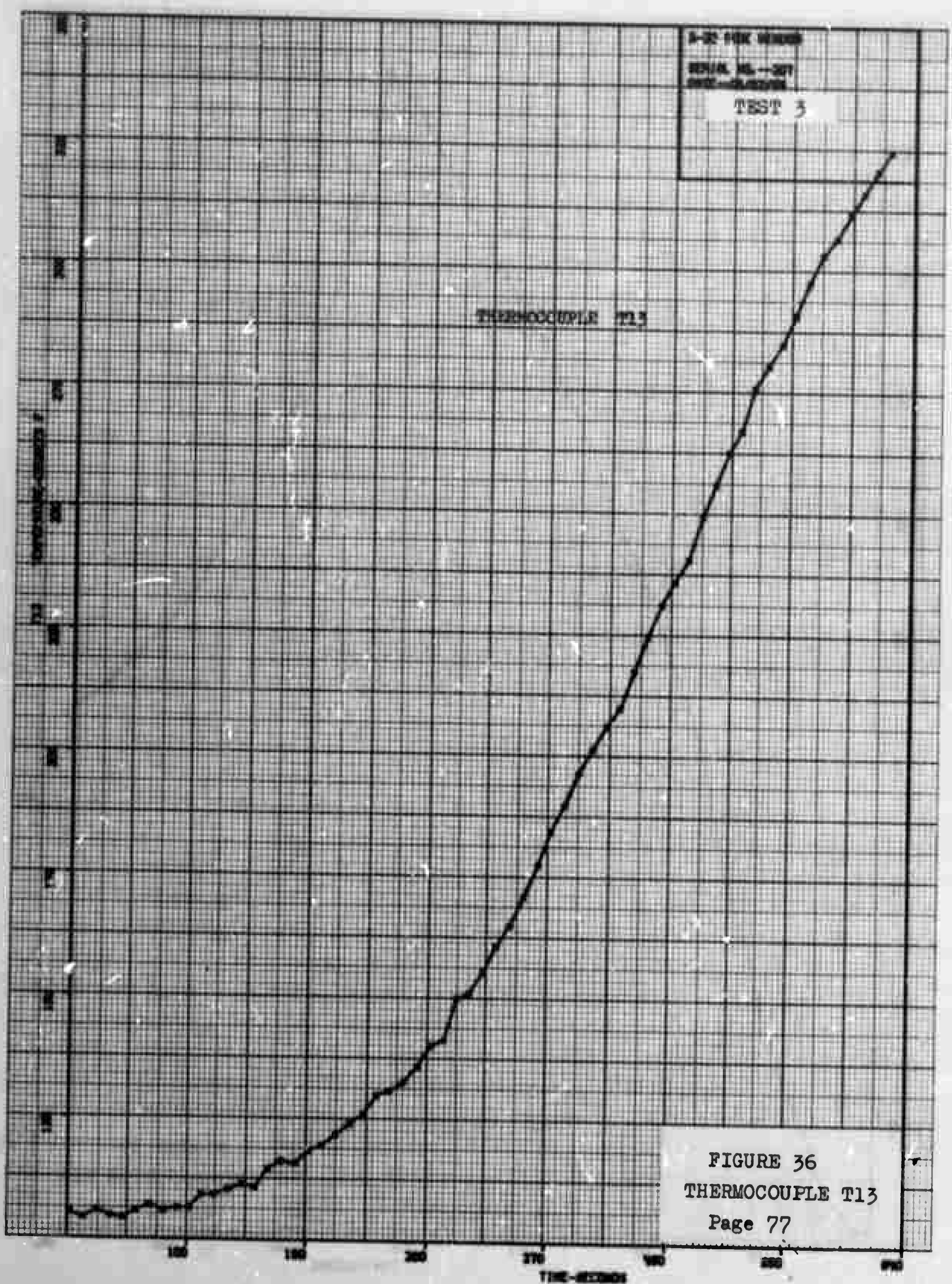

FIGURE 36
THERMOCOUPLE T13

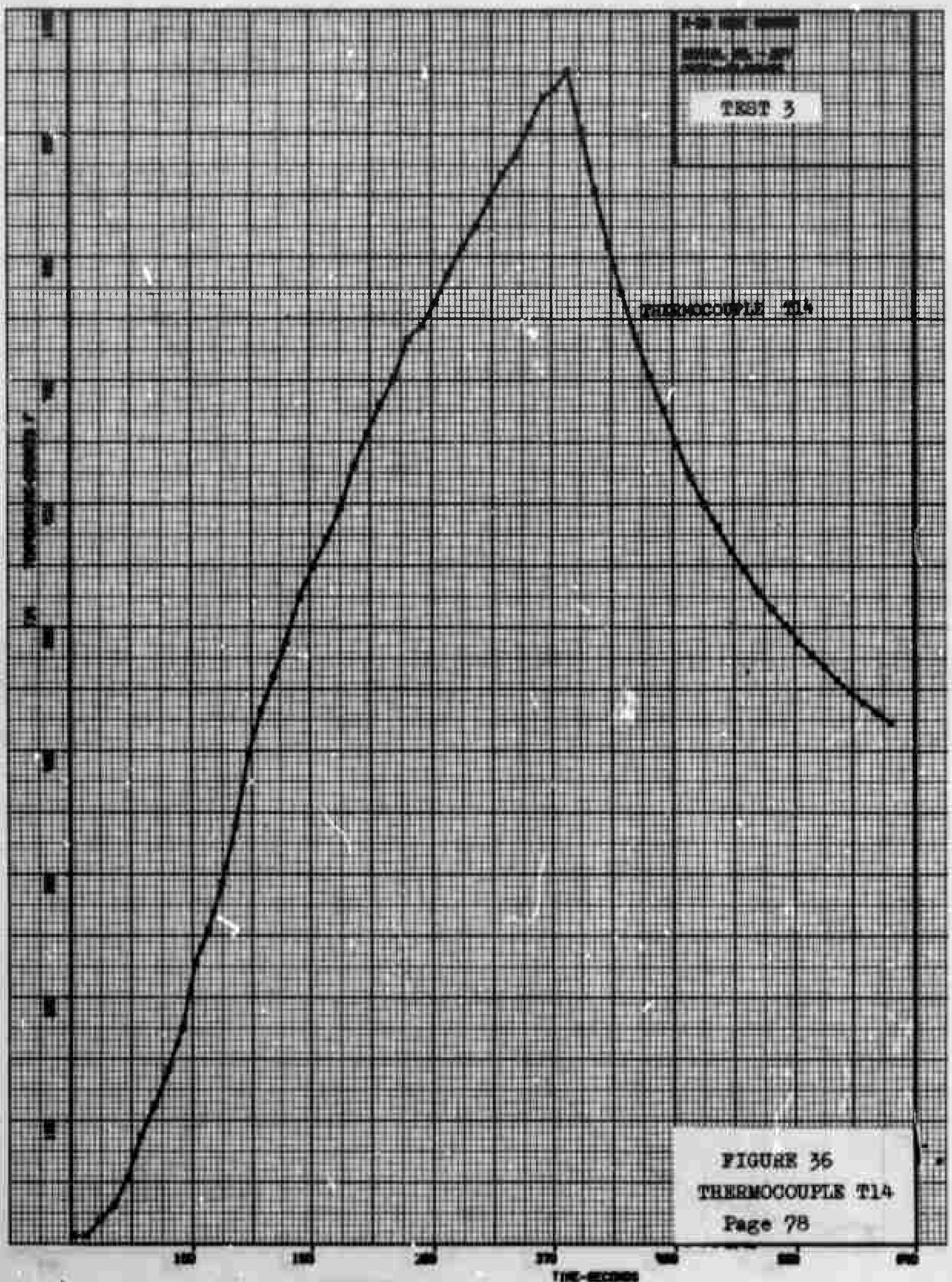

FIGURE 36
THERMOCOUPLE T14

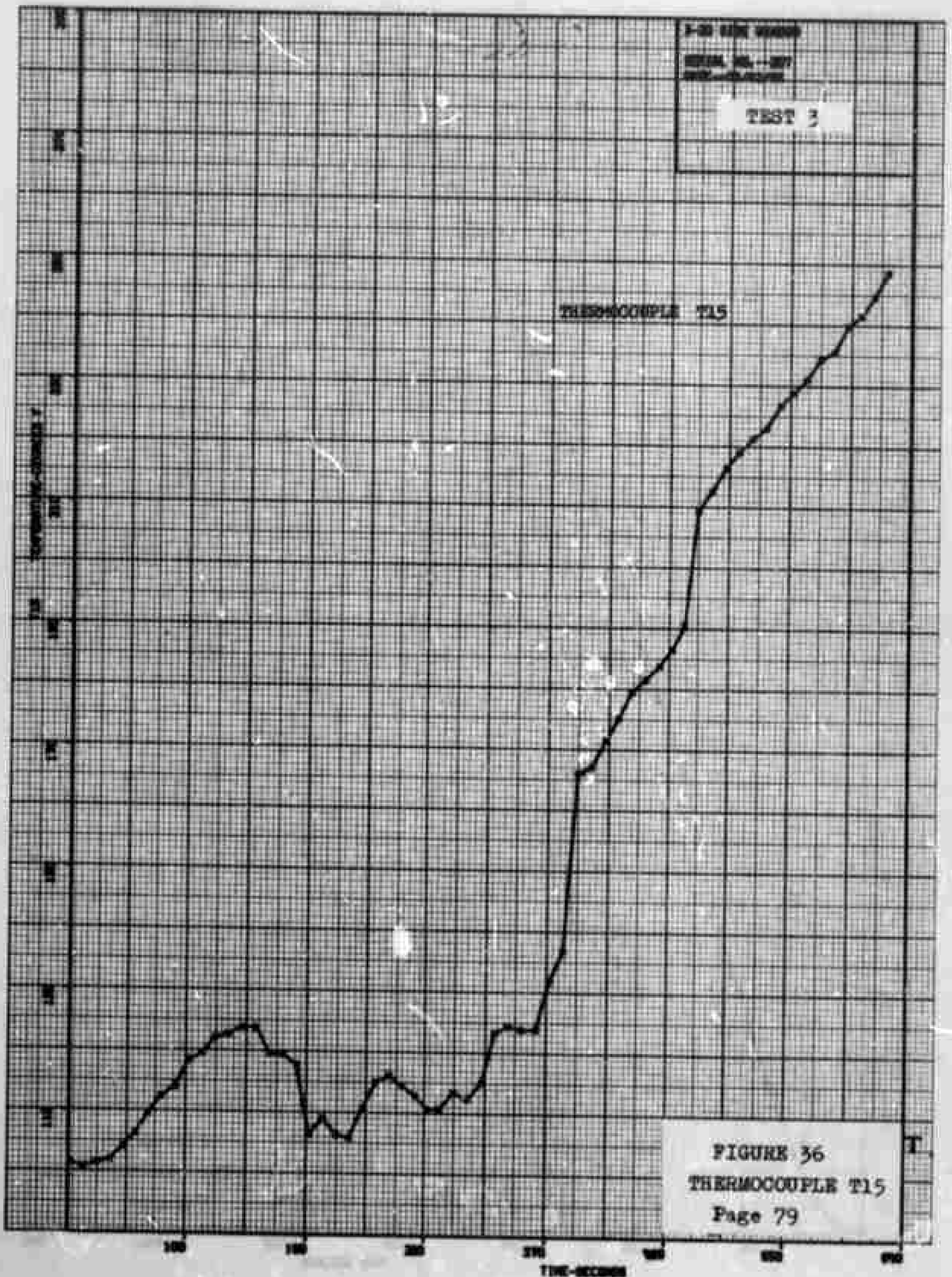

FIGURE 36
THERMOCOUPLE T15
Page 79

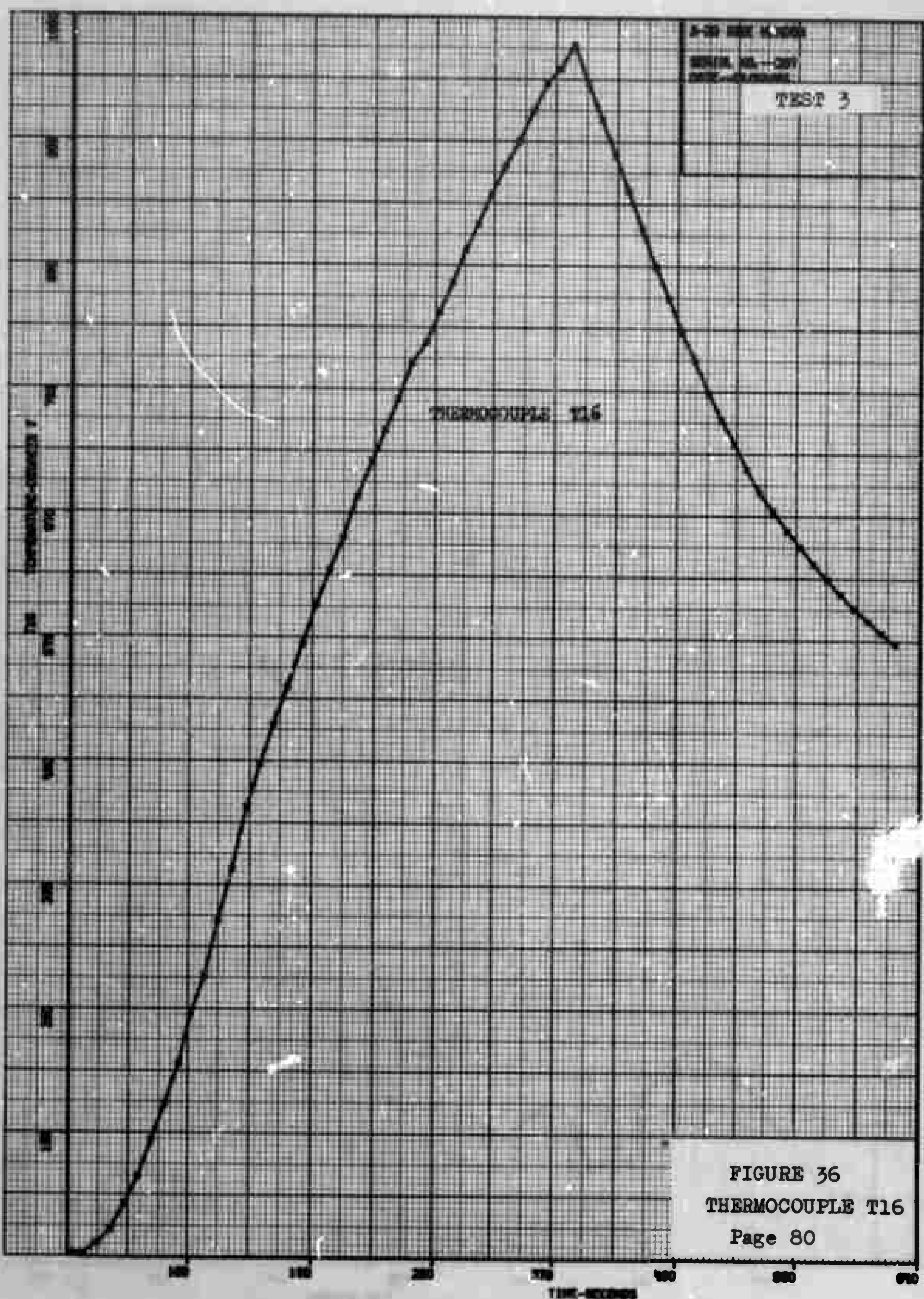

FIGURE 36
THERMOCOUPLE T16
Page 80

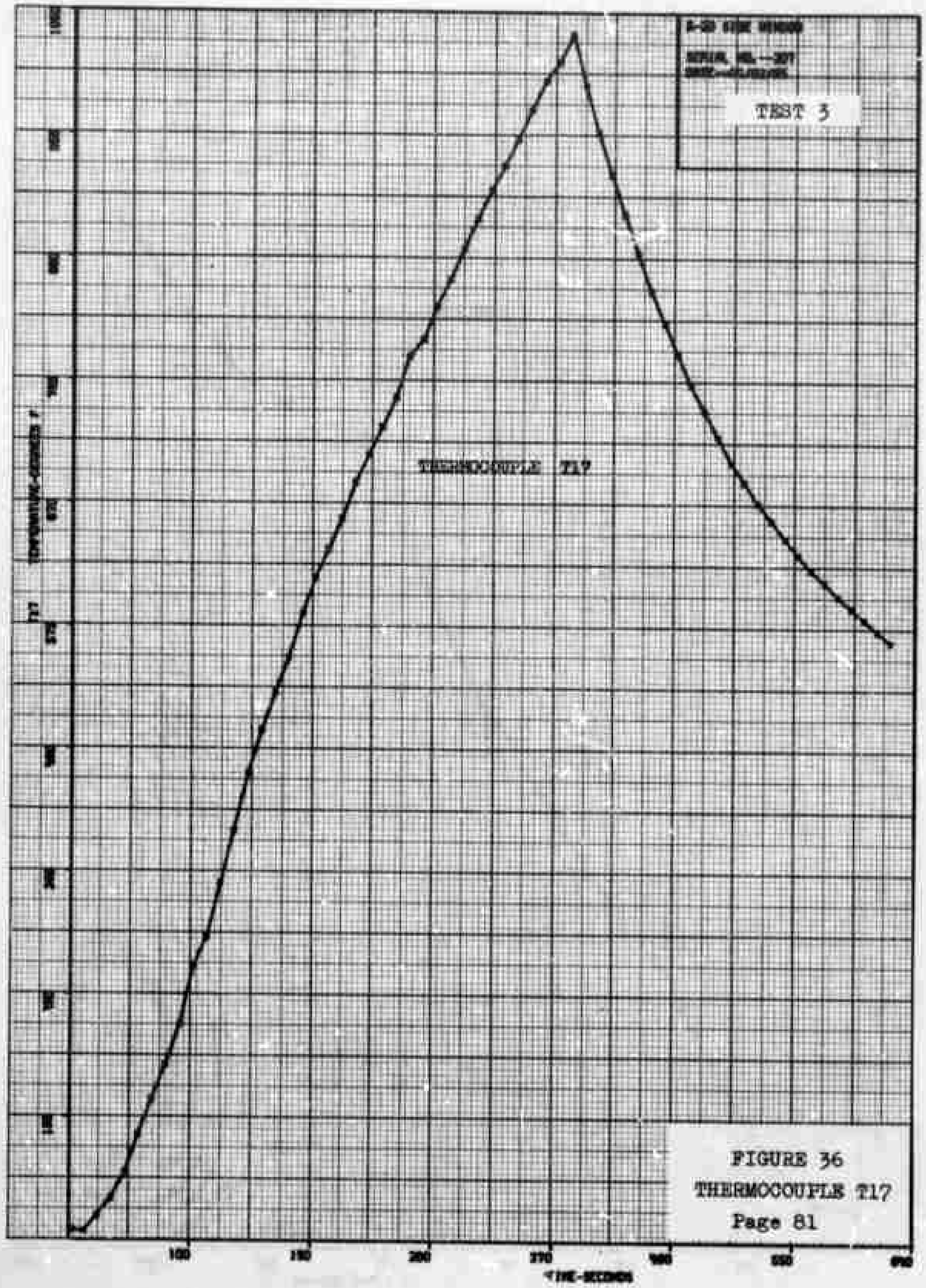

FIGURE 36
THERMOCOUPLE T17
Page 81

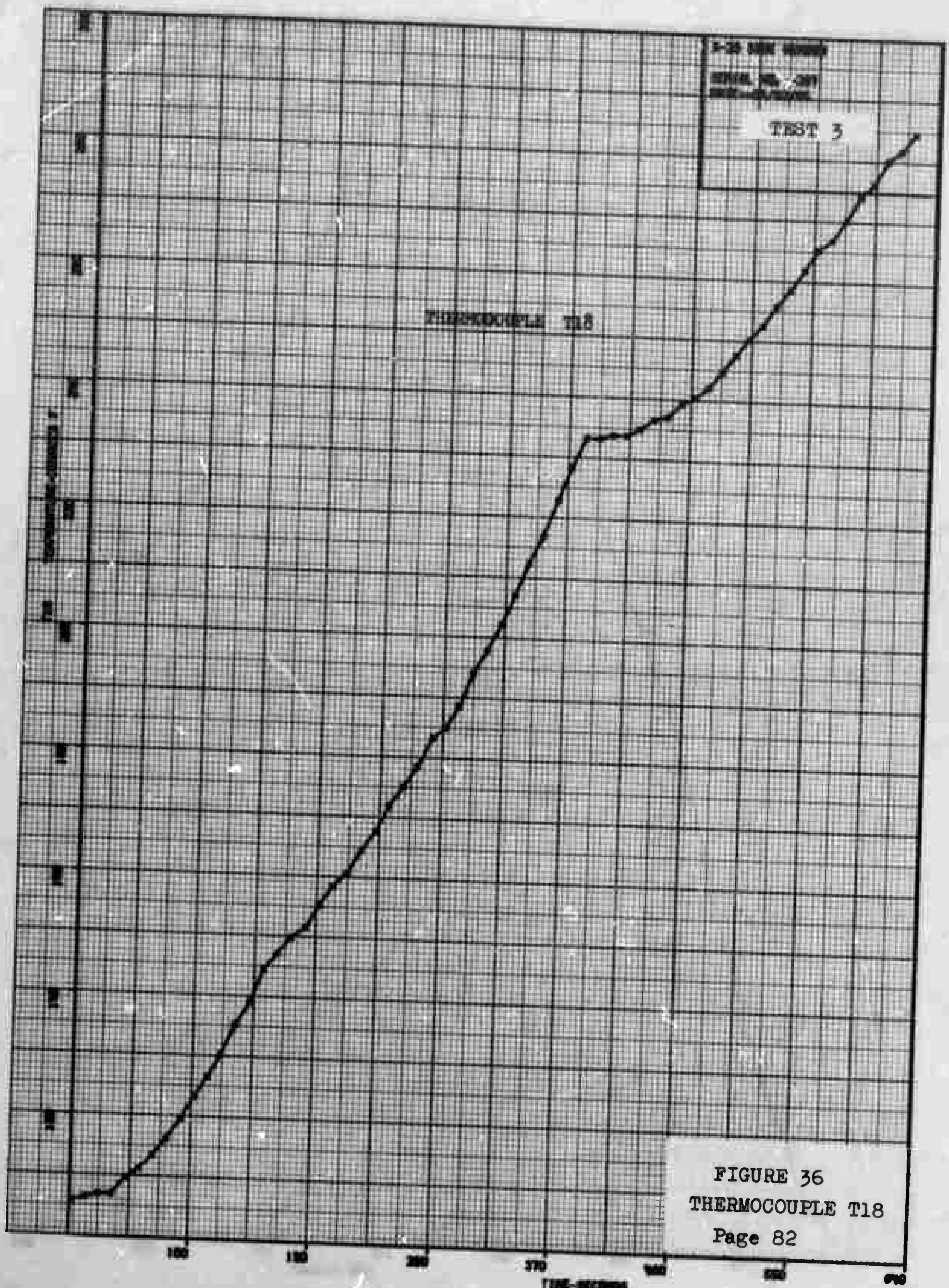

FIGURE 36
THERMOCOUPLE T18
Page 82

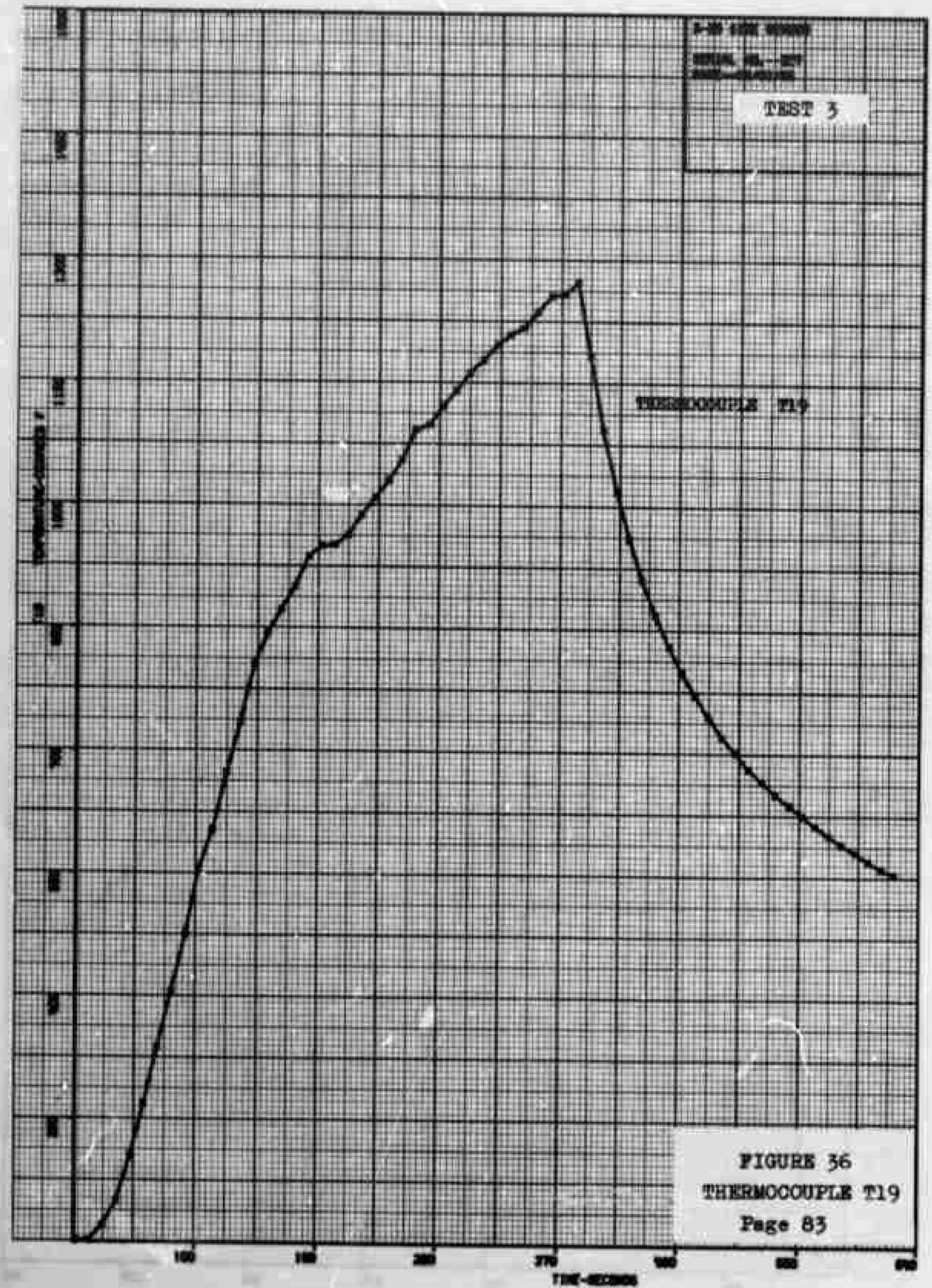

FIGURE 36
THERMOCOUPLE T19
Page 83

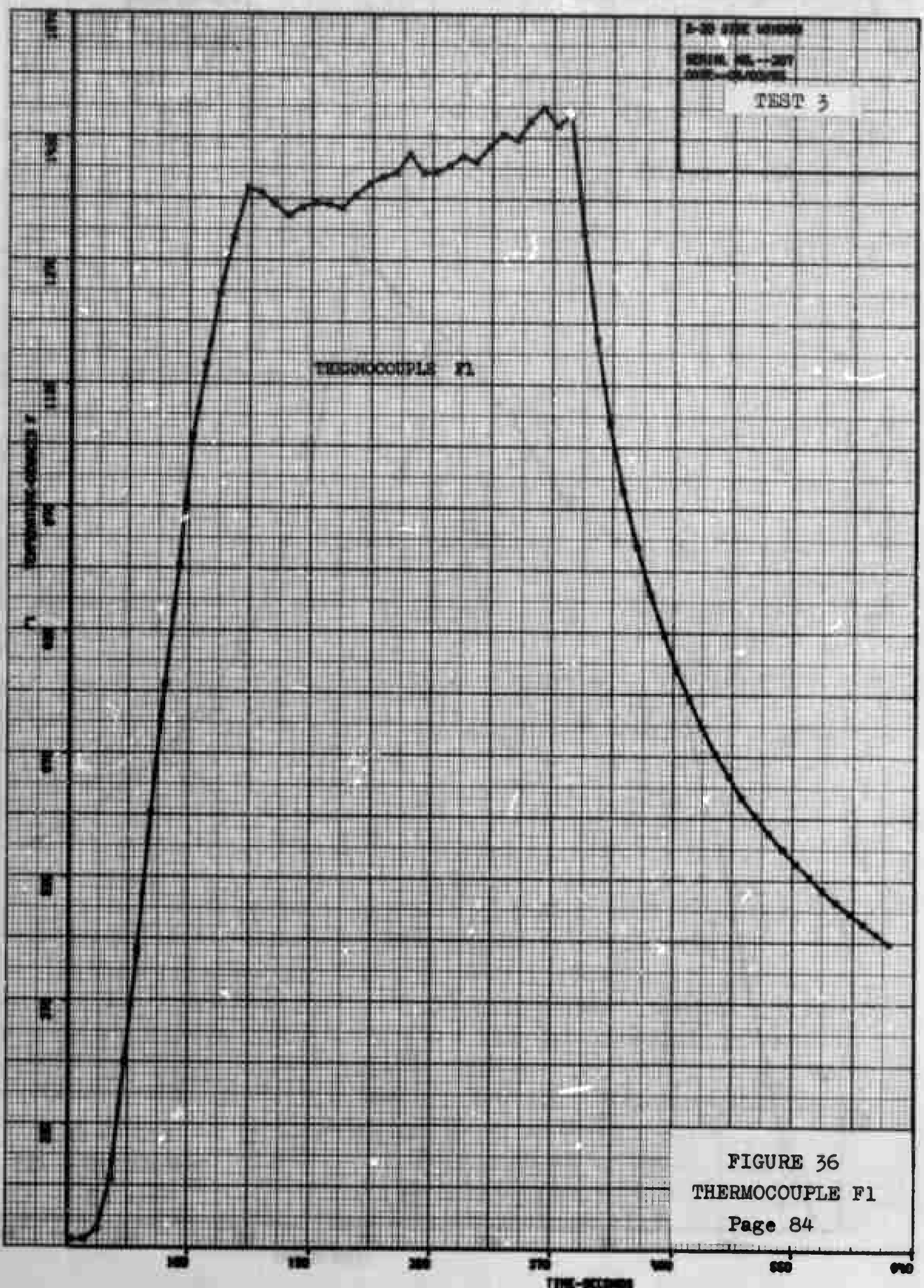

FIGURE 36
THERMOCOUPLE F1
Page 84

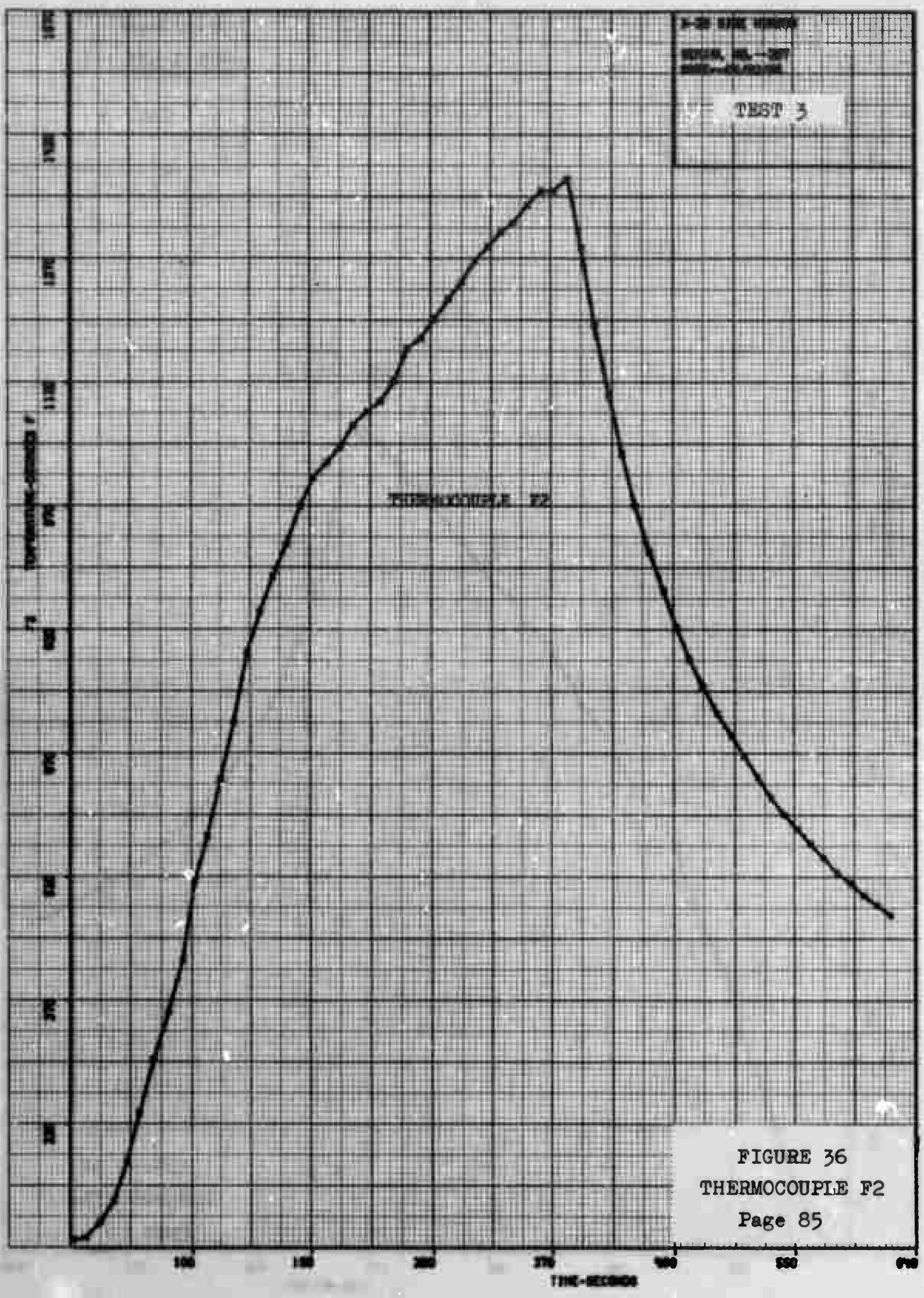

FIGURE 36
THERMOCOUPLE F2

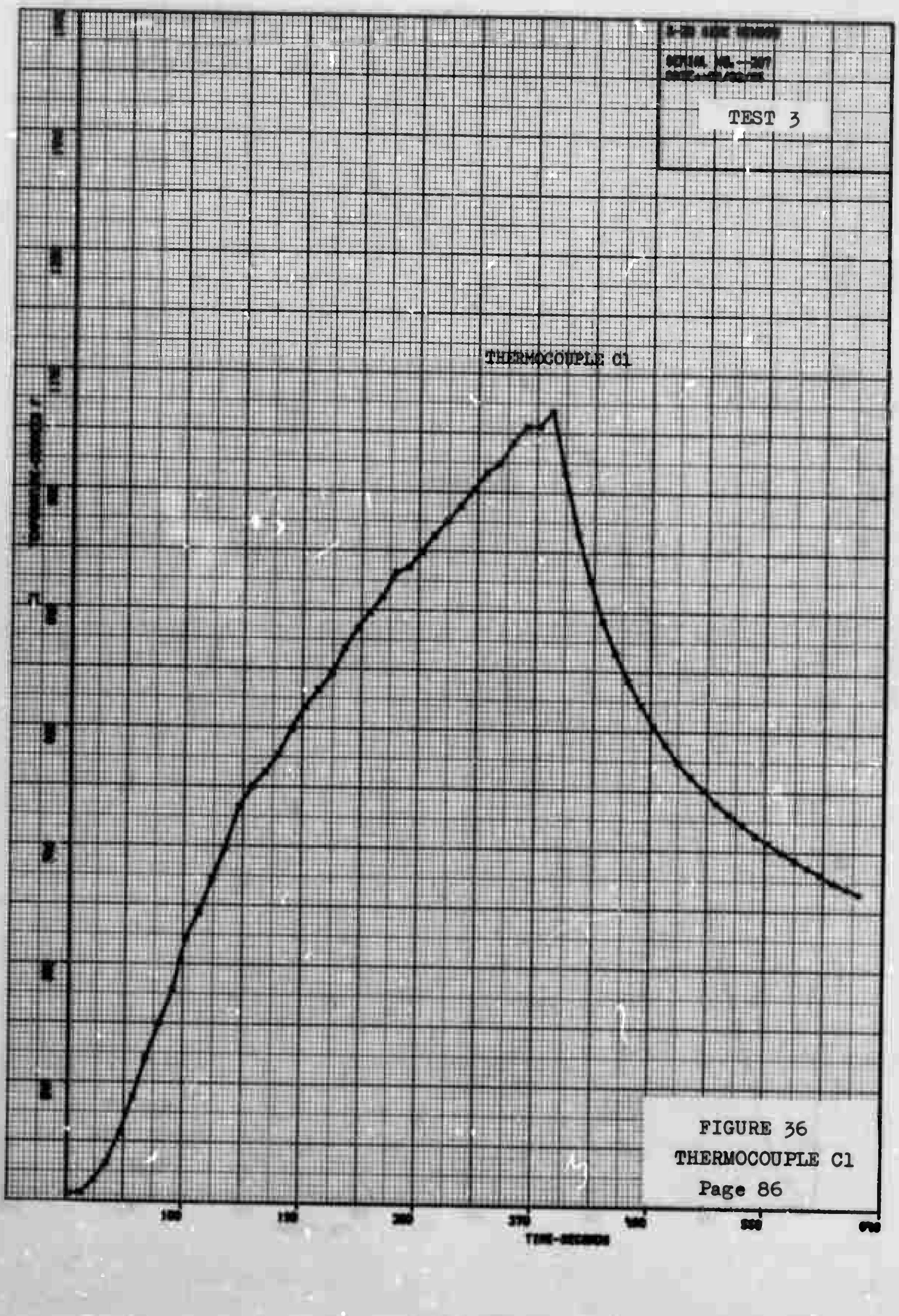

FIGURE 36
THERMOCOUPLE C1

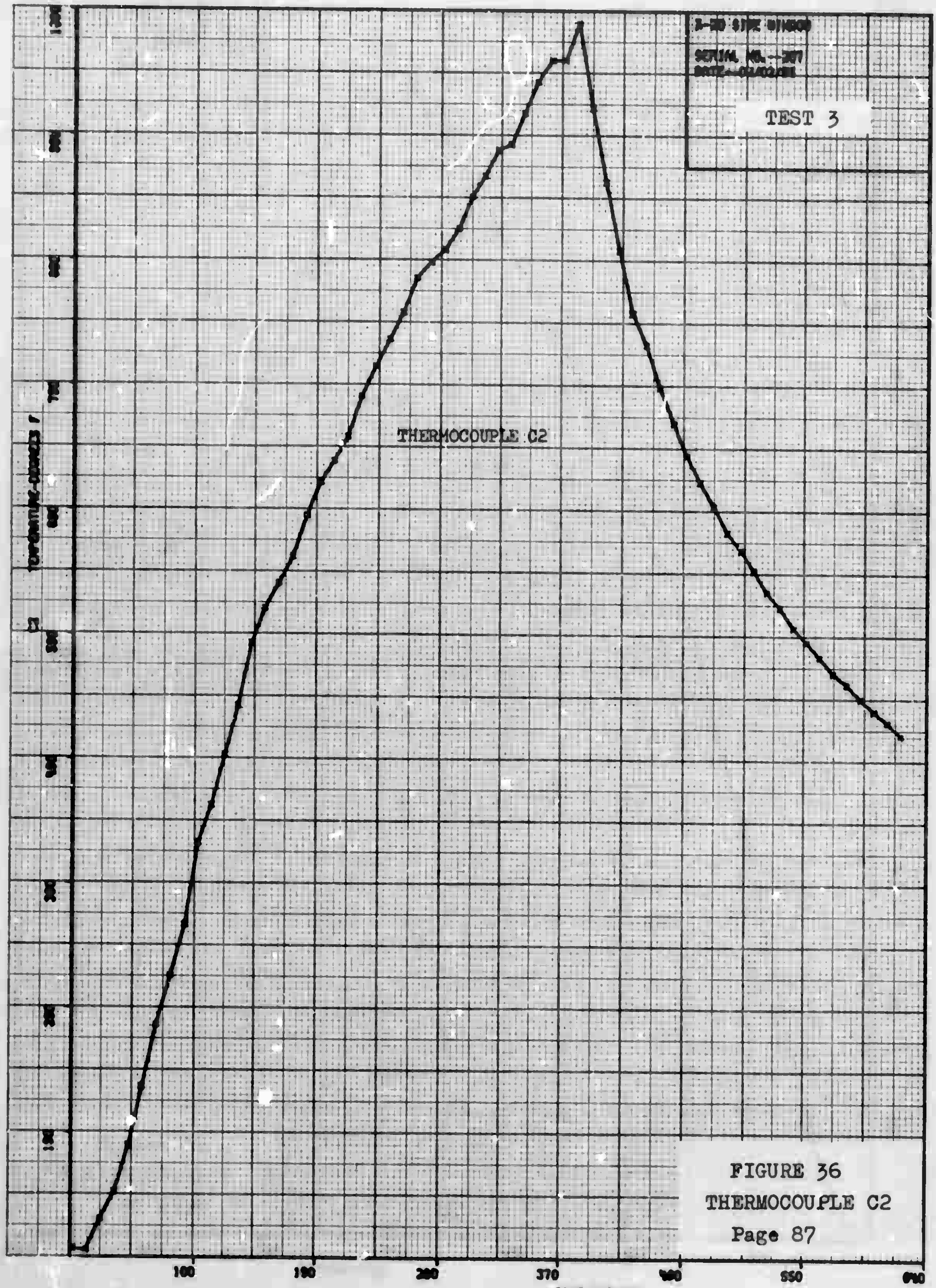

FIGURE 36
THERMOCOUPLE C2

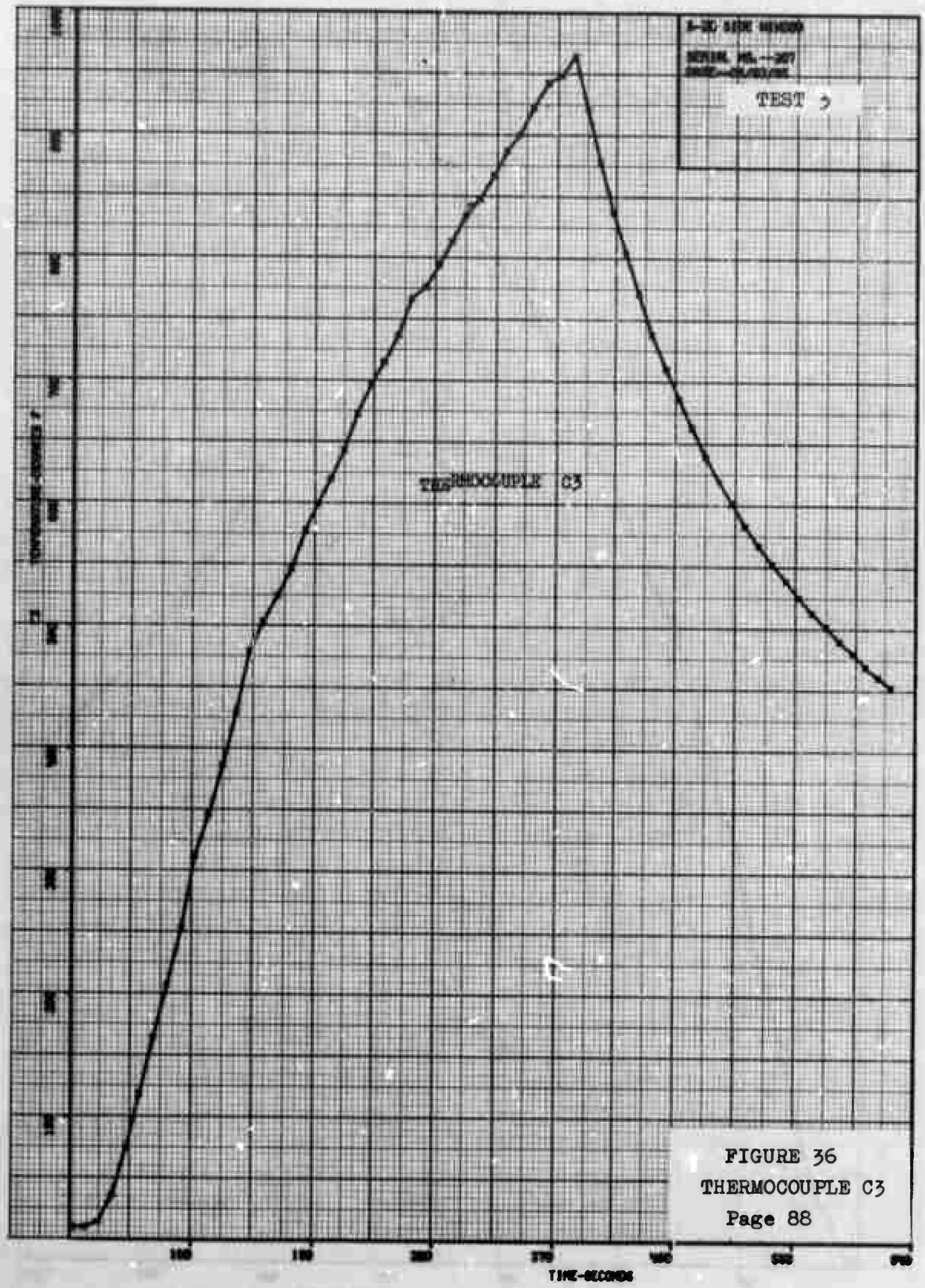

FIGURE 36
THERMOCOUPLE C3
Page 88

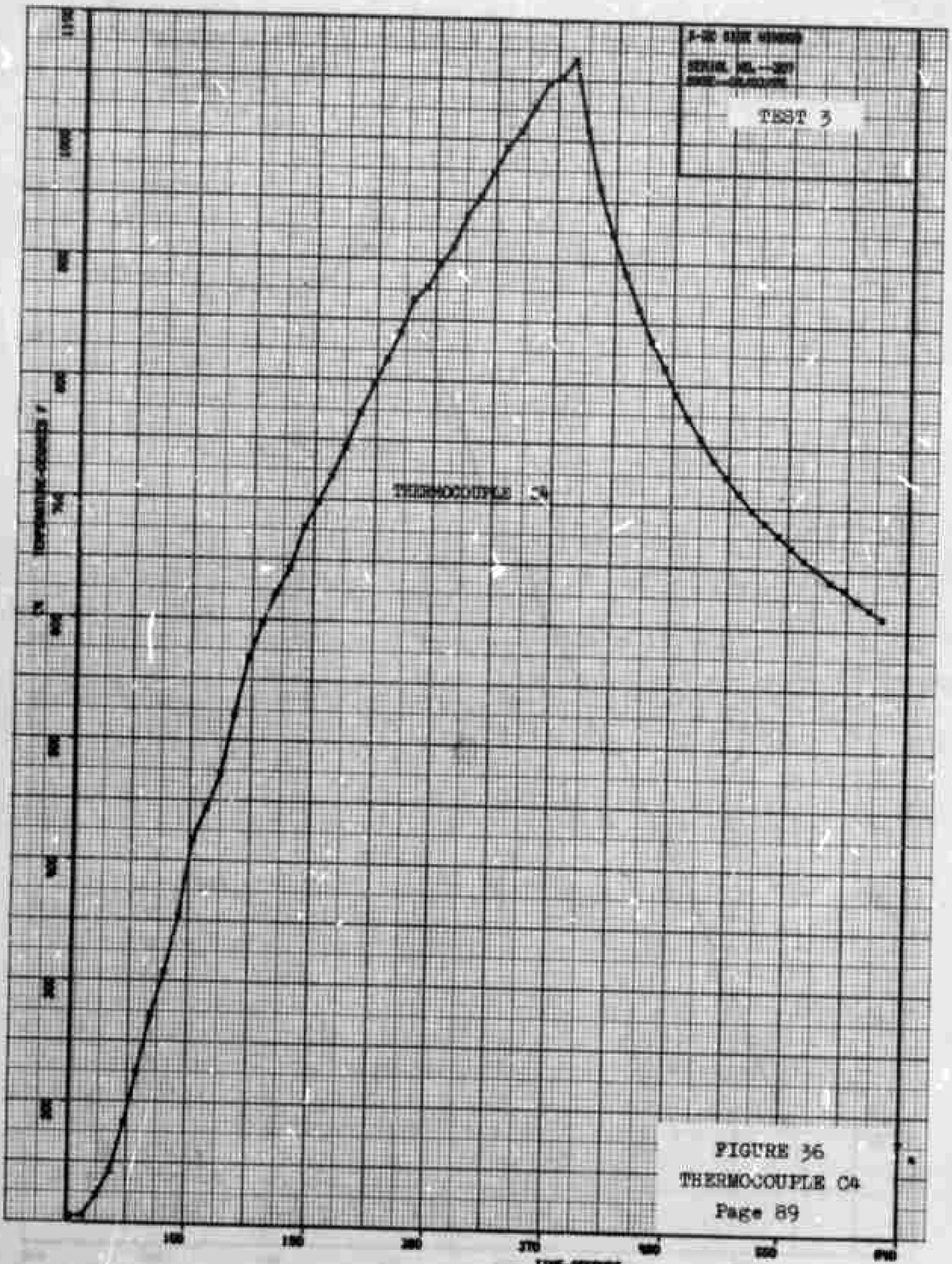

FIGURE 36
THERMOCOUPLE C4
Page 89

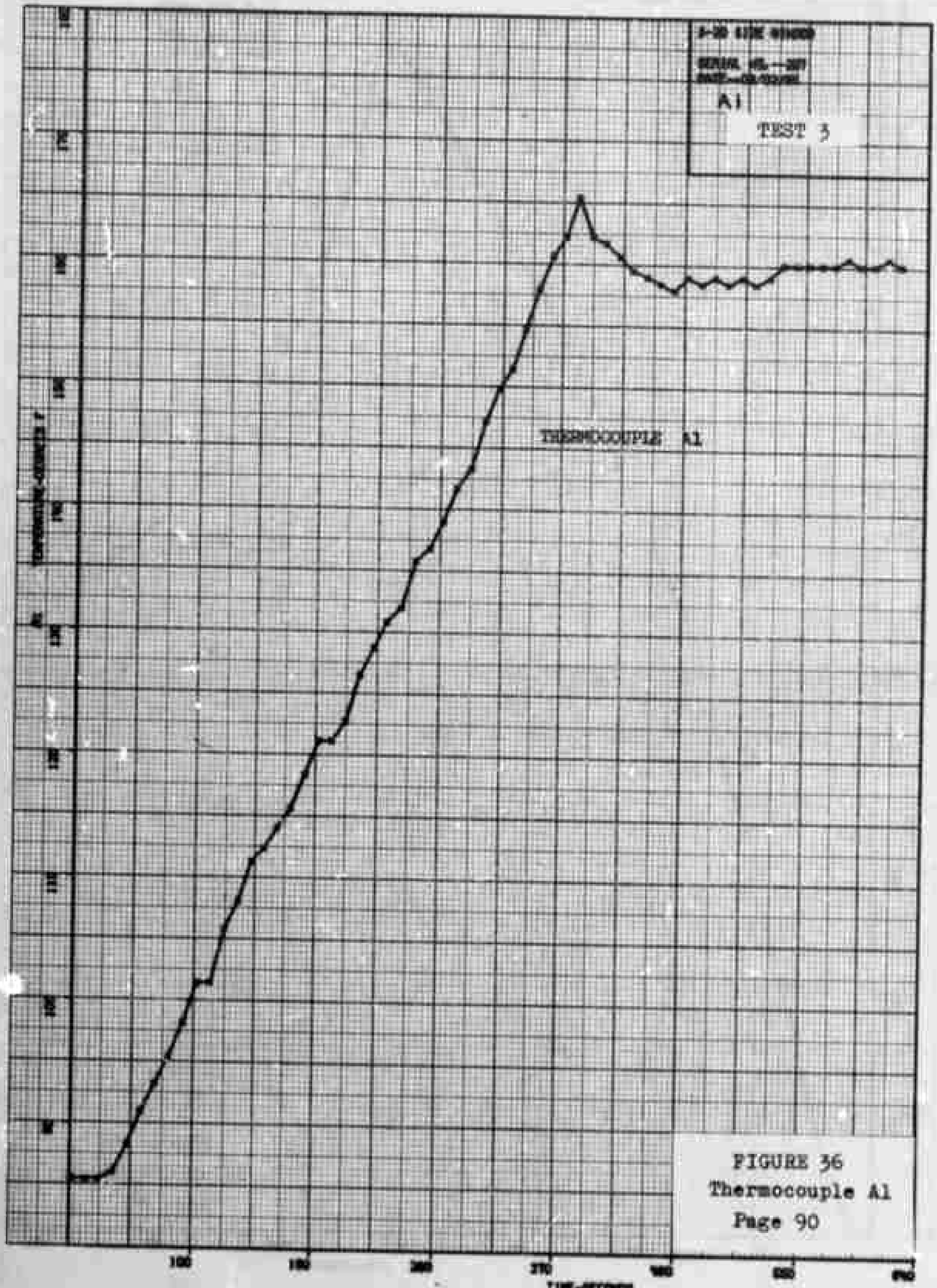

FIGURE 36
Thermocouple A1
Page 90

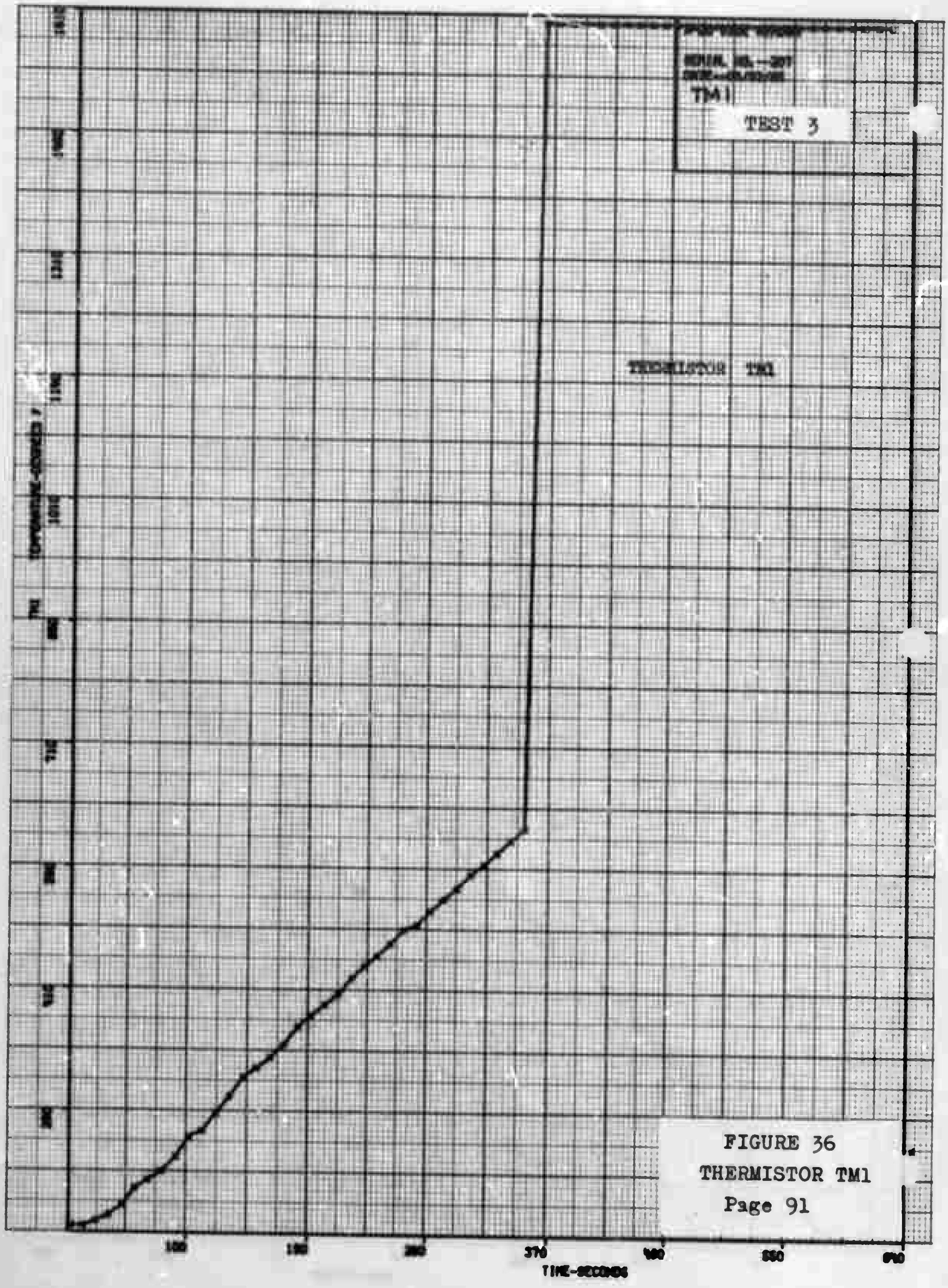

FIGURE 36
THERMISTOR TM1
Page 91

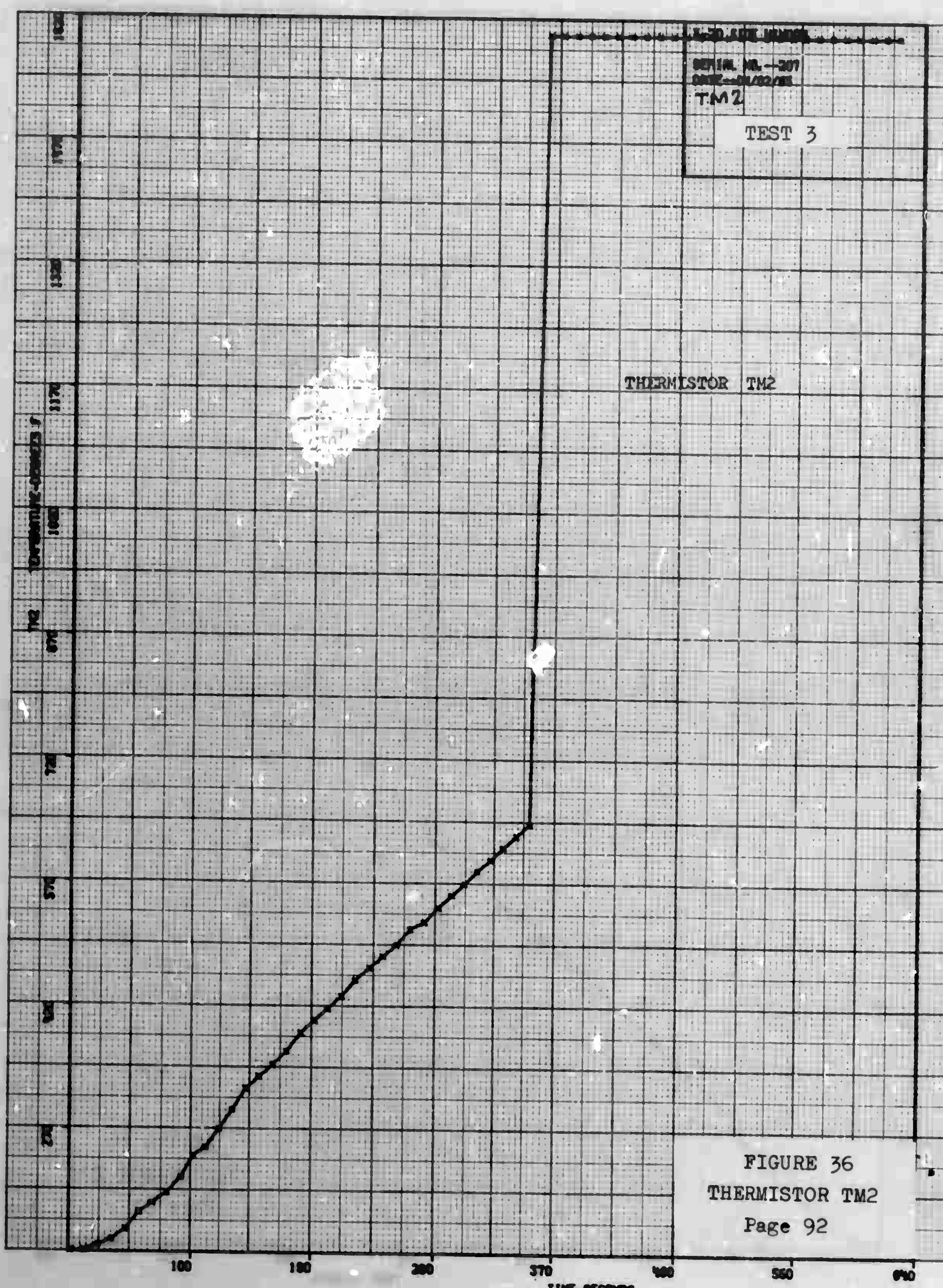

FIGURE 36
THERMISTOR TM2

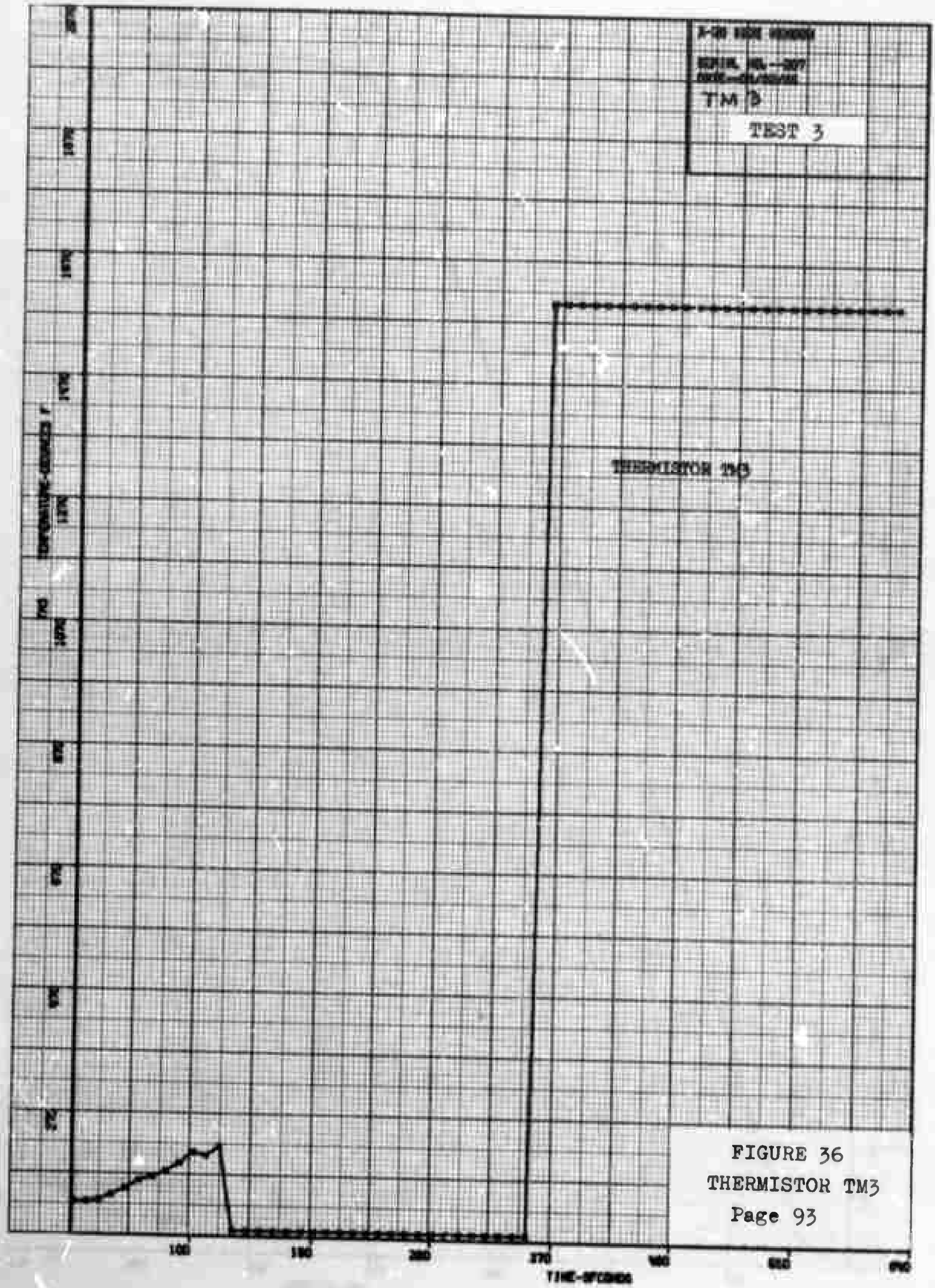

FIGURE 36
THERMISTOR TM3
Page 93

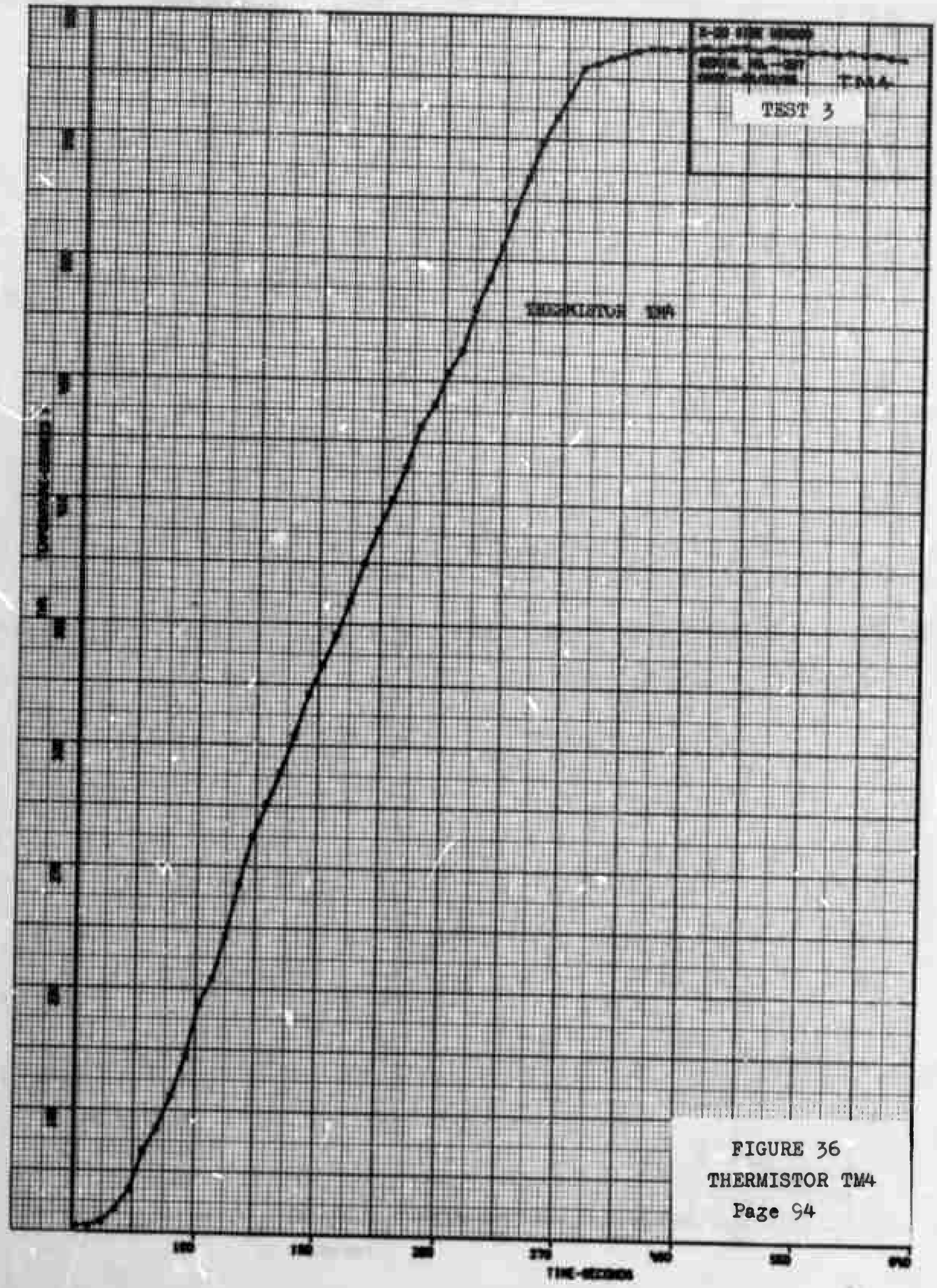

FIGURE 36
THERMISTOR TM4
Page 94

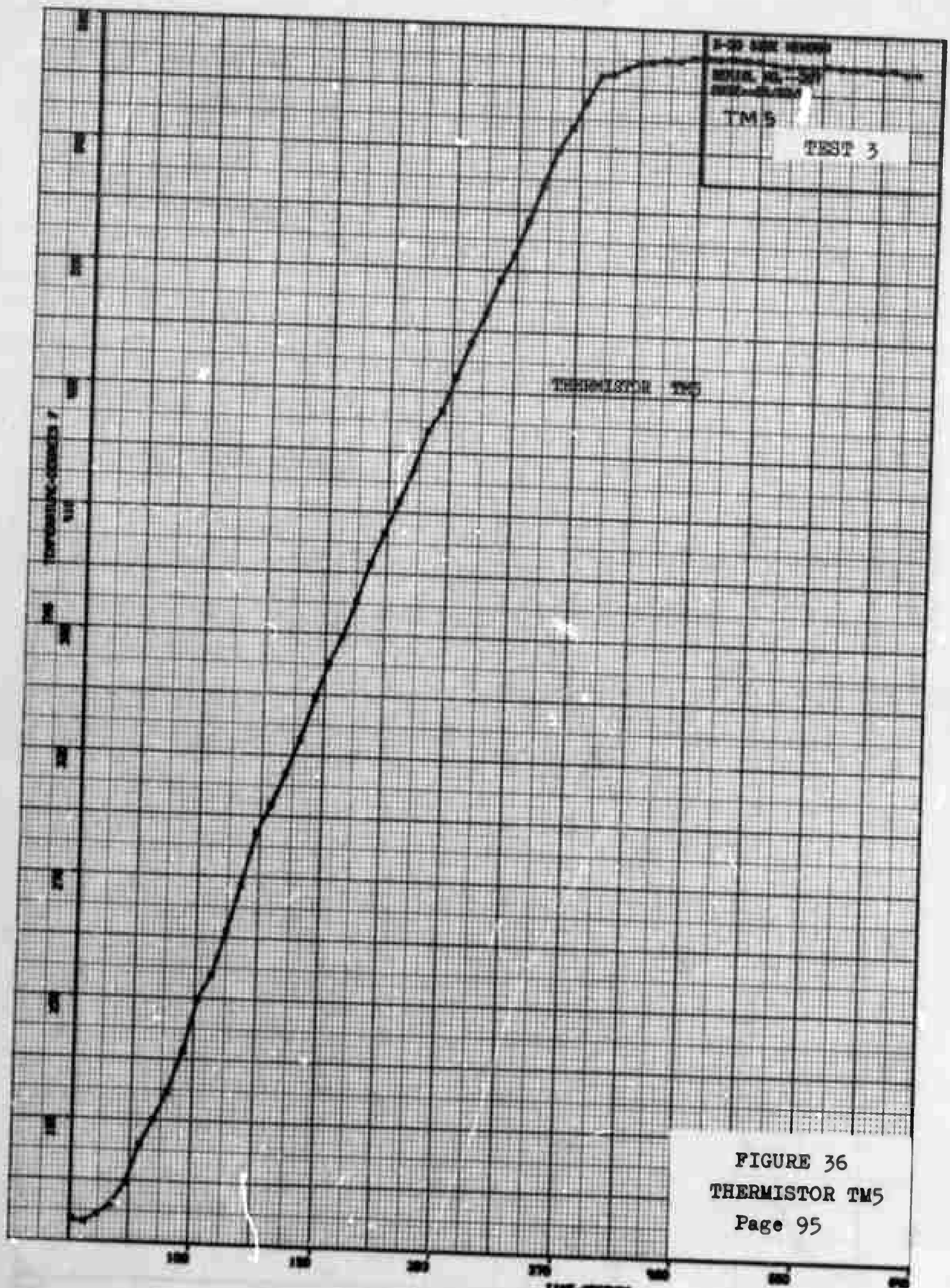

FIGURE 36
THERMISTOR TM5

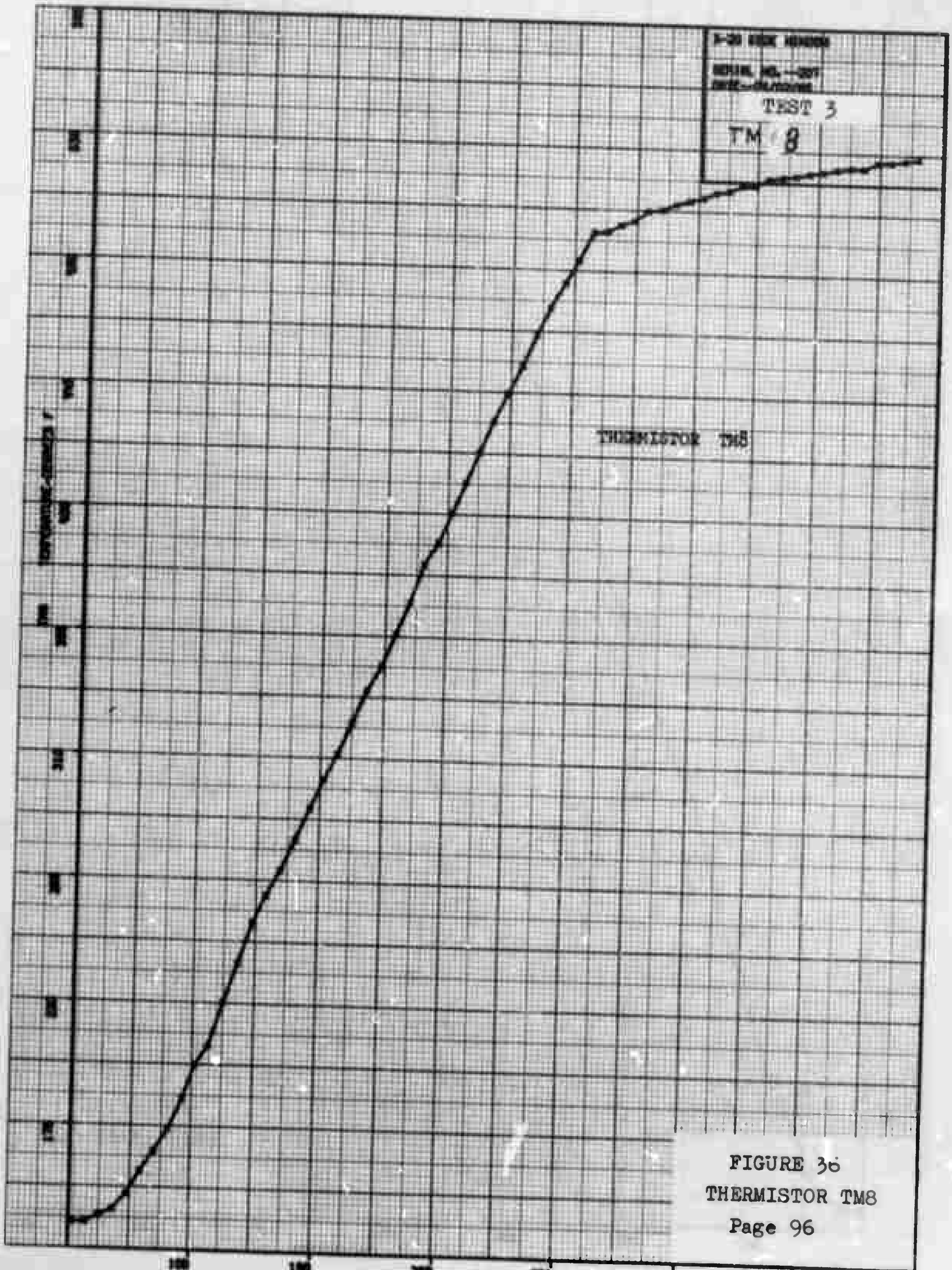

FIGURE 36
THERMISTOR TM8
Page 96

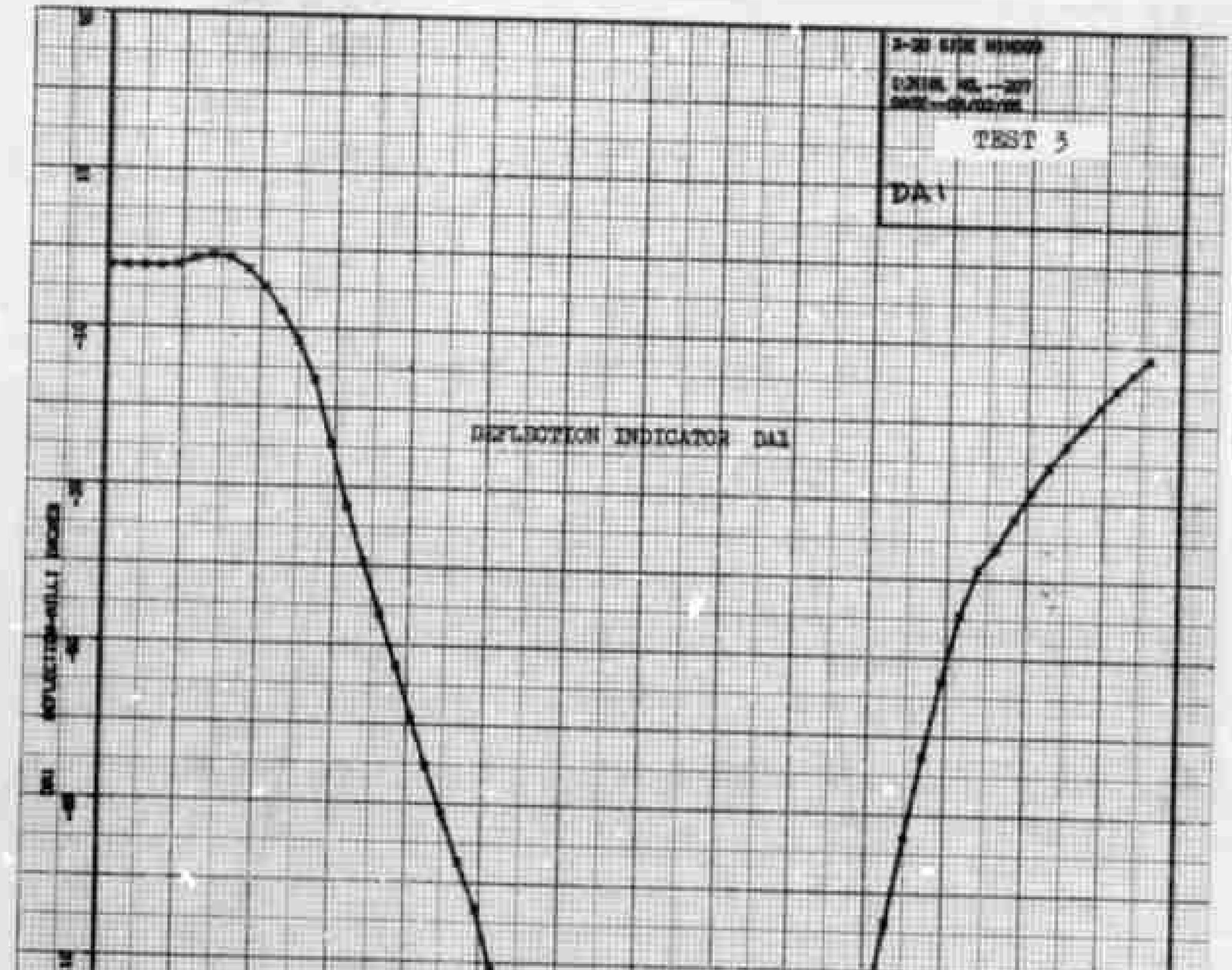

FIGURE 36
DEF. INDIC. DA1
Page 97

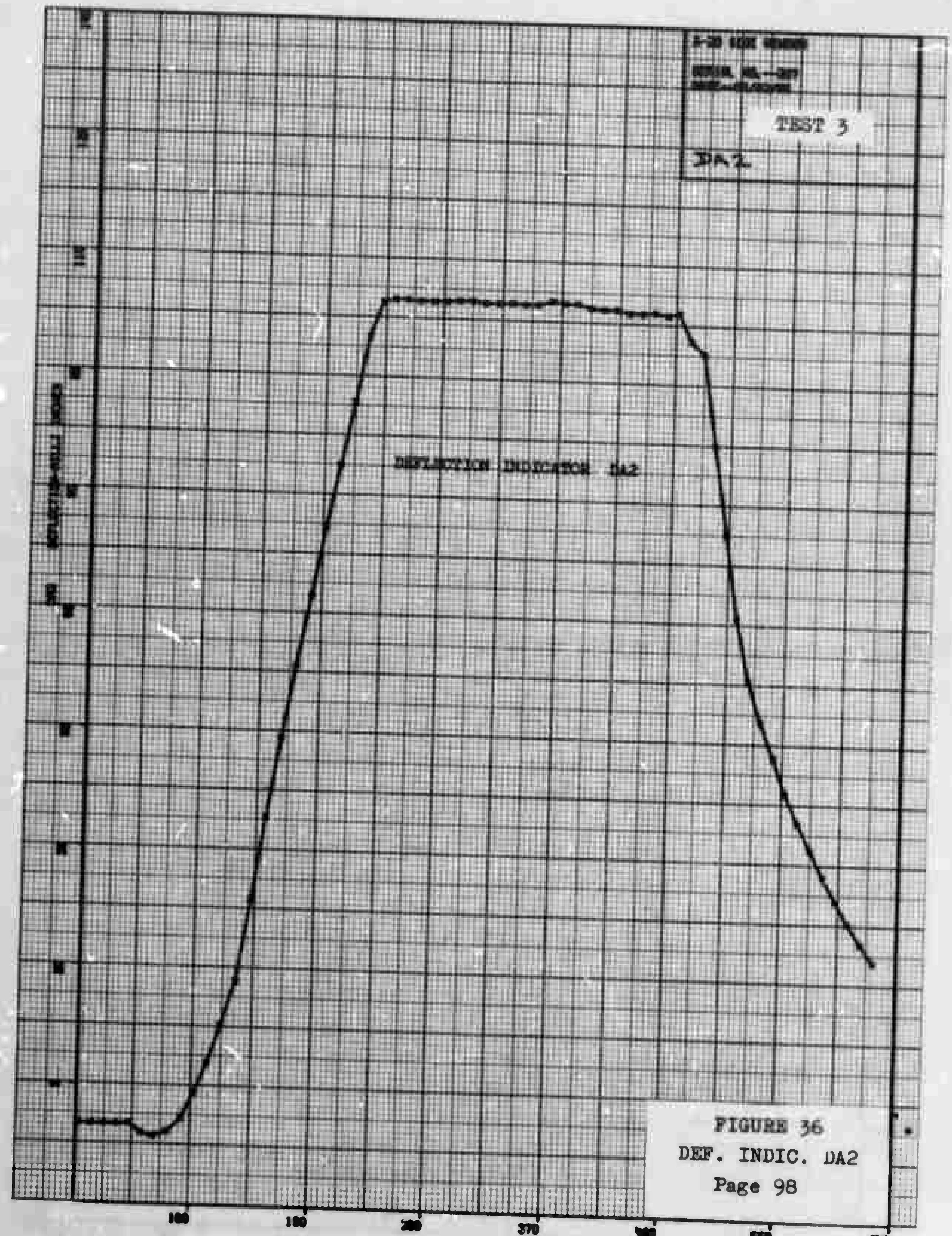

FIGURE 36
DEF. INDIC. DA2
Page 98

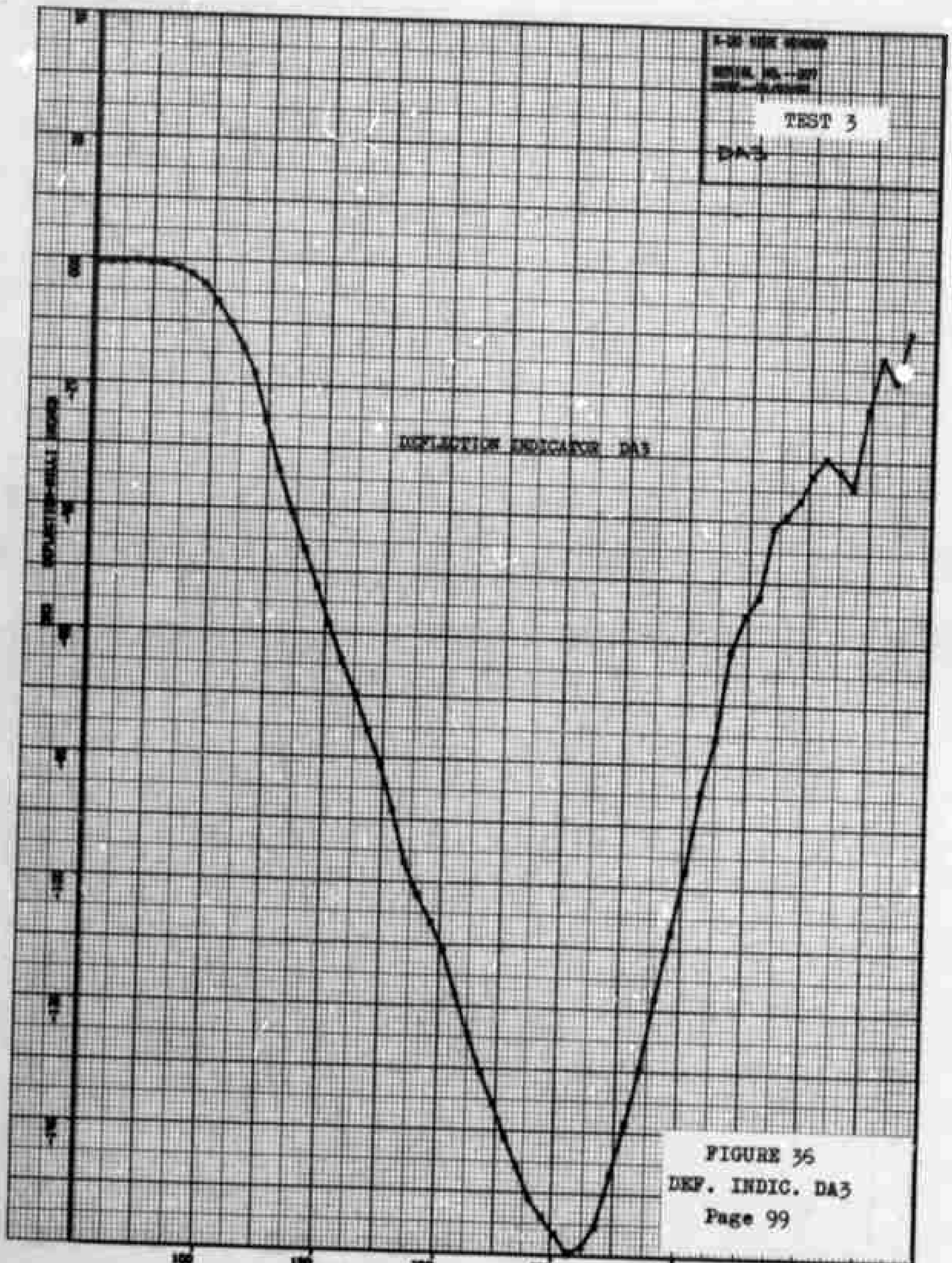

FIGURE 36
DEF. INDIC. DA3

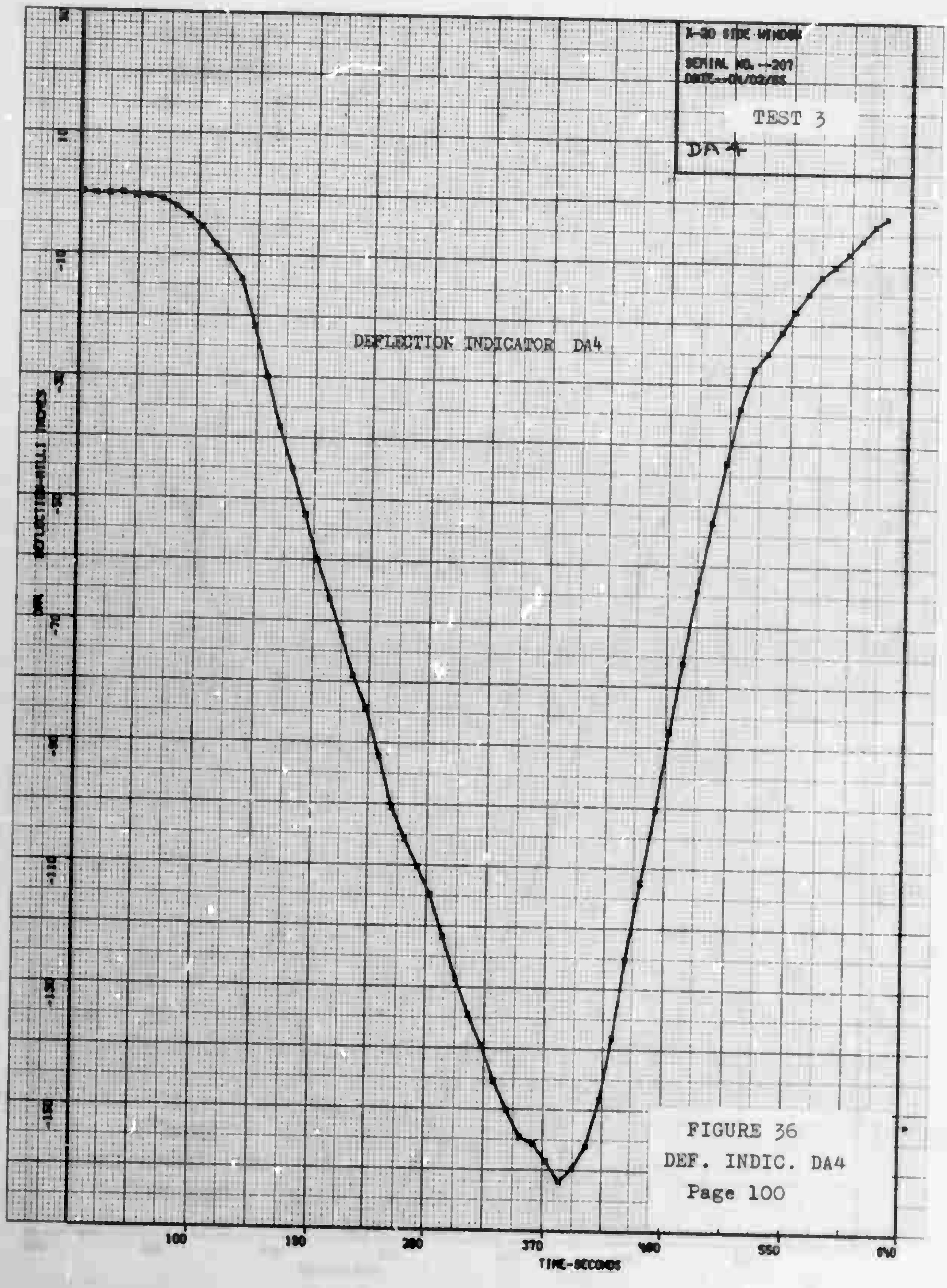

FIGURE 36
DEF. INDIC. DA4

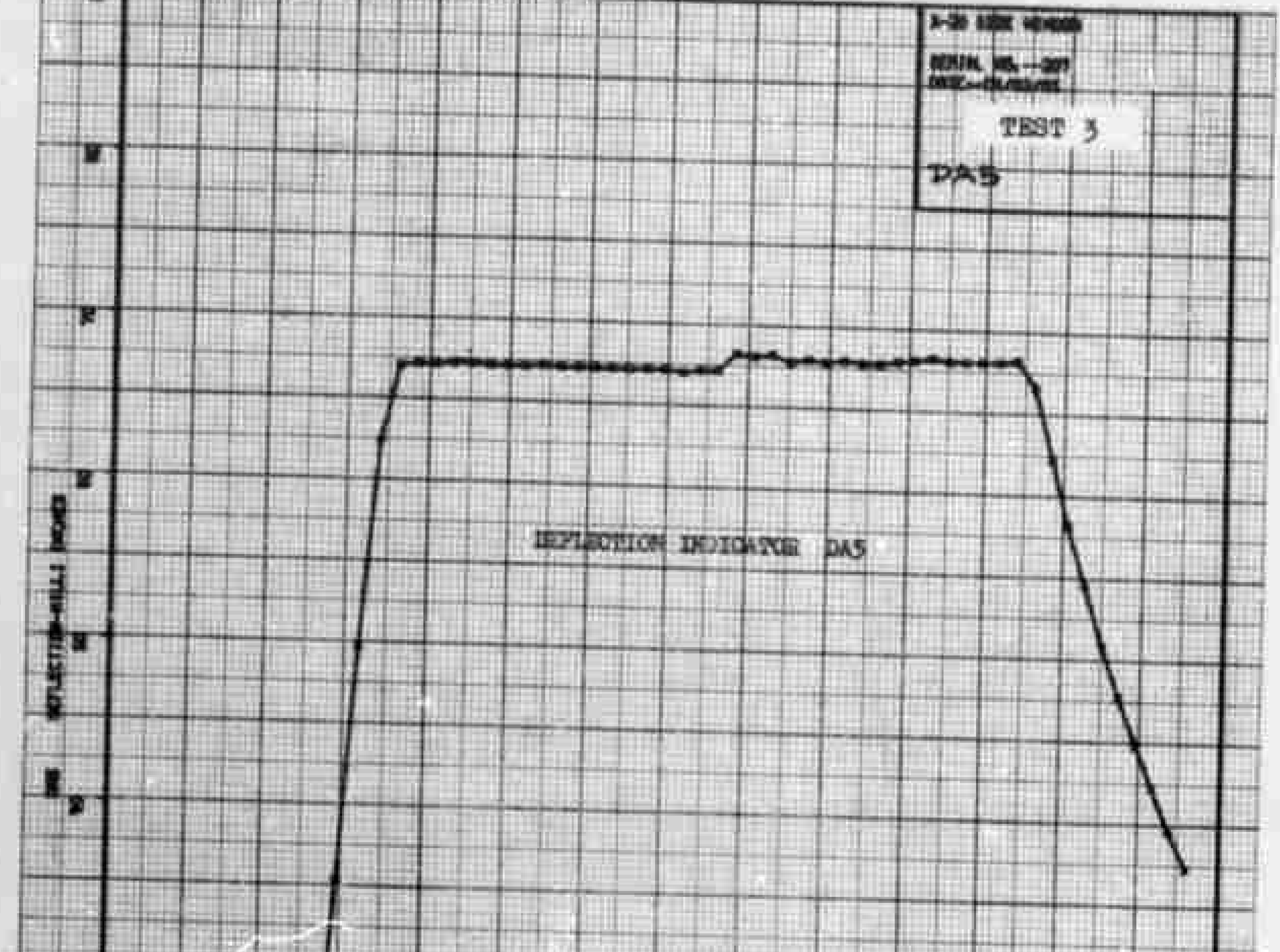

FIGURE 36
DEF. INDIC. DA5
Page 101

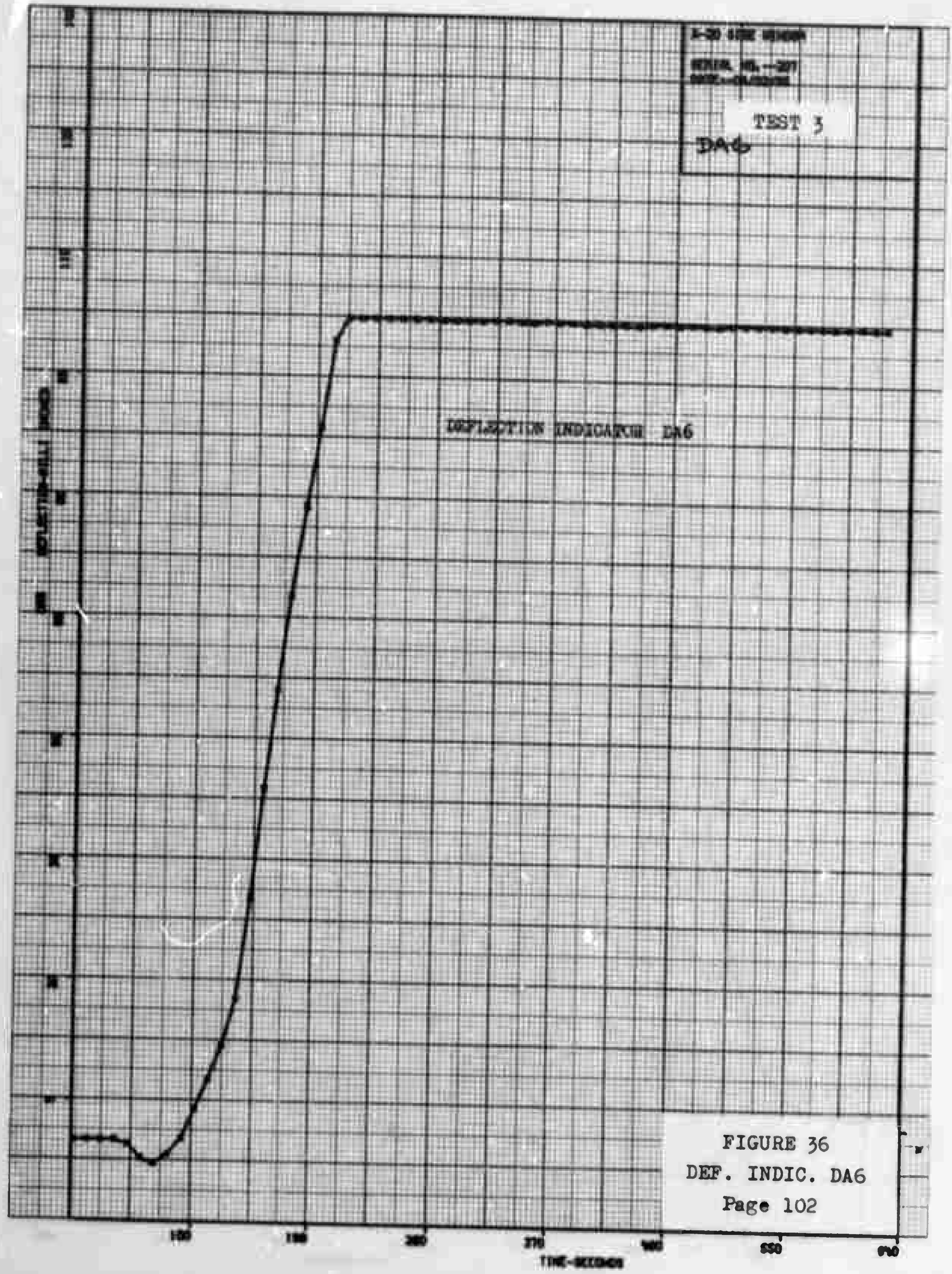

FIGURE 36
DEF. INDIC. DA6
Page 102

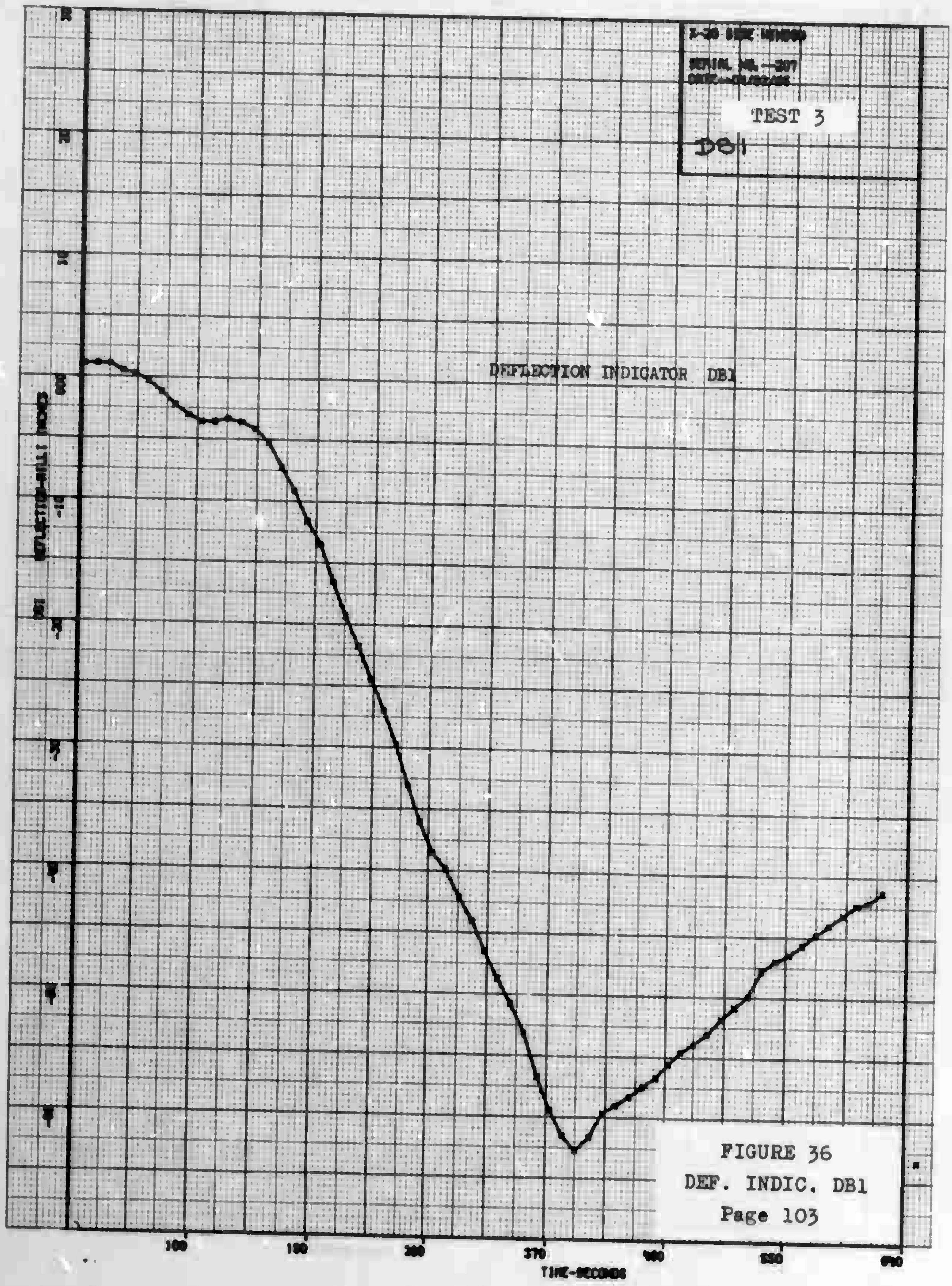

FIGURE 36
DEF. INDIC. DB1
Page 103

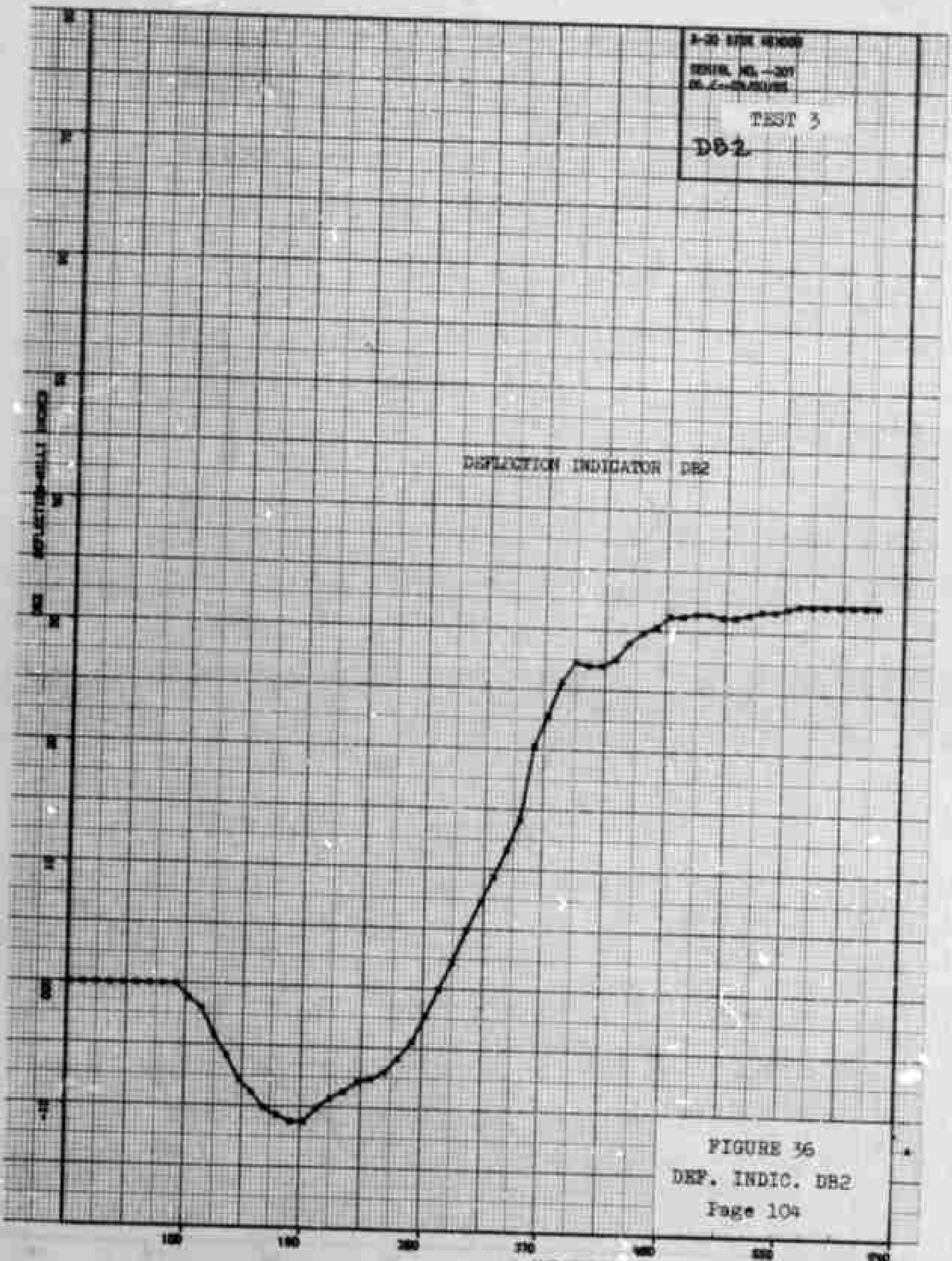

FIGURE 36
DEF. INDIC. DB2
Page 104

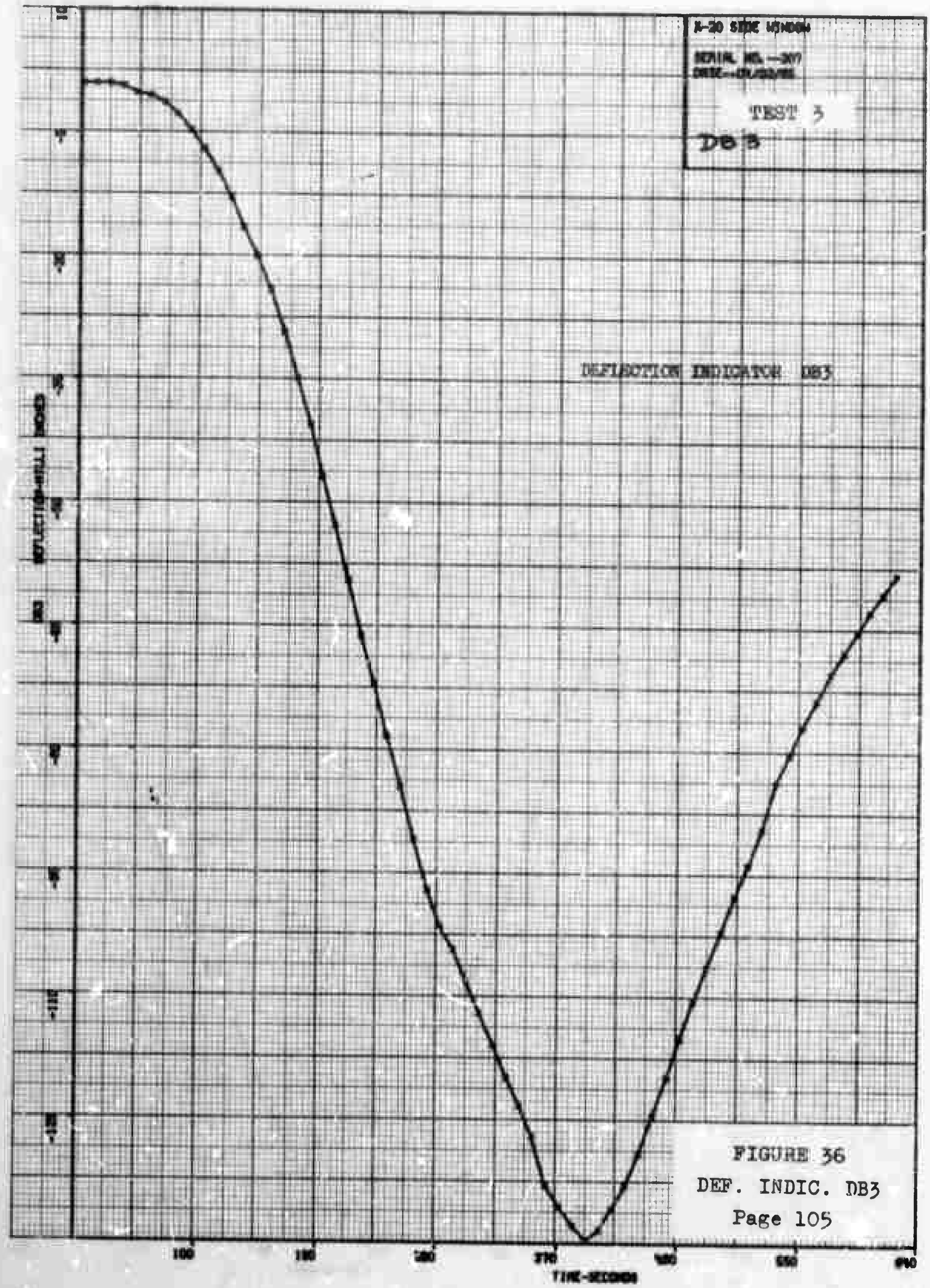

FIGURE 36
DEF. INDIC. DB3

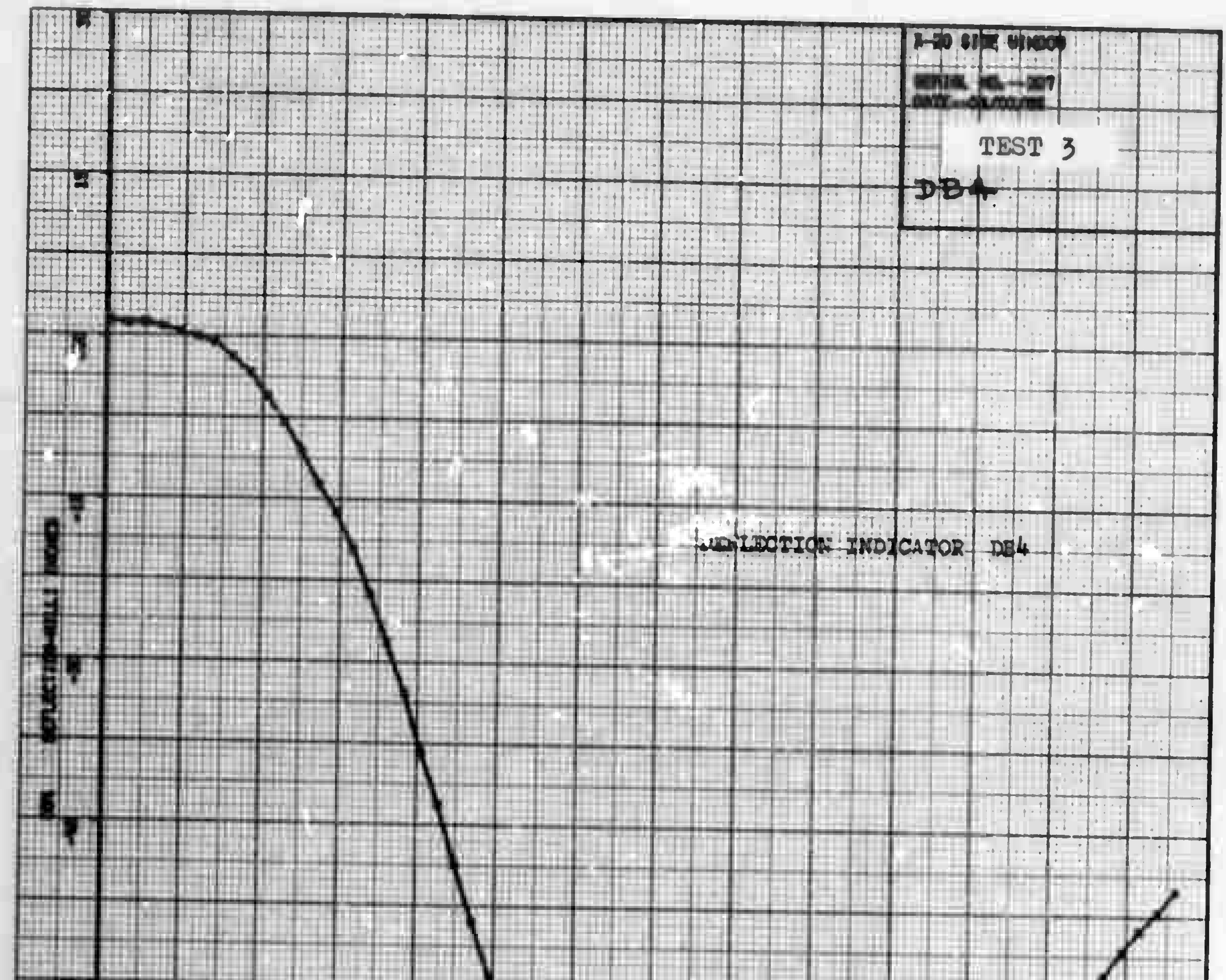

FIGURE 36
DEF. INDIC. DB4

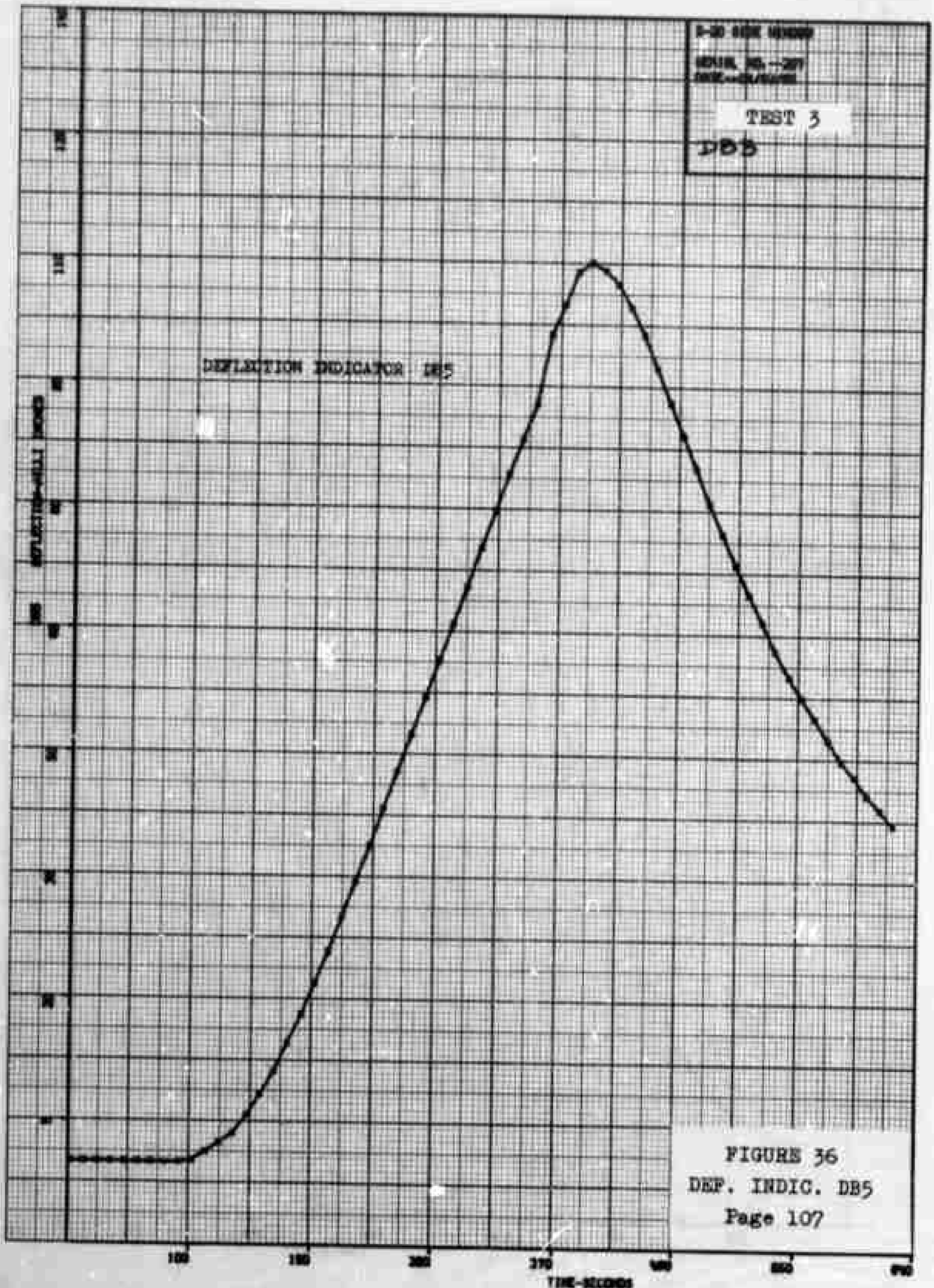

FIGURE 36
DEF. INDIC. DB5
Page 107

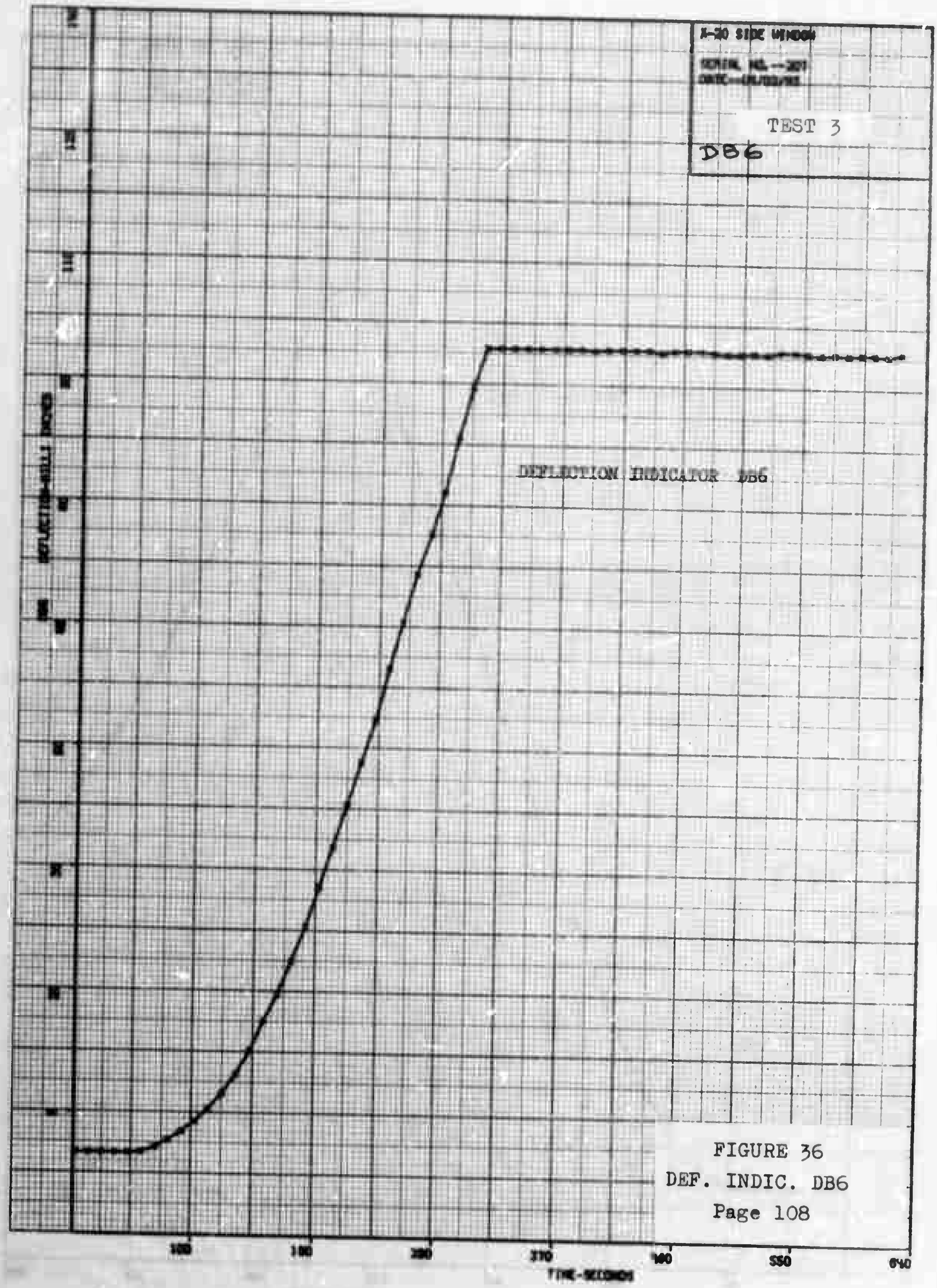

FIGURE 36
DEF. INDIC. DB6
Page 108

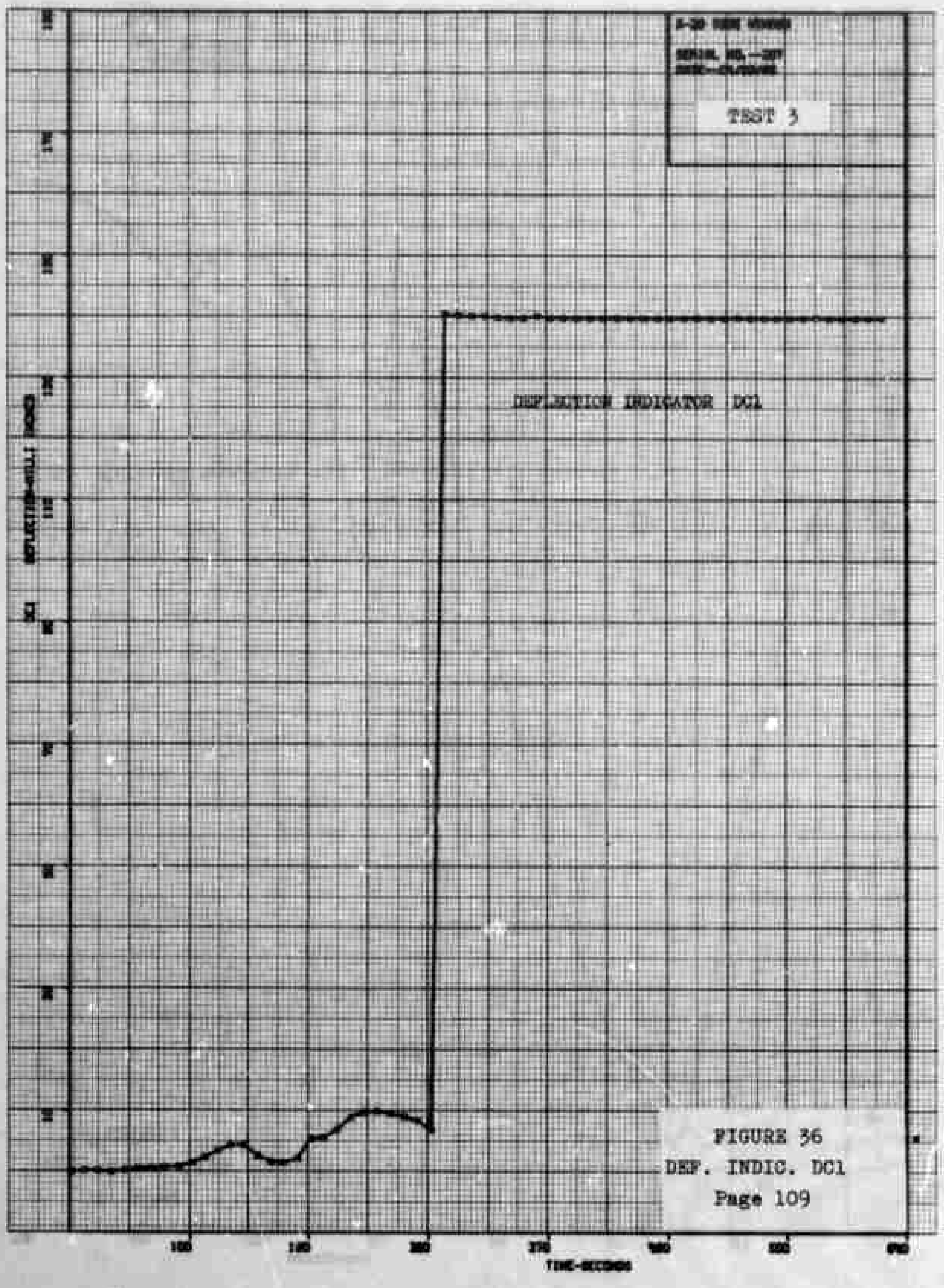

FIGURE 36
DEF. INDIC. DC1

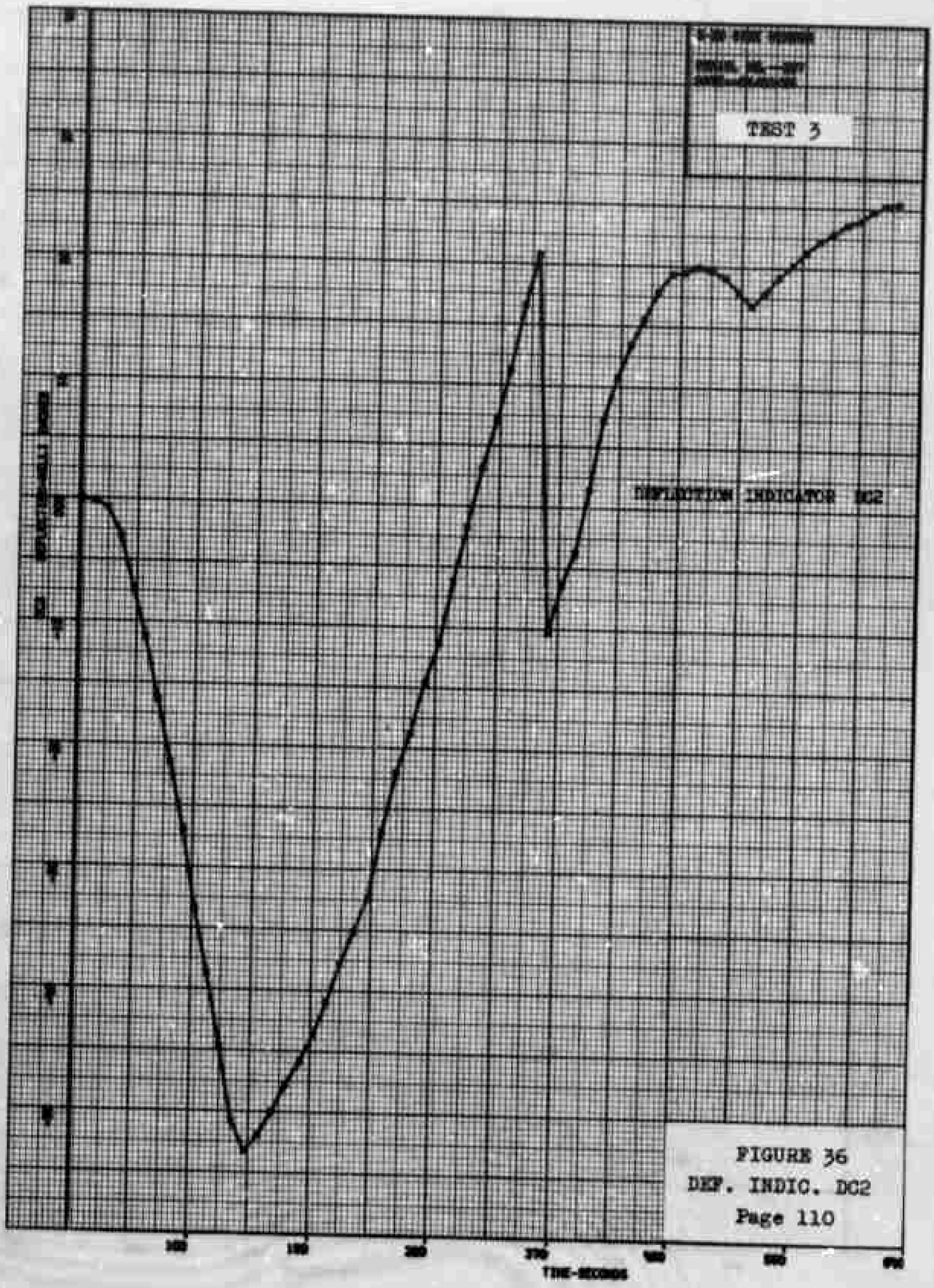

FIGURE 36
DEF. INDIC. DC2
Page 110

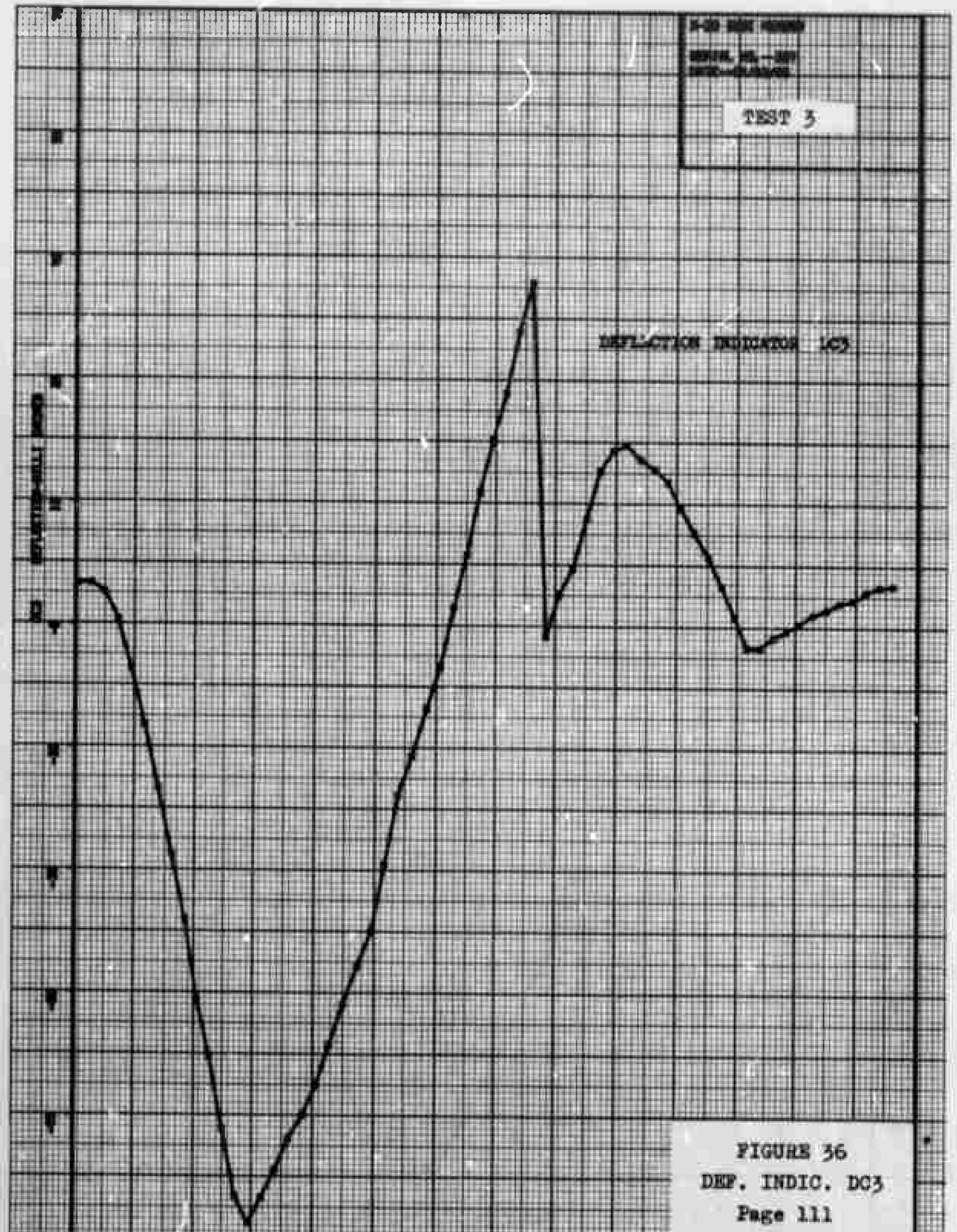

FIGURE 36
DEF. INDIC. DC3
Page 111

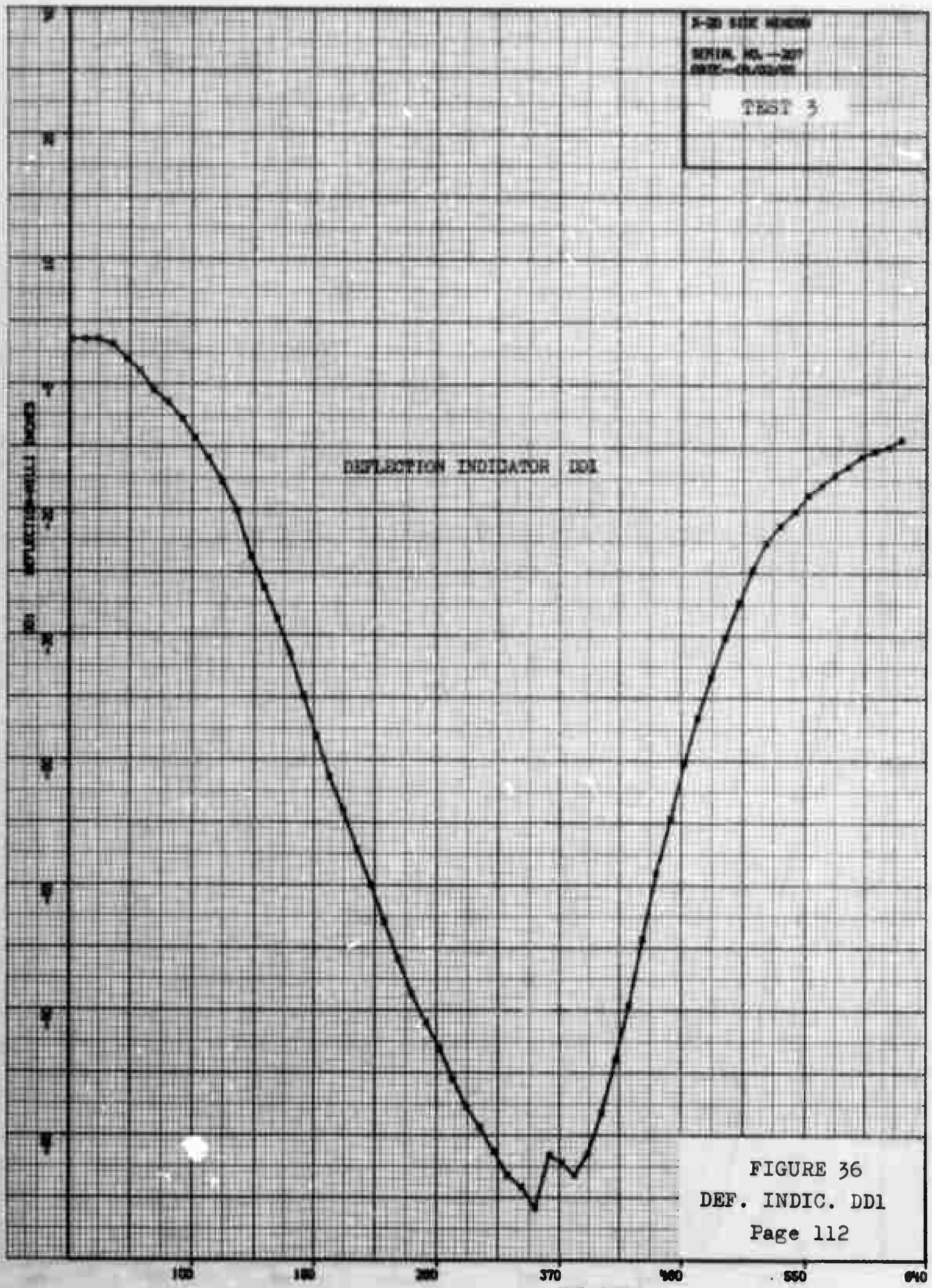

FIGURE 36
DEF. INDIC. DD1
Page 112

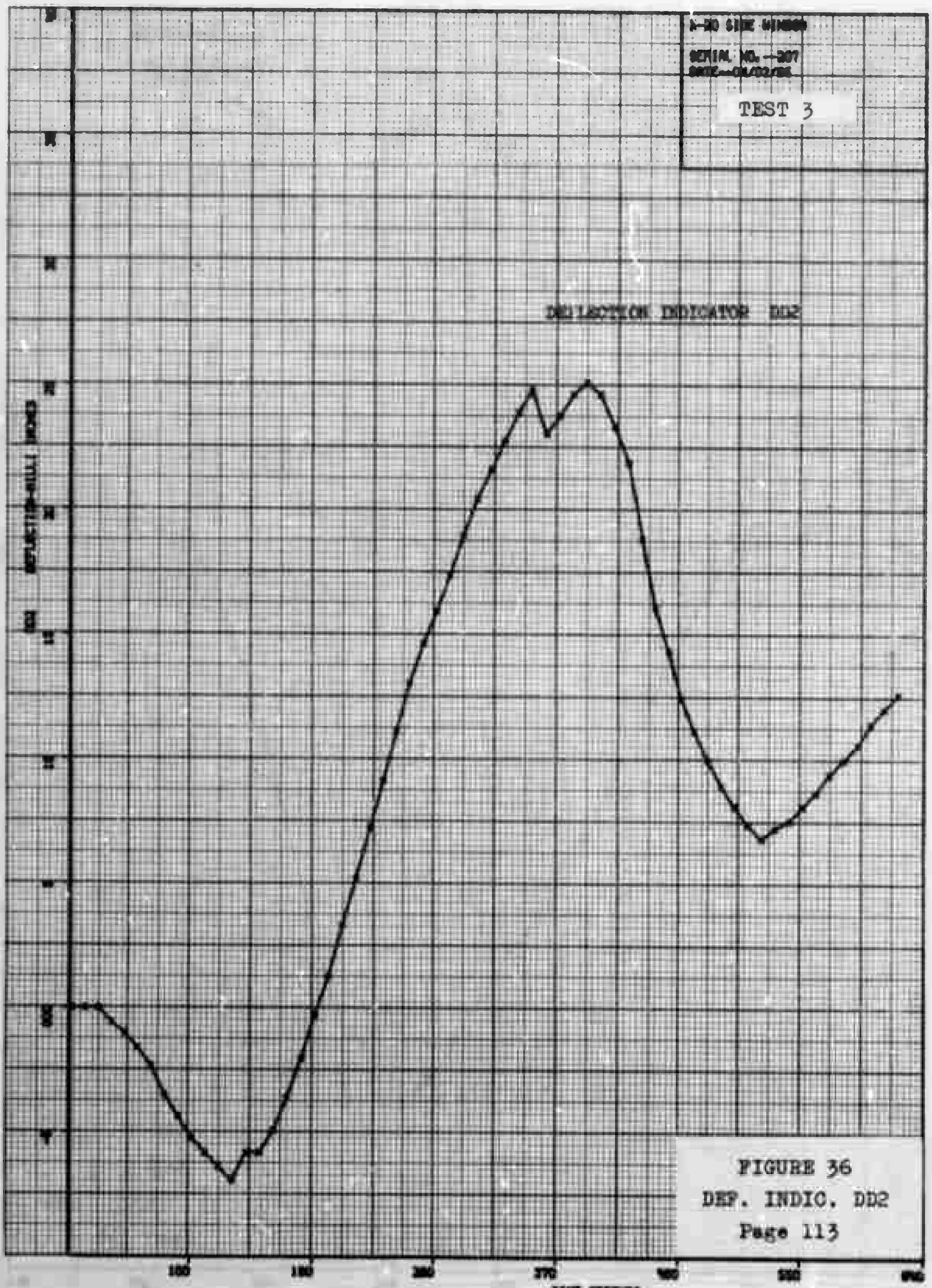

FIGURE 36
DEF. INDIC. DD2

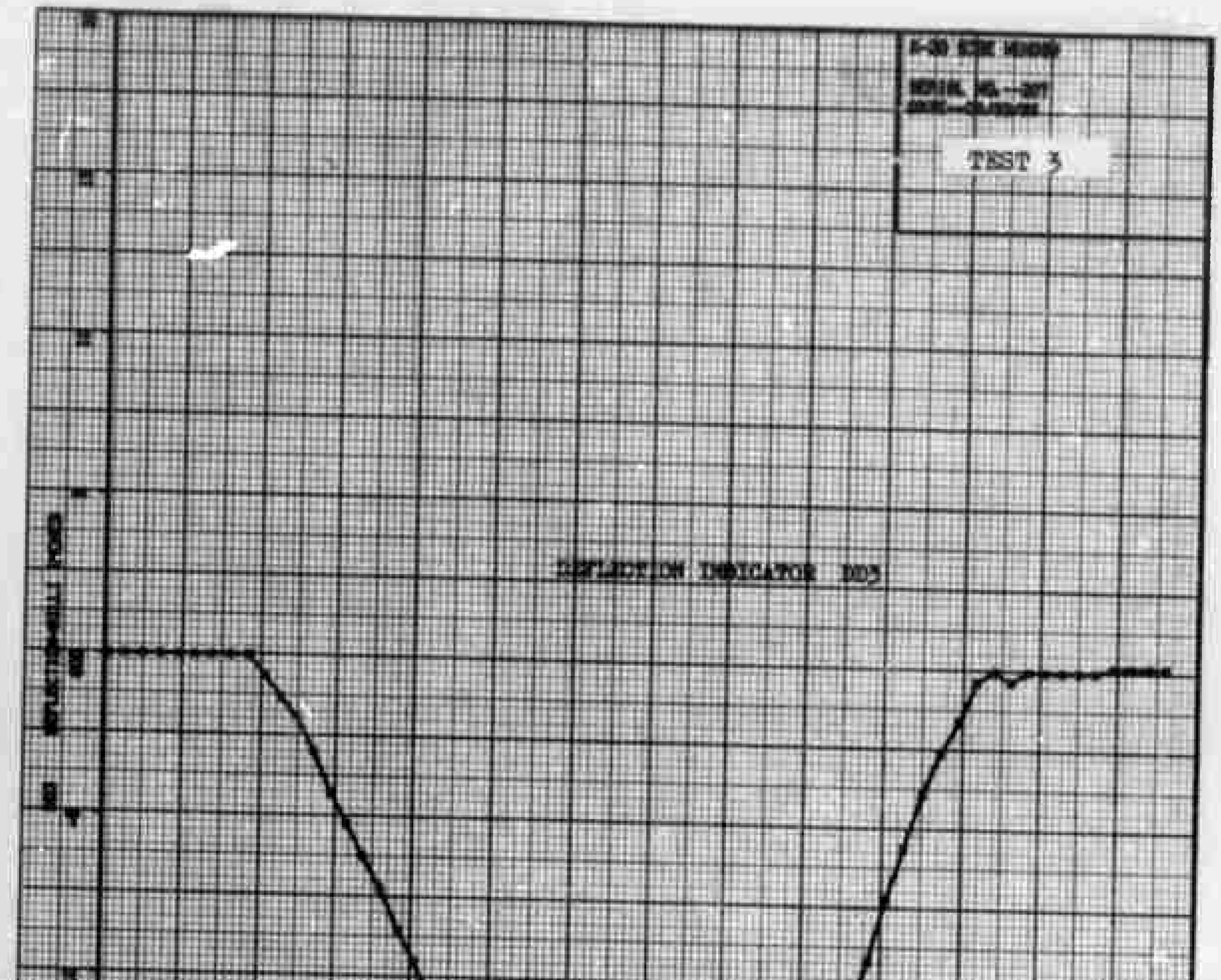

FIGURE 36
DEF. INDIC. DD3
Page 114

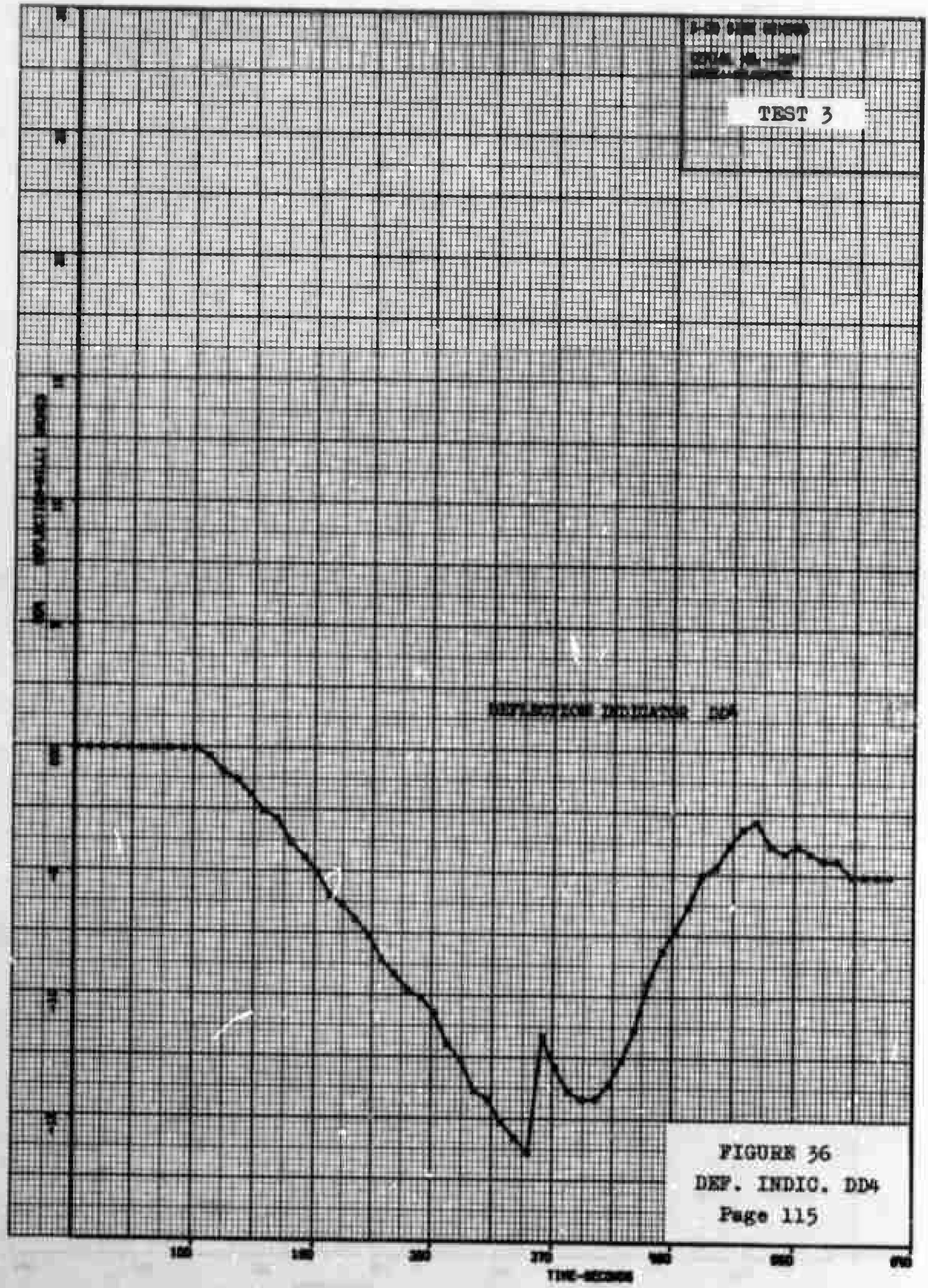

FIGURE 36
DEF. INDIC. DD4
Page 115

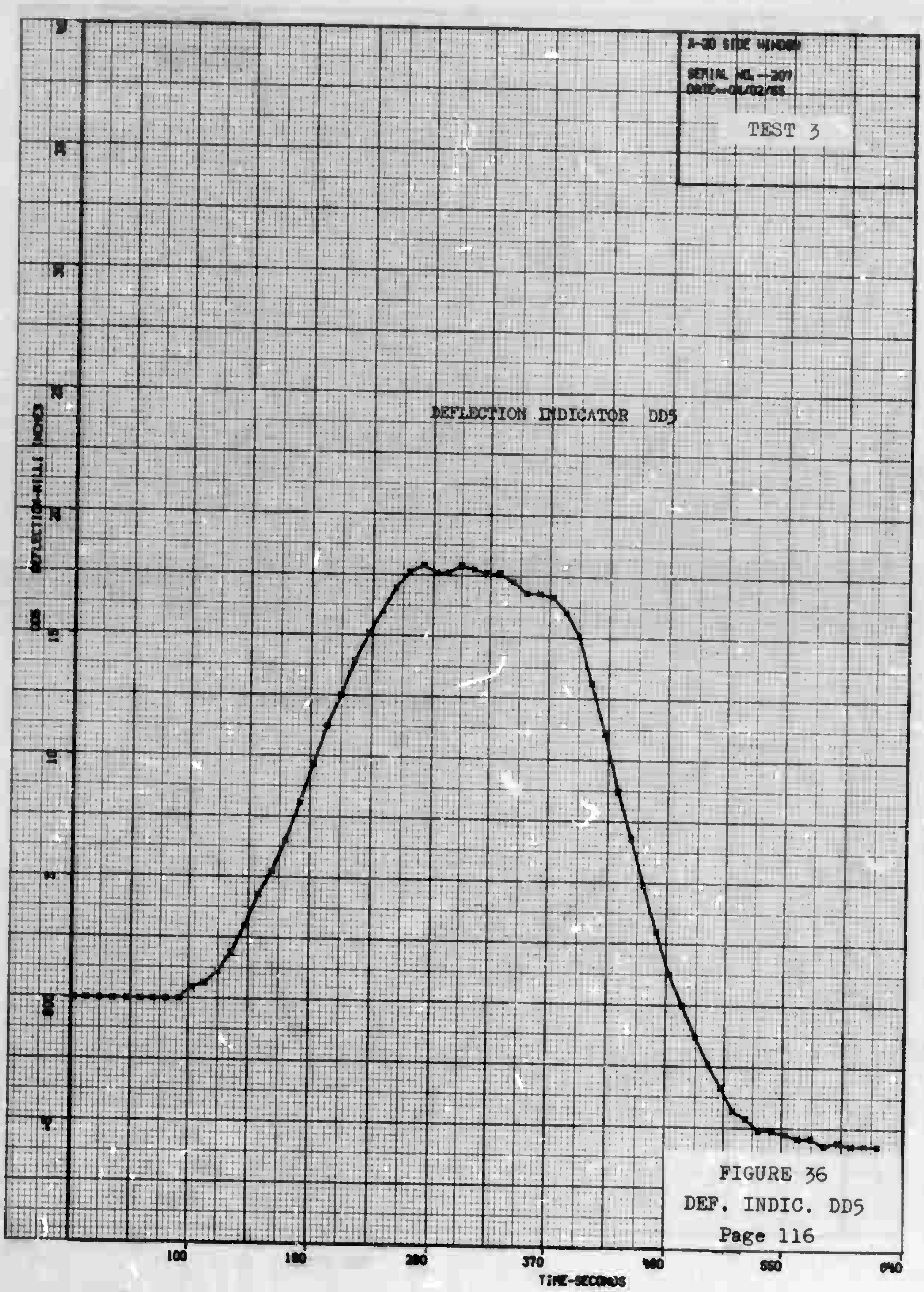

FIGURE 36
DEF. INDIC. DD5
Page 116

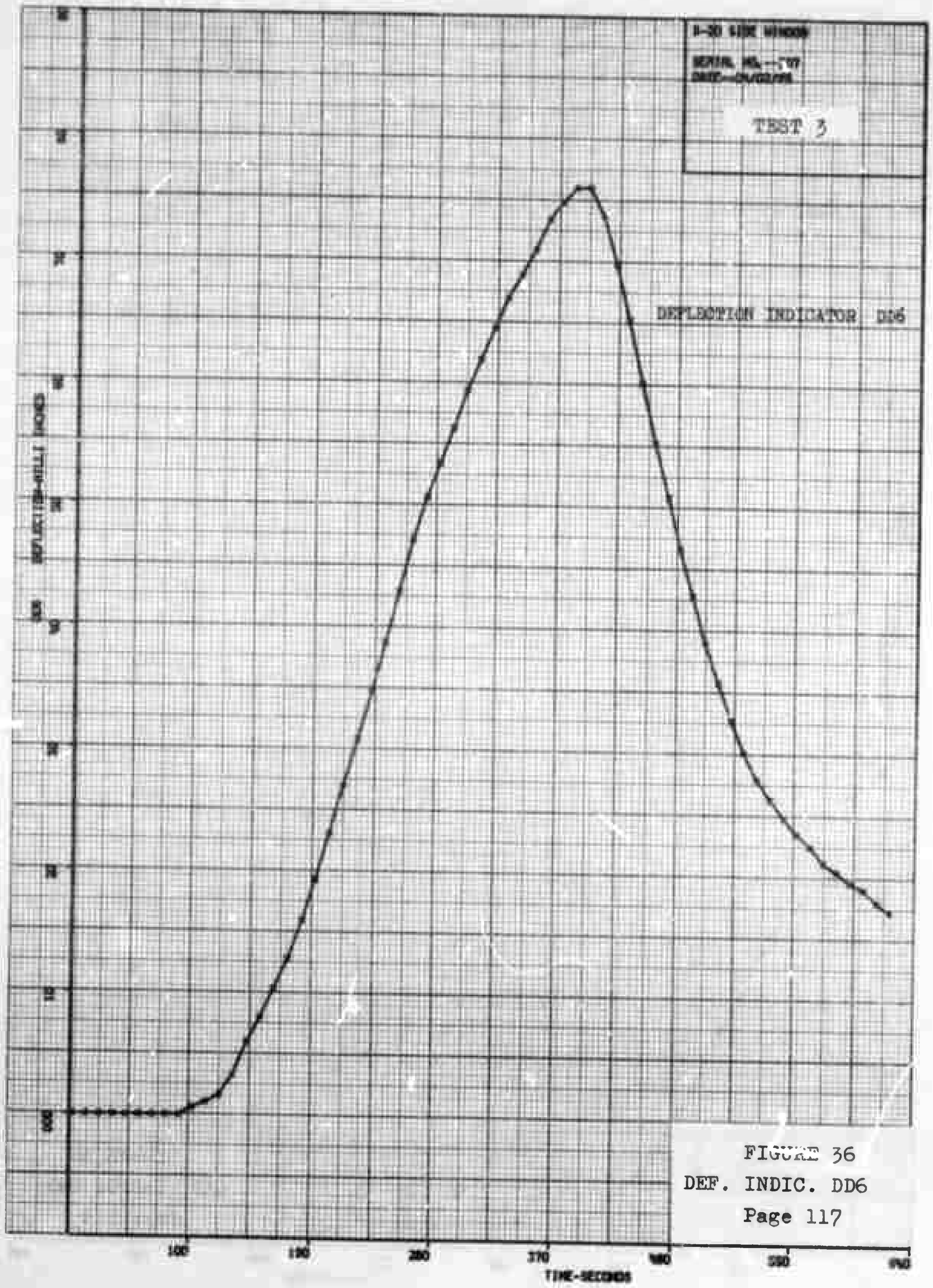

FIGURE 36
DEF. INDIC. DD6
Page 117

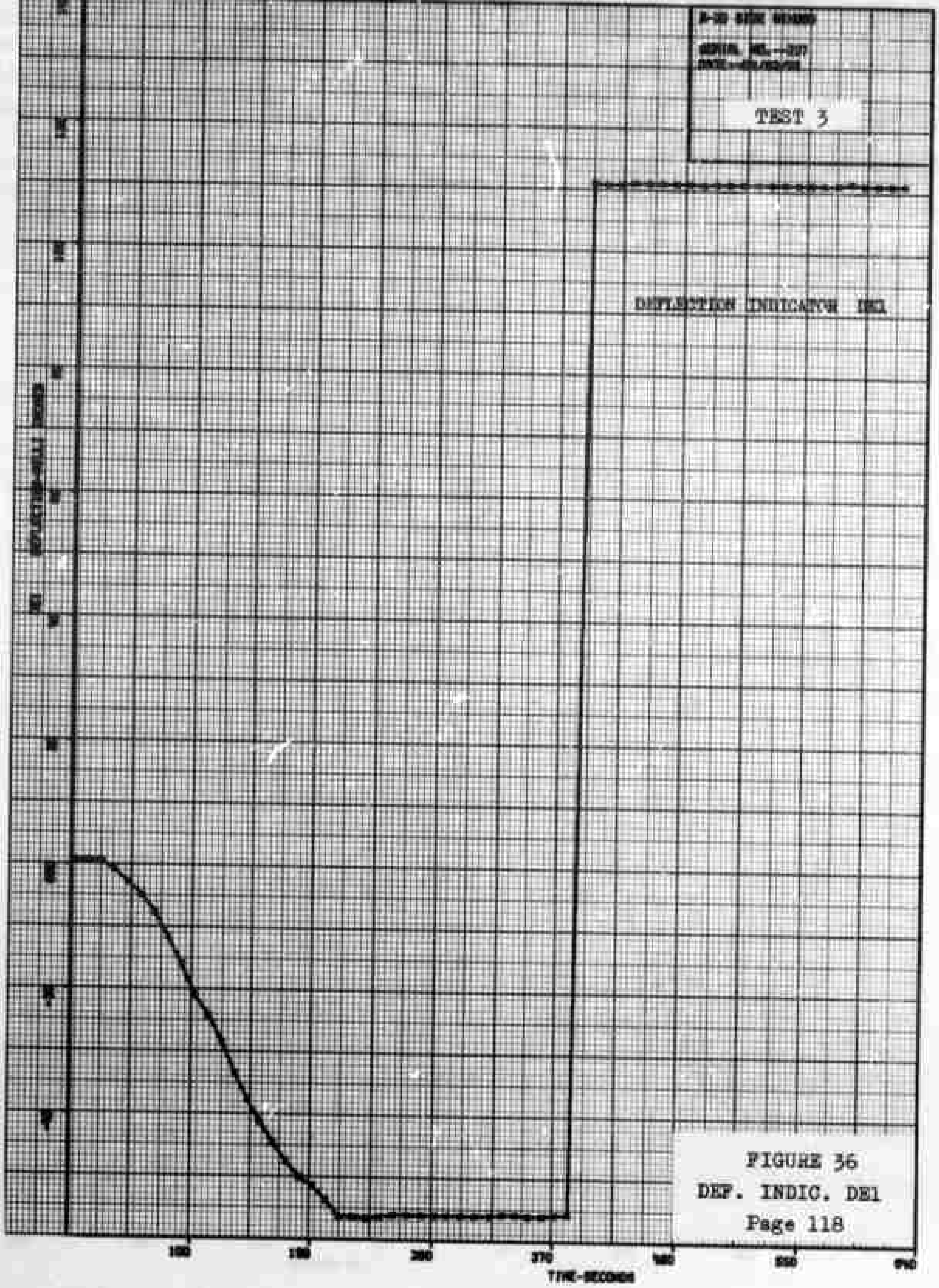

FIGURE 36
DEF. INDIC. DE1
Page 118

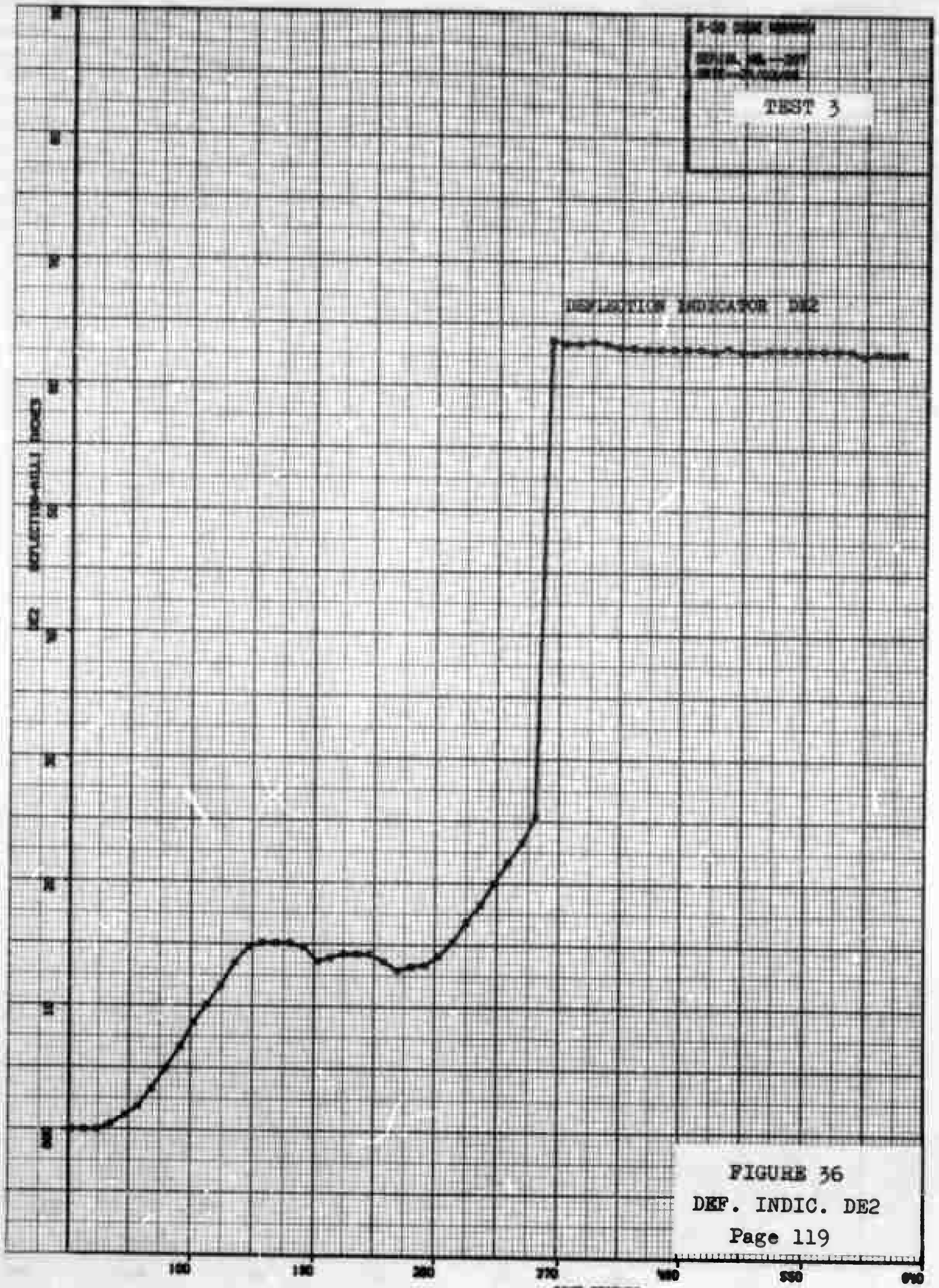

FIGURE 36
DEF. INDIC. DE2

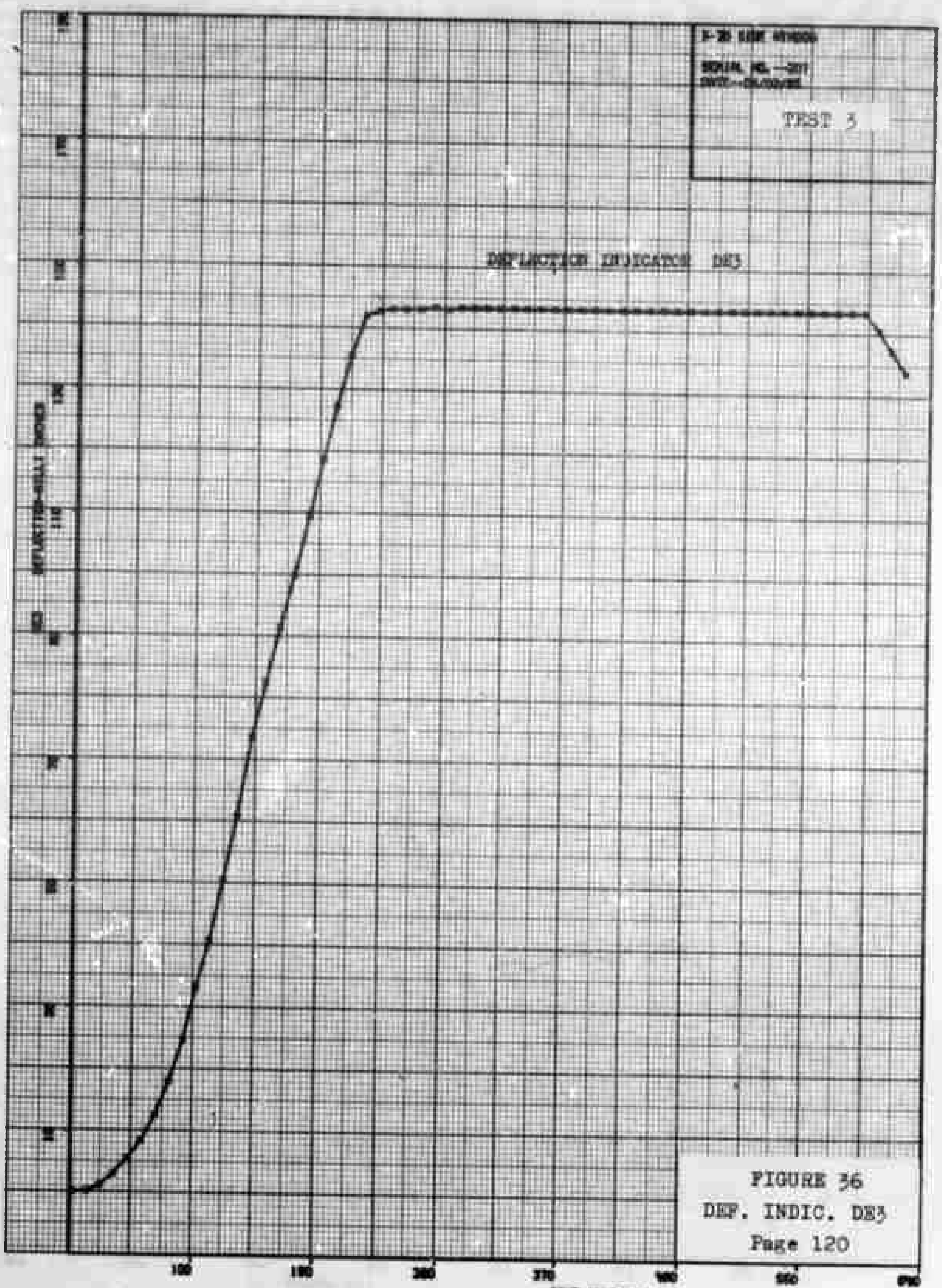

FIGURE 36
DEF. INDIC. DE3

FIGURE 37 WINDOW GAPS

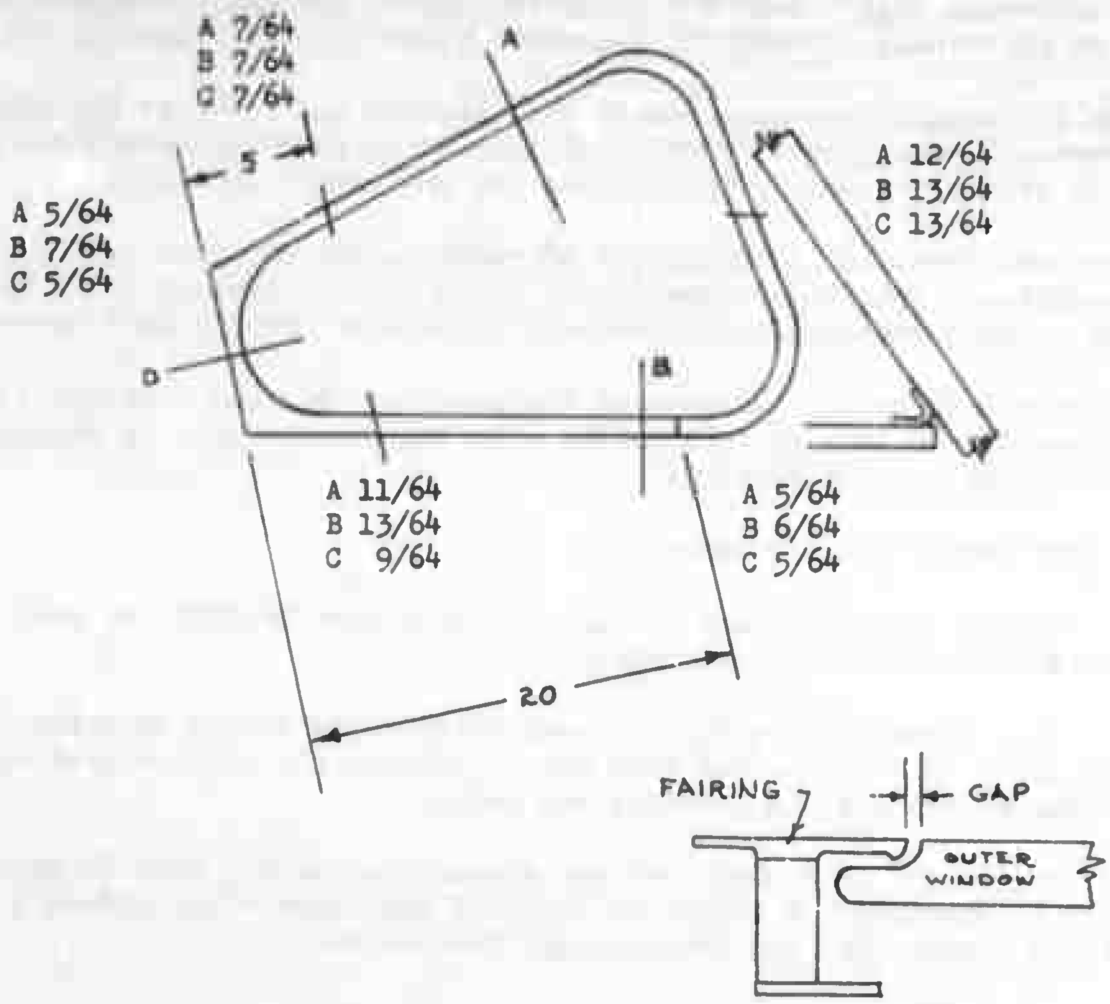

A BEFORE TEST 2
B AFTER TEST 2 & BEFORE TEST 3
C AFTER TEST 3

	INITIALS	DATE	REV BY INITIALS	DATE	TITLE	MODEL
CALC					WINDOW GAPS	X-20
CHECK						
APPD.						
APPD.						

U3 4038 8000 REV 10.64

4.4 DETERMINATION OF VISIBLE LIGHT TRANSMISSION FACTOR

4.4.1 INTRODUCTION

It was requested that a separate investigation of the light transmission factor of the window assembly be measured before and after heating the window.

A device for making this measurement was obtained but found to be inoperative. The Structures Test Branch (FDTT) instrumentation personnel assembled a device to attempt to obtain readings so the test could continue.

Following the heat test a second set of readings was obtained with a different photoconductor. This was followed by a third set of readings which were obtained using a standard Photo Research Spectra Brightness Spot Meter.

A doubt exists as to the validity of the readings obtained from the first two set-ups due to lack of information relating current drop to attenuation of light in the visible spectrum.

4.4.2 TEST SET-UP AND PROCEDURE

a. Figure 38 is a sketch of the apparatus made by FDTT and used for the preheat and post heat measurements.

1. A current reading was made without the window in place (through air). The window was then placed between the light source and the photoconductor and a second reading was made.

b. Figure 39 is a sketch of the standard apparatus used to make the third set of readings. A series of readings were made with different light intensities through air and then through the window.

4.4.3 TEST RESULTS

a. Before heat test with FDTT apparatus with RCA 7163 Photoconductor.

TABLE 2

Thru Air	Thru Window	Ratio $\frac{\text{Window in}}{\text{Window out}}$
.210 amps	.125 amps	.595
Light Intensity Increased:		
.280 amps	.165 amps	.589

4.4.3 TEST RESULTS (Continued)

TABLE 2 (Continued)

b. After heat test with PDTT apparatus with Layfette MS 791 Photoconductor.

Thru Air	Thru Window	Ratio Window in / Window out
Light Intensity Increased:		
.770 amps	.490 amps	.636
.245 amps	.142 amps	.580

c. After heat test with Photo Research Spectra Brightness Spot Meter UB1/2.

Thru Air Ft-Lamberts	Thru Window Ft-Lamberts	Ratio Window in / Window out
1000	650	.65
500	310	.62
240	120	.50
150	100	.67

FIGURE 38 FDIT LIGHT TRANSMISSION APPARATUS

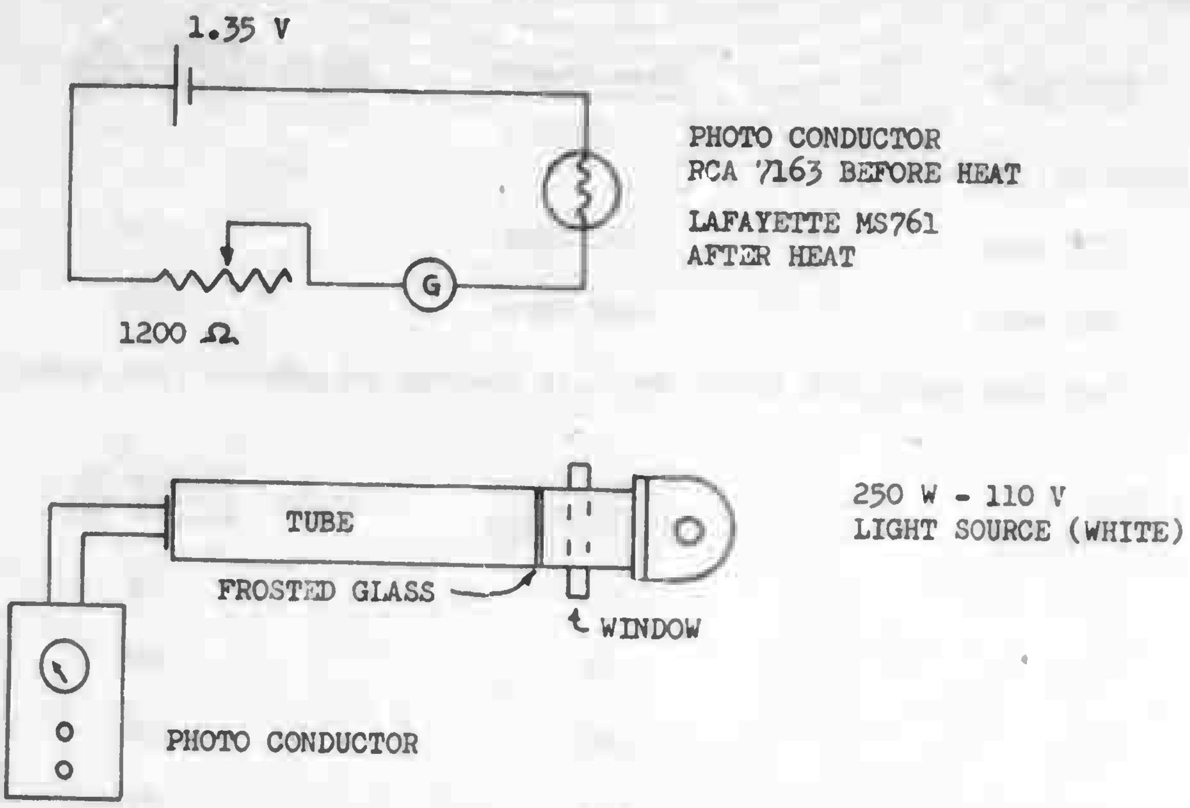

FIGURE 39 STANDARD LIGHT TRANSMISSION APPARATUS

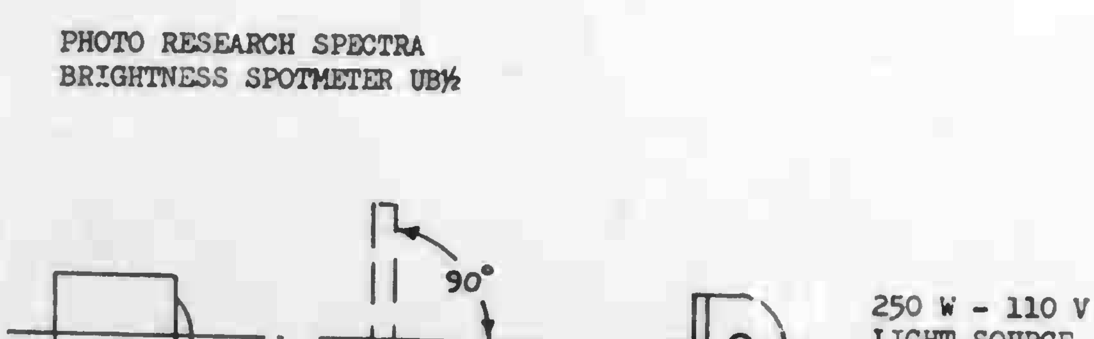

	INITIALS	DATE	REV BY INITIALS	DATE	TITLE	MODEL
CALC					LIGHT TRANSMISSION APPARATUS	X-20
CHECK						
APPD.						
APPD.						

5 ANALYSIS OF WINDOW FAILURE

5.1 THERMAL DEFLECTIONS

It is well known that a flat plate of uniform thickness "t" and of any shape will normally assume a spherical curvature with radius $t/\alpha\Delta T$ when subjected to a thickness temperature gradient. That is, one face is at a uniform temperature "T" and the other face is at a uniform temperature $T + \Delta T$, the temperature gradient between the faces being linear, where α is the coefficient of thermal expansion. No thermal stresses are involved provided that the deflections are not restrained. The X-20 hot side window frame is designed on this principle. The three point suspension system as described on page 16 gives the window frame freedom to deflect thermally and also prevents thermal or load distortions of the cab frame from being induced into the window frame.

The .65 inch thick outer glass would require a thermal gradient through its depth of approximately 10 times that of the 1.62 inch deep Rene' 41 frame in order to have the same thermal curvature. This is because the coefficient of expansion of the Rene' 41 frame is approximately 25 times that of the fused silica glass. In actual test measurements, however, the thermal gradient through the depth of the glass was insignificant. Therefore the window panes want to remain essentially flat during the temperature cycle.

The stiffness (EI) of the frame is approximately 50 times that of the glass at the point of maximum span. Therefore the constraint offered by the glass to the frame is small.

The vertical frame deflections that were recorded during Test No. 3 were plotted versus the recorded frame temperature gradients. The data were plotted for both the short time rapid heat pre-test condition and the actual Test No. 3 condition. The short time-rapid heat deflections are shown on page 126 . The actual Test No. 3 condition is shown on page 127. The test data has been corrected for rigid body movements as shown on page 195. In both of the test cases it can be seen that the recorded frame deflections agreed very closely with the theory discussed.

The actual deflection at the time of glass failure was obtained by extrapolation since some of the deflection indicators were inactive at that time. This deflection data is shown in Figure 42 on page 128. In Figure 42 page 128 the allowable glass curvature is shown based on the assumption of rigid seals.

Reference 5, Side Window Strength Check Notes, page 1.13.11, predicted an allowable frame temperature gradient of 260°F/inch which would be equivalent to 260 (1.62) = 420°F for the total frame.

FIGURE 40 THERMAL DEFLECTION COMPARISON - RAPID HEAT SN 206

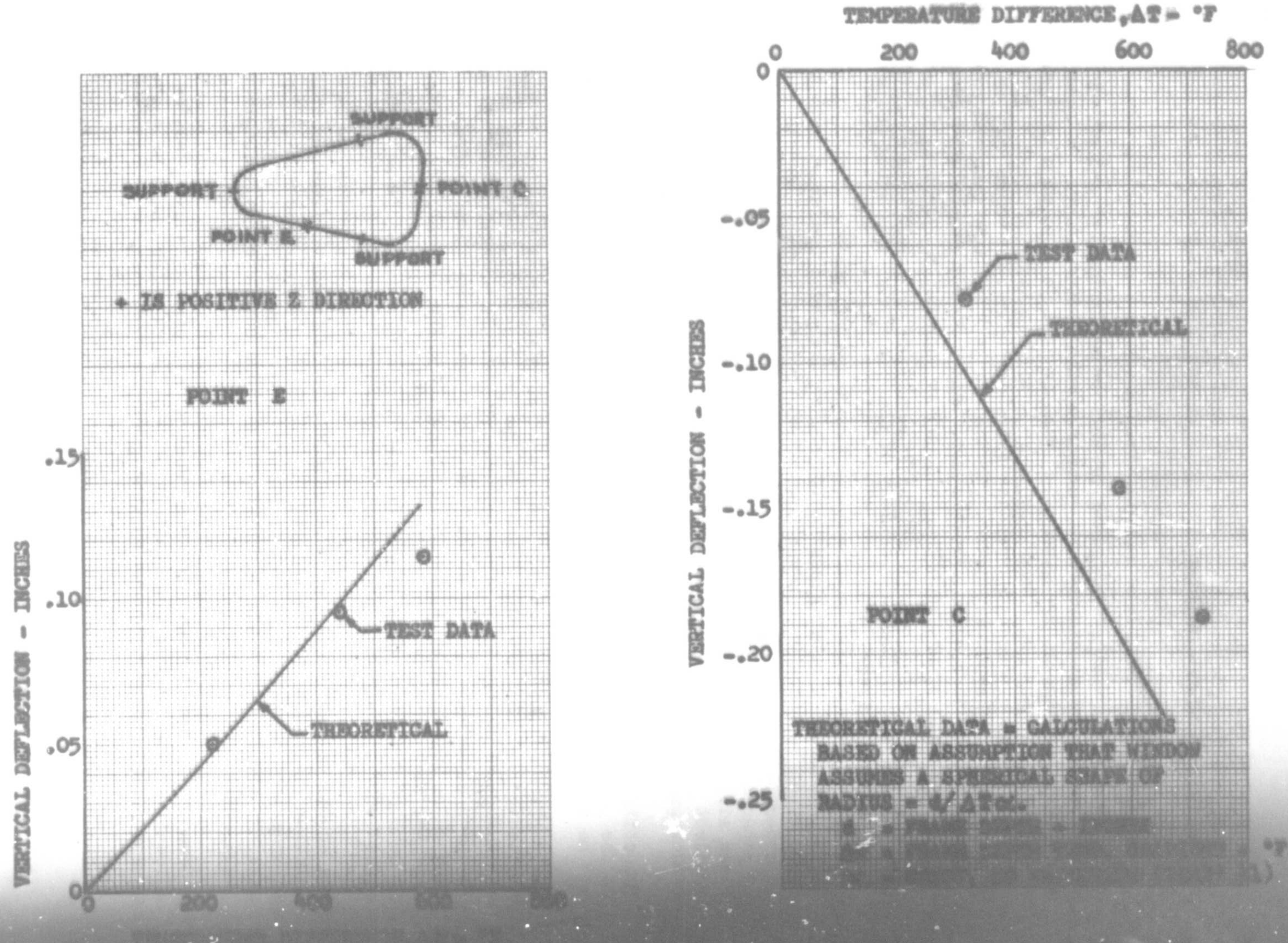

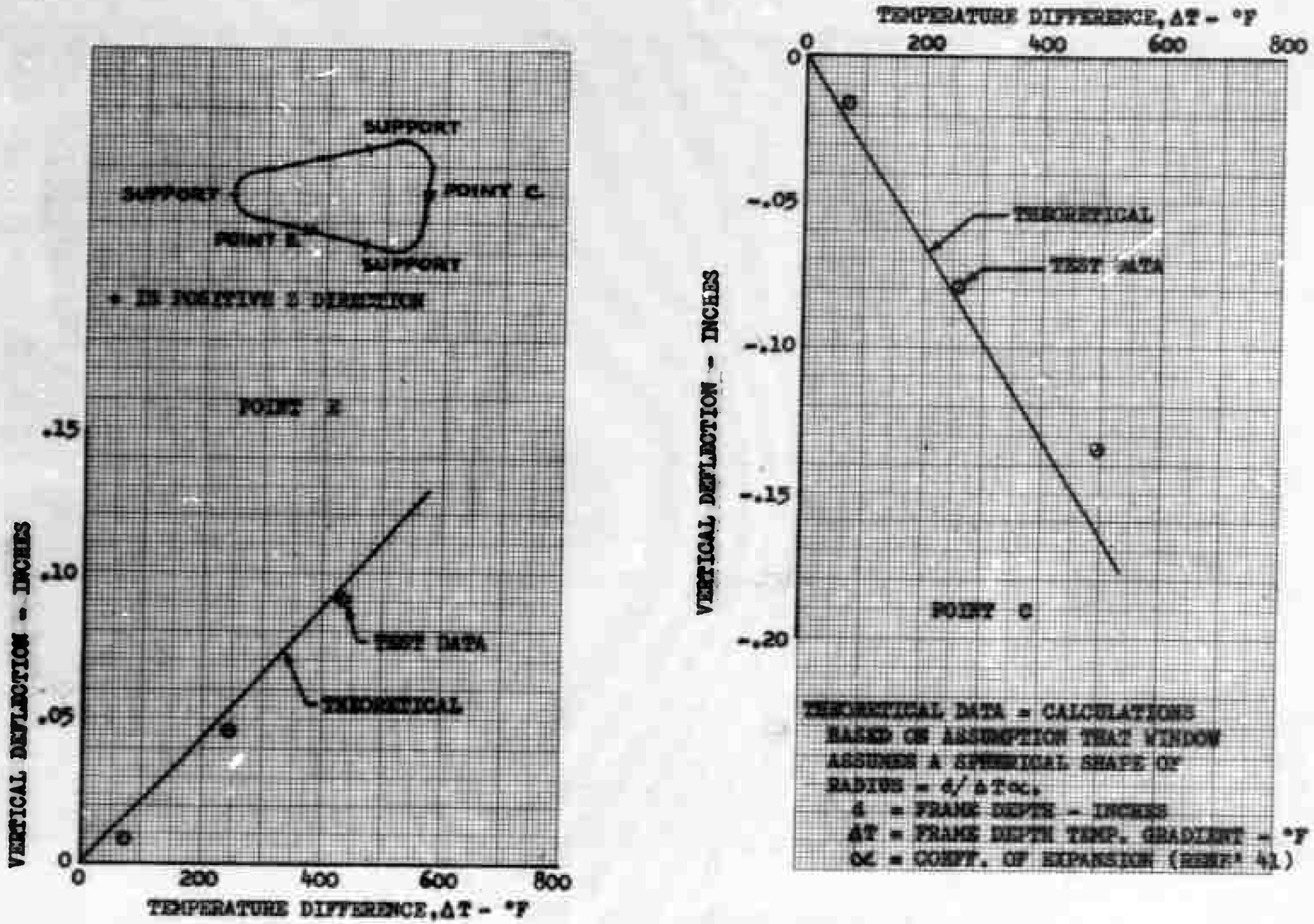

FIGURE 41 Thermal Deflection Comparison-Test No. 3 SN207

FIGURE 42
GLASS THERMAL CURVATURE COMPARISON

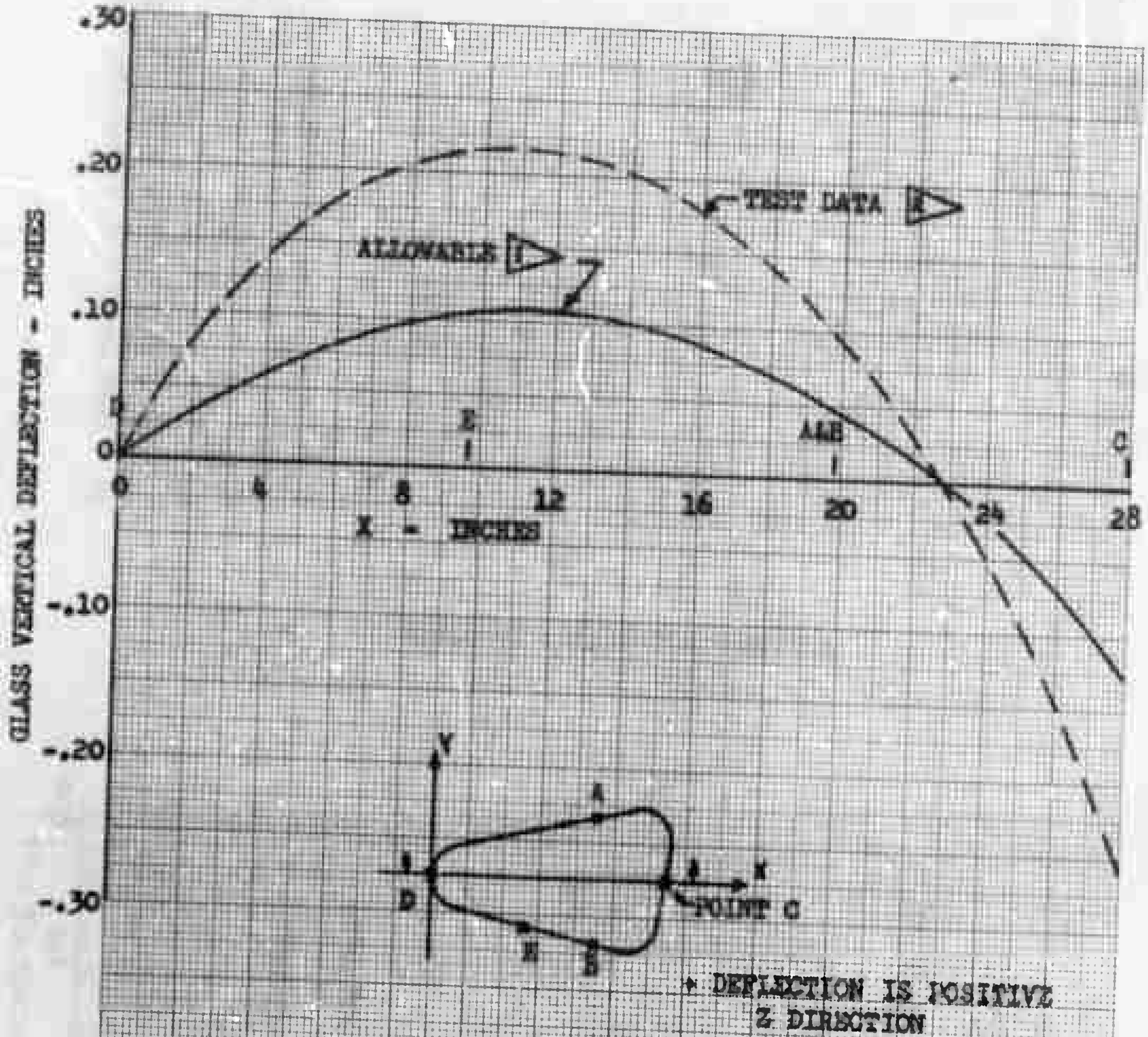

1 ALLOWABLE BENDING IN GLASS
RADIUS = 588. INCHES
FRAME ΔT = 344 °F
GLASS ΔT = 0 °F
INDUCED STRESS IN GLASS = 5800 LBS/IN^2 - RIGID SEALS

2 TEST DATA AT FAILURE (EXTRAPOLATED) - RIGID SEALS
RADIUS = 289. INCHES
FRAME ΔT = 757. °F

5.1 THERMAL DEFLECTIONS (Continued)

The actual measured temperatures at the time of failure are shown pictorially on Figure 43, page 130. It can be seen from Figure 43 that the frame temperature gradients were greater than the allowable. For instance, Section D-D shows a gradient of 1145° - 171° = 974°F.

In view of the good agreement between measured deflections and temperature gradients with elementary theory it is concluded that the primary cause of window failure was the high temperature gradient through the depth of the frame. The resulting frame temperature gradient produced window frame curvature which induced glass curvature in excess of allowable.

5.2 THERMAL ANALYSIS

During the window design phase the frame temperature gradient predictions had been based on significant interface conduction. This, of course, produced relatively low overall thermal gradients.

A new two-dimensional thermal analysis of the window frame was performed after the window pane failure occurred during Test No. 3. This thermal analysis used some relatively new approaches, particularly in the handling of interface thermal resistance. A recent X-20 continuation effort, "Hot Structures Thermal Correlation", (Reference 6) indicated that for materials such as Rene' 41 at high temperatures, the radiation mode of heat transfer across an interface is highly dominant, i.e., conduction can and should be neglected. This analysis assumes all window frame interfaces (including those due to the seal system) have radiation heat transfer only.

Two cases were analyzed. The results are shown on Figure 44, page 131, and Figure 45, page 132. Figure 40, page 144, is based on the available data from Test Condition 3 up to a time of 6 minutes at which time the window failure occurred. All external temperature boundary nodes were driven from the actual test data for this case. Figure 45, page 132, shows temperature gradients for a complete test profile. Variances from the test case include insulation around the periphery of the specimen and a slightly different control location on the fairing.

Of prime interest in both cases, Figures 44 and 45, is the correlation between the analysis and test data and the relatively lower gradient existing through the bulk of the frame (Nodes 17 through 21). Evidently the major gradient which induced the pane failure was that shown between Nodes 16 and 17. The frame's outermost element or fairing (Node 16) being a continuous structural member drove most of the frame curvature which resulted in pane bending and failure. These results suggest that a possible solution would be to redesign the outer fairing and inner backup strip frame elements to allow for differential expansion such as by segmentation. This would require a relocation of the basic seal plane to a more internal location such as the inner surface of the outer pane.

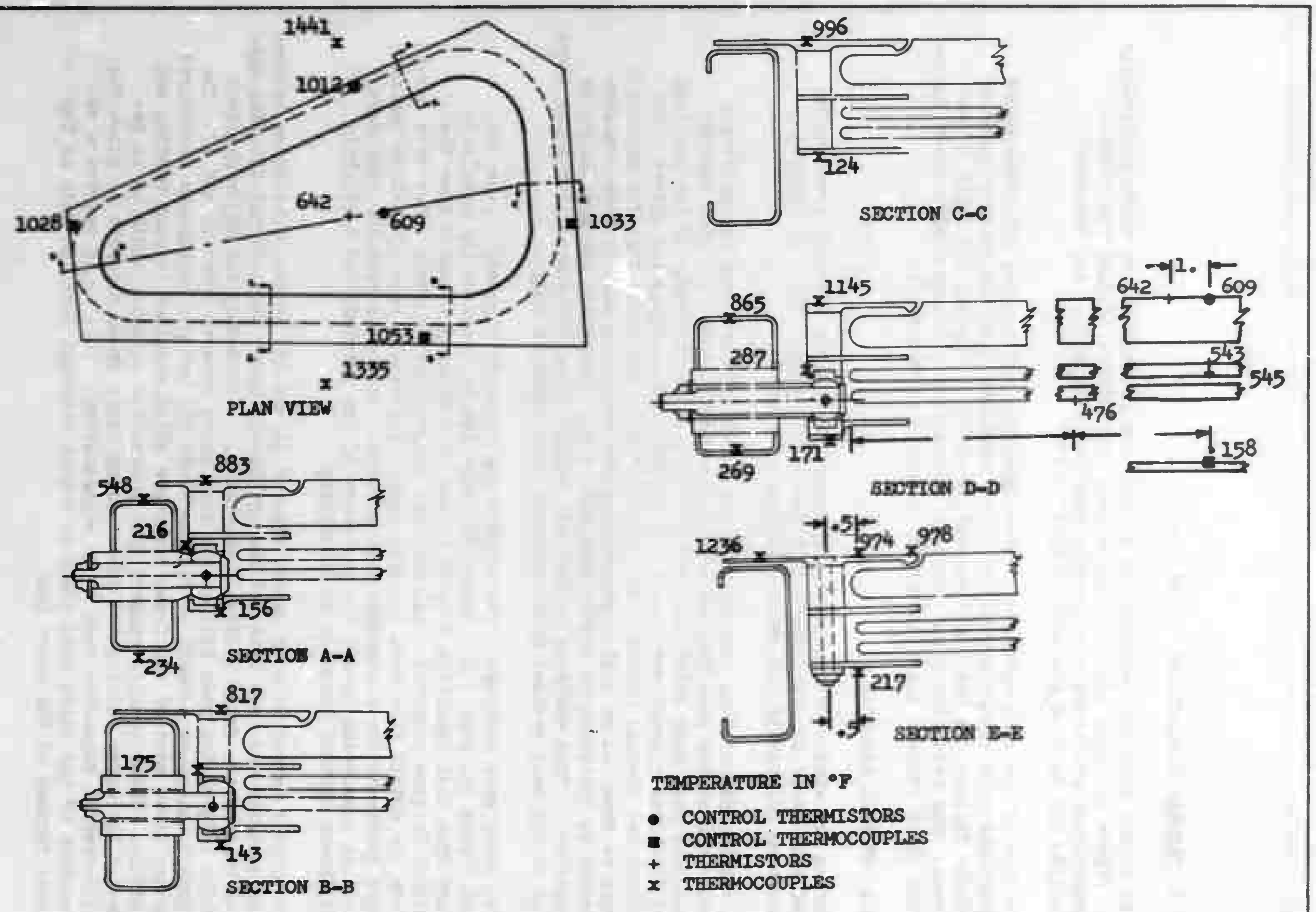

FIGURE 43 TEMPERATURE DISTRIBUTION AT TIME OF WINDOW FAILURE

FIGURE 44 THERMAL ANALYSIS OF TEST NO. 3

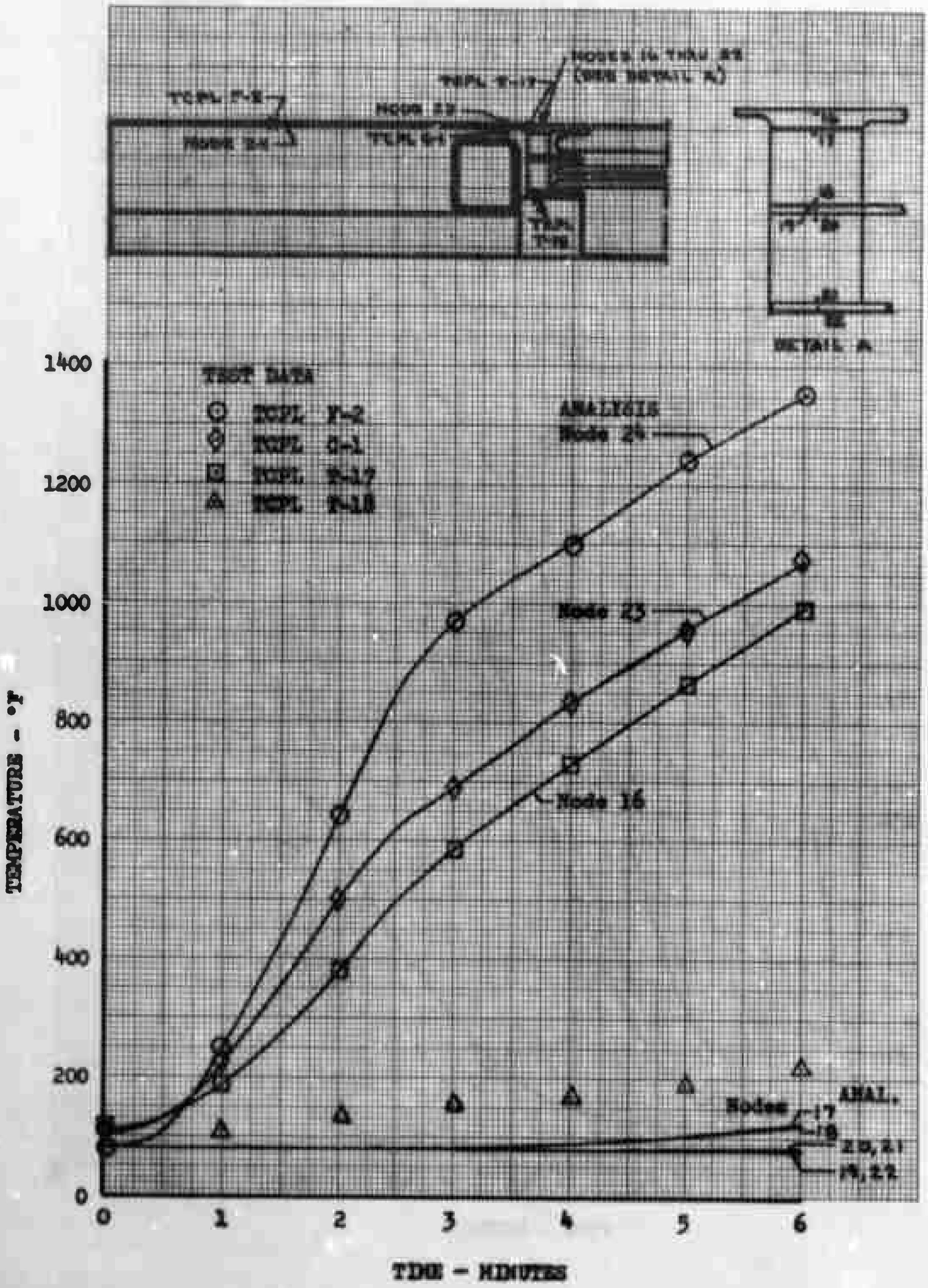

FIGURE 45 THERMAL ANALYSIS - REVISED TEST SET-UP

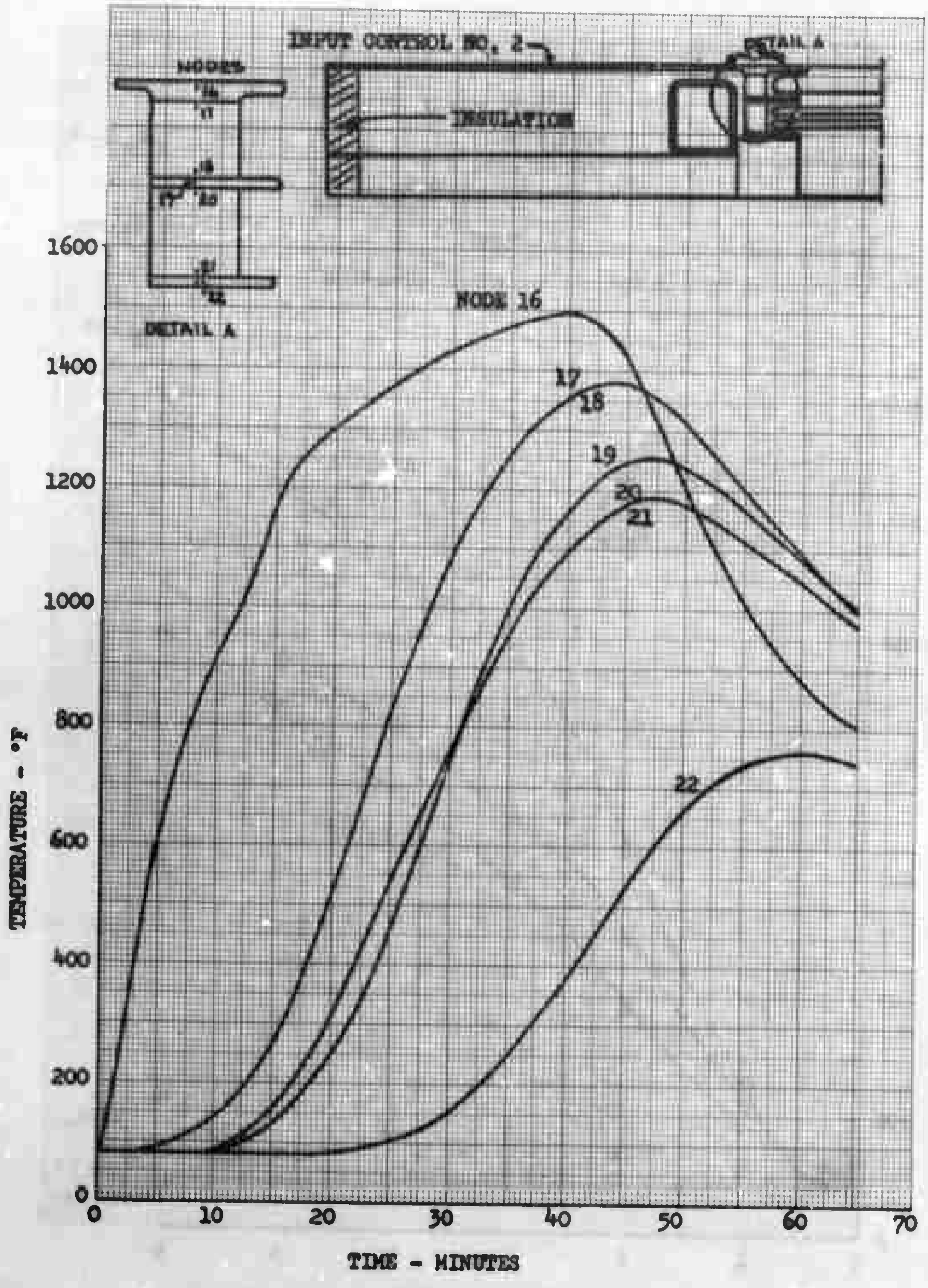

5.3 THERMISTOR LEADS

Upon examination of the crack pattern of the window pane as shown in Figure 35 page 63, it is evident that the crack originated at the location where four thermistor leads exited through the window seals. The wedge pattern of the crack near the thermistor leads indicates the outer surface of the glass was in tension as expected. The fissures indicate the crack traveled from the thermistor leads across the window then rebounded to a location approximately midway between the supports.

A secondary cause of failure is believed to be the hard point in the seals caused by the thermistor instrumentation leads running under the window seals as discussed on page 24. These leads would not be present on flight hardware, however.

6 CONCLUSIONS AND RECOMMENDATIONS

An X-20A (Dyna-Soar) high temperature side window assembly was fabricated from superalloys and fused silica panes. The window assembly was subjected to a series of tests simulating the X-20 environment to experimentally verify the design and to provide experience for improved window design. The window assembly successfully withstood a preliminary vibration survey and limit boost airload pressure. The outer window pane fractured during the simulated re-entry temperature cycle. The major cause of the window pane failure was the high temperature gradient through the depth of the window frame. The frame temperature gradient produced frame curvature which exceeded the allowable curvature of the glass. Although the full planned program of tests was not completed, limited tests were run for each of the three design environments—vibration, pressure, and temperature. The following specific conclusions and recommendations were made as a result of the limited tests and the analysis conducted on the window assembly:

6.1 INSTRUMENTATION

a. The hard point in the window seals caused by the thermistor instrumentation leads running under the window seals is believed to have caused a stress concentration which added to the cause of failure. This, however, is considered to be a secondary factor. In future window testing it is recommended that methods be designed to prevent stress concentrations caused by the instrumentation leads running through the window seals. It is possible that grooves could be manufactured in the seals but this also may cause some stress concentrations, and would prevent sealing the outer window. With some development it is envisioned that the gold thin film thermistor leads could be continued around the edge of the glass. The contacts could then be made on the edge of the glass and thus not alter the seals. The present X-20 frame design does not have sufficient clearance for this application, however.

6.2 TESTING

a. The test bed fixture weight for the vibration test was limited so as not to exceed the maximum load capability of the Ling A-300B shaker. The test bed fixture consisted of a two inch thick aluminum plate. High amplification factors were recorded during preliminary testing which indicated the test jig mounting plate had marginal stiffness.

It is recommended that future vibration testing of window specimens of equivalent weight and size be performed on a shaker of larger capacity so that the test bed could have a much greater stiffness. Such shakers as the Ling 249, L200, or MBC210 are recommended.

6.2 TESTING (Continued)

b. The heat control zone separation for the test was not sufficient to give ideal flight simulation. Results from Test No. 3 indicate that sufficient heat from Control Zone 2 was entering Control Zone 1 to heat the center of the window pane to the programmed levels. Thus the outer window pane regions were possibly hotter since they were closer to the energy source. This effect may have contributed to the window failure in a minor degree.

Future testing of window specimens should consider special baffles or close lamp spacing to the specimen (this would require separate test set-up for tests run with and without vacuum-pressure box for clearance reasons) and methods to prevent lamp reflector overlaps.

c. The insufficient separation of the heat control zones required the removal of most of the silicon carbide powder from the outside window pane in order to prevent overheating. This allowed some direct penetration of the heat lamp radiant energy to the interior regions of the window system. Since flight plasma radiation is insignificant in the side window region, such penetration is less than ideal flight simulation. This effect did not contribute to the window failure as it actually reduced the frame thermal temperature gradient slightly.

6.3 STRENGTH ANALYSIS

a. The comparison of window frame rotations (torsional angular twist) and vertical deflections due to limit boost air load with analyses based on the direct stiffness method as programmed for the digital IBM 7094 Computer show good correlation. In most cases the values lie between the fixed and pinned glass to frame analyses cases.

It is concluded that the good agreement between the analysis and test data for boost limit airload is evidence that the window assembly has no structural weakness. Extrapolation of this data to ultimate load indicates that the window assembly could withstand the ultimate pressure load without failure.

6.4 THERMAL ANALYSIS

a. The measured thermal deflections can be approximated with reasonable accuracy by elementary theory.

b. The window frame design was based on interface thermal conduction which resulted in low overall frame thermal gradient predictions. A new thermal analysis based on radiation heat transfer only across the interfaces agrees with the test data and predicts the high thermal gradients that were measured, and was the primary cause of the window failure.

6.4 THERMAL ANALYSIS (Continued)

c. The high frame thermal gradients were caused by the many interfaces (laminations) created by the buildup of bars, plates, and shims in the construction of the frame. These interfaces resulted in poor thermal conductivity through the window frame. A large temperature drop occurs across the first interface (fairing).

6.5 WINDOW DESIGN

a. The three point suspension system of the X-20 side window frame performed satisfactorily. The suspension system prevented the cab frame distortions from being induced into the window frame. The system also allowed relative movement of the window frame and the cab frame in the plane of the window without inducing redundant force systems.

b. Rene' 41 material is considered a suitable material for window frame material that must operate in the X-20 environment (1800°F) even though its coefficient of thermal expansion is somewhat larger than suitable refractory alloys. Thus Rene' 41 exhibits somewhat larger curvature due to frame thermal gradients. The problems of coatings, fabrication, and assembly of refractory alloys appear to offset the advantages offered by their somewhat lower coefficients of thermal expansion.

c. The use of the window leaf springs installed in series with the seals to maintain clamping forces after exposure to the heat environment and the side clamping and positioning springs are considered good design procedure.

d. The air leakage rate through the window seals exceeded the design target value by a factor of 10. The higher leakage rate is attributed to the thermistor lead wires passing across the window seal. The leakage rates are not considered conclusive of the sealing qualities of the window seals as the flight article would not have these thermistor leads. The use of the Hastelloy-X wire mesh high temperature seals is considered good design procedure.

e. The X-20A window design represents the most advanced technology for hypersonic re-entry vehicles. It is recommended that a redesign of the X-20A high temperature side window be considered incorporating design improvements based on the experience of this test program. The new design should then be subjected to the environmental tests as planned under this program. The potential value of such a program has application in many high temperature window requirements.

A redesign should consider the segmentation of the outer fairing (retainer) in order to allow this element to expand differentially. The other portions of the window frame should be made as continuous and homogeneous as possible.

APPENDIX I

STRUCTURAL ANALYSIS

I STRUCTURAL ANALYSIS

Summary

This secion presents the deflection and internal loads analysis of the X-20 external side window for the critical design condition, boost ultimate net pressure of 10.5 psi.

A description of the window and window environment, and the construction of a mathematical model for structural analysis are presented. The stiffness method as programmed for the digital IBM 7094 by The Boeing Company, and called "Cosmos", is used for analysis.

Results of the digital solution include translation and rotation, and internal loads in the glass pane and the window frame. A discussion of the stresses and strains in the critically stressed region of the glass pane is included.

External Loads

External loads are taken from D2-81142, "X-20 Boost, Hypersonic, Approach, and Air Launch Phase Load Conditions". The side window outer glass pane is critical for the boost environment. The critical condition during boost results in a net air load of 10.5 psi ultimate on the external side window.

The curve of page 140 shows hatch area boost pressures corresponding to the critical condition.

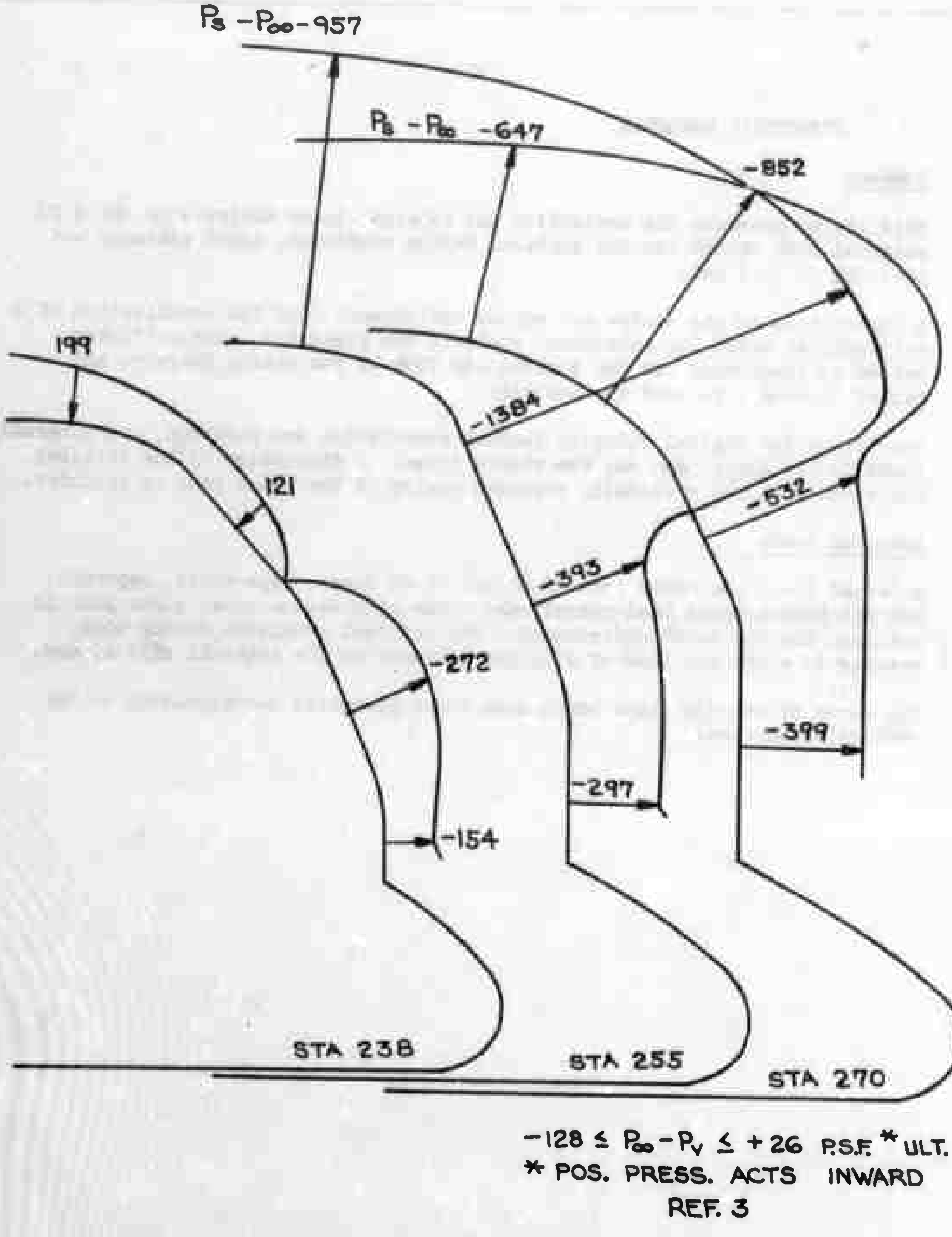

FIGURE 46 Boost Pressure Distribution - Hatch Area

Internal Loads

The side window outer glass pane is critical for the boost environment. This includes effects of air load, vibration, and installation. This paper deals with the effects of air loads on the glass.

The internal loads in the glass pane are affected by several design features of the window assembly.

1) The window frame is supported at three points. This tends to concentrate the load in the glass at the three support regions.

2) As the window frame is stiffened, the tendency for the stress trajectories to concentrate at support regions is reduced.

3) Support of the window by a system of seals and springs in series cushions the window edge as it is clamped in the frame.

4) The glass bears on the window frame through the seals. The center of action of the bearing force is conservatively estimated to be .92 inch from the shear and torsion center of the window frame. (See Figure 47 , page 143) Torsion moments are applied to the window frame when air load is transferred from the glass to the frame. The torsional rotation of the frame under these moments will force the glass to carry more of the airload toward the frame support points.

5) Springs around the periphery of the window are designed to fill the gap between the window pane and window frame. These springs position the window for all times during flight of the X-20, cushioning against vibration and inertia loads.

Idealization of the X-20 Side Window for the Stress Analysis

The mathematical model which simulates the structural behavior of the X-20 side window is shown in Figure 47 , page 143. The model is made up of four types of structural elements which together simulate the stiffnesses of the real structure. They are quadrilateral and triangular plate elements, six degree of freedom beam elements, and spar elements.

The quadrilateral and triangular plate elements are used to simulate the .65 inch thick fused silica glass pane. Quadrilateral plates are used in all areas except where a change in size of quadrilateral elements is desired, or where geometry of the real plate is such that it is naturally simulated by a triangular element (as in the case around the boundary of the side window).

The six degree of freedom beam elements are used to simulate the window frame bending and torsion stiffness. They also have the capability of defining the locus of the centers of shear and torsion to lie away from the points of load transfer from glass to frame by any dimension. This permits proper simulation of the coupling of torsion and bending in the window frame with the load transfer from glass to frame.

The spar elements are used to force displacement compatibility between the boundary of the real plate and the frame at the points of load transfer between glass and frame. Essentially the spar elements are used as a device for pinning the glass to the frame. Spar elements may be used to simulate seal and seal spring flexibility. The one inch length for spar elements is arbitrary as long as axial area is adjusted accordingly.

The actual assemblage of window pane and window frame with seals is shown for comparison with the idealized structure simulating the actual assemblage on page 143.

Nodes may be defined as points in the idealized structure at which loads may be applied, the structure may be supported, deflections and rotations of the structures may be obtained, continuity between the common structural elements may (or may not) be enforced (at the user's discretion).

Nodes for the plate elements are numbered 1 through 129. Nodes for the window frame six degree of freedom beam elements are located one inch "below" the boundary of the plate elements. The frame nodes are obtained simply by adding 200 to the corresponding window boundary node number. The spar elements simulating seal stiffness connect the window boundary nodes to their corresponding frame nodes.

Idealization of the X-20 Side Window for the Stress Analysis (Continued)

The side window frame is supported at three points. These points are indicated in the figure on page 145 . These support points are not located at frame nodes but, instead, at the center of shear and torsion of the frame. Some supports can be specified only at nodes, the support points for the frame are moved to frame nodes 201, 287, and 296. Appropriate moments are then applied at these frame nodes to correct for the movement of the support points to the frame nodes.

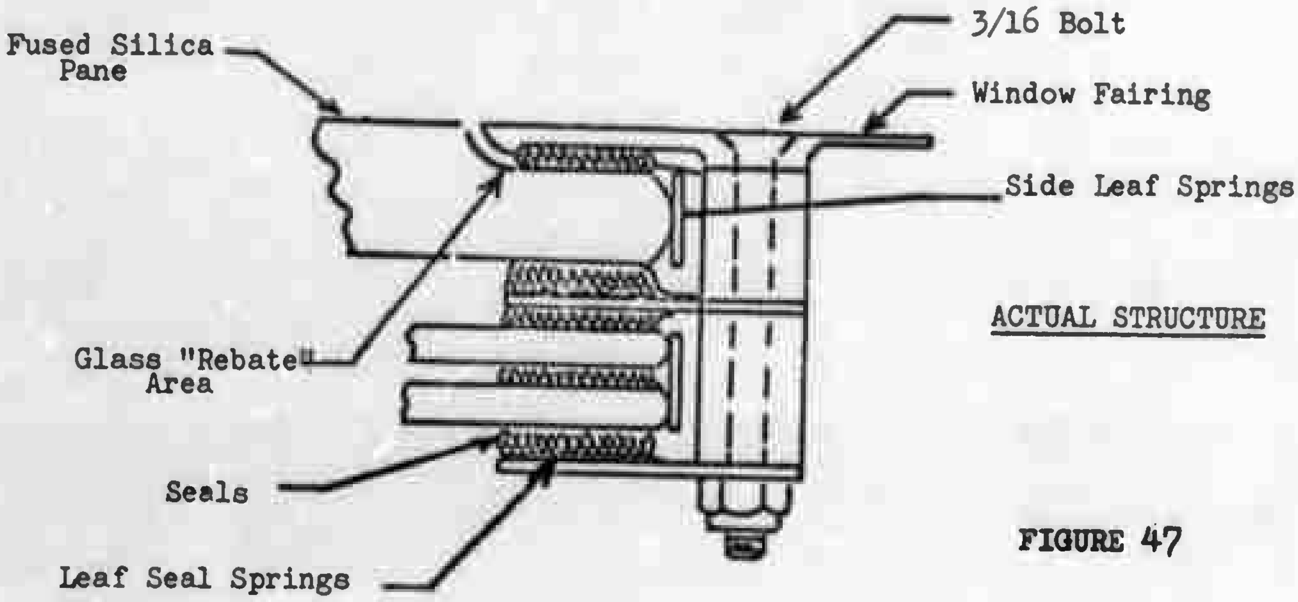

FIGURE 47

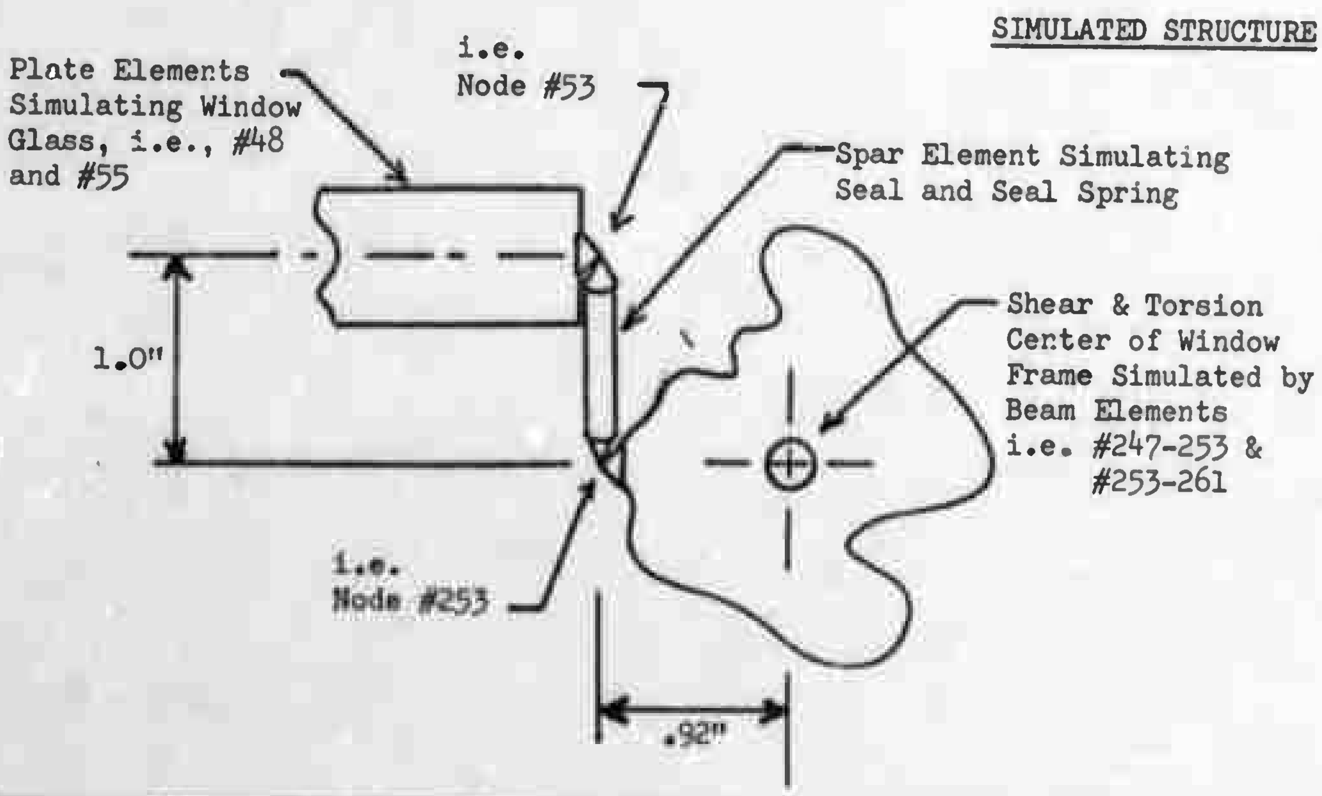

The following figure shows the arrangement of structural elements for the stress and deflection analysis of the X-20 side window. Also shown is the coordinate system and sign convention for displacement and rotation at the nodes.

An illustration of the simulation of the frame and pane is shown on page 143.

NOMENCLATURE

1. Node numbers for the glass plate elements are numbered 1 through 229.
2. To obtain window frame beam element node numbers, add 200 to the node numbers assigned to the glass plate periphery.
3. All panel numbers are underlined. Panels numbered 1 thru 121 represent the side window outer pane, .65 inch thick. Panels numbered 122 thru 163 are used only for proper allocation of airload on the window fairing to nodes.
4. ——— Indicates beam elements representing window frame. This line coincides with the locus of points lying on the window frame shear center.
5. ⌖ Indicates locations of three support points for window frame.

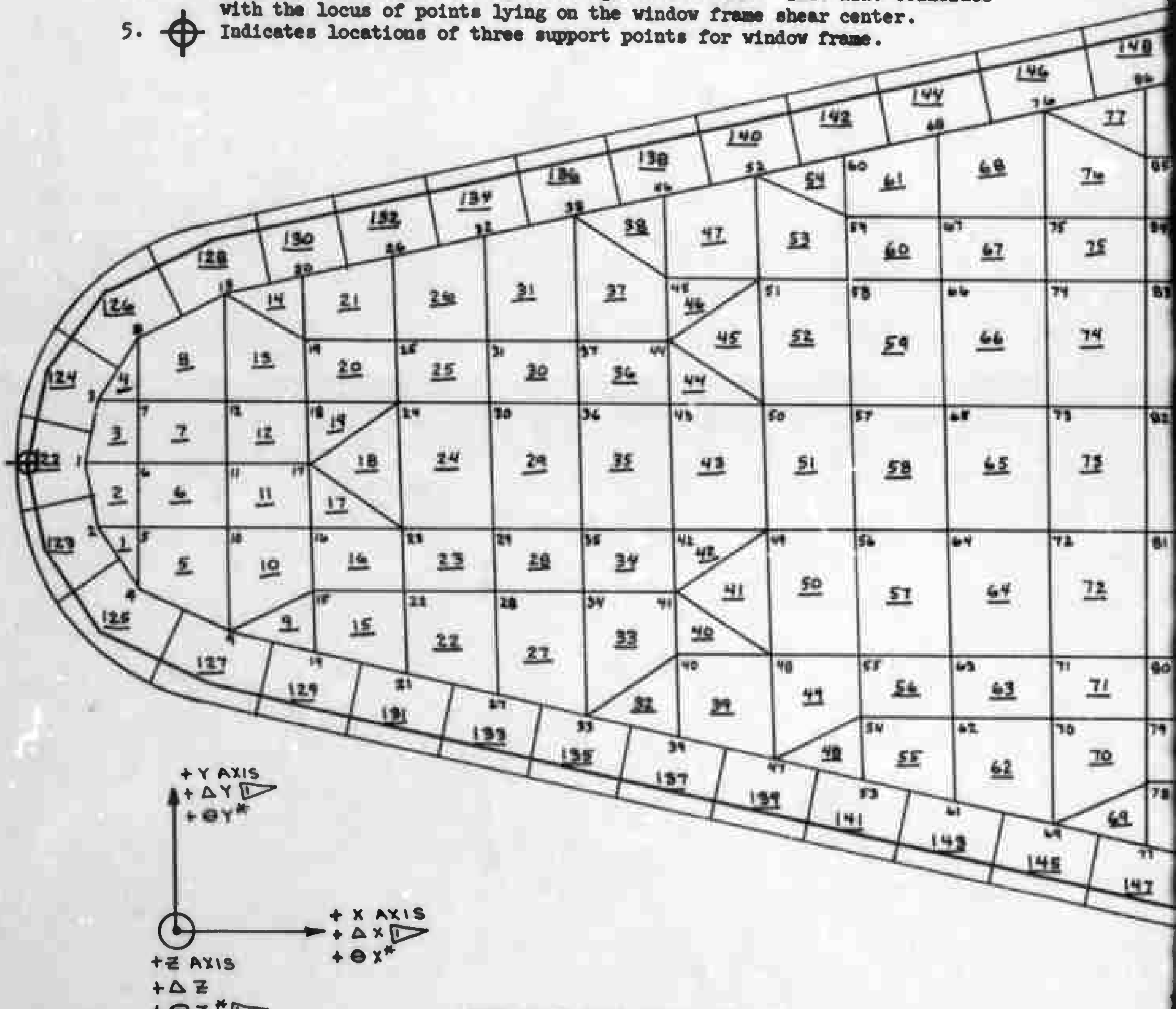

*Use right hand screw rule

▷ These node deformations are zero for this analysis

through 229.
0 to the node numbers

u 121 represent the
122 thru 163 are
fairing to nodes.
This line coincides
shear center.
dow frame.

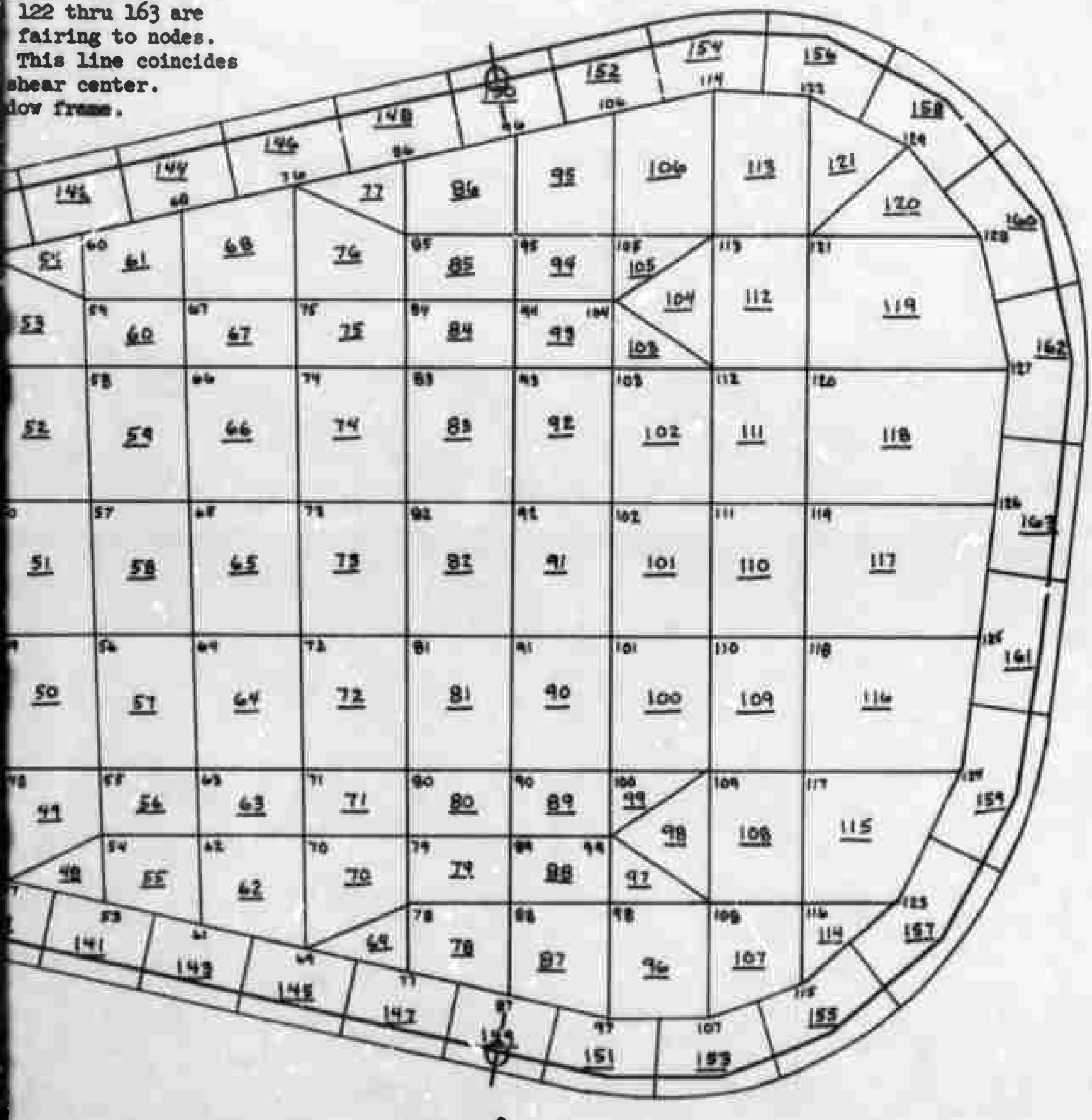

zero for this analysis

FIGURE 48
NODAL AND STRUCTURAL ELEMENT DIAGRAM

2

Description of Mathematical Model Structural Properties

The window glass is supported around its periphery by the window frame which, in turn, rests on three spherical bearings at the three support points. The glass bears on the frame through the seals and seal springs. The center of action of the bearing force is conservatively estimated to be .92 inch from the shear and torsion center of the frame.

A soft window frame in bending or in torsion will force the glass to carry more of the air load toward the window frame support points. Bending and torsion stiffnesses of the window frame are calculated on page 176.

Use of soft seals and seal springs around the edge of the glass results in a more uniform transfer of load from the glass to the frame. Becuase of the non-linearity expected for seal spring rates, seals and seal springs are simulated to be approximately 25 times stiffer than is expected at room temperature. Flexing of the window frame protruding flanges is conservatively neglected in calculating seal stiffness.

Elastic properties of Rene' 41 and fused silica glass are presented in the Appendix on pages 203 to 215.

External Loads for the Idealized Structure

A net uniform pressure of 4.3 psi is applied to the mathematical model. The pressure is applied in the positive z-direction. For other pressures a direct ratio may be employed as this solution is not non-linear. I.e., for the boost ultimate net pressure of 10.5 psi, external loads, internal loads, deflections, etc. may be obtained by multiplying the results presented here by the ratio of 10.5/4.3 = 2.442.

External loads can be applied to the mathematical model only at node points. To accomplish the transformation of uniform pressure to node loads, the surface of the window is simply divided into air load panels, and the resolution of load to the nodes is performed using principles of statics and engineering judgment.

Deflections

Deflection patterns of the glass pane and window frame when subjected to a uniform air load are shown on pages 149 and 151 respectively for z-axis translations. Translation vectors drawn slanting upward and to the left are in the positive z-direction.

Translations and rotations of all nodes for a uniform air load of 4.3 psi acting in the positive z-direction are tabulated on pages 153 through 162. The right hand screw rule is followed for rotations. See page 145 for pictorial presentation of deflection sign convention.

To obtain translations and rotations of the window structure when subjected to boost ultimate net pressure of 10.5 psi, multiply by 2.442.

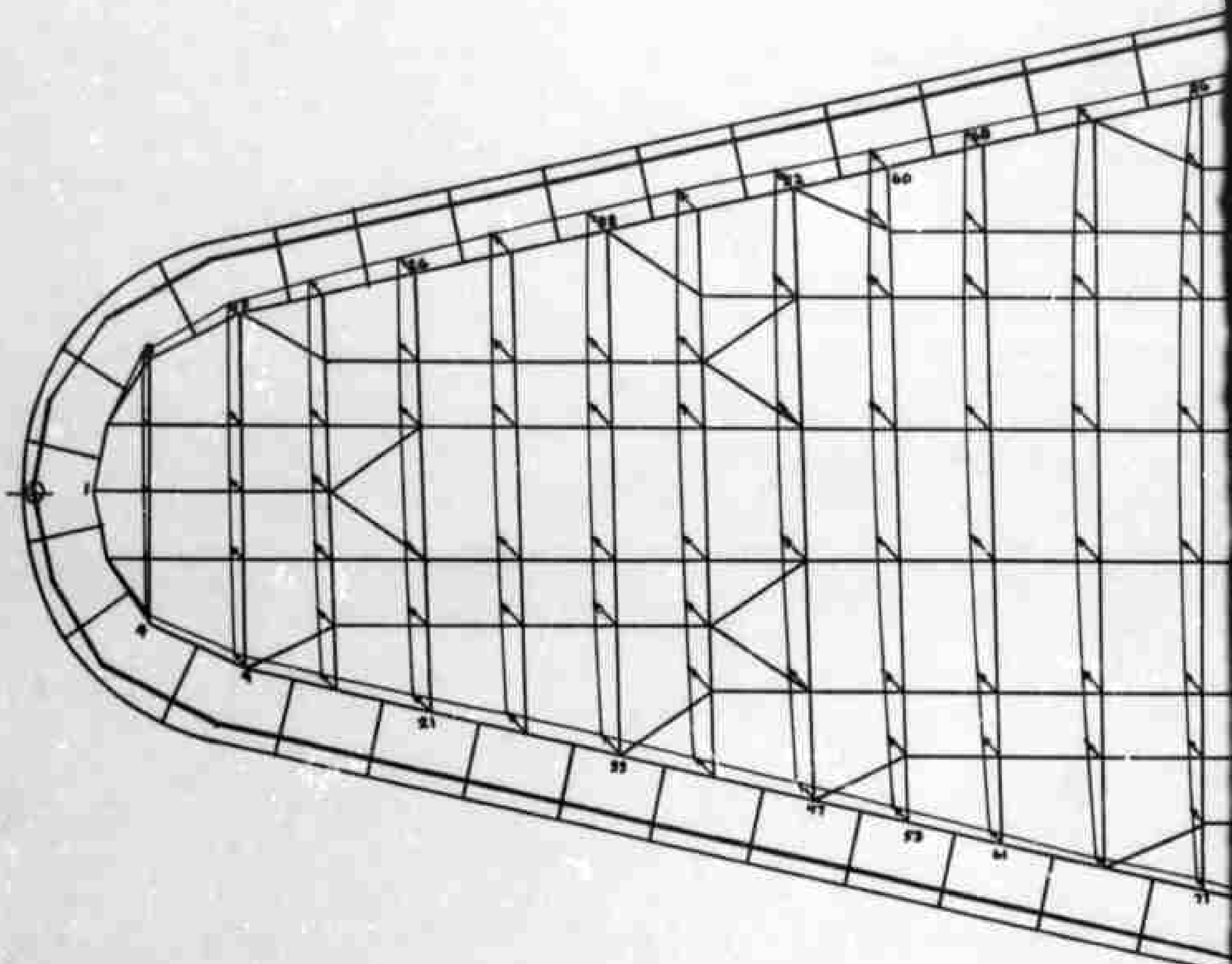

Load is normal to the window
and toward the reader.

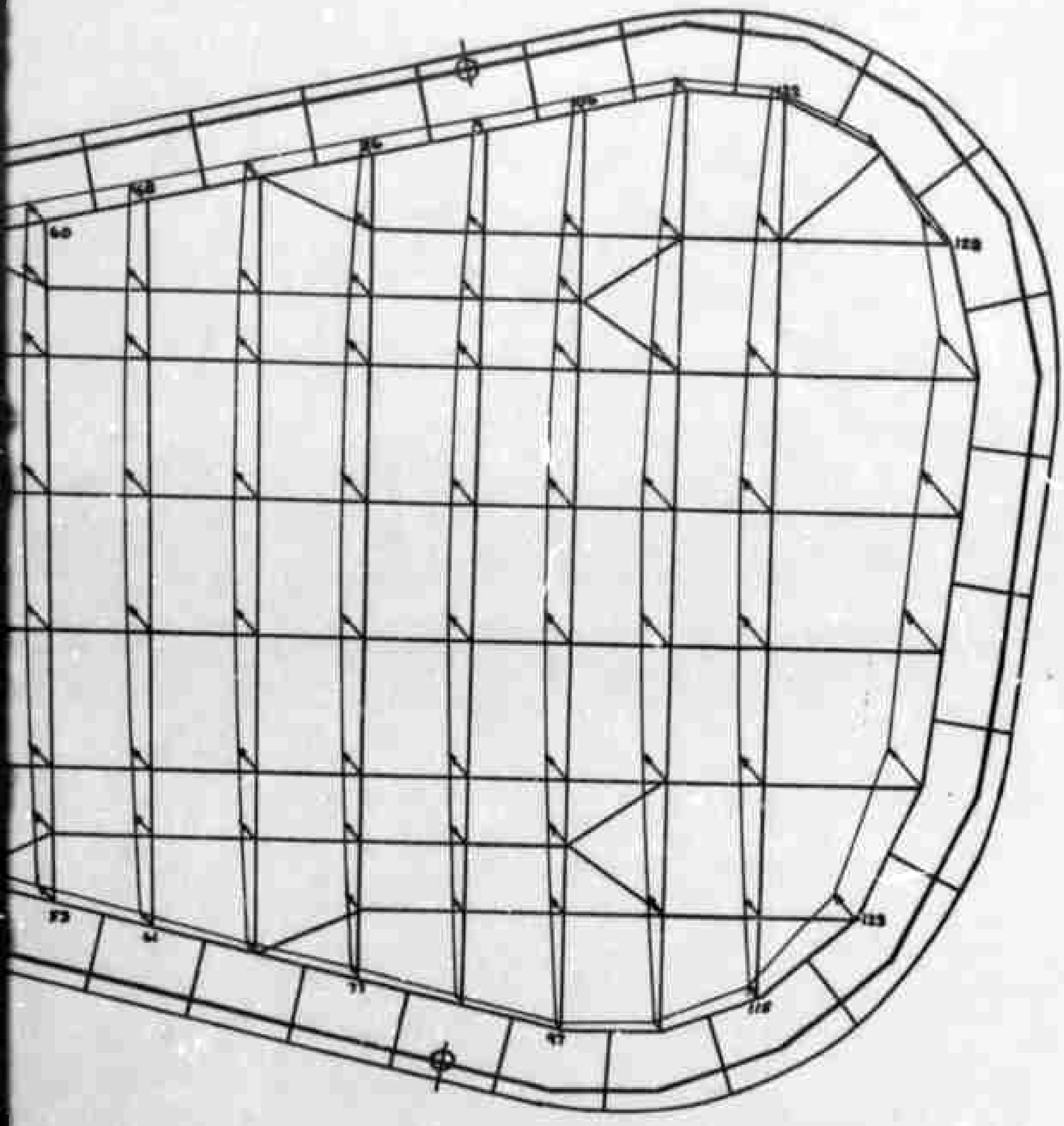

FIGURE 49

AIRLOAD DEFLECTION PATTERN

Pinned Case - Airload = 4.3 Lbs/In^2

2

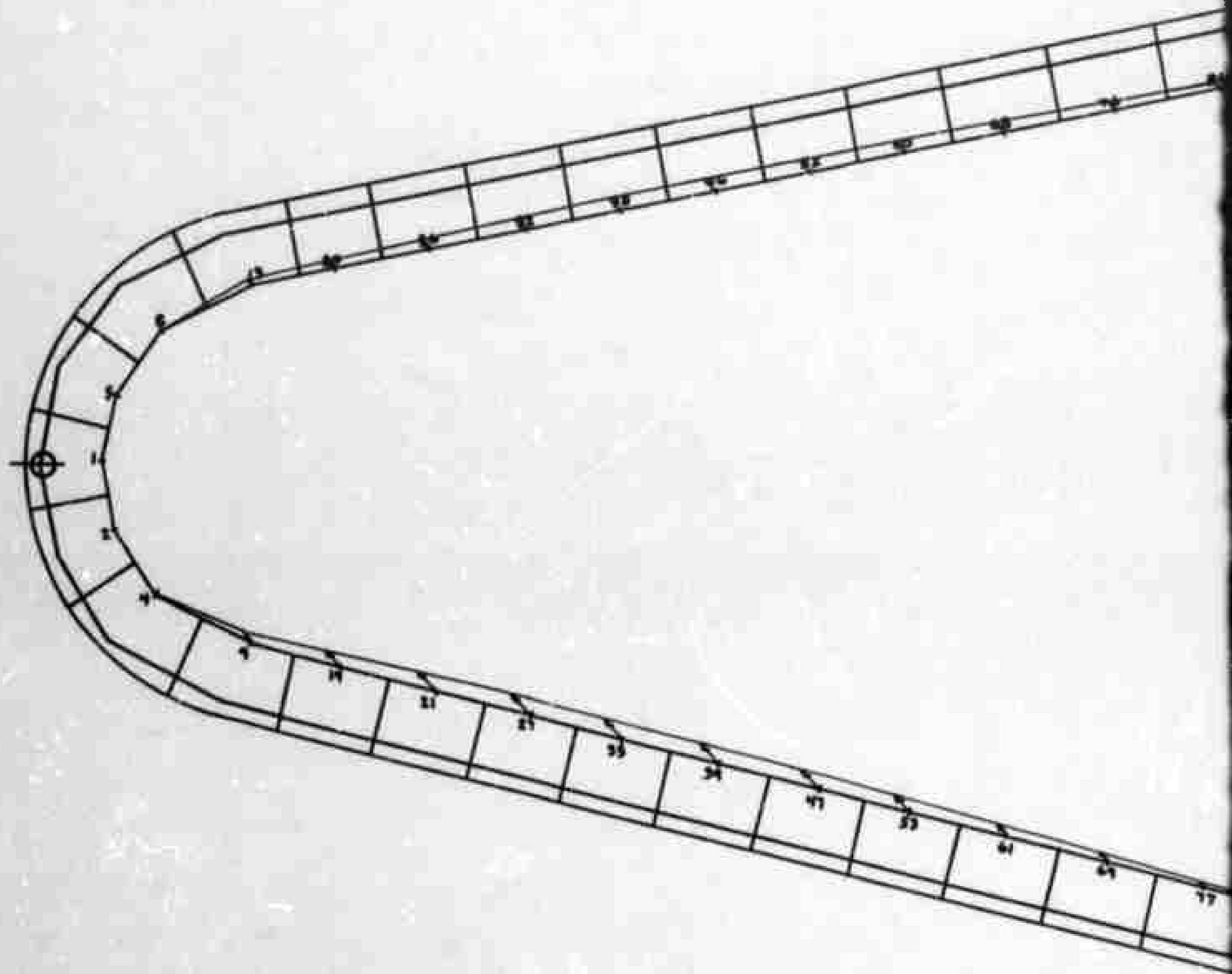

Load is normal to the frame
and toward the reader.

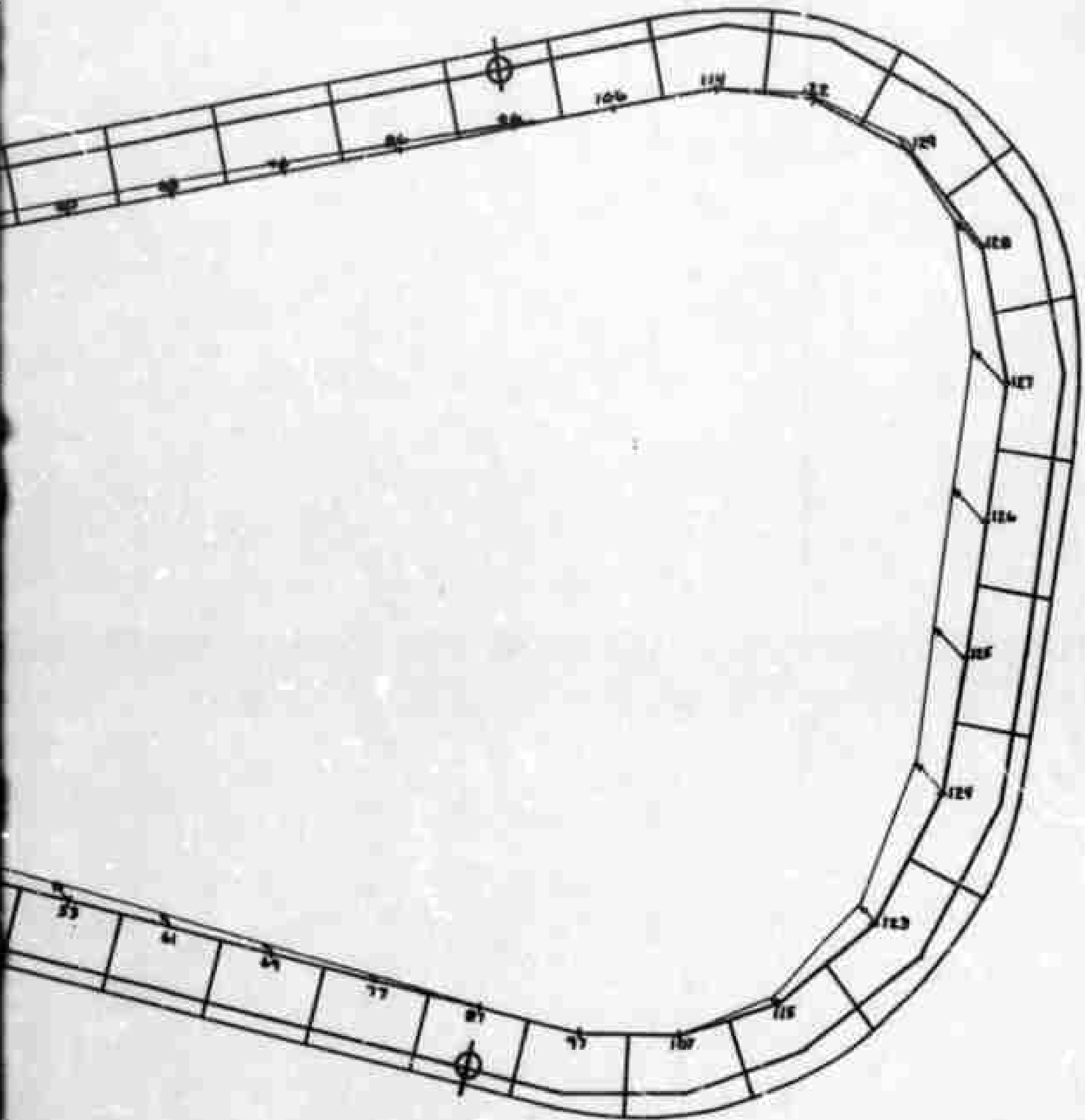

2

FIGURE 50
FRAME AIRLOAD DEFLECTION PATTERN
Pinned Case - Airload = 4.3 Lbs/I

TABLE 3 ROTATIONS AND DEFLECTIONS - PINNED CASE

Pressure = 4.3 psi

RY = θ_y - RADIANS
RX = θ_x - RADIANS
Z = ΔZ - INCHES

NODE	FREEDOM		NODE	FREEDOM	
1	RY	-2 -.10309921	17	Z	-2 +.41737234
1	RX	-3 -.10008610	18	RY	-3 -.87060937
1	Z	-3 +.59392566	18	RX	-3 -.13587298
2	RY	-2 -.10263542	18	Z	-2 +.40351832
2	RX	-4 -.75697320	19	RY	-3 -.86751173
2	Z	-3 +.89787785	19	RX	-3 -.16833000
3	RY	-2 -.10307034	19	Z	-2 +.38457096
3	RX	-3 -.12229998	20	RY	-3 -.85654965
3	Z	-3 +.68795080	20	RX	-3 -.17271722
4	RY	-2 -.10024731	20	Z	-2 +.36454800
4	RX	-4 -.53730180	21	RY	-3 -.62627717
4	Z	-2 +.16451625	21	RX	-4 +.46174014
5	RY	-2 -.10181153	21	Z	-2 +.53869758
5	RX	-4 -.70609816	22	RY	-3 -.67815602
5	Z	-2 +.15749265	22	RX	-4 +.32485974
6	RY	-2 -.10254908	22	Z	-2 +.54256400
6	RX	-4 -.98444681	23	RY	-3 -.70644380
6	Z	-2 +.14812860	23	RX	-4 -.16039641
7	RY	-2 -.10237956	23	Z	-2 +.54097900
7	RX	-3 -.12571457	24	RY	-3 -.72406521
7	Z	-2 +.13578398	24	RX	-3 -.14135247
8	RY	-2 -.10144813	24	Z	-2 +.52092281
8	RX	-3 -.14083086	25	RY	-3 -.71632650
8	Z	-2 +.12119790	25	RX	-3 -.18638586
9	RY	-3 -.93087357	25	Z	-2 +.50128611
9	RX	-4 -.27537489	26	RY	-3 -.68701922
9	Z	-2 +.30729662	26	RX	-3 -.19547176
10	RY	-3 -.96043775	26	Z	-2 +.47260937
10	RX	-4 -.53679347	27	RY	-3 -.41748154
10	Z	-2 +.29944174	27	RX	-3 +.12709813
11	RY	-3 -.97064738	27	Z	-2 +.61182206
11	RX	-4 -.93476823	28	RY	-3 -.50111958
11	Z	-2 +.29023760	28	RX	-4 +.83829669
12	RY	-3 -.97039144	28	Z	-2 +.62863291
12	RX	-3 -.13328395	29	RY	-3 -.53507935
12	Z	-2 +.27786387	29	RX	-4 +.12977459
13	RY	-3 -.95404546	29	Z	-2 +.63277687
13	RX	-3 -.15894785	30	RY	-3 -.55318845
13	Z	-2 +.25106772	30	RX	-3 -.15381867
14	RY	-3 -.80702765	30	Z	-2 +.61537906
14	RX	-5 +.40839874	31	RY	-3 -.53523647
14	Z	-2 +.43312814	31	RX	-3 -.22046464
15	RY	-3 -.83301001	31	Z	-2 +.59520029
15	RX	-5 -.21248197	32	RY	-3 -.48052887
15	Z	-2 +.43197529	32	RX	-3 -.25076304
16	RY	-3 -.85411555	32	Z	-2 +.55200559
16	RX	-4 -.36964402	33	RY	-3 -.20192301
16	Z	-2 +.42689141	33	RX	-3 +.24800835
17	RY	-3 -.86781731	33	Z	-2 +.64959300
17	RX	-4 -.86817950	34	RY	-3 -.32764988

TABLE 3 ROTATIONS AND DEFLECTIONS - PINNED CASE (CONTINUED)

34RX	-3	+.15001886
34 Z	-2	+.68923364
35RY	-3	-.36457602
35RX	-4	+.46533804
35 Z	-2	+.69819922
36RY	-3	-.38009824
36RX	-3	-.17133888
36 Z	-2	+.68419038
37RY	-3	-.35975929
37RX	-3	-.27184229
37 Z	-2	+.66109669
38RY	-3	-.26474787
38RX	-3	-.35774896
38 Z	-2	+.59581754
39RY	-6	+.21925155
39RX	-3	+.36473948
39 Z	-2	+.65267010
40RY	-3	-.10192926
40RX	-3	+.31716936
40 Z	-2	+.69913317
41RY	-3	-.16703102
41RX	-3	+.21401341
41 Z	-2	+.72561017
42RY	-3	-.20812735
42RX	-4	+.84016229
42 Z	-2	+.74036001
43RY	-3	-.22430736
43RX	-3	-.19214028
43 Z	-2	+.72841124
44RY	-3	-.19976423
44RX	-3	-.31949539
44 Z	-2	+.70196886
45RY	-3	-.15202709
45RX	-3	-.41655161
45 Z	-2	+.66428757
46RY	-4	-.70248733
46RX	-3	-.45293559
46 Z	-2	+.60620146
47RY	-3	+.17066587
47RX	-3	+.56088387
47 Z	-2	+.62026625
48RY	-4	+.20399831
48RX	-3	+.43364610
48 Z	-2	+.70475454
49RY	-4	-.87683460
49RX	-3	+.13146668
49 Z	-2	+.76189357
50RY	-3	-.10491385
50RX	-3	-.22115402
50 Z	-2	+.75229362
51RY	-4	-.32809761
51RX	-3	-.51381425
51 Z	-2	+.67737799
52RY	-4	+.90026937
52RX	-3	-.63013775
52 Z	-2	+.58122235
53RY	-3	+.28259008
53RX	-3	+.74444868
53 Z	-2	+.55994278
54RY	-3	+.19218273
54RX	-3	+.67799352
54 Z	-2	+.63305202
55RY	-4	+.98269913
55RX	-3	+.54585299
55 Z	-2	+.69502193
56RY	-4	-.13621109
56RX	-3	+.17655541
56 Z	-2	+.76829990
57RY	-4	-.31082725
57RX	-3	-.24503373
57 Z	-2	+.76126374
58RY	-4	+.45110592
58RX	-3	-.60347797
58 Z	-2	+.67556442
59RY	-3	+.11975667
59RX	-3	-.72497398
59 Z	-2	+.60890620
60RY	-3	+.19336330
60RX	-3	-.77629087
60 Z	-2	+.53545007
61RY	-3	+.33352270
61RX	-3	+.93237685
61 Z	-2	+.48215083
62RY	-3	+.20666553
62RX	-3	+.82262414
62 Z	-2	+.60258567
63RY	-3	+.12069840
63RX	-3	+.65937919
63 Z	-2	+.67784908
64RY	-4	+.12155835
64RX	-3	+.22296612
64 Z	-2	+.76722962
65RY	-5	-.49049096
65RX	-3	-.26675640
65 Z	-2	+.76281545
66RY	-4	+.70369760
66RX	-3	-.69327376
66 Z	-2	+.66599491
67RY	-3	+.13978958
67RX	-3	-.84929786

TABLE 3 ROTATIONS AND DEFLECTIONS - PINNED CASE (CONTINUED)

67 Z	-2 +.58841393	84RX	-2 -.10847418
68RY	-3 +.24960614	84 Z	-2 +.56260579
68RX	-3 -.94872858	85RY	-4 +.28519461
68 Z	-2 +.47053329	85RX	-2 -.12593830
69RY	-3 +.30761772	85 Z	-2 +.44961270
69RX	-2 +.11893346	86RY	-4 +.96947350
69 Z	-2 +.38861536	86RX	-2 -.13666565
70RY	-3 +.15698143	86 Z	-2 +.30136469
70RX	-3 +.97805571	87RY	-5 +.14578138
70 Z	-2 +.57271875	87RX	-2 +.15203237
71RY	-4 +.80133190	87 Z	-2 +.23258860
71RX	-3 +.77330908	88RY	-4 -.65209238
71 Z	-2 +.66104437	88RX	-2 +.13789223
72RY	-4 -.16574134	88 Z	-2 +.43512320
72RX	-3 +.27018857	89RY	-3 -.11372473
72 Z	-2 +.76630638	89RX	-2 +.11842522
73RY	-4 -.33601539	89 Z	-2 +.56415816
73RX	-3 -.28537647	90RY	-3 -.15371427
73 Z	-2 +.76466944	90RX	-3 +.93914265
74RY	-4 +.29736617	90 Z	-2 +.66880729
74RX	-3 -.78285876	91RY	-3 -.20926967
74 Z	-2 +.65682915	91RX	-3 +.34690268
75RY	-4 +.90436687	91 Z	-2 +.79834668
75RX	-3 -.98110553	92RY	-3 -.23221889
75 Z	-2 +.56813674	92RX	-3 -.29917855
76RY	-3 +.22711385	92 Z	-2 +.80356660
76RX	-2 -.11801937	93RY	-3 -.21937623
76 Z	-2 +.38164026	93RX	-3 -.89545207
77RY	-3 +.18690543	93 Z	-2 +.68385667
77RX	-2 +.13788087	94RY	-3 -.19768953
77 Z	-2 +.29995273	94RX	-2 -.11501650
78RY	-3 +.12028893	94 Z	-2 +.58133918
78RX	-2 +.12797491	95RY	-3 -.16855103
78 Z	-2 +.43693718	95RX	-2 -.13438476
79RY	-4 +.43718634	95 Z	-2 +.46115996
79RX	-2 +.11003543	96RY	-3 -.11148242
79 Z	-2 +.55648584	96RX	-2 -.15115433
80RY	-4 -.16769635	96 Z	-2 +.24156549
80RX	-3 +.86855803	97RY	-3 -.23005770
80 Z	-2 +.65543180	97RX	-2 +.16503145
81RY	-4 -.95146873	97 Z	-2 +.19064429
81RX	-3 +.31205117	98RY	-3 -.25798275
81 Z	-2 +.77433093	98RX	-2 +.14441735
82RY	-3 -.11458066	98 Z	-2 +.45655337
82RX	-3 -.29718720	99RY	-3 -.27883916
82 Z	-2 +.77579797	99RX	-2 +.12363087
83RY	-4 -.73450568	99 Z	-2 +.59133140
83RX	-3 -.85268815	100RY	-3 -.29760279
83 Z	-2 +.65992005	100RX	-3 +.97889290
84RY	-4 -.28775979	100 Z	-2 +.70277603

TABLE 3 ROTATIONS AND DEFLECTIONS - PINNED CASE (CONTINUED)

101RY	-3	-.32925882
101RX	-3	+.37156929
101 Z	-2	+.83853352
102RY	-3	-.35210505
102RX	-3	-.29141563
102 Z	-2	+.84691139
103RY	-3	-.36218503
103RX	-3	-.90681322
103 Z	-2	+.72681395
104RY	-3	-.36270267
104RX	-2	-.11732768
104 Z	-2	+.62280780
105RY	-3	-.35783149
105RX	-2	-.13846206
105 Z	-2	+.49991595
106RY	-3	-.35049306
106RX	-2	-.16103003
106 Z	-2	+.22247795
107RY	-3	-.44720769
107RX	-2	+.16539388
107 Z	-2	+.24270626
108RY	-3	-.44493815
108RX	-2	+.14594174
108 Z	-2	+.50980650
109RY	-3	-.43801882
109RX	-3	+.99809057
109 Z	-2	+.75703833
110RY	-3	-.44830631
110RX	-3	+.38677681
110 Z	-2	+.89694664
111RY	-3	-.46948704
111RX	-3	-.27453681
111 Z	-2	+.90821192
112RY	-3	-.50193895
112RX	-3	-.89755844
112 Z	-2	+.79149691
113RY	-3	-.54151128
113RX	-2	-.13822511
113 Z	-2	+.56788074
114RY	-3	-.58230963
114RX	-2	-.16419407
114 Z	-2	+.24357952
115RY	-3	-.60352242
115RX	-2	+.15763146
115 Z	-2	+.40329389
116RY	-3	-.60628241
116RX	-2	+.14343018
116 Z	-2	+.58731989
117RY	-3	-.56525872
117RX	-3	+.98552745
117 Z	-2	+.83218078
118RY	-3	-.55599718
118RX	-3	+.39372980
118 Z	-2	+.97205053
119RY	-3	-.57632198
119RX	-3	-.25168300
119 Z	-2	+.98692706
120RY	-3	-.62376069
120RX	-3	-.86055209
120 Z	-2	+.87629667
121RY	-3	-.69433246
121RX	-2	-.13357959
121 Z	-2	+.66102191
122RY	-3	-.76358078
122RX	-2	-.15881489
122 Z	-2	+.35902887
123RY	-3	-.69921002
123RX	-2	+.13232745
123 Z	-2	+.71075109
124RY	-3	-.73877188
124RX	-3	+.92513917
124 Z	-2	+.98599394
125RY	-3	-.73202226
125RX	-3	+.39040131
125 Z	-1	+.11405212
126RY	-3	-.76895763
126RX	-3	-.20986233
126 Z	-1	+.11788369
127RY	-3	-.83686511
127RX	-3	-.76470302
127 Z	-1	+.10978080
128RY	-3	-.88074459
128RX	-2	-.12077401
128 Z	-2	+.86712015
129RY	-3	-.86753212
129RX	-2	-.14510742
129 Z	-2	+.59181687
201RY	-3	-.64759403
201RX	-3	-.12149032
202RY	-3	-.59514164
202RX	-3	-.10485621
202 Z	-3	+.20761655
203RY	-3	-.61485460
203RX	-3	-.14208567
203 Z	-4	-.23648766
204RY	-3	-.61864796
204RX	-4	+.36923770
204 Z	-3	+.74907559
208RY	-3	-.64565829
208RX	-3	-.27973752

TABLE 3   ROTATIONS AND DEFLECTIONS - PINNED CASE (CONTINUED)

208 Z	-3 +.26721636	261RX	-2 +.52143168
209RY	-3 -.75433048	261 Z	-2 +.33986681
209RX	-3 +.77490611	268RY	-3 -.46079500
209 Z	-2 +.21200754	268RX	-2 -.55883835
213RY	-3 -.80056968	268 Z	-2 +.32834739
213RX	-2 -.10118558	269RY	-3 -.34191876
213 Z	-2 +.14836553	269RX	-2 +.53675856
214RY	-3 -.75108536	269 Z	-2 +.22294201
214RX	-2 +.15304324	276RY	-3 -.53879294
214 Z	-2 +.35044945	276RX	-2 -.57684551
220RY	-3 -.81378595	276 Z	-2 +.20301300
220RX	-2 -.18162990	277RY	-3 -.48000417
220 Z	-2 +.28310174	277RX	-2 +.53628380
221RY	-3 -.70474838	277 Z	-2 +.10054137
221RX	-2 +.22572339	286RY	-3 -.72235043
221 Z	-2 +.46028554	286RX	-2 -.57509751
226RY	-3 -.78061163	286 Z	-3 +.91046006
226RX	-2 -.25544239	287RY	-3 -.72901386
226 Z	-2 +.39401040	287RX	-2 +.51628381
227RY	-3 -.63165675	296RY	-2 -.10515973
227RX	-2 +.29207156	296RX	-2 -.55262027
227 Z	-2 +.53126081	297RY	-3 -.94551972
232RY	-3 -.71861664	297RX	-2 +.47888486
232RX	-2 -.32509736	297 Z	-3 -.70829647
232 Z	-2 +.47358515	306RY	-2 -.13236503
233RY	-3 -.54329042	306RX	-2 -.51821007
233RX	-2 +.35265288	306 Z	-3 -.19352098
233 Z	-2 +.56651571	307RY	-2 -.10941918
238RY	-3 -.64427326	307RX	-2 +.37907984
238RX	-2 -.38787092	307 Z	-4 -.42390452
238 Z	-2 +.51160388	314RY	-2 -.14336570
239RY	-3 -.45065335	314RX	-2 -.46073052
239RX	-2 +.40680815	314 Z	-4 -.70692254
239 Z	-2 +.55501044	315RY	-2 -.15374946
246RY	-3 -.56854842	315RX	-2 +.24807035
246RX	-2 -.44365730	315 Z	-2 +.21785628
246 Z	-2 +.51549821	322RY	-2 -.15962569
247RY	-3 -.36536874	322RX	-2 -.34347008
247RX	-2 +.45674087	322 Z	-2 +.14730404
247 Z	-2 +.52256525	323RY	-2 -.25095706
252RY	-3 -.50407526	323RX	-2 +.11619786
252RX	-2 -.49065028	323 Z	-2 +.62720933
252 Z	-2 +.47163452	324RY	-2 -.32883755
253RY	-3 -.31104715	324RX	-3 +.40968389
253RX	-2 +.49342390	324 Z	-2 +.94375602
253 Z	-2 +.43738387	325RY	-2 -.33964935
260RY	-3 -.46215428	325RX	-4 +.79131575
260RX	-2 -.52940942	325 Z	-1 +.10714711
260 Z	-2 +.41232772	326RY	-2 -.35401477
261RY	-3 -.29476332	326RX	-3 -.24578806

TABLE 3 ROTATIONS AND DEFLECTIONS - PINNED CASE (CONTINUED)

326 Z	-1	+.11245380
327RY	-2	-.36938127
327RX	-3	-.56045034
327 Z	-1	+.11001143
328RY	-2	-.31767382
328RX	-3	-.98896342
328 Z	-2	+.85973899
329RY	-2	-.22434835
329RX	-2	-.19804522
329 Z	-2	+.48608930

TABLE 4 ROTATIONS AND DEFLECTIONS - FIXED CASE

Pressure = 4.3 psi

RY = θ_y - RADIANS
RX = θ_x - RADIANS
Z = ΔZ - INCHES

NODE, FREEDOM			NODE, FREEDOM		
1RY	-3	-.95399749	18RY	-3	-.74157756
1RX	-5	-.79689990	18RX	-4	-.91096547
2RY	-3	-.93058870	18 Z	-2	+.30975214
2RX	-4	-.30525402	19RY	-3	-.71027529
2 Z	-3	+.20156564	19RX	-3	-.15418230
3RY	-3	-.93157497	19 Z	-2	+.29437892
3RX	-4	+.14182351	20RY	-3	-.60317158
3 Z	-3	+.17621992	20RX	-3	-.22262791
4RY	-3	-.86296415	20 Z	-2	+.27426890
4RX	-5	-.42780251	21RY	-3	-.42865405
4 Z	-3	+.79556379	21RX	-3	+.33078446
5RY	-3	-.90065696	21 Z	-2	+.36706737
5RX	-4	+.13582426	22RY	-3	-.56138557
5 Z	-3	+.80290130	22RX	-3	+.20759720
6RY	-3	-.91557047	22 Z	-2	+.40098663
6RX	-5	-.80484200	23RY	-3	-.59925816
6 Z	-3	+.79804663	23RX	-3	+.10247112
7RY	-3	-.90134364	23 Z	-2	+.41436728
7RX	-4	-.29981052	24RY	-3	-.60307090
7 Z	-3	+.76853149	24RX	-3	-.12282882
8RY	-3	-.86757003	24 Z	-2	+.40871488
8RX	-5	-.86261377	25RY	-3	-.57187177
8 Z	-3	+.72774473	25RX	-3	-.22509494
9RY	-3	-.73470877	25 Z	-2	+.38875596
9RX	-4	+.99458392	26RY	-3	-.44359216
9 Z	-2	+.19518753	26RX	-3	-.34238141
10RY	-3	-.84440306	26 Z	-2	+.34919386
10RX	-4	+.42889759	27RY	-3	-.25039452
10 Z	-2	+.20557820	27RX	-3	+.47076178
11RY	-3	-.85587845	27 Z	-2	+.41240133
11RX	-5	-.76986401	28RY	-3	-.40536900
11 Z	-2	+.20580354	28RX	-3	+.26705374
12RY	-3	-.84715978	28 Z	-2	+.47167335
12RX	-4	-.58368794	29RY	-3	-.43794745
12 Z	-2	+.20148593	29RX	-3	+.13152021
13RY	-3	-.74113403	29 Z	-2	+.49098235
13RX	-3	-.10610203	30RY	-3	-.44349532
13 Z	-2	+.18616260	30RX	-3	-.15409500
14RY	-3	-.59638211	30 Z	-2	+.48604375
14RX	-3	+.20974969	31RY	-3	-.41402874
14 Z	-2	+.29287463	31RX	-3	-.28744833
15RY	-3	-.70676172	31 Z	-2	+.46288020
15RX	-3	+.14143878	32RY	-3	-.26950181
15 Z	-2	+.30832730	32RX	-3	-.48300926
16RY	-3	-.73838777	32 Z	-2	+.39768868
16RX	-4	+.76172529	33RY	-4	-.70854083
16 Z	-2	+.31656394	33RX	-3	+.60518884
17RY	-3	-.75283040	33 Z	-2	+.42656231
17RX	-5	-.82662610	34RY	-3	-.23931535
17 Z	-2	+.31708206	34RX	-3	+.33016901

TABLE 4 ROTATIONS AND DEFLECTIONS - FIXED CASE (Continued)

34 Z	-2	+.51875354
35RY	-3	-.27330471
35RX	-3	+.16056428
35 Z	-2	+.54264179
36RY	-3	-.27751803
36RX	-3	-.18432819
36 Z	-2	+.53913758
37RY	-3	-.24886867
37RX	-3	-.35228061
37 Z	-2	+.51165842
38RY	-4	-.91418547
38RX	-3	-.61906225
38 Z	-2	+.41425317
39RY	-3	+.10795766
39RX	-3	+.74453524
39 Z	-2	+.40786825
40RY	-4	-.50156996
40RX	-3	+.56572200
40 Z	-2	+.49466316
41RY	-4	-.92499468
41RX	-3	+.39078115
41 Z	-2	+.54268547
42RY	-3	-.12234798
42RX	-3	+.18984875
42 Z	-2	+.57162420
43RY	-3	-.12748392
43RX	-3	-.21300316
43 Z	-2	+.56863010
44RY	-3	-.10317546
44RX	-3	-.41062566
44 Z	-2	+.53697268
45RY	-4	-.66838596
45RX	-3	-.58042900
45 Z	-2	+.48674079
46RY	-4	+.79274812
46RX	-3	-.74992652
46 Z	-2	+.40067327
47RY	-3	+.24899802
47RX	-3	+.91067032
47 Z	-2	+.36535954
48RY	-4	+.64964136
48RX	-3	+.63855361
48 Z	-2	+.49361212
49RY	-5	-.28184712
49RX	-3	+.22026676
49 Z	-2	+.58046151
50RY	-5	-.76072481
50RX	-3	-.24241437
50 Z	-2	+.57816043
51RY	-4	+.48662954
51RX	-3	-.65141184
51 Z	-2	+.48805492
52RY	-3	+.21705140
52RX	-3	-.90671860
52 Z	-2	+.35985409
53RY	-3	+.34819015
53RX	-2	+.10653785
53 Z	-2	+.29624968
54RY	-3	+.19780194
54RX	-3	+.90024611
54 Z	-2	+.39464671
55RY	-3	+.14656964
55RX	-3	+.71686572
55 Z	-2	+.47658605
56RY	-4	+.77661927
56RX	-3	+.24491[illegible]54
56 Z	-2	+.57404824
57RY	-4	+.73989791
57RX	-3	-.26553606
57 Z	-2	+.57[illegible]37999
58RY	-3	+.13355034
58RX	-3	-.72451464
58 Z	-2	+.47333770
59RY	-3	+.18069495
59RX	-3	-.89907983
59 Z	-2	+.39205871
60RY	-3	+.31723509
60RX	-2	-.10477657
60 Z	-2	+.29889563
61RY	-3	+.38308025
61RX	-2	+.12130981
61 Z	-2	+.21376813
62RY	-3	+.22250625
62RX	-3	+.99300286
62 Z	-2	+.36245561
63RY	-3	+.17111548
63RX	-3	+.78093287
63 Z	-2	+.45222543
64RY	-3	+.11295719
64RX	-3	+.26865569
64 Z	-2	+.55858219
65RY	-3	+.11093550
65RX	-3	-.28701128
65 Z	-2	+.55723465
66RY	-3	+.16561666
66RX	-3	-.78581393
66 Z	-2	+.44989712
67RY	-3	+.21419226
67RX	-3	-.98758332
67 Z	-2	+.36110332

TABLE 4 ROTATIONS AND DEFLECTIONS - FIXED CASE (Continued)

68RY	-3	+.35769393	84 Z	-2	+.31117350
68RX	-2	-.11871152	85RY	-4	+.36024119
68 Z	-2	+.22060533	85RX	-2	-.12895827
69RY	-3	+.32906450	85 Z	-2	+.19505480
69RX	-2	+.13616048	86RY	-3	+.12501004
69 Z	-2	+.12663122	86RX	-2	-.14178349
70RY	-3	+.17380125	86 Z	-3	+.43818525
70RX	-2	+.10704354	87RY	-3	-.12711160
70 Z	-2	+.33075313	87RX	-2	+.15010656
71RY	-3	+.13688726	88RY	-3	-.13653978
71RX	-3	+.83853635	88RX	-2	+.13201073
71 Z	-2	+.42698085	88 Z	-2	+.19637168
72RY	-4	+.94369470	89RY	-3	-.11263511
72RX	-3	+.28869615	89RX	-2	+.11110460
72 Z	-2	+.54064692	89 Z	-2	+.31857062
73RY	-4	+.92339458	90RY	-4	-.90711373
73RX	-3	-.30374092	90RX	-3	+.86730955
73 Z	-2	+.53936189	90 Z	-2	+.41591587
74RY	-3	+.13153597	91RY	-4	-.72609993
74RX	-3	-.84146753	91RX	-3	+.30492329
74 Z	-2	+.42427547	91 Z	-2	+.53375066
75RY	-3	+.16739727	92RY	-4	-.87421608
75RX	-2	-.10617942	92RX	-3	-.29683897
75 Z	-2	+.32875009	92 Z	-2	+.53470474
76RY	-3	+.30272141	93RY	-3	-.13025157
76RX	-2	-.13318396	93RX	-3	-.85255049
76 Z	-2	+.12452557	93 Z	-2	+.41941629
77RY	-3	+.16988413	94RY	-3	-.16157232
77RX	-2	+.14616502	94RX	-2	-.10921892
77 Z	-3	+.47159345	94 Z	-2	+.32197502
78RY	-4	+.66509617	95RY	-3	-.19344274
78RX	-2	+.13199035	95RX	-2	-.12775642
78 Z	-2	+.18859123	95 Z	-2	+.20792220
79RY	-4	+.55244975	96RY	-3	-.22320398
79RX	-2	+.11271656	96RX	-2	-.14309760
79 Z	-2	+.31176669	97RY	-3	-.42568345
80RY	-4	+.42504887	97RX	-2	+.14790102
80RX	-3	+.87326893	97 Z	-4	-.42552099
80 Z	-2	+.41211760	98RY	-3	-.31425910
81RY	-4	+.26321178	98RX	-2	+.12449073
81RX	-3	+.30134666	98 Z	-2	+.22887764
81 Z	-2	+.53015963	99RY	-3	-.25408918
82RY	-4	+.19468759	99RX	-2	+.10523429
82RX	-3	-.30915359	99 Z	-2	+.34432211
82 Z	-2	+.52933691	100RY	-3	-.20968188
83RY	-4	+.23375014	100RX	-3	+.82727623
83RX	-3	-.87042358	100 Z	-2	+.43885583
83 Z	-2	+.41068475	101RY	-3	-.17005658
84RY	-4	+.31920374	101RX	-3	+.30120150
84RX	-2	-.11142613	101 Z	-2	+.55224593

TABLE 4 ROTATIONS AND DEFLECTIONS - FIXED CASE (Continued)

102RY	-3 -.19034770	118 Z	-2 +.63344082
102RX	-3 -.26891086	119RY	-3 -.39477293
102 Z	-2 +.55568197	119RX	-3 -.19306829
103RY	-3 -.26308711	119 Z	-2 +.64339842
103RX	-3 -.79706541	120RY	-3 -.47260729
103 Z	-2 +.44877859	120RX	-3 -.63684074
104RY	-3 -.32046528	120 Z	-2 +.56029441
104RX	-2 -.10207467	121RY	-3 -.60324843
104 Z	-2 +.35783415	121RX	-3 -.95939975
105RY	-3 -.38632891	121 Z	-2 +.40364167
105RX	-2 -.11993646	122RY	-3 -.84365233
105 Z	-2 +.25124997	122RX	-2 -.11716590
106RY	-3 -.53207751	122 Z	-2 +.18600349
106RX	-2 -.13683681	123RY	-3 -.73448214
106 Z	-3 +.13133920	123RX	-3 +.96237187
107RY	-3 -.60755492	123 Z	-2 +.46184269
107RX	-2 +.13904404	124RY	-3 -.71334924
107 Z	-3 +.69111637	124RX	-3 +.61043558
108RY	-3 -.41875998	124 Z	-2 +.66180489
108RX	-2 +.11445198	125RY	-3 -.66384828
108 Z	-2 +.28430631	125RX	-3 +.26481599
109RY	-3 -.30563332	125 Z	-2 +.76838745
109RX	-3 +.77486975	126RY	-3 -.68568933
109 Z	-2 +.47715542	126RX	-4 -.97148760
110RY	-3 -.26732493	126 Z	-2 +.79671528
110RX	-3 +.29588217	127RY	-3 -.76802809
110 Z	-2 +.58537698	127RX	-3 -.45250329
111RY	-3 -.29004101	127 Z	-2 +.74792722
111RX	-3 -.23188165	128RY	-3 -.84701058
111 Z	-2 +.59181568	128RX	-3 -.78710416
112RY	-3 -.37192404	128 Z	-2 +.59118946
112RX	-3 -.72127184	129RY	-3 -.87817168
112 Z	-2 +.49660626	129RX	-2 -.10074193
113RY	-3 -.51334081	129 Z	-2 +.38294418
113RX	-2 -.10823735		
113 Z	-2 +.31956082		
114RY	-3 -.73064109		
114RX	-2 -.12896709		
114 Z	-3 +.66033475		
115RY	-3 -.69489340		
115RX	-2 +.12428589		
115 Z	-2 +.21642043		
116RY	-3 -.52421848		
116RX	-2 +.10366528		
116 Z	-2 +.35357168		
117RY	-3 -.41601539		
117RX	-3 +.71665998		
117 Z	-2 +.53098116		
118RY	-3 -.37665292		
118RX	-3 +.29100445		

Glass Bending Moments and Shear

Bending moment patterns in the glass pane for M_x and M_y when subjected to a uniform air load are shown on page 165. Ordinates of the moment diagrams are drawn slanting upward and to the left when moment is positive. Plate element bending moments are positive if tension is produced in the outside fiber (relative to glider).

Bending moments for plate elements for a uniform air load of 4.3 psi acting in the + z-direction are presented on page 167.

To obtain glass bending moments for the boost ultimate net pressure of 10.5 psi, multiply by 2.442. Glass bending stress is 14.2 x moment. Glass rebate bending stress is 2.085 x glass bending stress.

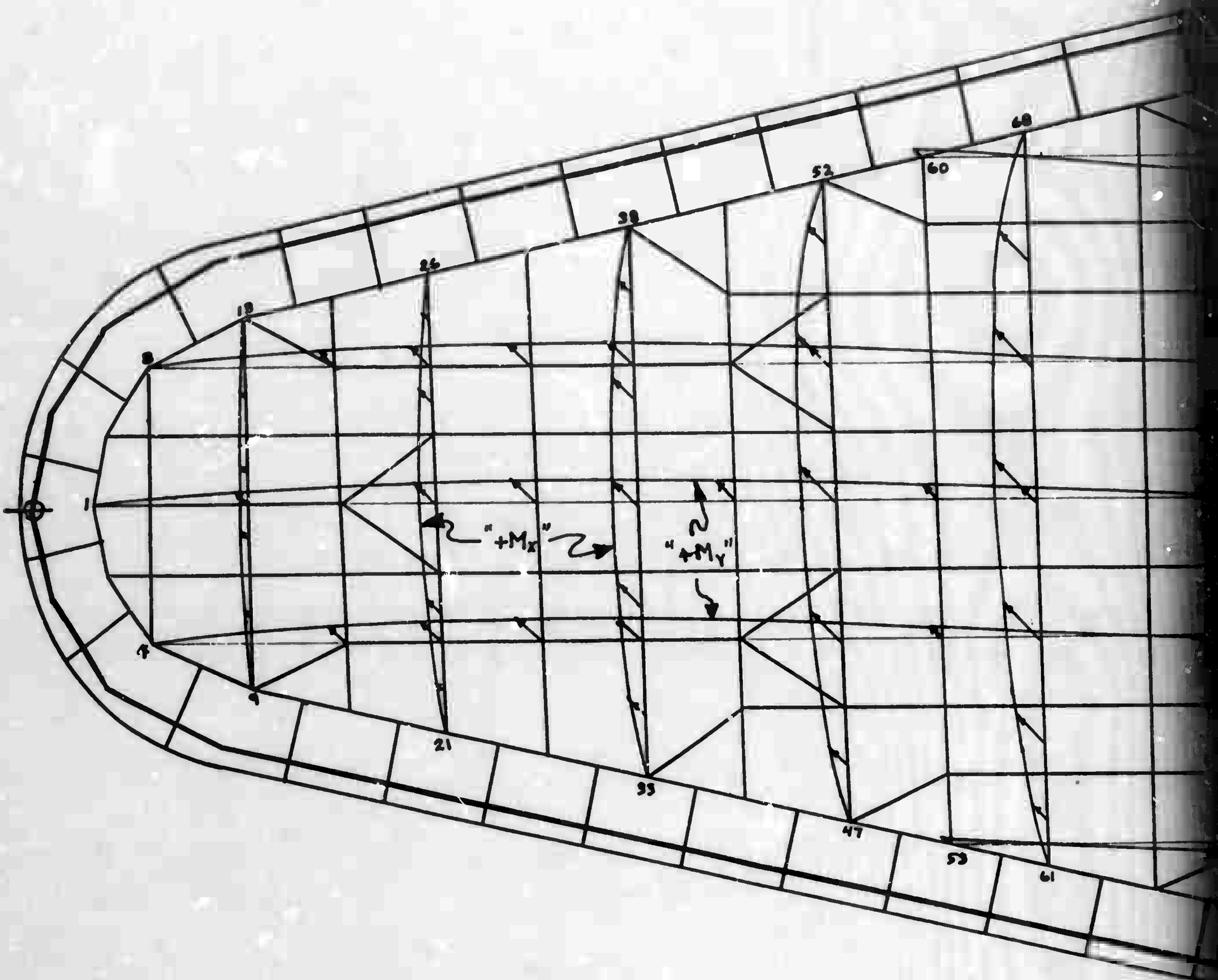

$M_x \sim \xrightarrow{+}$

$M_y \sim +\uparrow$

Moments here result from airload being applied in the +z direction, i.e. toward the reader. Positive moments result in tension in the glass on the side toward the reader.

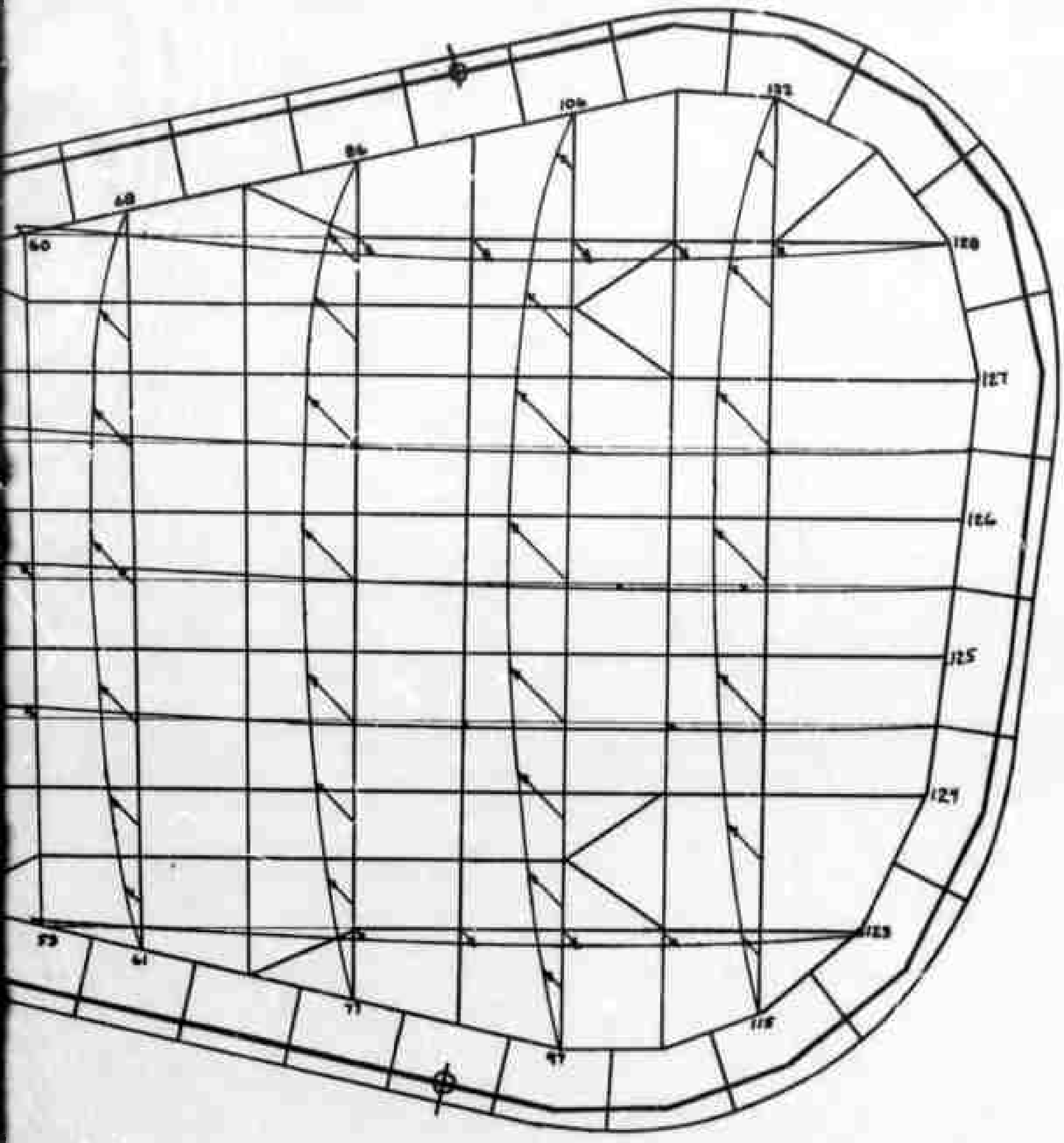

FIGURE 51

MOMENT DIAGRAMS ~ M_X AND M_{Y_2}

Pinned Case - Airload = 4.3 Lbs/In

2

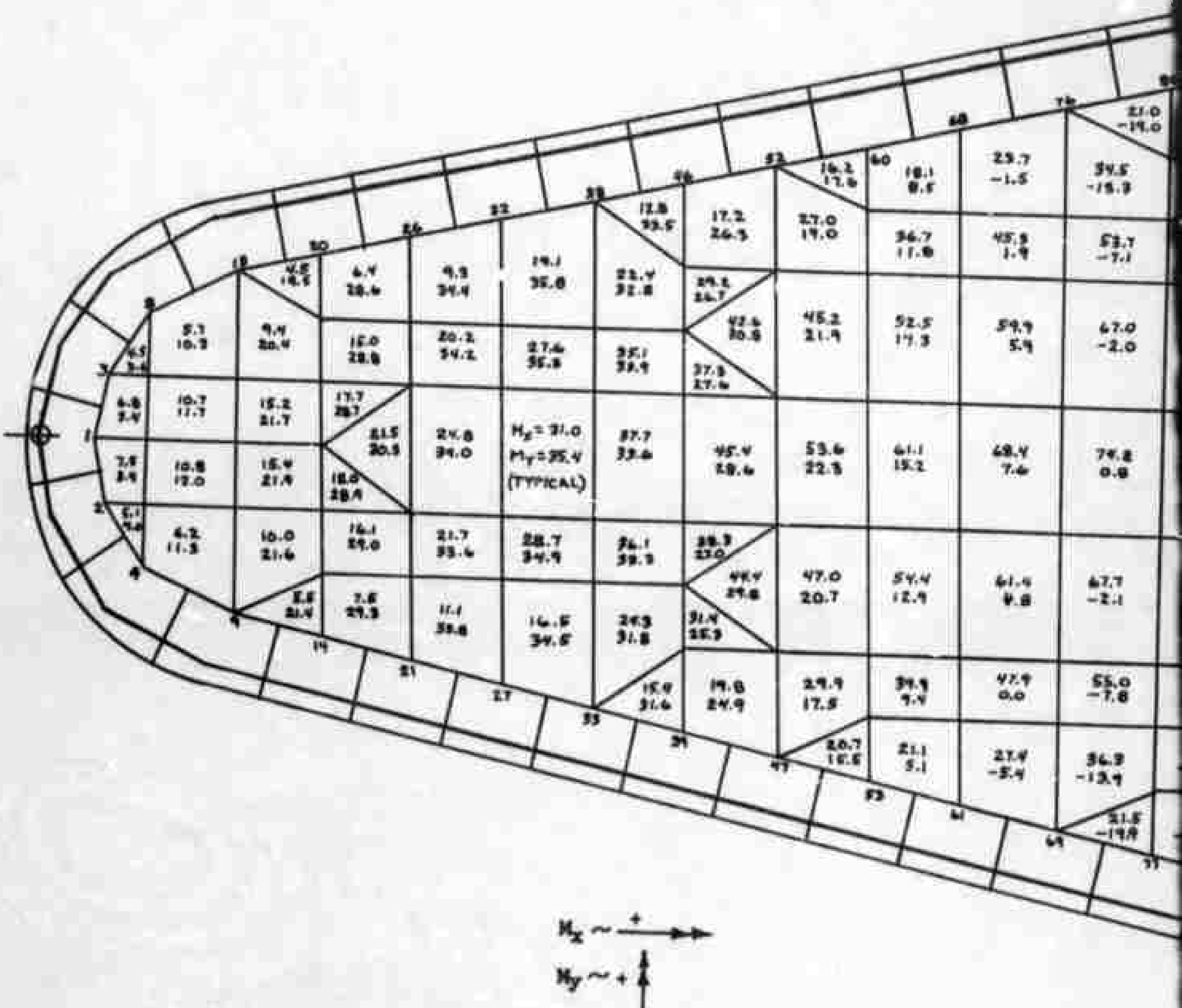

Positive M_x produces tension in the outer surface
Positive M_y produces tension in the outer surface
Glass stress = 14.2 x moment
Rebate stress = 2.085 x glass stress

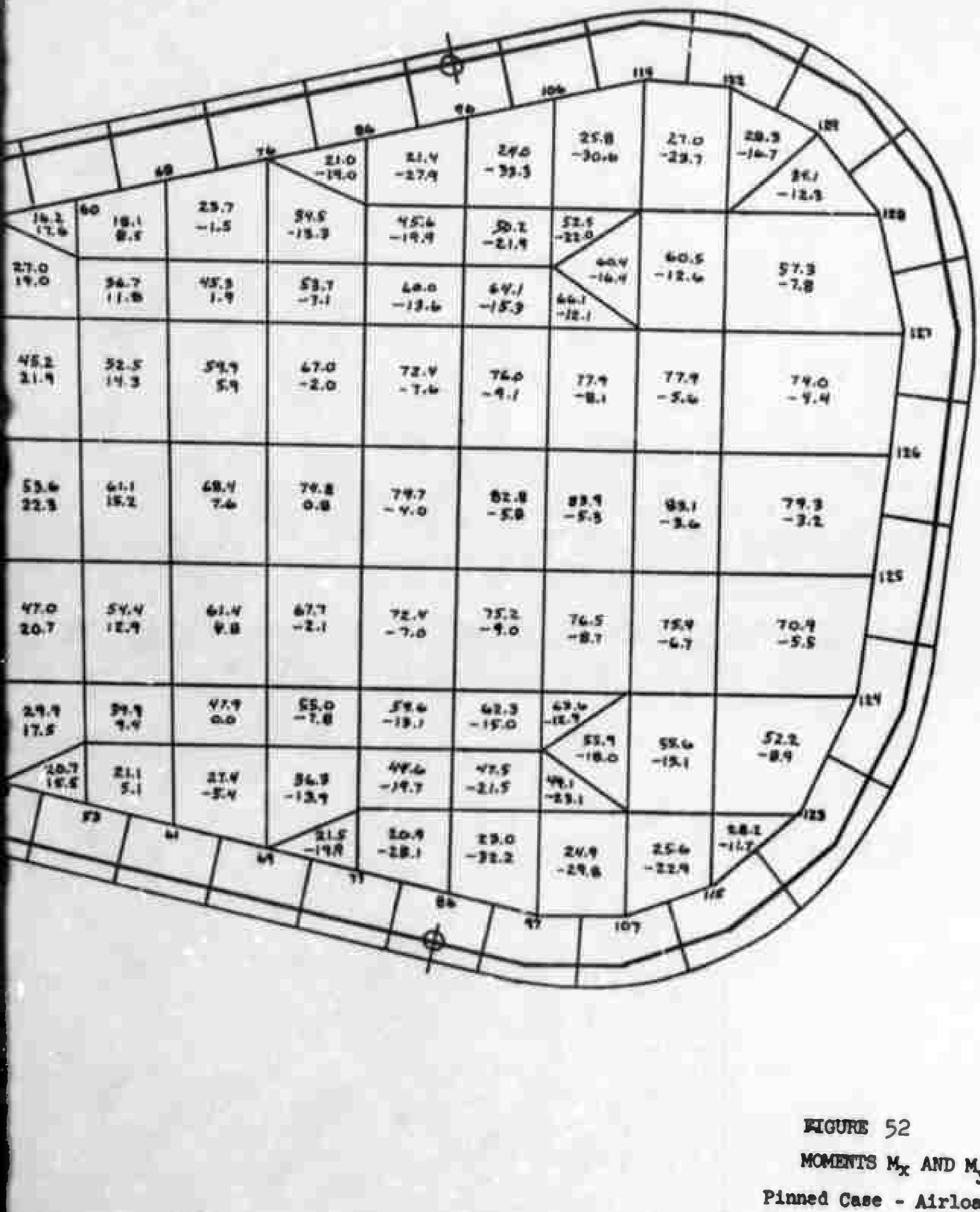

FIGURE 52

MOMENTS M_x AND M_y ~ IN.LBS/IN.

Pinned Case - Airload = 4.3 Lbs/In^2

2

Glass Out-of-Plane Shear

Out-of-plane shears Q_x and Q_y on glass elements corresponding to a net air load of 4.3 psi on the glass surface, acting outward (+ z-direction), are presented along with the sign convention for shears. Shears for 10.5 psi ultimate boost net pressure are 2.442 times larger.

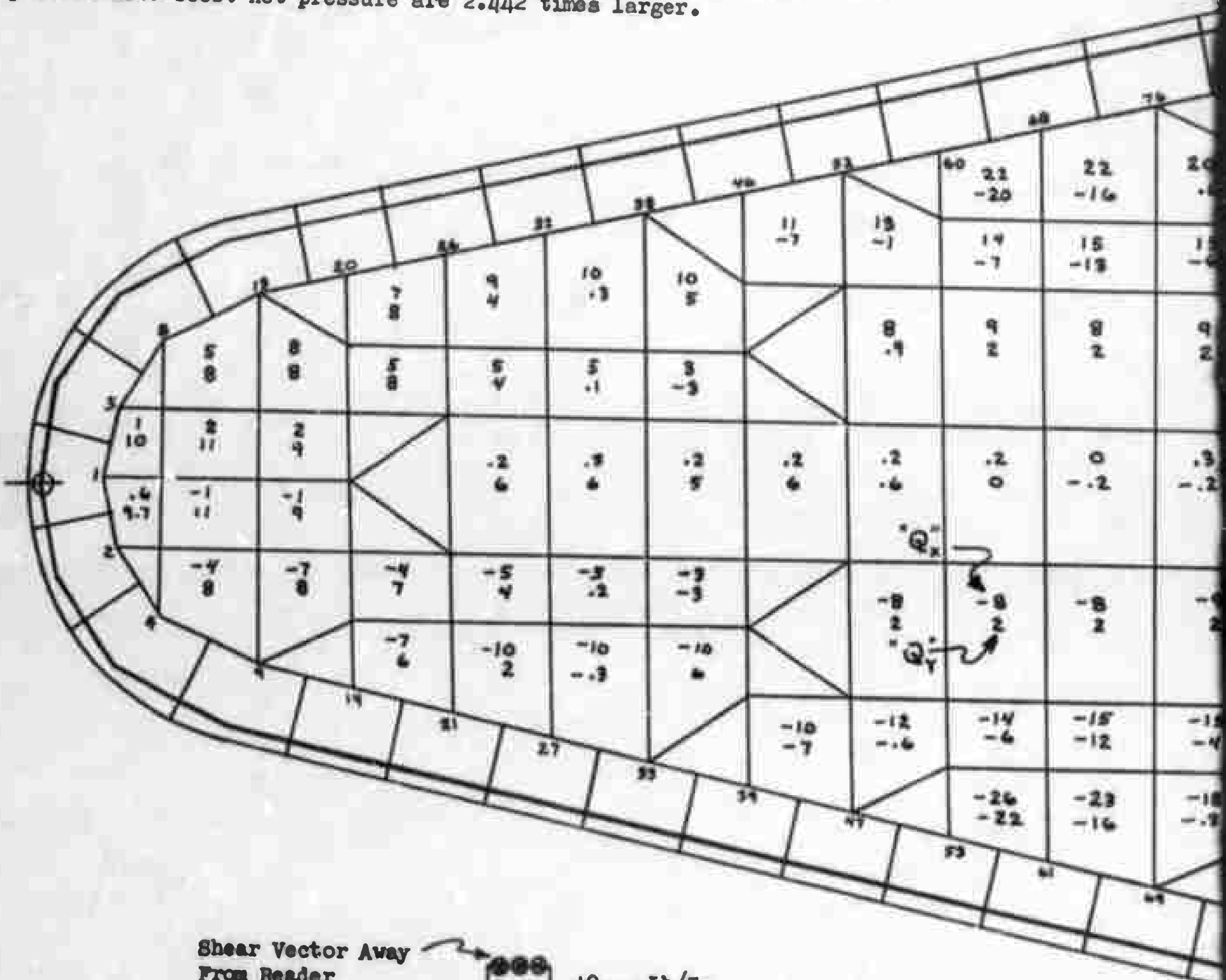

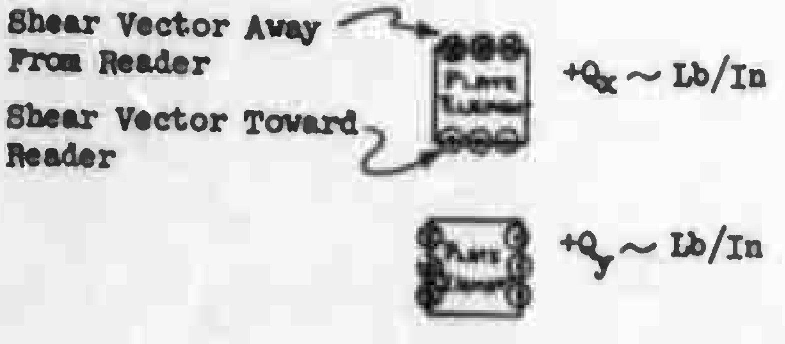

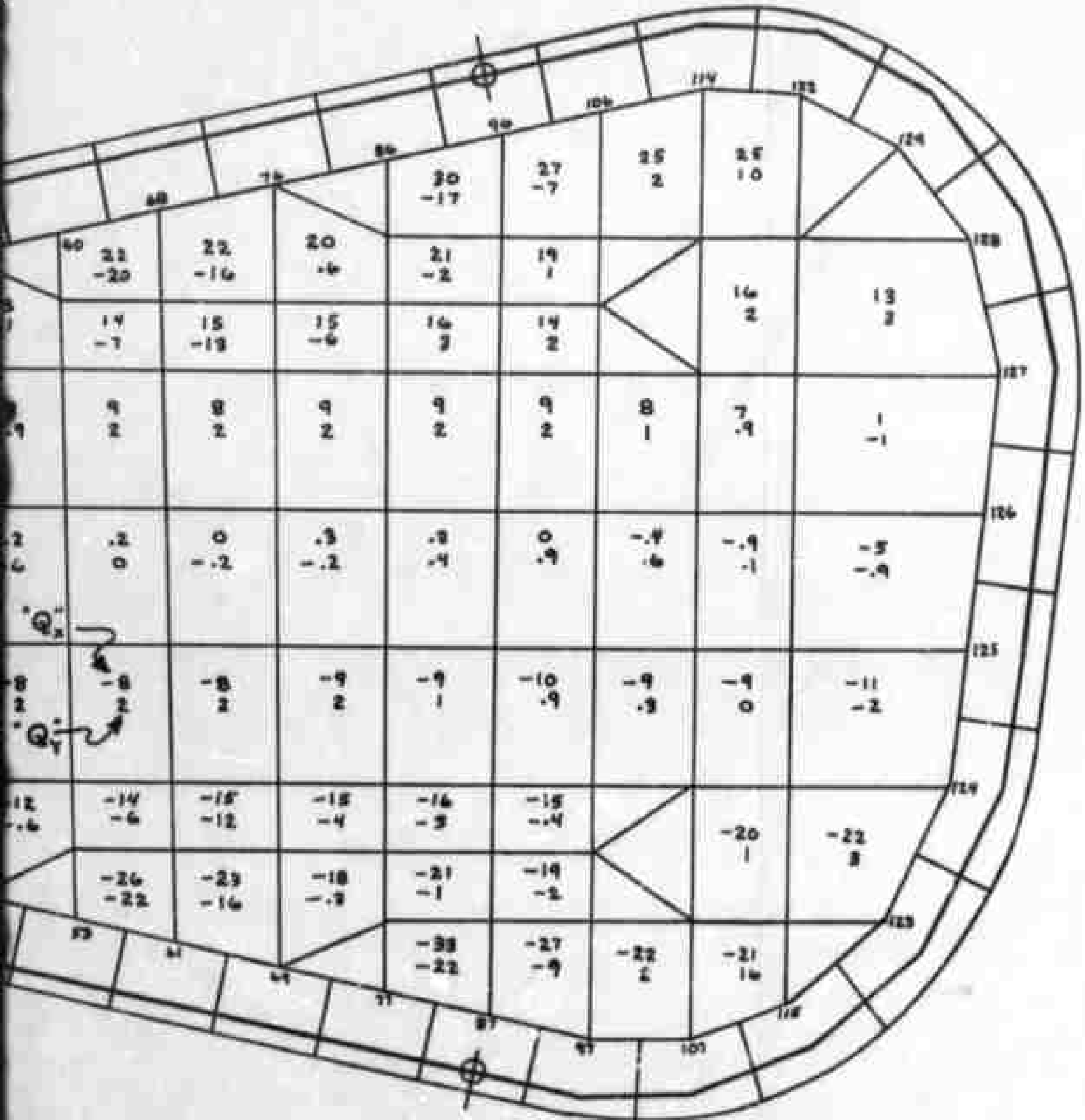

FIGURE 53
OUT-OF-PLANE SHEAR ON PLATE ELEMENTS
Pinned Case - Airload = 4.3 Lbs/In^2

2

Glass Torsion

Torsion moment M_{xy} for plate elements when subjected to a uniform net air load of 4.3 psi in the + z-direction is shown along with the sign convention for torsion moment. To obtain glass torsion moments for the boost ultimate net pressure of 10.5 psi, multiply by 2.442. Glass shear stress due to torsion is 14.2 x glass torsion moment.

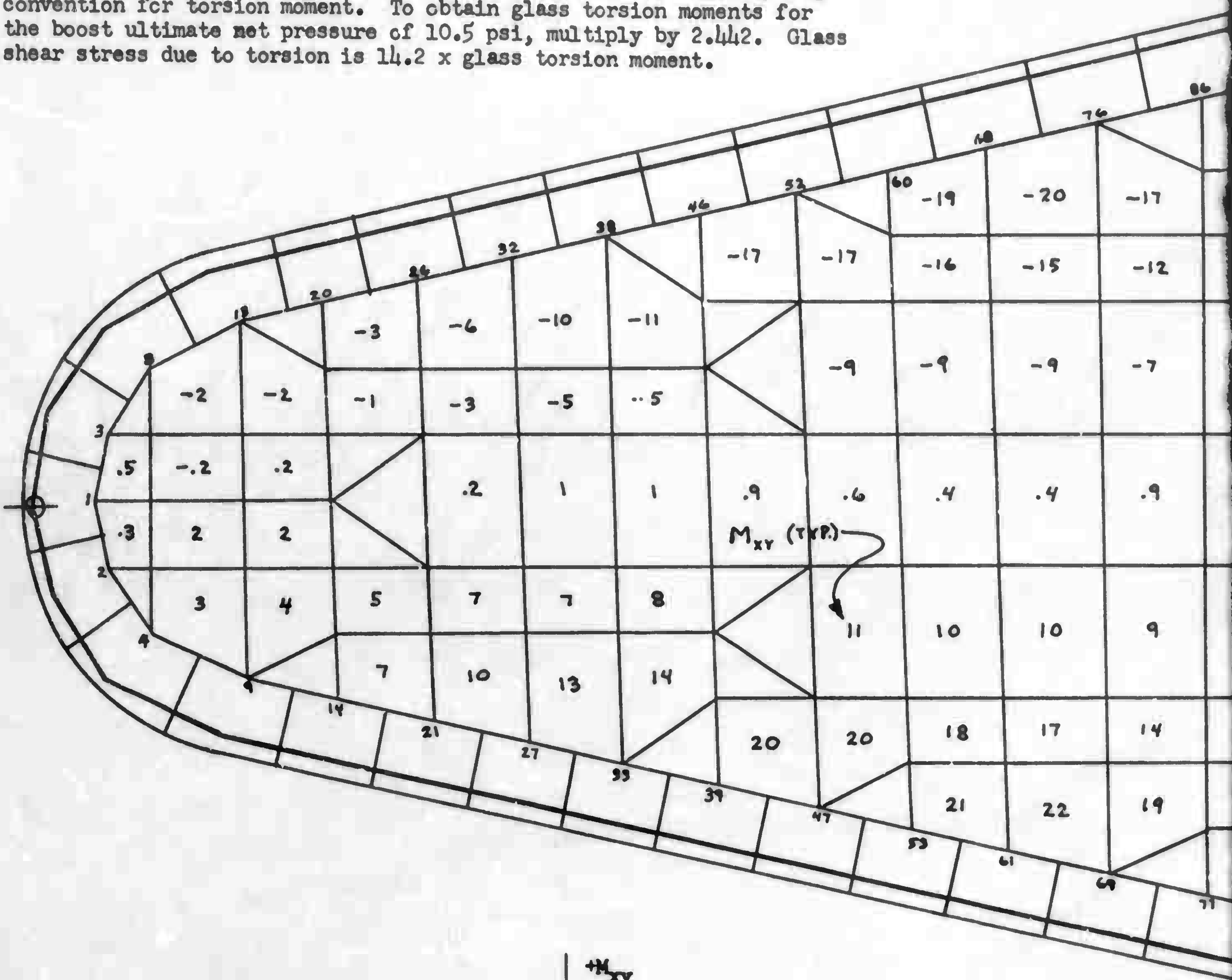

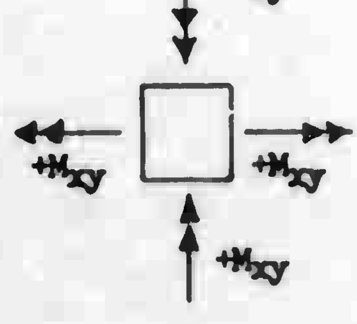

Torsion on Plate Elements ~ In.Lb/In.

net
sign
or
Glass

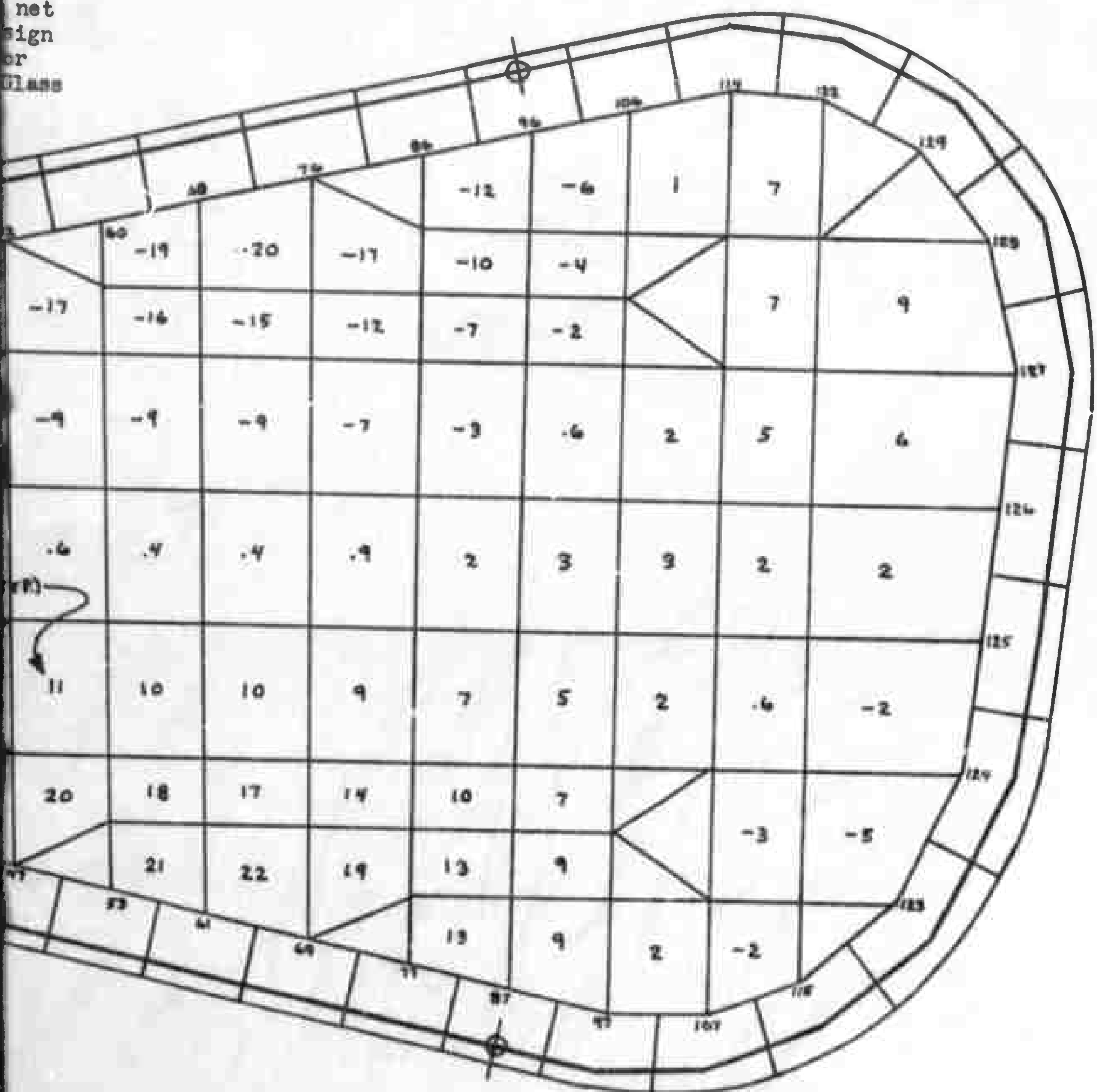

/In.

FIGURE 54
MOMENT M_{xy} (TORSION) ON PLATE ELEMENTS
Pinned Case - Airload = 4.3 Lbs/In^2

2

Window Frame Bending Moment and Shear

Bending moments and shears in the side window frame for 4.3 psi net air load acting outward on the window are shown together with the moment and shear sign convention. Maximum bending moments and shears, occurring during boost when a net air load of 10.5 psi boost is applied to the window, may be obtained by multiplying by 2.442.

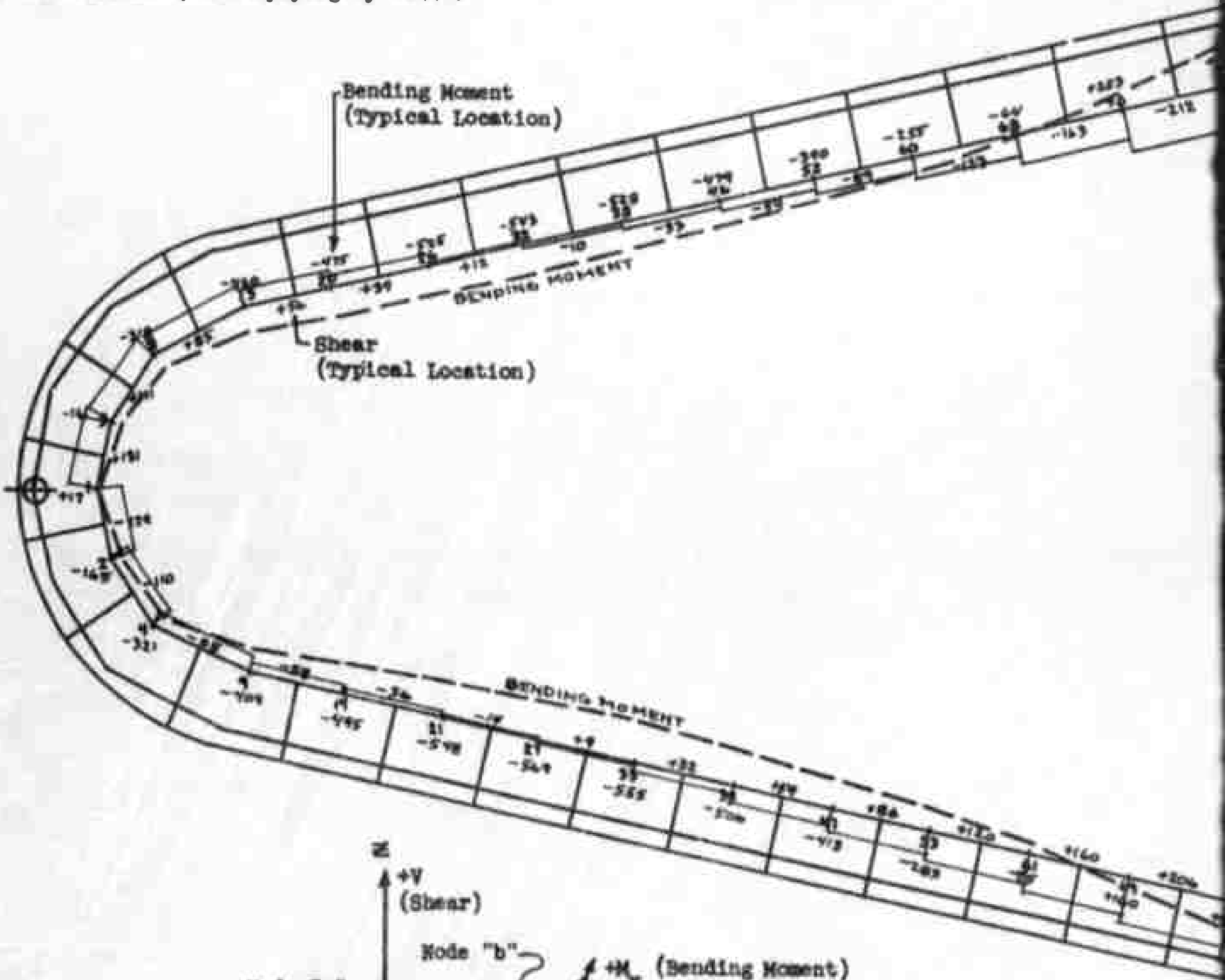

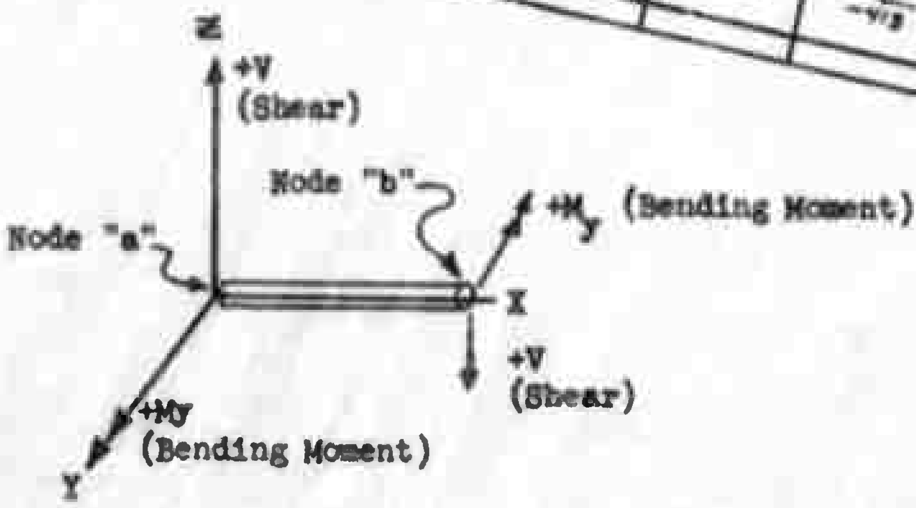

Node "b" is always counterclockwise around the frame from node "a".
Bending moments are written at nodes.
Shear is written between nodes.

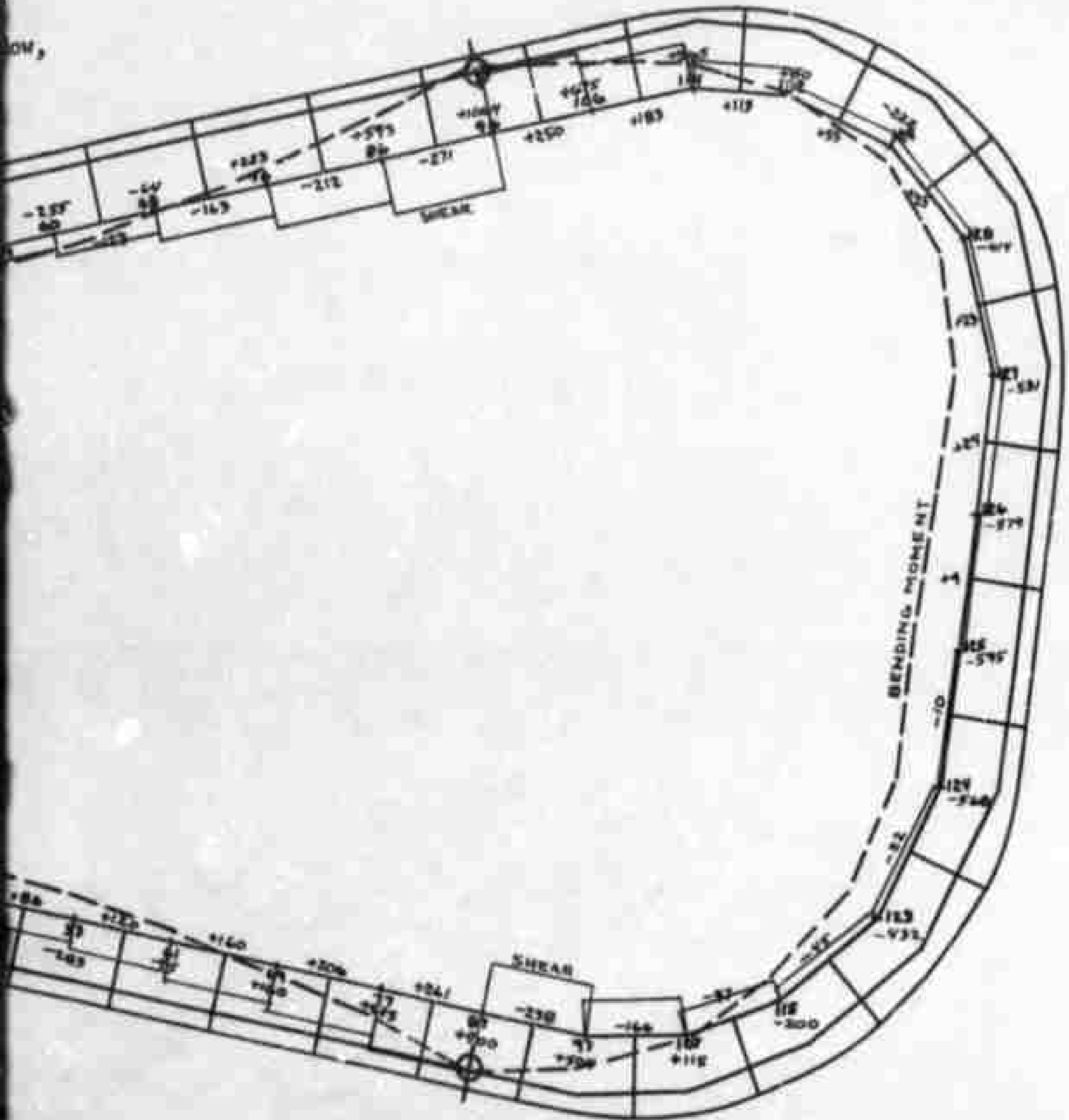

frame from node "a".

FIGURE 55
WINDOW FRAME SHEAR AND BENDING MOMENT
Pinned Case - Airload = 4.3 Lbs/In^2

2

Seal Loads

The seal and seal spring stiffness is simulated by the spar elements as discussed on page 142 . The axial loads in the spar elements represent the load transferred from the glass to the frame.

Spar element axial loads are tabulated below. Axial load in a spar is positive when the spar is subjected to tension. See page 143 for a pictorial representation of the spar element.

TABLE 5

Spar Node Numbers	Axial Load	Spar Node Numbers	Axial Load
1-201	16.5	86-286	58.5
2-202	19.2	87-287	64.7
3-203	19.8	96-296	67.2
4-204	24.9	97-297	72.7
8-208	26.3	106-306	67.2
9-209	26.5	107-307	68.7
13-213	28.6	114-314	69.7
14-214	23.0	115-315	51.6
20-220	22.6	122-322	58.9
21-221	21.8	123-323	23.2
26-226	21.8	124-324	11.7
27-227	22.4	125-325	19.2
32-232	21.8	126-326	15.1
33-233	23.1	127-327	0
38-238	23.4	128-328	2.1
39-239	27.1	129-329	29.4
46-246	25.2		
47-247	27.2		
52-252	30.5		
53-253	34.1		
60-260	34.2		
61-261	39.6		
68-268	39.5		
69-269	46.1		
76-276	49.7		
77-277	55.4		

STRESS ANALYSIS

FRAME SECTION

The frame section is not stress critical but is deflection critical. This is because small deflections can lead to high stresses in the glass. The 3/16 inch diameter frame clamping bolts in Class I holes do not develop sufficient friction between the frame elements to prevent unwanted shear slippage. The internal frame elements are riveted together with 1/4 inch diameter Rene' 41 rivets to provide shear continuity.

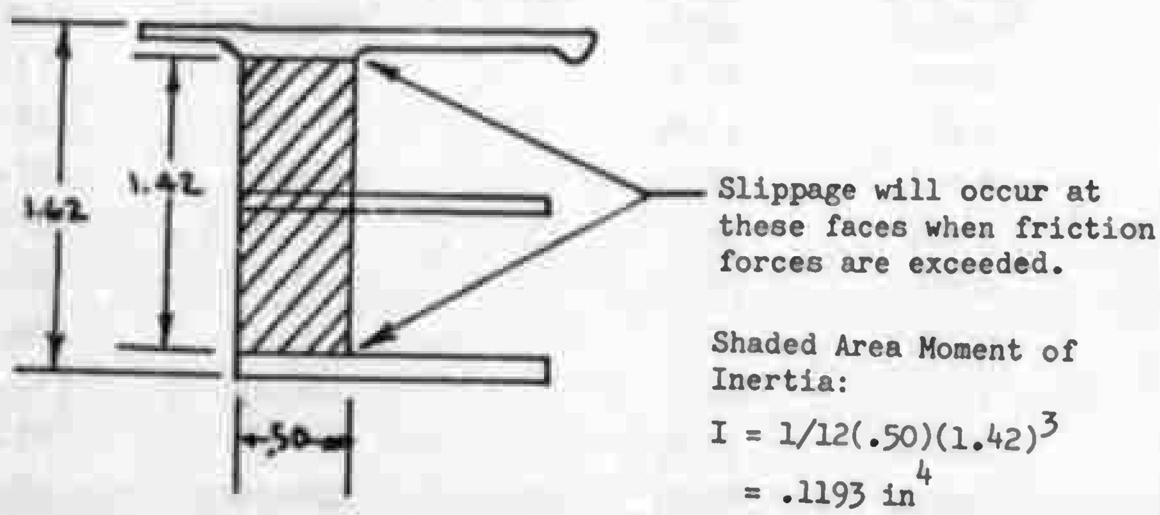

Shaded Area Moment of Inertia:

$$I = 1/12(.50)(1.42)^3 = .1193 \text{ in}^4$$

The 3/16 inch diameter clamping bolts and counterbores for the 1/4 inch diameter rivets reduce the stiffness of the frame section by 4%. The flanges (outer fairing and inner back-up strip) are only partially effective in bending because of the Class I holes. Using the effectiveness based on flange friction with bolts torqued to 20-25 inch-pound torque (700 pounds/bolt) and μ = .40 gives an increase in stiffness of 25%.

FINAL FRAME MOMENT OF INERTIA

$$I = .1193 \times .96 \times 1.25 = .1432 \text{ inch}^4 \text{ (Computer Analysis used .1397)}$$

FRAME TORSIONAL STIFFNESS

$$J_s = a\, b^3 \left[\frac{16}{3} - 3.36\, \frac{b}{a}\left(1 - \frac{b^4}{12a^4}\right)\right] = .04606 \text{ inch}^4$$

STRESS ANALYSIS (Continued)

GLASS SECTION

The high stress condition for the center of the glass occurs when the glass edges are supported on knife edges, i.e. pinned case.

Using the results from the digital solution the critical stress element at the plate center is 102-101-111-110.

For 4.3 psi outward acting this plate element has the .ollowing stresses, from the digital solution:

σ_{xx} = 1191.4 psi

σ_{yy} = -75.4 psi

τ_{xy} = 39.6 psi

Stress elements for external and internal surfaces:

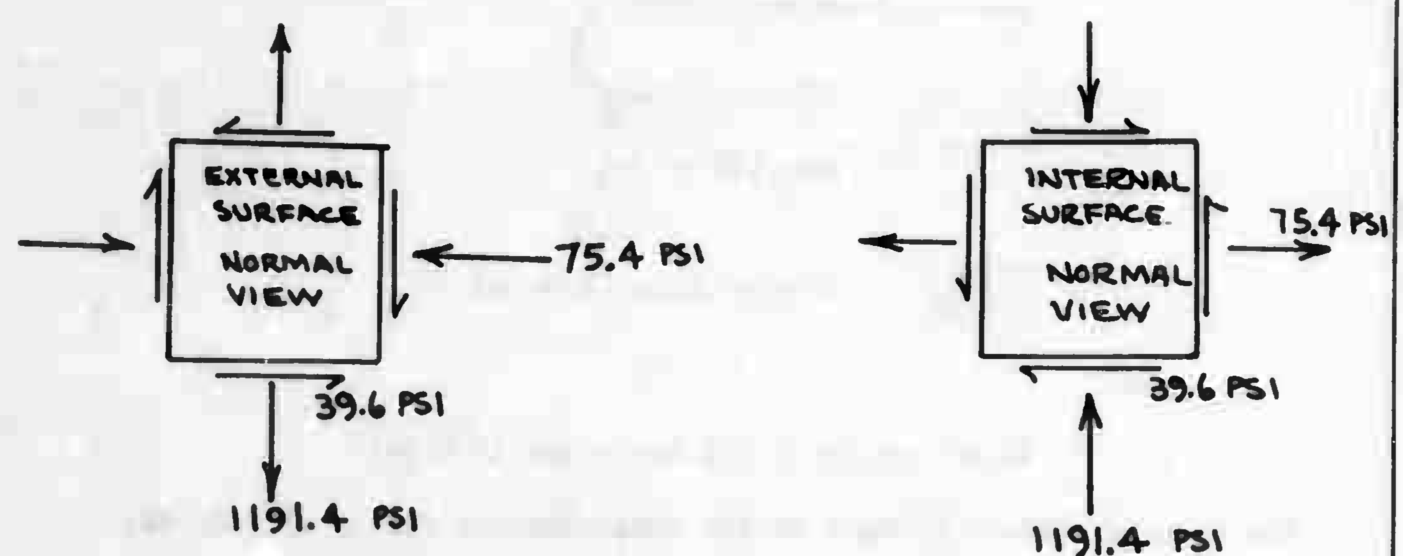

The principal stresses are calculated:

$$\sigma_{\substack{max \\ min}} = \frac{1}{2}(1191.4 - 75.4) \pm \sqrt{\left[\frac{1}{2}(1191.4 + 75.4)\right]^2 + 39.6^2}$$

for 4.3 psi airload

$$= 558 \pm 635 = \left.\begin{matrix} +\ 1193 \\ -\ 77 \end{matrix}\right\} \text{PSI}$$

STRESS ANALYSIS (Continued)

GLASS SECTION (Continued)

For 10.5 psi airload:

$\sigma_{\text{Allowable in Bending}} = 5800$ psi

$$\text{M.S.}_{\text{Max Stress Theory}} = \frac{5800}{1193 \times \frac{10.5}{4.3}} - 1 = \underline{\underline{.991}}$$

Examine the stress in the rebate - pinned boundary.

The shear to rebate is maximum at elements $\underbrace{87\text{-}97\text{-}107}_{\text{2 beams}}$

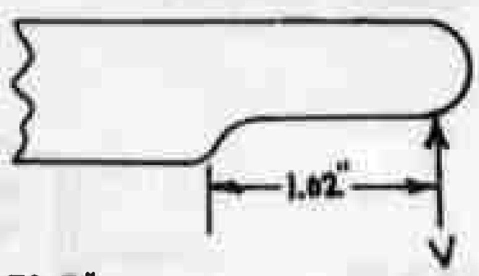

$$= \frac{72.7\#}{1.5 \text{ in}} = 48.47\#/\text{in for } 4.3 \text{ psi}$$

or

$$= 48.47 \times 2.442 = 118.4\#/\text{in for } 10.5 \text{ psi}$$

The bending stress, using a stress concentration factor of 1.2, is:

$$= \frac{118.4 \times 6 \times 1.2}{1 \times .45^2} = 4209 \text{ psi}$$

Realistically, the force V will act at 2/3 of 1.02 or .68 inch

$$= \frac{2}{3} \times 4209 = 2803 \text{ psi} \quad \text{(does not include installation stress)}$$

It is noted that rebate is critical since installation stresses are largest in the rebate area and are unknown.

APPENDIX II

WINDOW SEAL AND SPRING TESTS

II. WINDOW SEAL AND SPRING TESTS

PURPOSE

The purpose of these tests was to obtain stress relaxation and load-deflection data for one window seal configuration.

TEST SPECIMENS

Test 1: Two foil-jacketed "Hastelloy-X" mesh seals (per Drawing 25-86203-1) and one 5-leaf Rene' 41 spring (per Drawing 25-83879-1), all three inches in length.

Test 2: One foil-jacketed "Hastelloy-X" mesh seal, three inches in length (per Drawing 25-86203-1).

Test 3: One "Hastelloy-X" mesh seal with no jacket, three inches in length (per Drawing 25-83879).

INSTRUMENTATION

Specimen deflections were measured by recording the amount of head travel on the universal test machine.

Specimen temperatures were measured using chromel-alumel thermocouples spot welded to the test specimen as shown in Figure 56 page 182.

TEST SETUP

The test specimens were installed in a 120,000-pound Baldwin-Lima-Hamilton test machine. Refer to Figures 56, 57 and 58 for the test setup of each specimen.

TEST PROCEDURE AND RESULTS

Test 1: The seal specimen was compressed at room temperature to a load of 90 pounds and a thickness of 0.28 inch was recorded. The load was then increased to 105 pounds and a thickness of 0.27 inch was recorded. The load was again increased to 220 pounds and a thickness of 0.22 inch was recorded. The specimen was unloaded and then compressed again to a thickness of 0.22 inch under a load of 225 pounds (refer to Figures 60 and 61.) The heat cycle was then applied per Figure 59 . The seal thickness was held constant and load decay was continuously recorded during the heat cycle (refer to Figure 61). Load and heat were removed and the seal thickness measured was 0.24 inch.

FIGURE 56 TEST SETUP - TEST 1

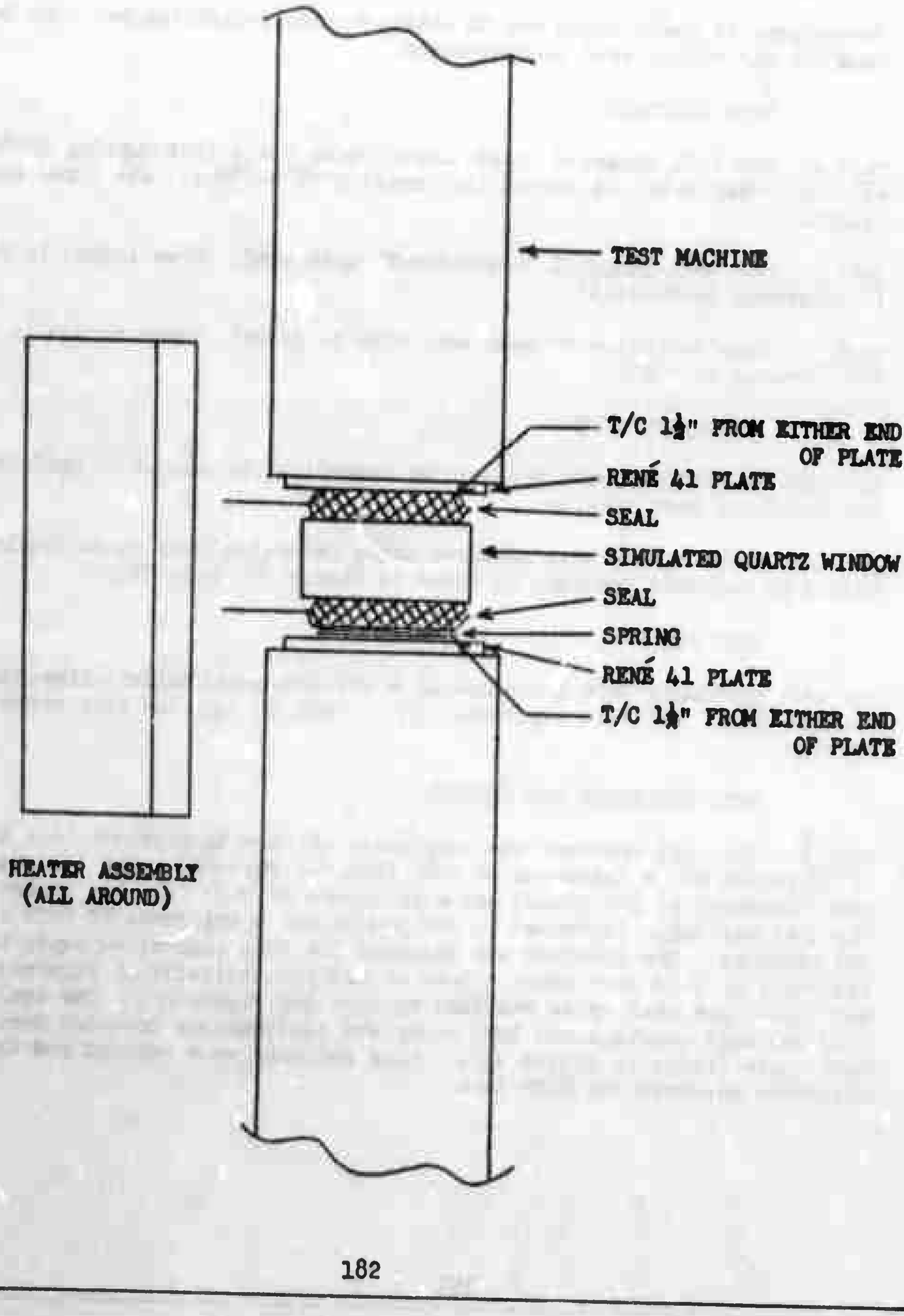

FIGURE 57 TEST SETUP - TEST 2

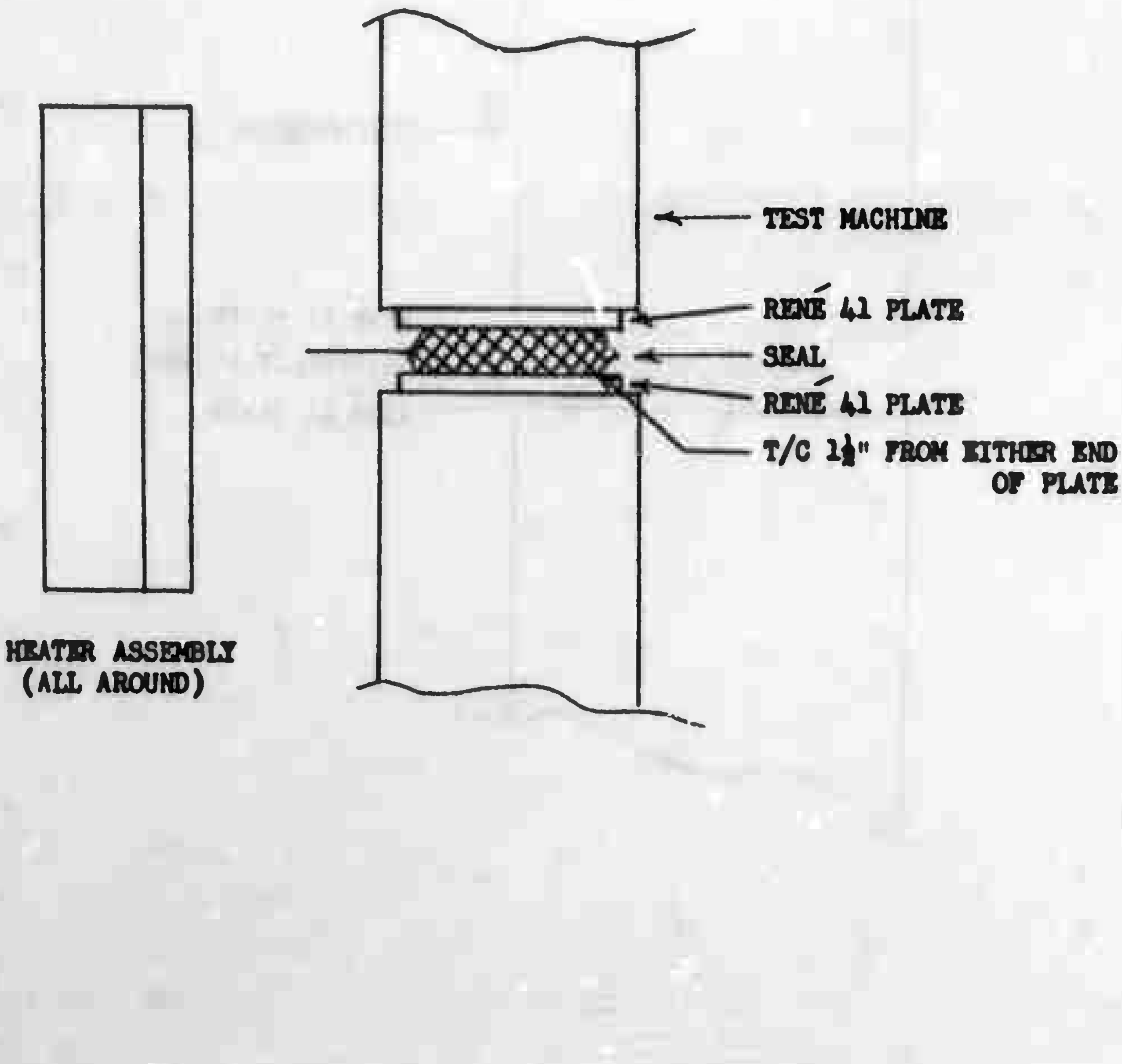

FIGURE 58 TEST SETUP - TEST 3

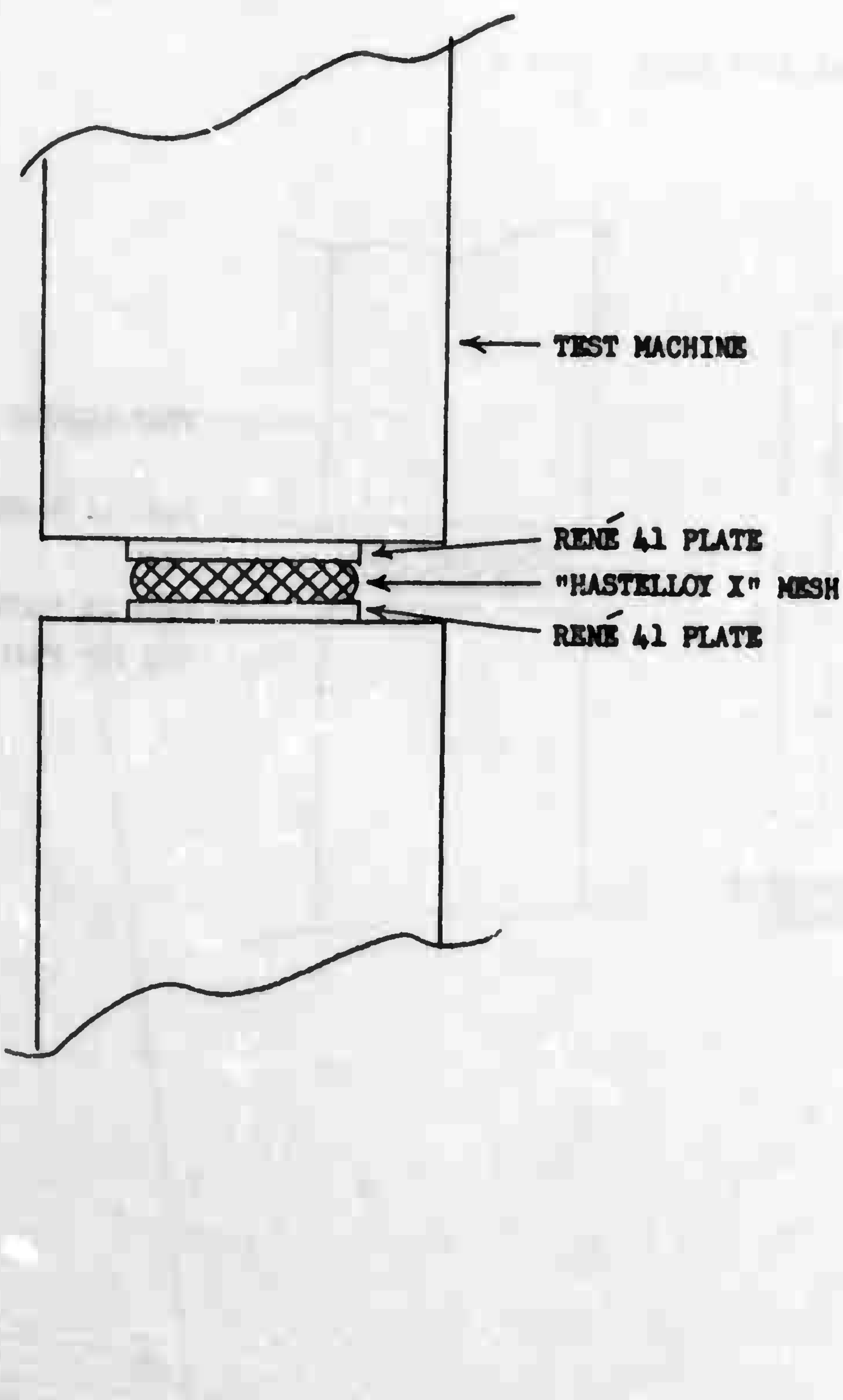

FIGURE 59 TIME - TEMPERATURE CURVE - TEST 1 AND 2

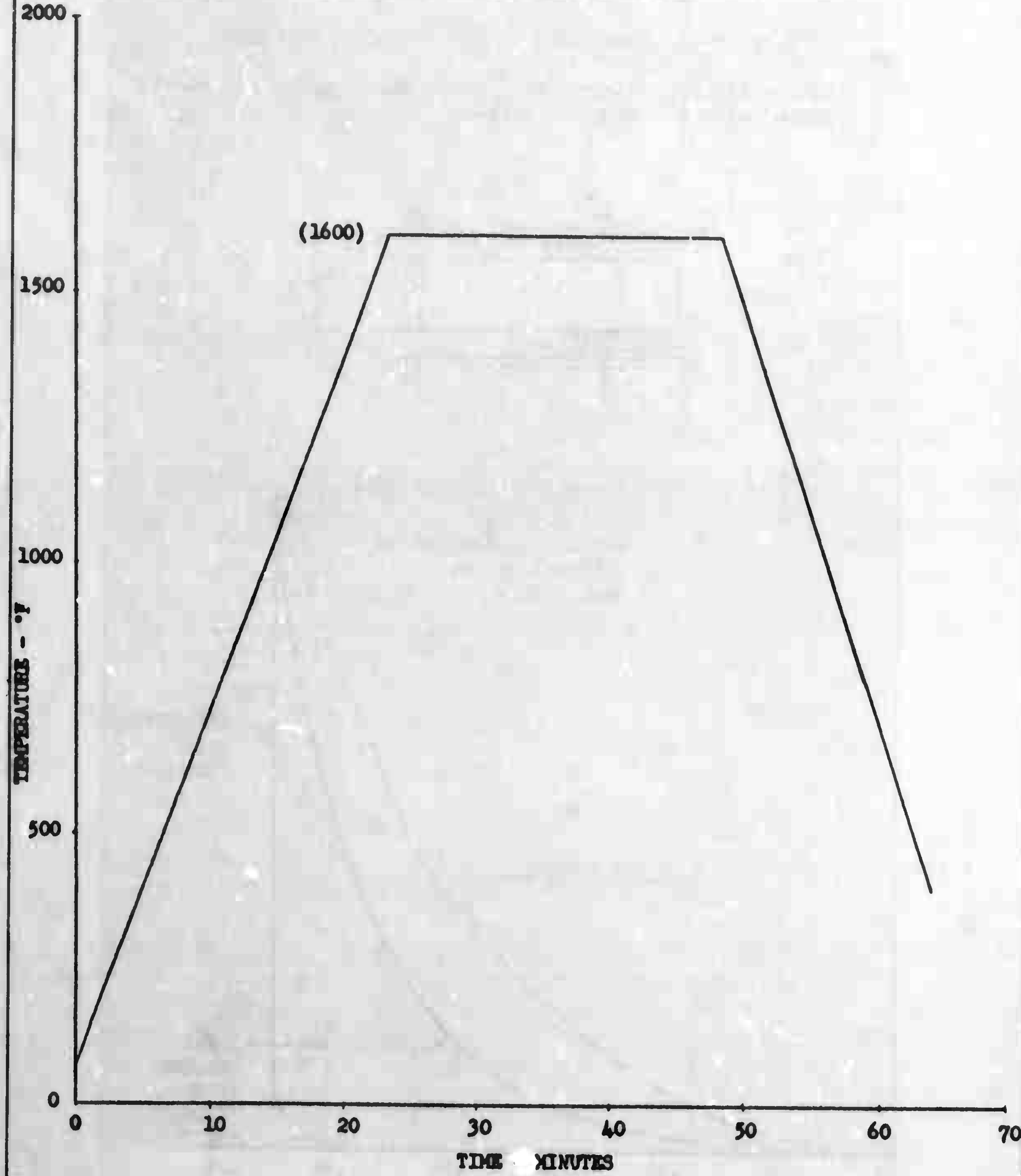

FIGURE 60 WINDOW SEAL AND SPRING TEST - TEST 1

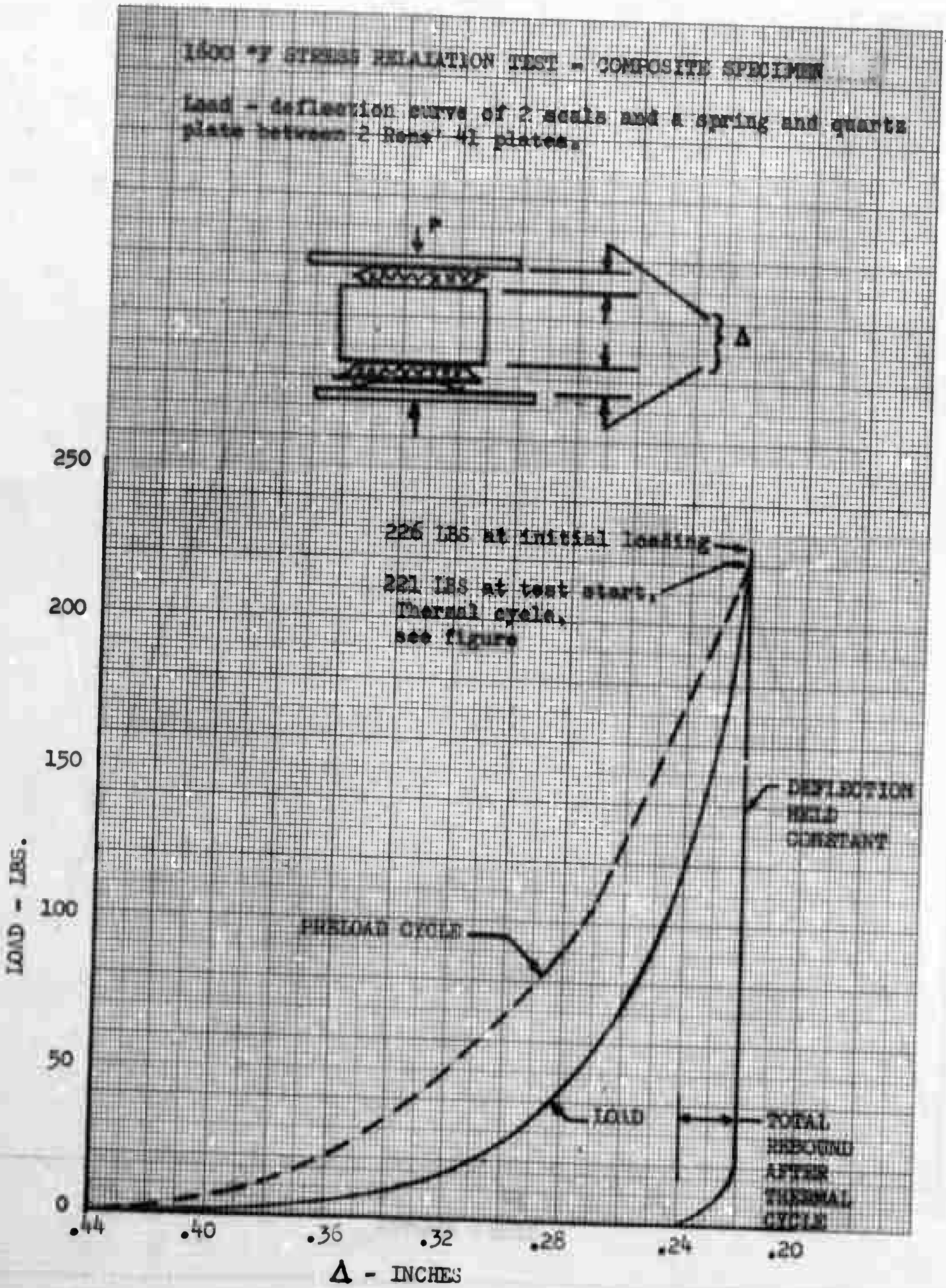

FIGURE 61 WINDOW SEAL AND SPRING TEST - TEST 1

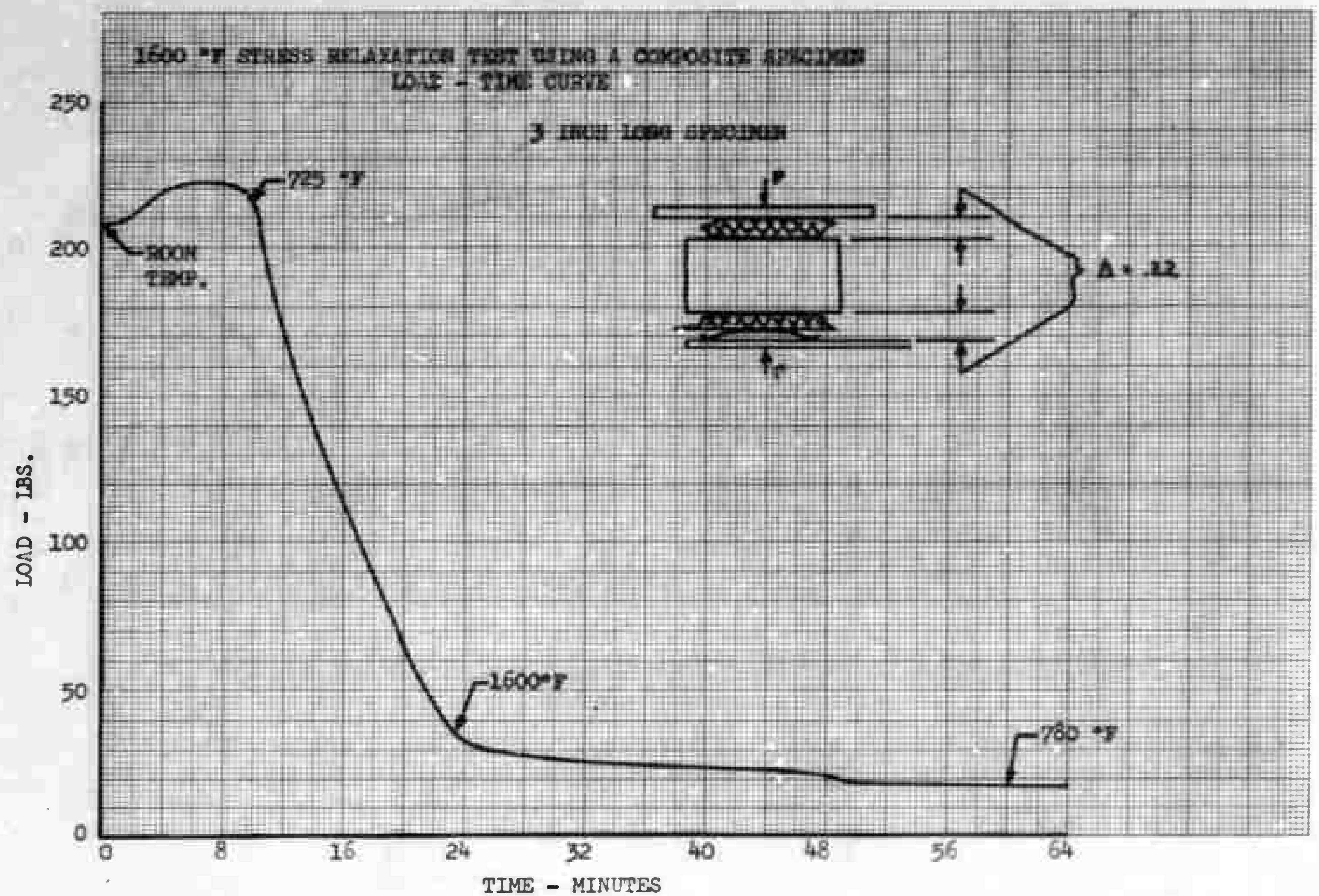

FIGURE 62 WINDOW SEAL AND SPRING TEST - TEST 2

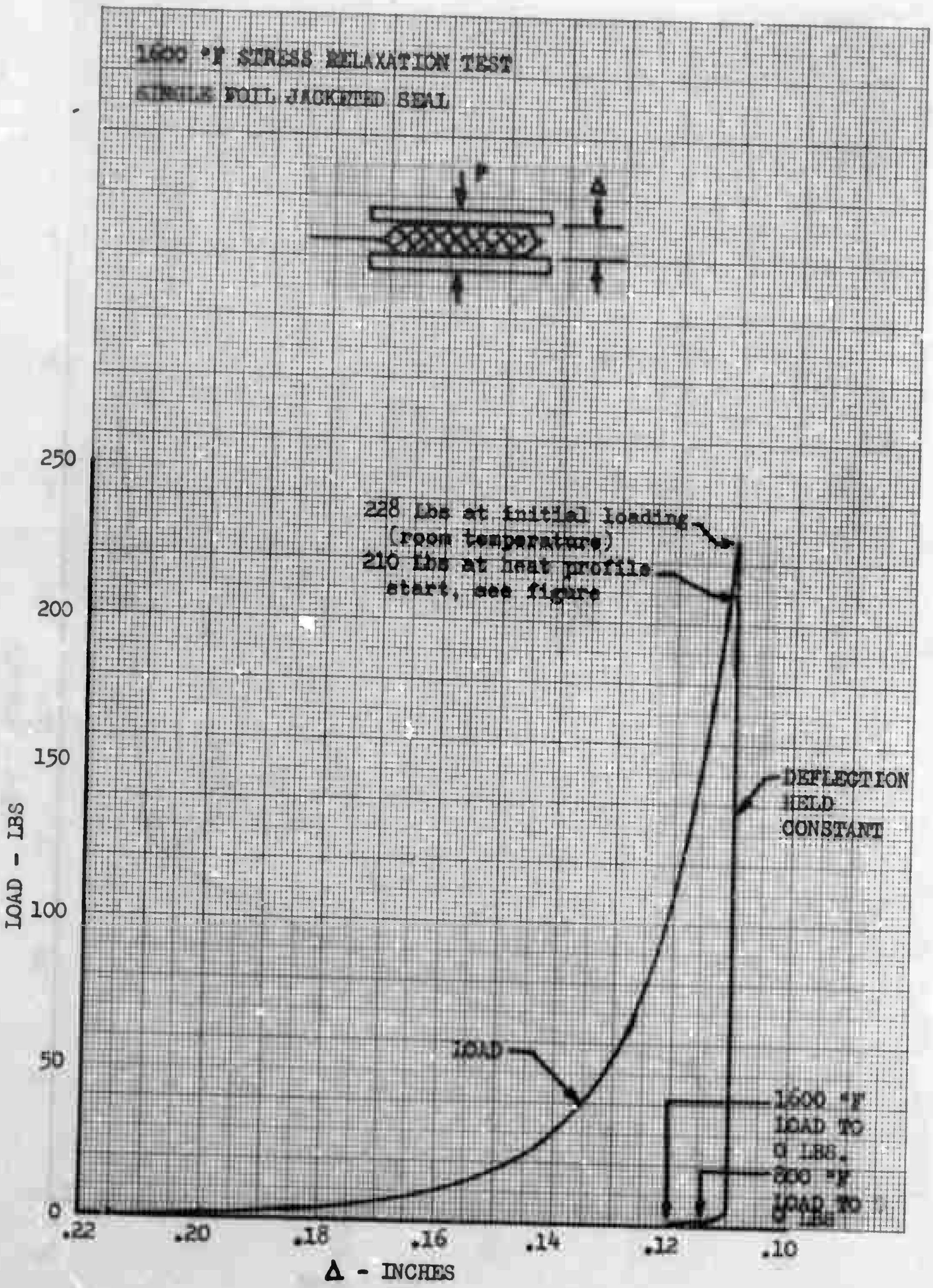

FIGURE 63 WINDOW SEAL AND SPRING TEST - TEST 2

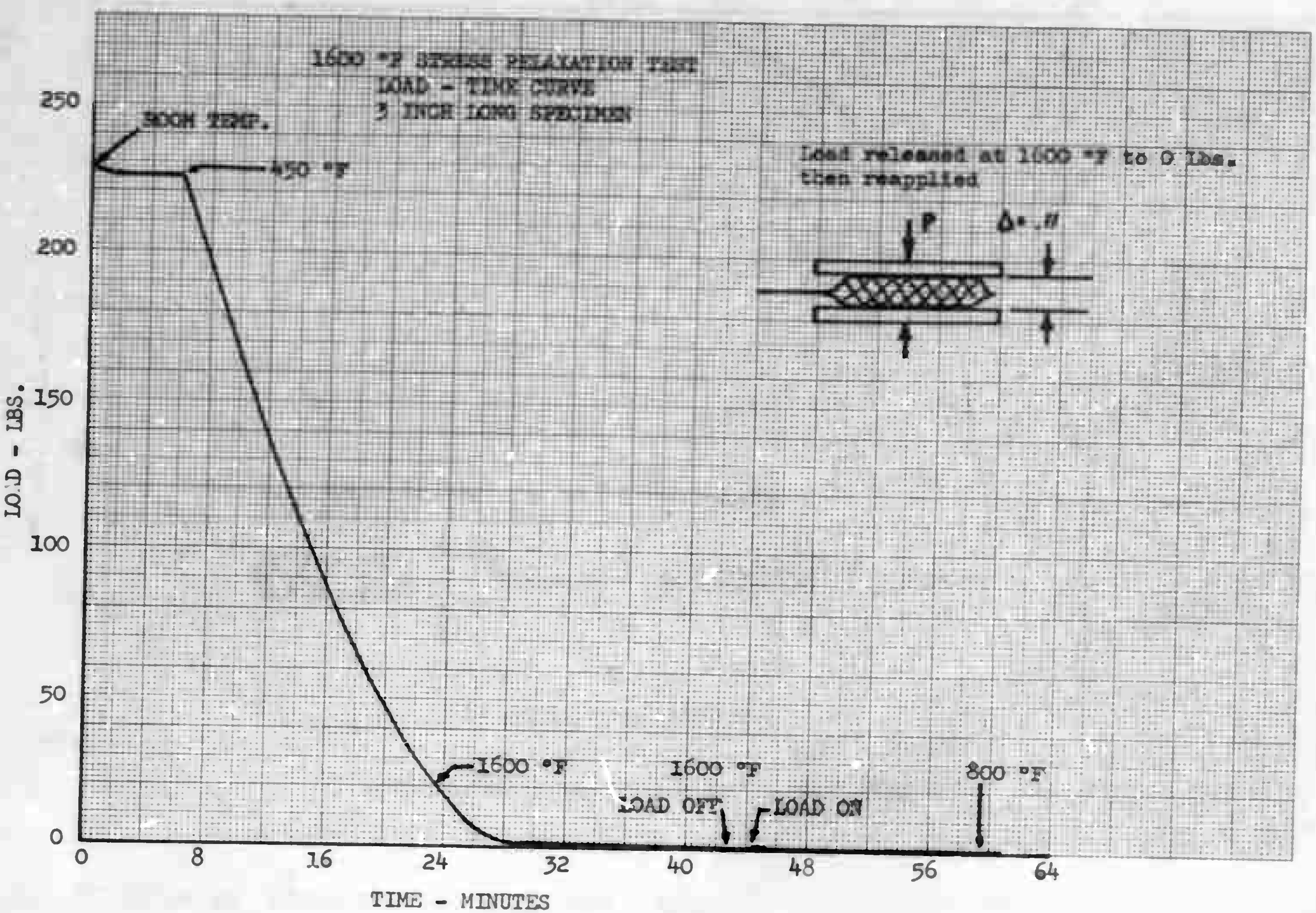

FIGURE 64 WINDOW SEAL AND SPRING TEST - TEST 3

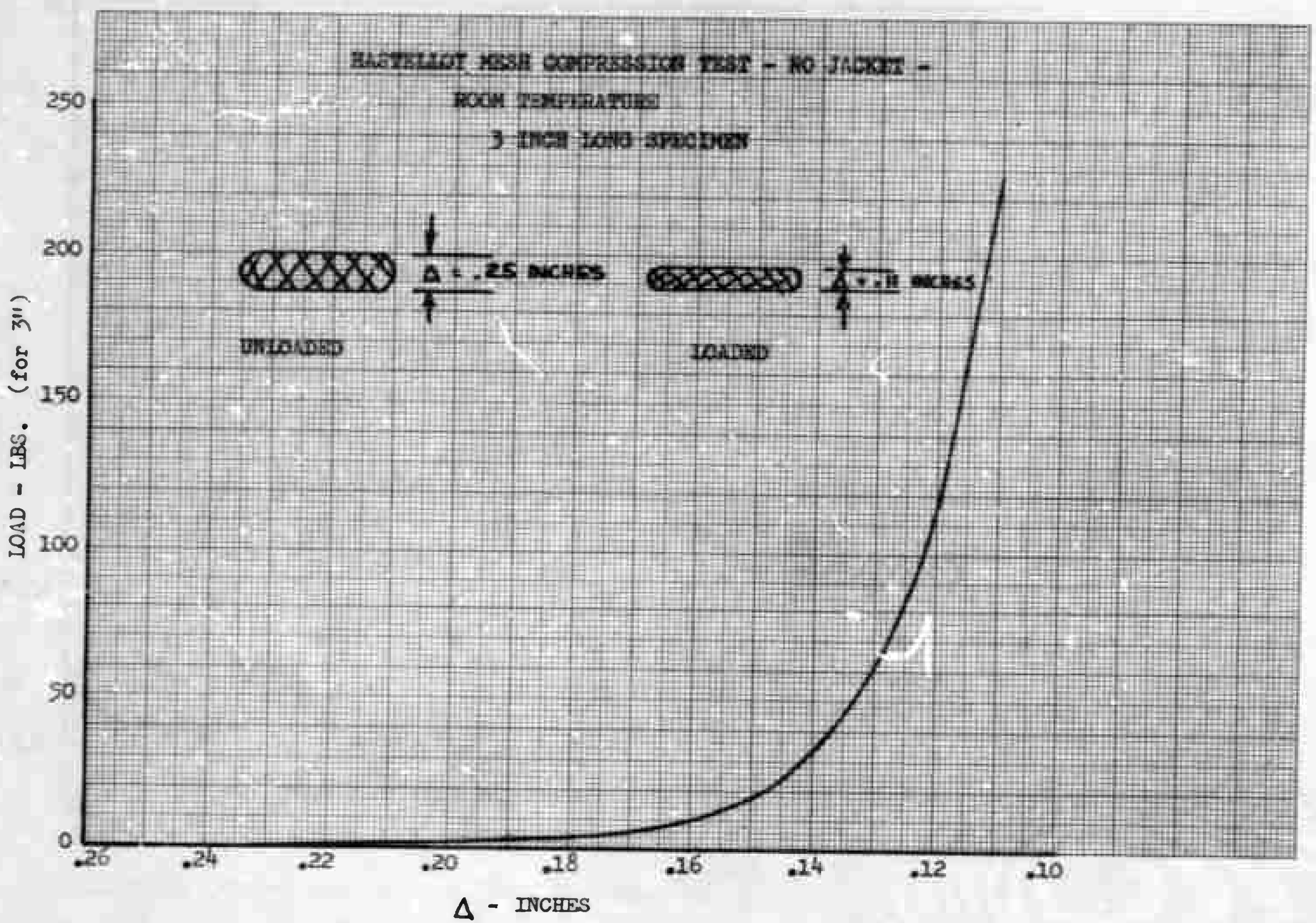

FIGURE 65 WINDOW CLAMPING FORCE

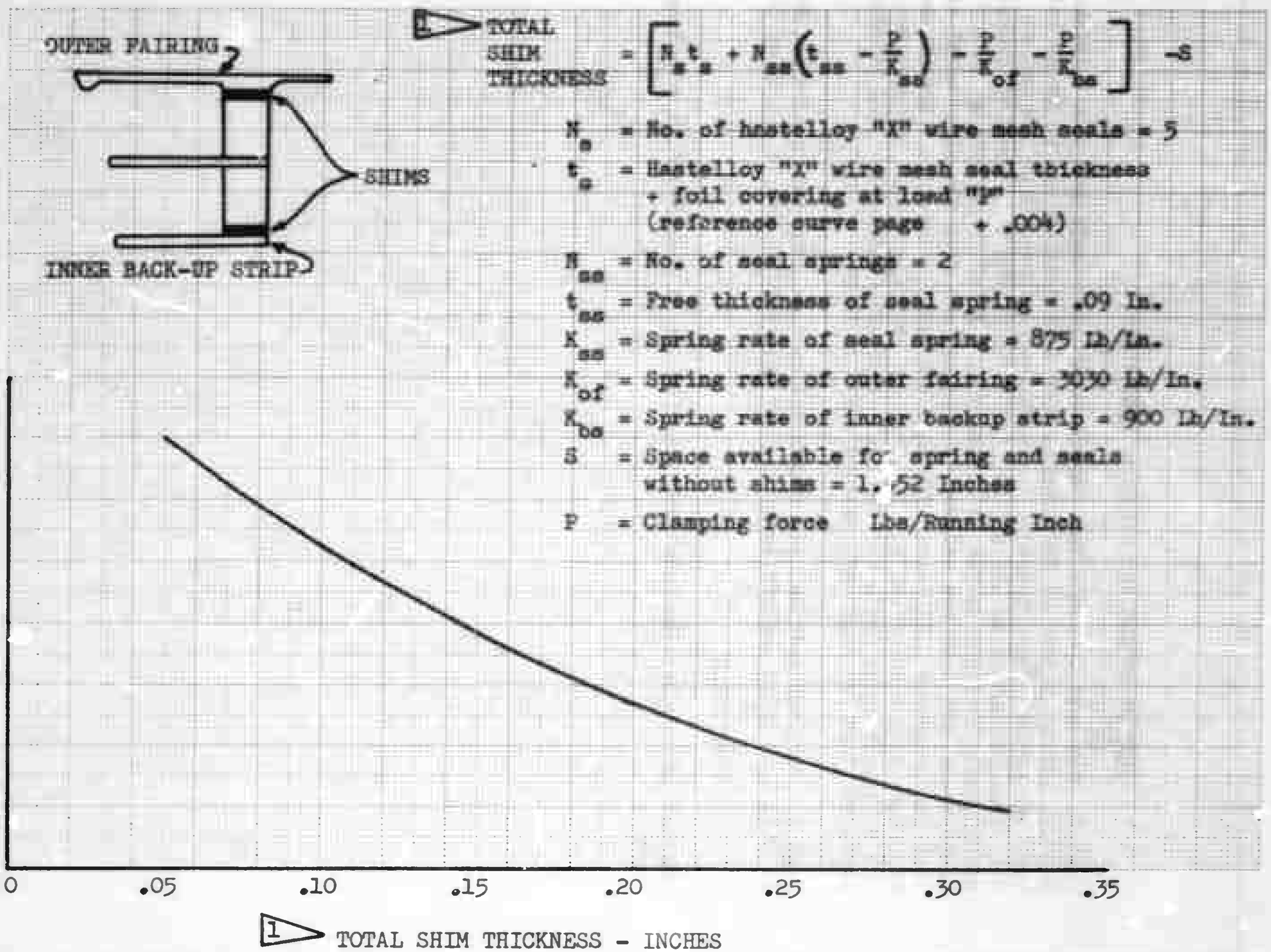

1 TOTAL SHIM THICKNESS $= \left[N_s t_s + N_{ss}\left(t_{ss} - \frac{P}{K_{ss}}\right) - \frac{P}{K_{of}} - \frac{P}{K_{bs}} \right] - S$

N_s = No. of hastelloy "X" wire mesh seals = 5

t_s = Hastelloy "X" wire mesh seal thickness + foil covering at load "P" (reference curve page + .004)

N_{ss} = No. of seal springs = 2

t_{ss} = Free thickness of seal spring = .09 In.

K_{ss} = Spring rate of seal spring = 875 Lb/In.

K_{of} = Spring rate of outer fairing = 3030 Lb/In.

K_{bs} = Spring rate of inner backup strip = 900 Lb/In.

S = Space available for spring and seals without shims = 1.52 Inches

P = Clamping force Lbs/Running Inch

TEST PROCEDURE AND RESULTS (Continued)

Test 2: The seal specimen was compressed at room temperature to a thickness of 0.11 inch at a load of 228 pounds. The load decayed to 210 pounds before heat was applied (see Figure 62 . With the thickness held constant at 0.11 inch, a heat cycle was applied (refer to Figure 59) and load decay continuously recorded (refer to Figure 63. After 15 minutes at 1600°F temperature, the load was reduced to 0 pounds and then reapplied until the seal thickness was 0.11 inch. The load was again reduced to 0 pounds when the heat cycle reached 800°F. The load was reapplied until the specimen was 0.11 inch thick again and the heat cycle was completed. Seal thickness after the load and heat were removed was 0.11 inch.

Test 3: The test specimen was compressed at room temperature to a thickness of 0.11 inch and a load-deflection curve was recorded (refer to Figure 64).

CONCLUSION

Similar load-deflection data were obtained for all specimens at room temperature.

APPENDIX III

TEST DATA REDUCTION METHODS

III. TEST DATA REDUCTION METHODS

VERTICAL DEFLECTION COMPARISON

Test data and analytic data were adjusted to the same reference for comparison as follows:

1. TEST DATA
The vertical deflections were corrected for rigid body rotation.

$$V_{corrected} = V - V_D + R_{xx}(\overline{Y}) + R_{yy}(\overline{X})$$

V = Vertical deflection data - Inches
V_D = Vertical deflection at point D (DD6) - Inches

$$R_{xx} = \frac{DA6 - DB6}{14.88} \quad \text{- Inches/Inch}$$

$$R_{yy} = \frac{DD6 - \frac{DA6 + DB6}{2}}{19.81} \quad \text{- Inches/Inch}$$

$\overline{X}$ = X-Distance from point D - Inches
$\overline{Y}$ = Y-Distance from point D - Inches

2. ANALYTIC DATA
The vertical deflection at the node was corrected to the deflection gage.

$$V = V_z + Rd$$

V_z = Vertical deflection from analysis - Inches
R = Rotation - Inches/Inch (see page 50)
d = Distance from node to point - Inches

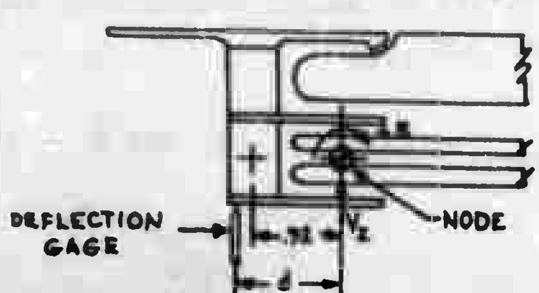

which is then corrected for rigid body movement

$$V_{corrected} = V - V_D + R_{xx}(\overline{Y}) + R_{yy}(\overline{X})$$

V = Vertical deflection at gage - Inches
V_D = Vertical deflection at gage (point D) - Inches

$$R_{xx} = \frac{V_A - V_B}{14.88} \quad \text{- Inches}$$

$$R_{yy} = \frac{V_D - \frac{V_A + V_B}{2}}{19.81} \quad \text{- Inches}$$

$\overline{X},\overline{Y}$ = X- and Y-Distance from point D - Inches

ROTATION COMPARISON

Test data and analytic data were adjusted to the same reference for comparison as follows:

1. TEST DATA

From D_1 and D_2 find R_{frame}.

$$R_{frame} = \frac{D_1 + D_2}{L} \quad \text{- Radians.}$$

which is then corrected for rigid body rotation.

$$R_{frame\ corr.} = R_{frame} - (R_{xx} \cos\phi - R_{yy} \sin\phi) \text{ - RADIANS}$$

$$R_{xx} = \frac{DA6 - DB6}{14.7} \quad \text{- RADIANS}$$

$$R_{yy} = \frac{DD6 - \left(\frac{DA6+DB6}{2}\right)}{19.6} \quad \text{- RADIANS}$$

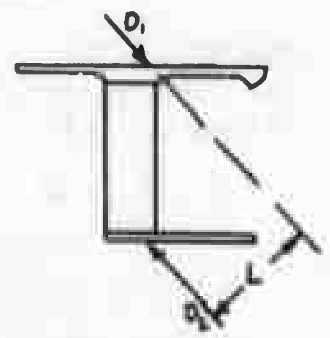

2. ANALYTIC DATA

From Rx and Ry analysis data find components to determine R_{frame}.

$$R_{frame} = Rx \cos\phi - Ry \sin\phi \text{ - RADIANS}$$

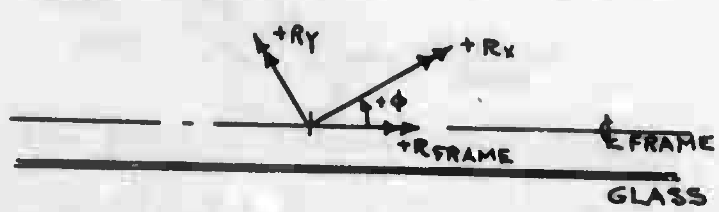

THERMAL DEFLECTION COMPARISON

Test data and analytic data were adjusted to the same reference for comparison as follows:

1. TEST DATA
   The vertical deflections were corrected for rigid body rotation. See page 195.

2. ANALYTIC DATA
   The vertical deflections were calculated based on the assumption that the window frame assumes a spherical shape of radius $d/\Delta T \alpha$.

   d = Frame depth - Inches
   ΔT = Frame depth temperature gradient - °F
   α = Coefficient of thermal expansion of Rene' 41. Inch/Inch/°F

   With points A, B and D fixed at $Z = 0$, determind Z_C and Z_E from the equation of a sphere:

   $$(X - h)^2 + (Y - k)^2 + (Z - l)^2 = R^2$$

   where (h,k,l) is the center of the sphere.

GLASS THERMAL CURVATURE COMPARISON

The allowable bending of the glass was compared with the extrapolated thermal deflection analysis assuming rigid seals and a spherical shape as follows:

1. ALLOWABLE BENDING OF THE GLASS
The allowable radius of curvature of the glass

$$R = \frac{C\,E}{f} = 588.\ \text{Inches}$$

$C = .325$ Inches (half the thickness of the glass)

$E = 10.5 \times 10^{6}$ PSI (modulus of elasticity)

$f = 5800.$ PSI (allowable bending stress)

and the allowable frame temperature gradient (ΔT) was calculated

$$\Delta T = d/R\alpha = 344\ °F$$

$d = 1.62$ Inches (frame depth)

$R = 588.$ Inches (radius of curvature)

$\alpha = 8. \times 10^{-6}$ Inches/Inch/°F (coeff. of expansion) (Rene' 41)

The glass vertical deflection along the X-axis was calculated from the equation of a sphere. See figure 42 page 128.

2. TEST DATA AT FAILURE
The frame depth temperature gradient (ΔT) = 757 °F at the time of failure with a resultant radius of curvature

$$R = d/\alpha\Delta T = 289.\ \text{Inches}$$

$d = 1.62$ Inches (frame depth)

$\Delta T = 757\ °F$

$\alpha = 7.4 \times 10^{-6}$ Inches/Inch/°F (coeff. of expansion - Rene' 41)

The glass vertical deflection along the X-axis was calculated from the equation of a sphere. See figure 42 page 128.

APPENDIX IV

TEST SPECIMEN DRAWING LIST

FIGURE 66 X-20 SIDE WINDOW TEST SPECIMEN DRAWING TREE

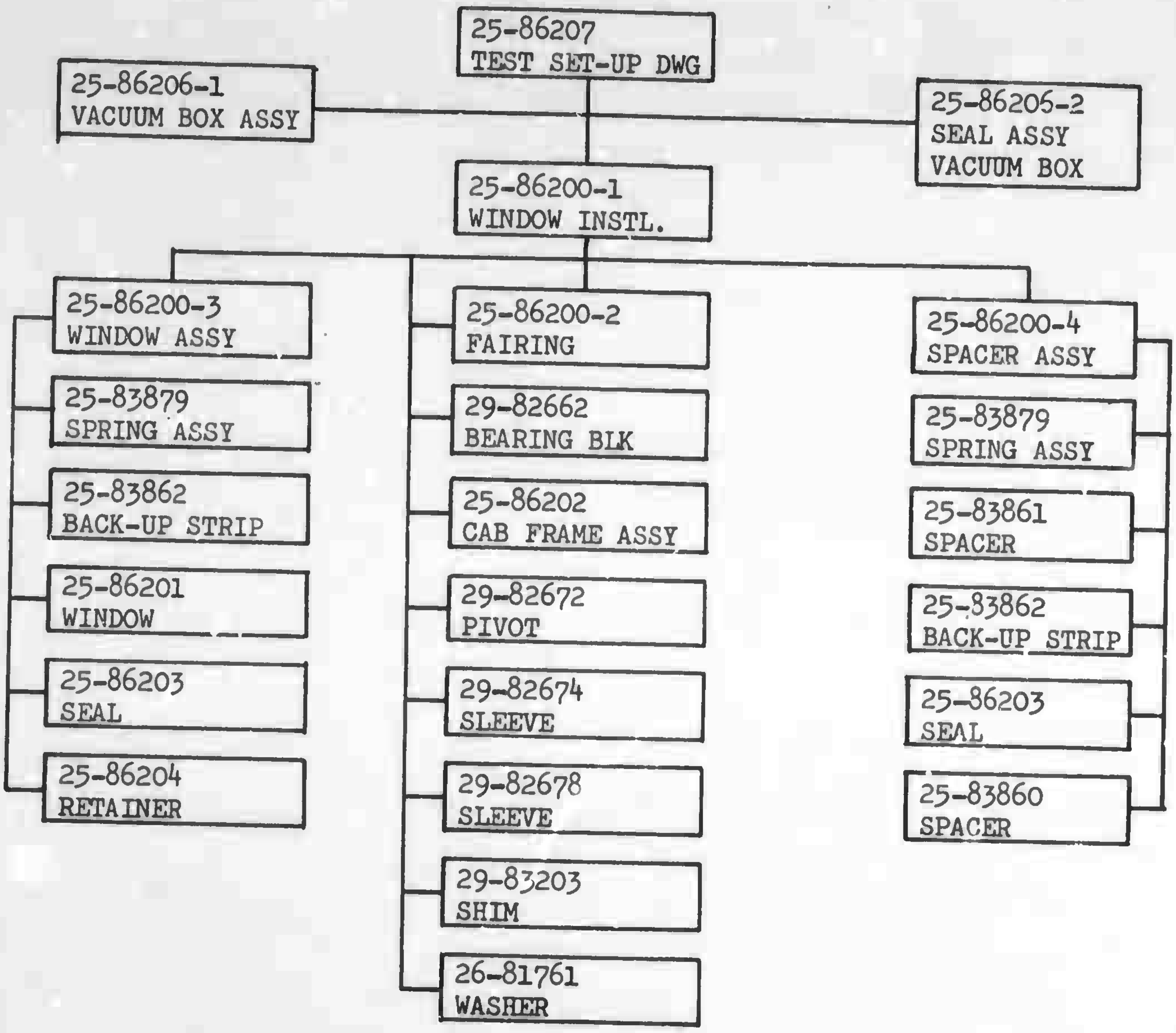

APPENDIX V

MATERIAL PROPERTIES AND ALLOWABLES DATA

FIGURE 67
PHYSICAL PROPERTIES

THERMAL PROPERTIES

RENE' 41 (BMS 7-95, BMS 7-96, BMS 7-119, BMS 7-120) ALL FORMS

PRIOR ENVIRONMENTAL CONDITIONING: NONE

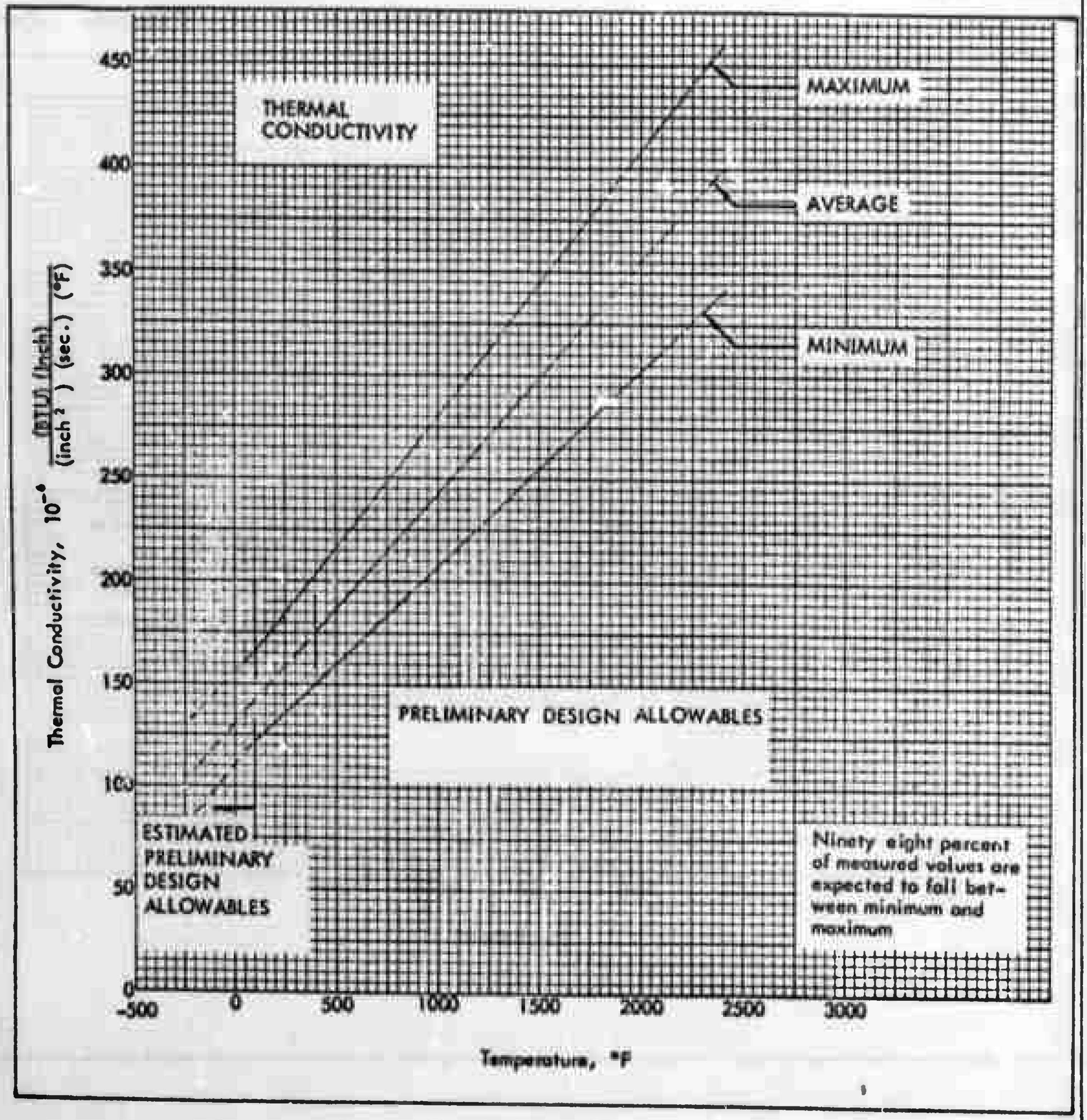

FIGURE 67 PHYSICAL PROPERTIES (CONTINUED)

THERMAL PROPERTIES

RENE' 41 (BMS 7-95, BMS 7-96, BMS 7-119, BMS 7-120) ALL FORMS

PRIOR ENVIRONMENTAL CONDITIONING: NONE

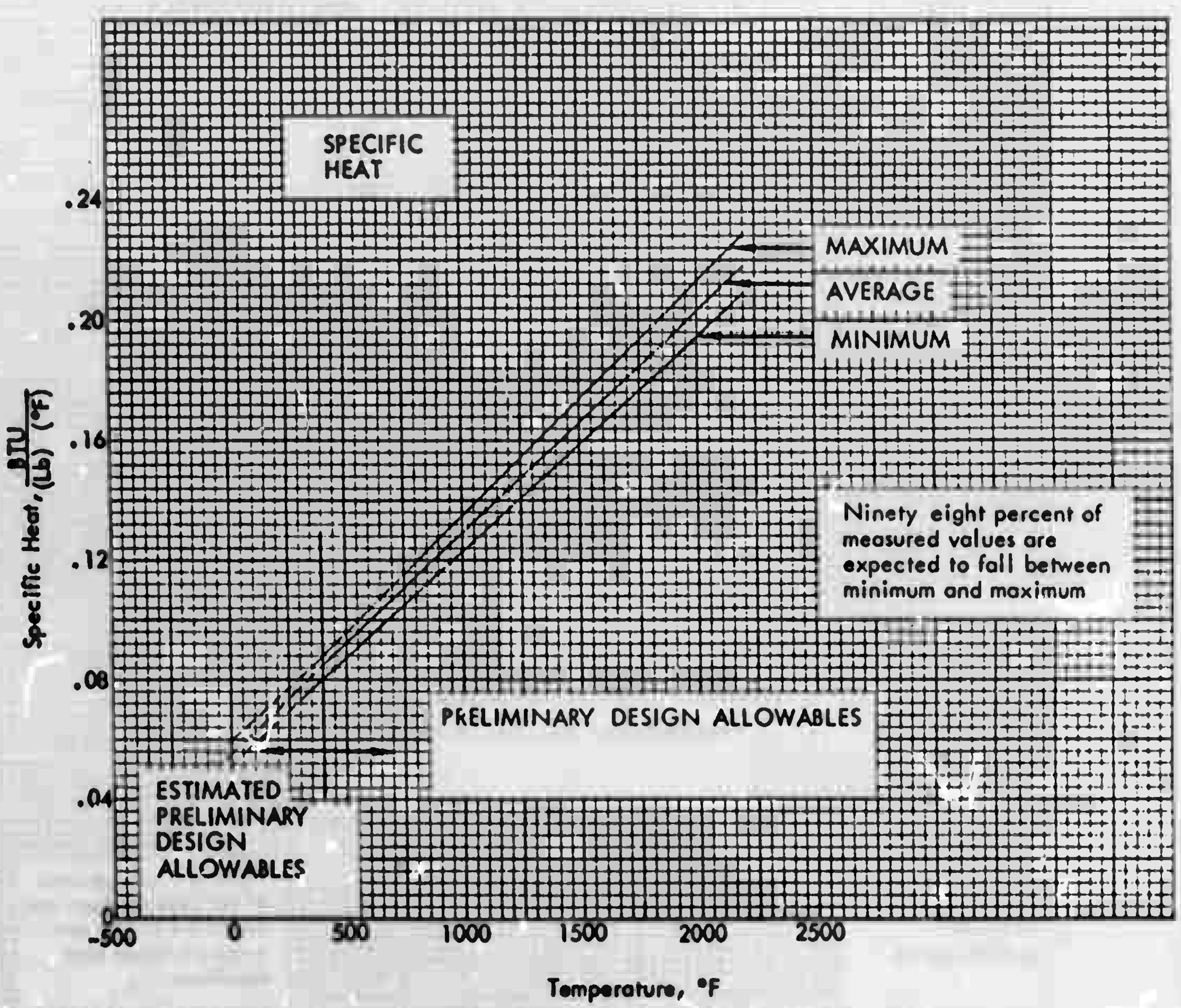

FIGURE 67 PHYSICAL PROPERTIES (CONTINUED)

THERMAL EXPANSION

RENE' 41 (BMS 7-95, BMS 7-96, BMS 7-119, BMS 7-120) ALL FORMS

PRIOR ENVIRONMENTAL CONDITIONING: NONE

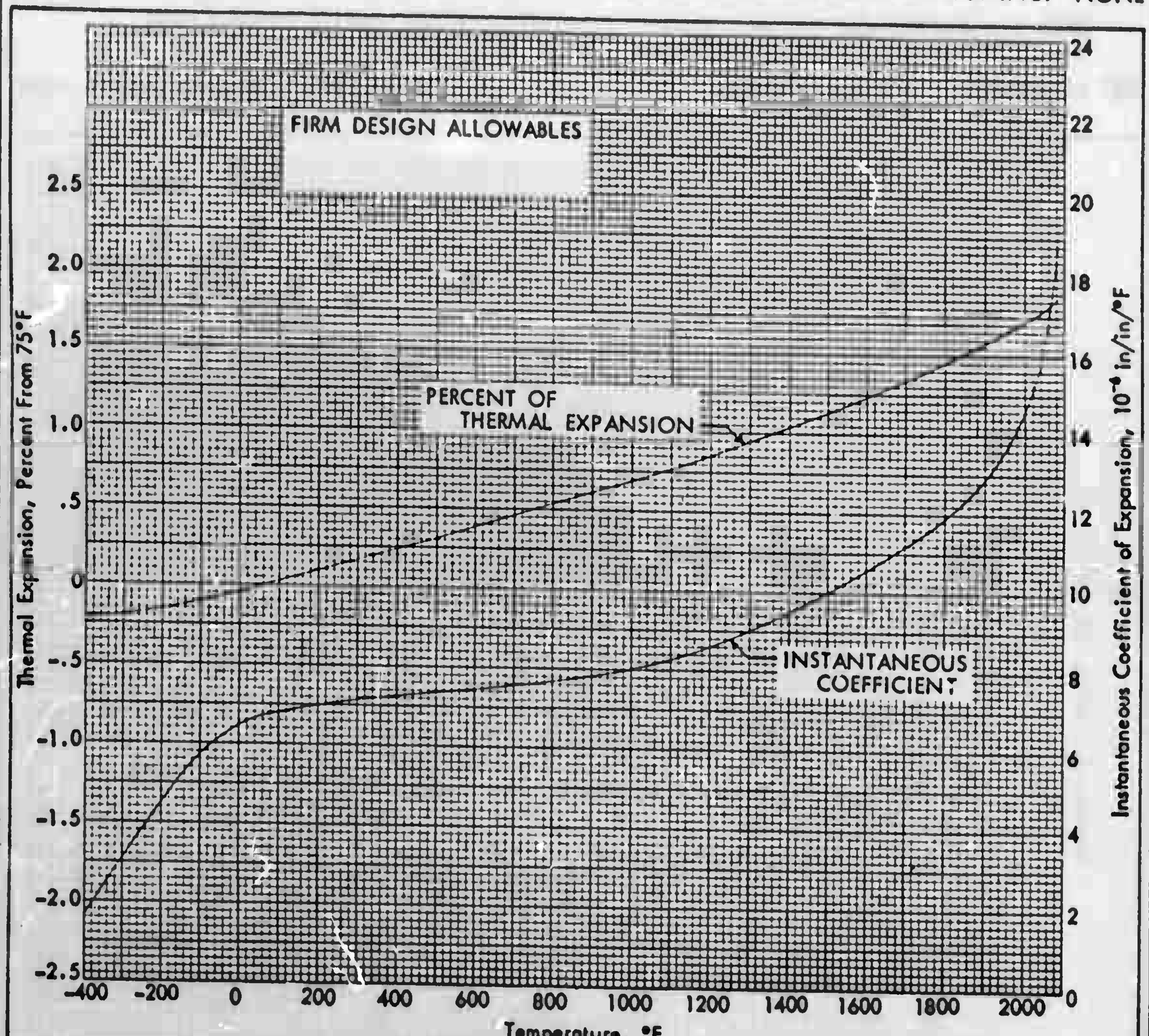

FIGURE 67 PHYSICAL PROPERTIES (CONTINUED)

BASIC MECHANICAL PROPERTIES

RENE' 41 (BMS 7-95, BMS 7-96, BMS 7-119, BMS 7-120) SHEET, PLATE, BAR AND FORGINGS

SOLUTION HEAT TREATED AT 1975°F, WATER QUENCHED; AGED AT 1650°F FOR 1 HOUR, AIR COOLED; AGED AT 1400°F FOR 10 HOURS, AIR COOLED

PRIOR ENVIRONMENTAL CONDITIONING: CONDITION A (ALL CYCLIC CONDITIONS)

TEST CONDITION: .2 HOUR EXPOSURE STRAIN RATE: .002-.005 IN./IN./MIN

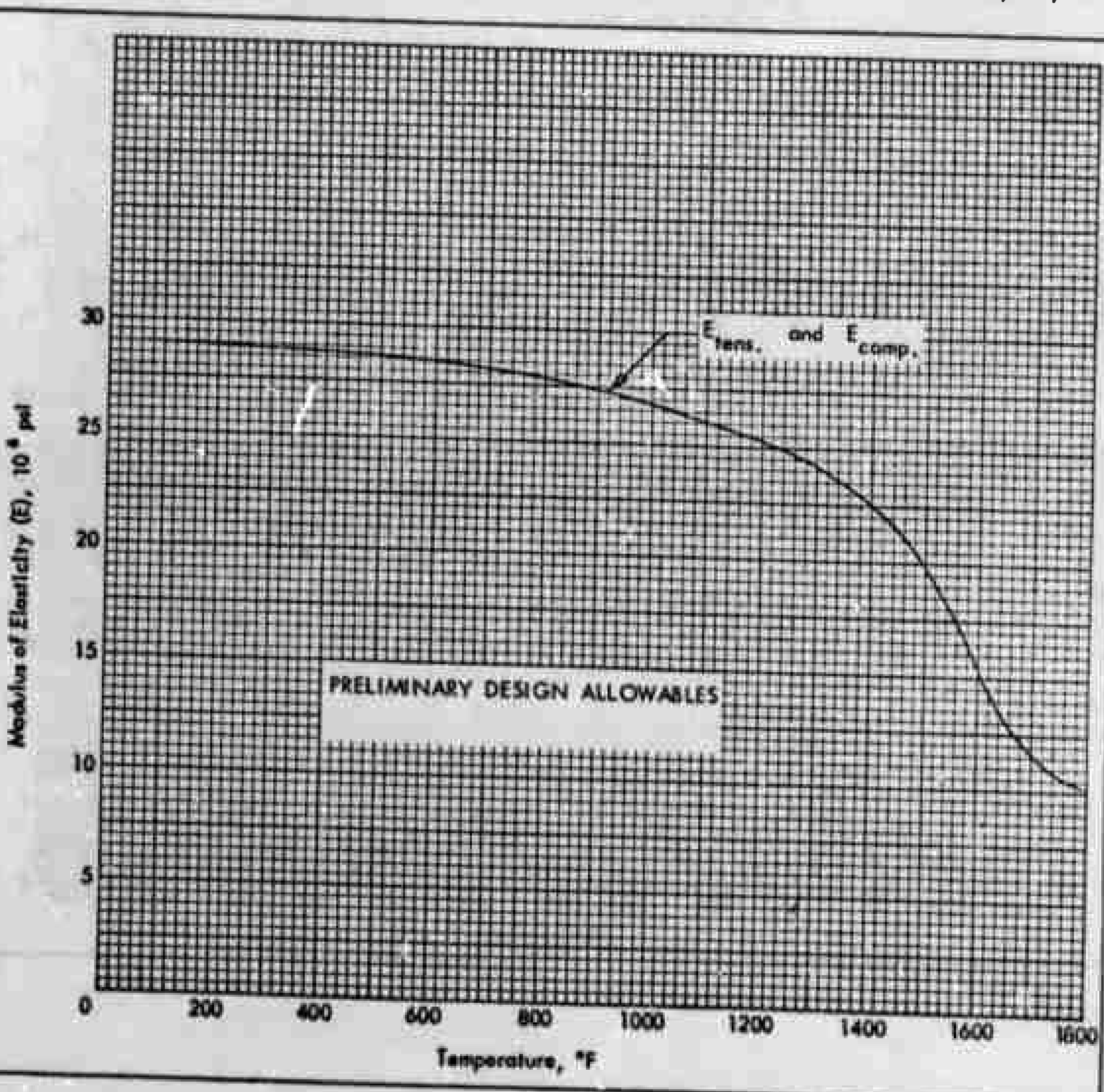

FUSED SILICA

GENERAL NOTES

Fused silica is an extremely pure 100% SiO_2 glass. The 2880°F softening point is the highest temperature capability of all the materials commonly considered for aircraft glazing.

MANUFACTURING PROCESSES

Regular glass cutting methods may be used to cut this material.

PROCUREMENT INFORMATION

Fused silica produced by Corning Glass Works is designated No. 7940 and is manufactured in industrial, optical, and ultrasonic grades. It is available in diameters up to 60 inches. Prices listed are typical for the optical grade.

THICKNESS	COST/IN^2
1/8"	$ 3.75
1/4"	5.25
3/8"	6.50
1/2"	7.80
5/8"	8.60
3/4"	10.30
7/8"	11.70
1"	12.85

FIG 68 PHYSICAL PROPERTIES

Density	.0796 lb/in^3
Softening Point	2880°F

FIGURE 68 PHYSICAL PROPERTIES (CONTINUED)

FUSED SILICA: LOW AND ELEVATED TEMPERATURE LINEAR THERMAL EXPANSION

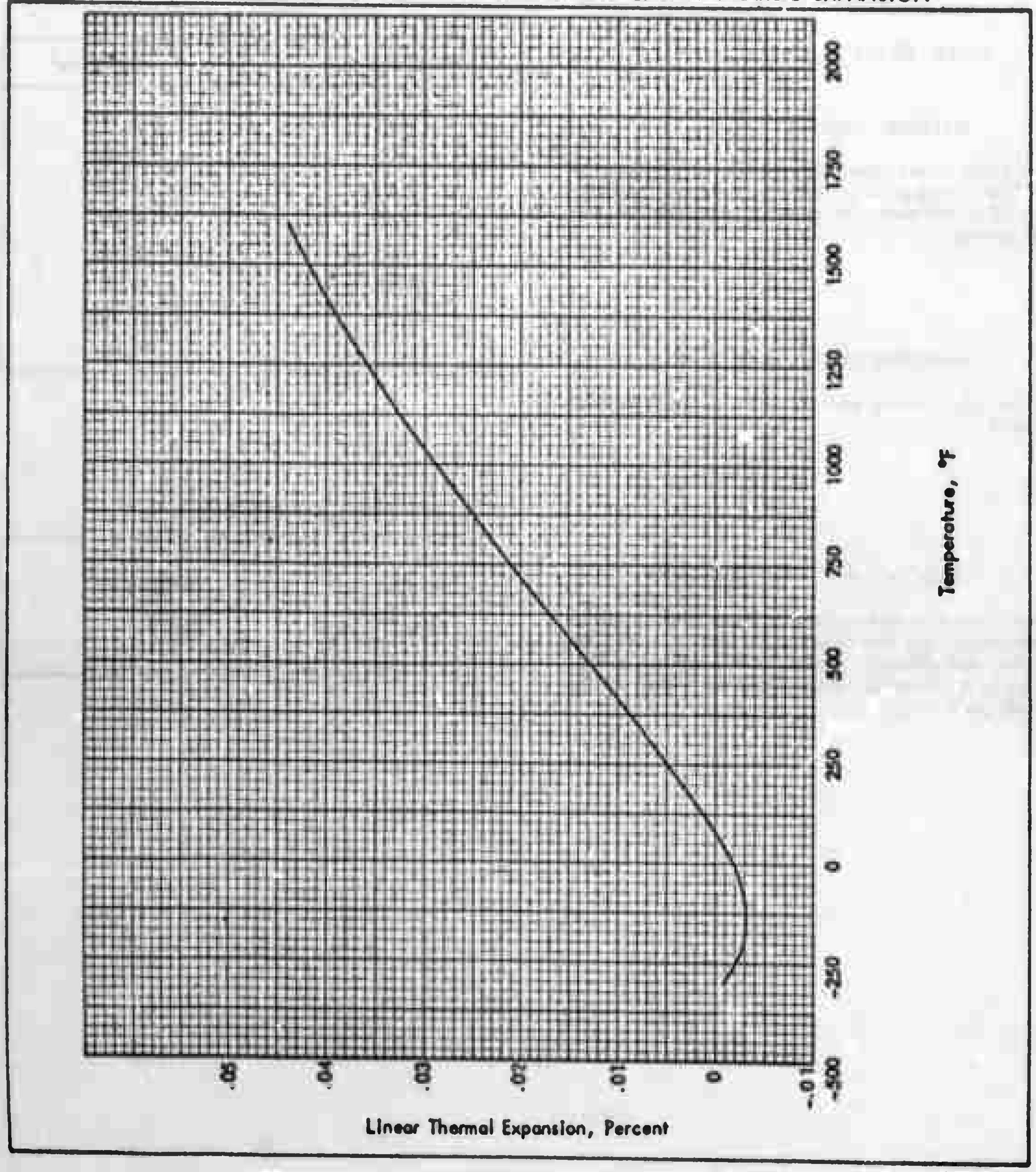

FIGURE 68 PHYSICAL PROPERTIES (CONTINUED)

FUSED SILICA: ROOM AND ELEVATED TEMPERATURE THERMAL CONDUCTIVITY

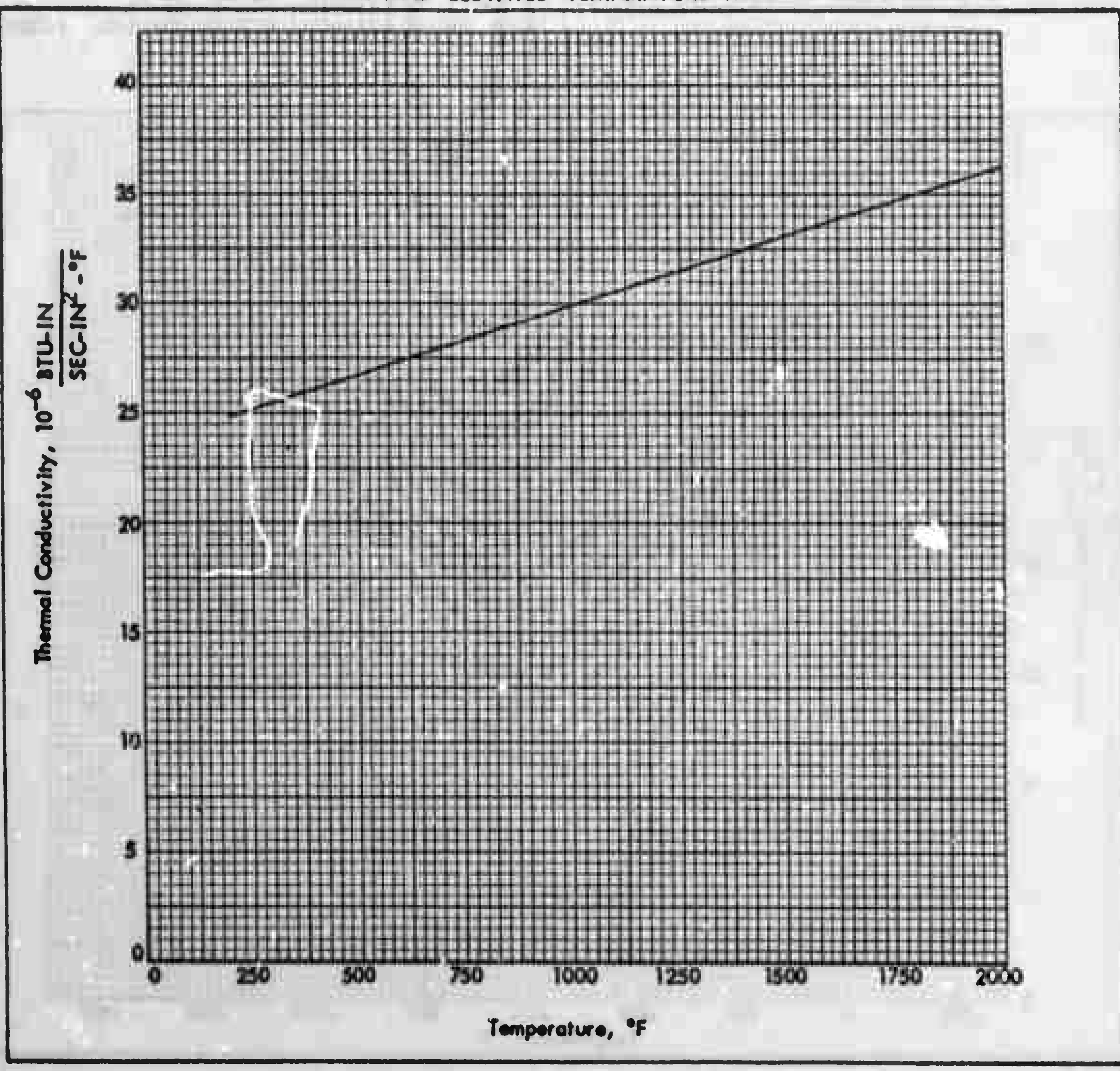

FIGURE 68 PHYSICAL PROPERTIES (CONTINUED)

SPECIFIC HEAT

FUSED SILICA GLASS (CORNING GLASS WORKS NO. 7940)

PRIOR ENVIRONMENTAL CONDITIONING: NONE

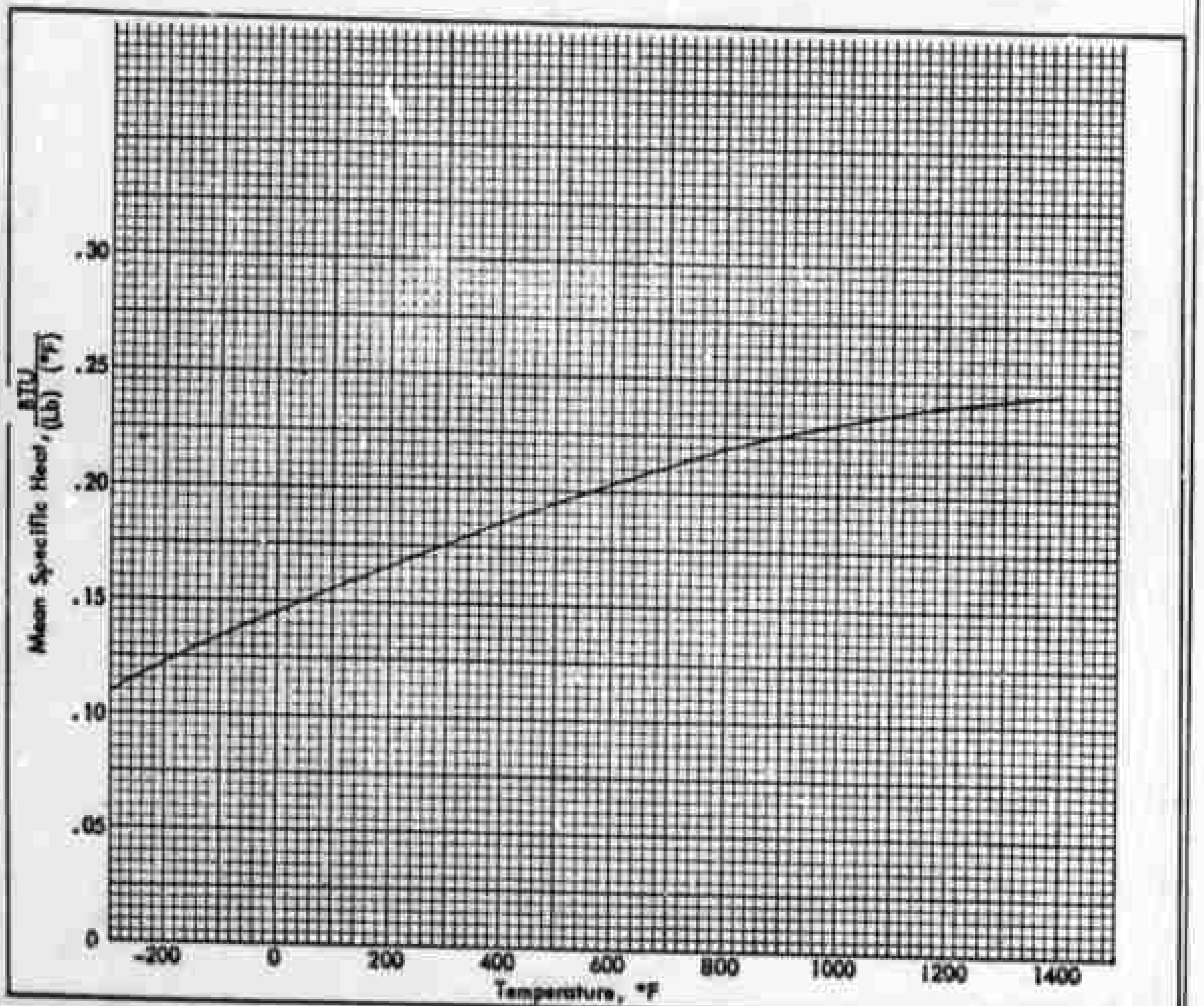

FIG. 68 PHYSICAL PROPERTIES (CONTINUED)

TOTAL NORMAL EMITTANCE

FUSED SILICA GLASS (CORNING GLASS WORKS NO. 7940)

MATERIAL AND COATING PER SOURCE CONTROL DRAWING 10-81001

PRIOR ENVIRONMENTAL CONDITIONING: NONE

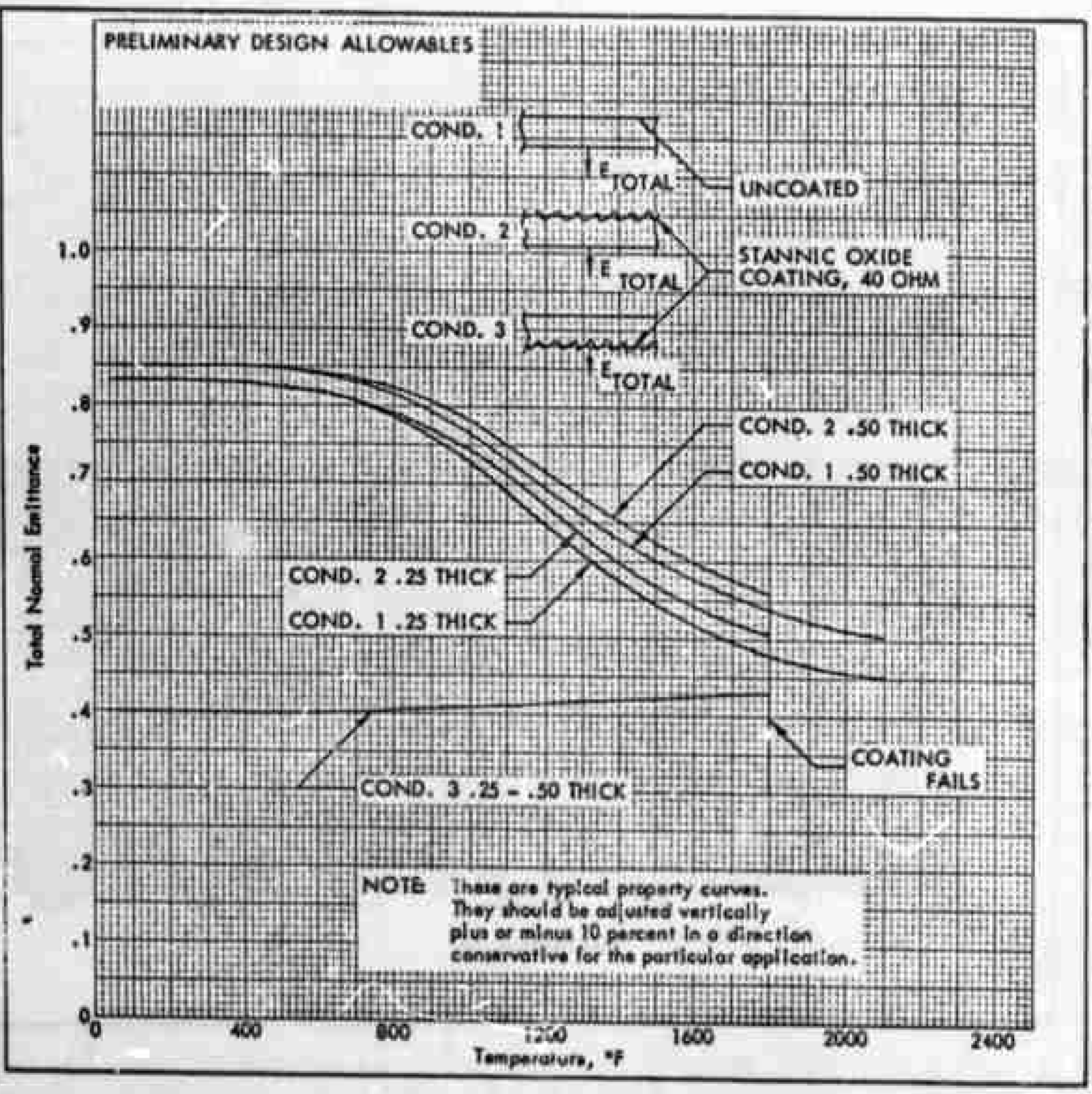

FIG. 69 MECHANICAL PROPERTIES

BASIC MECHANICAL PROPERTIES

FUSED SILICA GLASS (CORNING GLASS WORKS NO. 7940)

MATERIAL PER SOURCE CONTROL DRAWING 10-81001

PRIOR ENVIRONMENTAL CONDITIONING: NONE

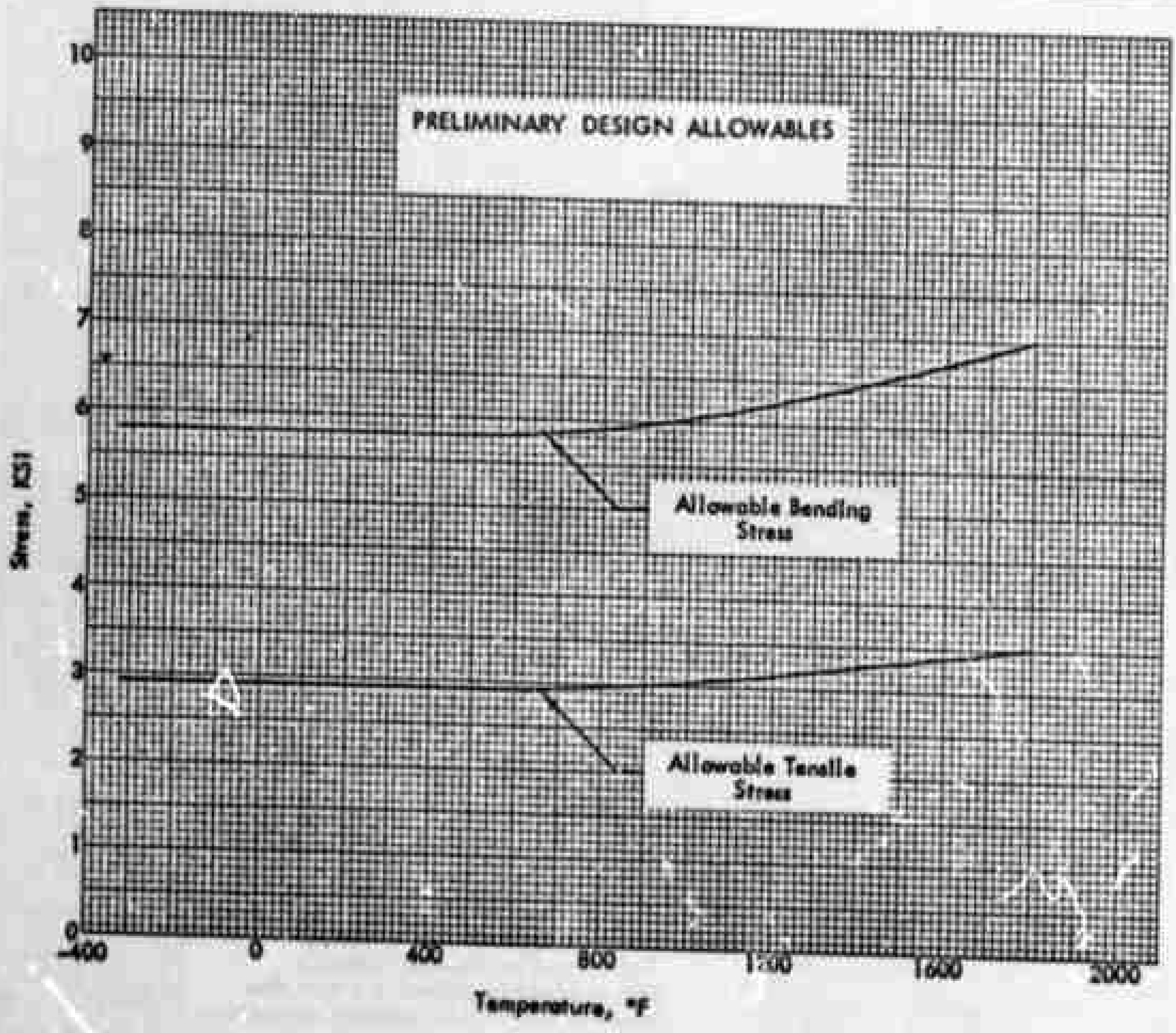

FIG. 69 MECHANICAL PROPERTIES (CONTINUED)

FUSED SILICA: ROOM AND ELEVATED TEMPERATURE MODULUS OF ELASTICITY (E)

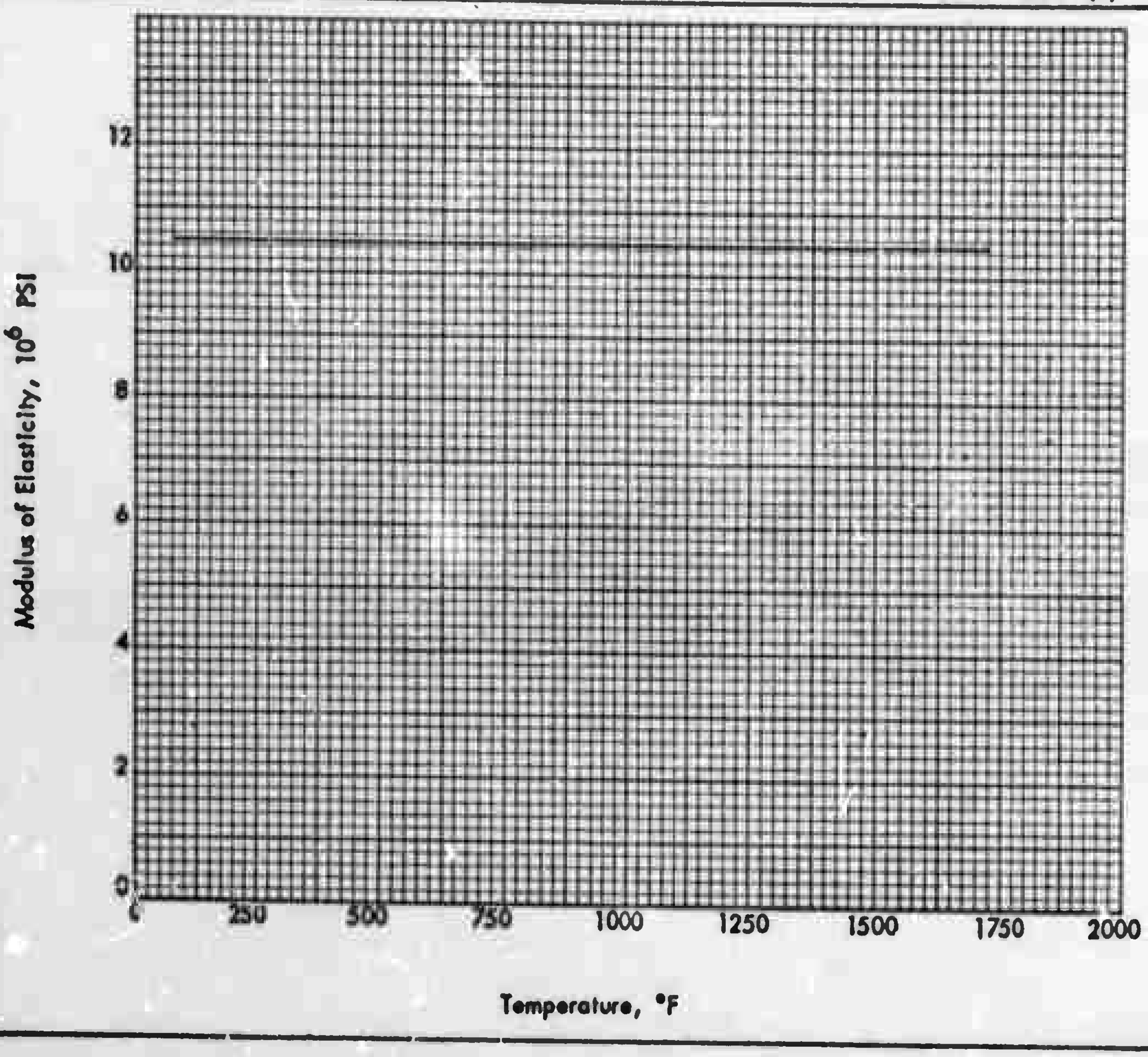

REFERENCES

1. D2-80088, Window Development - Dyna-Soar

2. D2-80706, Smoothness, Sealing and Venting Specifications for X-20 Glider and Transition

3. D2-81142, X-20 Boost, Hypersonic, Approach, and Air Launch Phase Load Conditions

4. D2-81293, X-20 Side Window Vibration, Heat, and Load Test Plan

5. D2-81300, Side Window Strength Check Notes - Model X-20

6. D2-90709-1, Hot Structures Thermal Correlation

7. 10-81001, Code Ident. No. 81205 Size A Source Control Drawing, Dyna-Soar Transparent Structures

Unclassified
Security Classification

DOCUMENT CONTROL DATA - R&D
(Security classification of title, body of abstract and indexing annotation must be entered when the overall report is classified)

1. ORIGINATING ACTIVITY (Corporate author) The Boeing Company, Aerospace Division 7755 E. Marginal Way Seattle, Washington	2a. REPORT SECURITY CLASSIFICATION Unclassified 2b. GROUP

3. REPORT TITLE

X-20 High Temperature Side Window Test Evaluation

4. DESCRIPTIVE NOTES (Type of report and inclusive dates)

Contractor's Final Technical Report 27 April 1964 - 1 August 1965

5. AUTHOR(S) (Last name, first name, initial)

John C. McGinnis

6. REPORT DATE	7a. TOTAL NO. OF PAGES	7b. NO. OF REFS
November 1965	217	7

8a. CONTRACT OR GRANT NO. AF 33(615)-2013 b. PROJECT NO. 1368 c. Task No. 136802 d.	9a. ORIGINATOR'S REPORT NUMBER(S) D2-81310-1 Code Ident. No. 81205 9b. OTHER REPORT NO(S) (Any other numbers that may be assigned this report) AFFDL-TR-65-155

10. AVAILABILITY/LIMITATION NOTICES Qualified requesters may obtain copies of this report from DDC. This document is subject to special export controls & each transmittal to foreign governments or foreign nationals may be made only with prior approval of AF Flight Dynamics Laboratory, Wright-Patterson AFB, Ohio.

11. SUPPLEMENTARY NOTES N/A	12. SPONSORING MILITARY ACTIVITY Structures Division Design Concepts Group - FDTS AFFDL - Wright-Patterson AFB, Ohio.

13. ABSTRACT

The purpose of this program was to experimentally verify the X-20A side window assembly and provide experience for improved window design. The objective of this program was to verify the structural integrity of an X-20A high temperature window design in the X-20A flight environment and provide test data to evaluate the design analysis and development procedures utilized.

The window was subjected to a low-level boost vibration environment, outward acting (partial vacuum) limit boost pressure of 7.7 psia, and a simulated re-entry heating time-temperature history.

The window failed during the re-entry temperature cycle. The primary cause of failure was the high temperature gradient through the depth of the window frame of approximately 850°F which exceeded by a factor of 2 the ultimate design value. The extreme thermal gradient caused thermal curvature of the window frame which induced glass curvature in excess of allowable.

Measured temperature and deflections are presented and compared with analytical values. A thermal analysis is presented and compared with test values. Deficiencies of the X-20 window design as determined from the test program are pointed out and suggested methods of improvement are given.

DD FORM 1 JAN 64 1473

Unclassified
Security Classification

Unclassified
Security Classification

14. KEY WORDS	LINK A ROLE	LINK A WT	LINK B ROLE	LINK B WT	LINK C ROLE	LINK C WT
Fused silica window panes High temperature windows High temperature seals Hypersonic re-entry vehicles Structural test of high temperature windows Superalloys						

INSTRUCTIONS

1. ORIGINATING ACTIVITY: Enter the name and address of the contractor, subcontractor, grantee, Department of Defense activity or other organization *(corporate author)* issuing the report.

2a. REPORT SECURITY CLASSIFICATION: Enter the overall security classification of the report. Indicate whether "Restricted Data" is included. Marking is to be in accordance with appropriate security regulations.

2b. GROUP: Automatic downgrading is specified in DoD Directive 5200.10 and Armed Forces Industrial Manual. Enter the group number. Also, when applicable, show that optional markings have been used for Group 3 and Group 4 as authorized.

3. REPORT TITLE: Enter the complete report title in all capital letters. Titles in all cases should be unclassified. If a meaningful title cannot be selected without classification, show title classification in all capitals in parenthesis immediately following the title.

4. DESCRIPTIVE NOTES: If appropriate, enter the type of report, e.g., interim, progress, summary, annual, or final. Give the inclusive dates when a specific reporting period is covered.

5. AUTHOR(S): Enter the name(s) of author(s) as shown on or in the report. Enter last name, first name, middle initial. If military, show rank and branch of service. The name of the principal author is an absolute minimum requirement.

6. REPORT DATE: Enter the date of the report as day, month, year; or month, year. If more than one date appears on the report, use date of publication.

7a. TOTAL NUMBER OF PAGES: The total page count should follow normal pagination procedures, i.e., enter the number of pages containing information.

7b. NUMBER OF REFERENCES: Enter the total number of references cited in the report.

8a. CONTRACT OR GRANT NUMBER: If appropriate, enter the applicable number of the contract or grant under which the report was written.

8b, 8c, & 8d. PROJECT NUMBER: Enter the appropriate military department identification, such as project number, subproject number, system numbers, task number, etc.

9a. ORIGINATOR'S REPORT NUMBER(S): Enter the official report number by which the document will be identified and controlled by the originating activity. This number must be unique to this report.

9b. OTHER REPORT NUMBER(S): If the report has been assigned any other report numbers *(either by the originator or by the sponsor)*, also enter this number(s).

10. AVAILABILITY/LIMITATION NOTICES: Enter any limitations on further dissemination of the report, other than those imposed by security classification, using standard statements such as:

(1) "Qualified requesters may obtain copies of this report from DDC."

(2) "Foreign announcement and dissemination of this report by DDC is not authorized."

(3) "U. S. Government agencies may obtain copies of this report directly from DDC. Other qualified DDC users shall request through ________________."

(4) "U. S. military agencies may obtain copies of this report directly from DDC. Other qualified users shall request through ________________."

(5) "All distribution of this report is controlled. Qualified DDC users shall request through ________________."

If the report has been furnished to the Office of Technical Services, Department of Commerce, for sale to the public, indicate this fact and enter the price, if known.

11. SUPPLEMENTARY NOTES: Use for additional explanatory notes.

12. SPONSORING MILITARY ACTIVITY: Enter the name of the departmental project office or laboratory sponsoring *(paying for)* the research and development. Include address.

13. ABSTRACT: Enter an abstract giving a brief and factual summary of the document indicative of the report, even though it may also appear elsewhere in the body of the technical report. If additional space is required, a continuation sheet shall be attached.

It is highly desirable that the abstract of classified reports be unclassified. Each paragraph of the abstract shall end with an indication of the military security classification of the information in the paragraph, represented as *(TS)*, *(S)*, *(C)*, or *(U)*.

There is no limitation on the length of the abstract. However, the suggested length is from 150 to 225 words.

14. KEY WORDS: Key words are technically meaningful terms or short phrases that characterize a report and may be used as index entries for cataloging the report. Key words must be selected so that no security classification is required. Identifiers, such as equipment model designation, trade name, military project code name, geographic location, may be used as key words but will be followed by an indication of technical context. The assignment of links, rules, and weights is optional.

Unclassified
Security Classification